DANMARKS OG GRØNLANDS GEOLOGISKE UNDERSØGELSE RAPPORT 2006/29

Seismic and petrophysical properties of Faroes basalts (the SeiFaBa project) Final Report

Funded by the Sindri group

Peter Japsen, Morten Sparre Andersen, Lars Ole Boldreel,
Regin Waagstein, Robert S. White, Michael Worthington
& The SeiFaBa group

GEOLOGICAL SURVEY OF DENMARK AND GREENLAND
MINISTRY OF THE ENVIRONMENT

G E U S

DANMARKS OG GRØNLANDS GEOLOGISKE UNDERSØGELSE RAPPORT 2006/29

Seismic and petrophysical properties of Faroes basalts (the SeiFaBa project) Final Report

Funded by the Sindri group

Peter Japsen,[1] Morten Sparre Andersen,[1, 2] Lars Ole Boldreel,[3]
Regin Waagstein,[1] Robert S. White,[4] Michael Worthington[5]
& the SeiFaBa group

[1] Danmarks og Grønlands Geologiske Undersøgelse (GEUS)
[1, 2] University of Faroe Islands
[3] University of Copenhagen
[4] University of Cambridge
[5] University of Oxford

Released 01.01.2008

GEOLOGICAL SURVEY OF DENMARK AND GREENLAND
MINISTRY OF THE ENVIRONMENT

G E U S

Introduction

The SeiFaBa project ('Seismic and petrophysical properties of Faroes Basalt', 2002–2006) was funded by the Sindri Group as part of the programmes for licensees within the Faroese offshore area. The aim of the project was to provide a unique dataset and new understanding of the seismic and petrophysical properties of the Faroes basalts with special focus on the subaerially extruded flood basalts. Drilling of a new well at Glyvursnes and relogging of the Vestmanna-1 well in combination with the extensive dataset for the Lopra-1 borehole would provide valuable new stratigraphic control of the Upper, Lower and Middle Basalt Formations as well as understanding of the physical differences between these formations. The proposed well site at Glyvursnes gave optimal conditions for combining VSP offset with onshore and offshore surface seismic experiments. The relations of sonic velocities of basalt to porosity, composition, stress and fluid content could be studied through detailed analysis of well logs and core material. Such studies would aim at achieving explanations for the sonic response of basalt in terms of physical and compositional properties, bridging the gap between the different scales of data acquired from outcrops, cores, well logs and surface seismic as well as a better understanding of the seismic signatures of flood basalt successions.

The SeiFaBa project is based on a Research Agreement between Atlanticon on behalf of the Sindri Committee and the Geological Survey of Denmark and Greenland (GEUS) on behalf on the scientific partners in the project (the universities of Cambridge, Copenhagen, Oxford and the Faroe Islands). The purpose of the Research Agreement was to specify the conditions governing the payments to be made in respect to the project by Atlanticon and to set out the rights and obligations of the parties; e.g. scope of the work, project period, work plans as well as progress and milestone reports. GEUS and the scientific partners signed a Collaboration Agreement to specify the organization of the work of the project and to set out the rights and obligations of the parties; e.g. semi-annual meetings in the Project Coordinating Committee.

Milestone reports as outlined in the Research Agreement including this Final report have been submitted to the Sindri group as well as eight SeiFaBa progress reports. Additional work will be carried out after the submission of the Final report: The research of Dr Giovanni Bais at the University of Cambridge will last as planned until October 1 2006 (under the direction of Prof Robert White). The PhD thesis of Felicia Shaw at the University of Oxford will be completed in the summer 2006 (under the direction of Prof Michael Worthington). The PhD thesis of Uni K. Petersen at the University of the Faroe Islands is also to be completed in the summer 2006 (under the direction of Dr Morten S. Andersen). Publication of a number of scientific papers documenting the results of the SeiFaBa project are thus to be expected over the coming years.

The present report contains a Summary of activities and results that highlights several aspects of the outcome of the project related to the investigations ranging from studies of core samples to surface seismic investigations with a focus on Faroes basalt, but including parallels to the properties of the Palaeogene basalts in the waters east of the Faroes and of Plio-Pleistocene basalts on Iceland. Moreover, the report contains a chapter with summaries of the project reports, a chapter with papers published during the project or in press and papers from the PhD thesis under preparation and finally a chapter with extended abstracts and abstracts to be presented at the Sindri Conference in Tórshavn, September 2006. The final report is accompanied with a cd containing pdf files with all items in the List of reports and publications.

Summary of activities and results

Drilling and logging at Glyvursnes and Vestmanna

A new 700 m deep scientific well (Glyvursnes-1*)* with continuous coring was successfully drilled autumn 2002 near Tórshavn through the boundary between the Upper Basalt Formation (UBF) and the Middle Basalt Formation (MBF) and the existing Vestmanna-1 well was reamed prior to running an extensive logging programme (Waagstein & Andersen 2004).

The Glyvursnes-1 well, located on the headland 2 km southeast of Tórshavn with the top of the surface casing at 16.6 m above sea level was drilled by the Finnish drilling contractor SMOY. The drilling method was diamond core drilling with fresh water flushing. The core was partly described visually on-site and later fully using a set of high quality digital core photos. The observed structural and petrographic features allowed the drilled succession to be subdivided into flow-units based on abundance and size of vesicles and presence of chilled surfaces and sediments.

The existing 660 m deep Vestmanna-1 borehole penetrating the lower part of the MBF with TD 100 m into the Lower Basalt Formation (LBF) was originally drilled in 1980. It had to be reamed prior to logging due to partly blocking by precipitation of white tufa along the wellbore. The reaming operation was terminated at 615 m due to stuck pipe.

An extensive suite of slim hole wire-line logs was run in both wells by Robertson Geologging. The logging programme comprised acquisition of the following logs: optical televiewer, three arm caliper, formation density, focussed electric, full waveform/compensated sonic, natural gamma spectroscopy and temperature/conductivity. The log quality is generally acceptable except for the spectral gamma logs due to lack of proper calibration. The full waveform sonic logs recorded with a tool with only two receivers are affected by high frequency noise causing difficulties to pick the shear waves. As the processing results from RG of the full waveform sonic logs were considered unsatisfactory time-consuming additional processing passes to enhance results were undertaken both by the Norwegian company Logtek and by GEUS.

The logging runs were made with only one tool at a time. As a good integration of wire-line log and core data is paramount to the project a tedious task of depth matching was carried out. It was carried out in two steps. First the formation density runs were chosen as the master run to which the depths of all other runs were compared. Afterwards the wire-line log runs were compared and adjusted with the drill cores. The depth shifts have been applied to the composite logs and composite LAS-files.

The well results are highlighted in the composite logs in the scale 1:500 showing all log runs together with general lithology and petrography of the cores. For simplicity only a distinction between sediments, brecciated lava crust, vesicular lava crust and massive lava core is made in the lithology column. The wire-line logs reflect clearly the bedding and other features seen in the core. For example the massive core of thicker flow-units comes out clearly with high bulk density, high sonic velocities, high resistivity and low neutron porosity.

The boundary between the Upper (UBF) and Middle Basalt formations (MBF) in the new Glyvursnes-1 well was picked at a depth of 355 m. It is picked at the base of 9 m simple flow of aphyric basalt with a very low gamma ray response morphologically and lithological similar to the so-called C-horizon exposed some 6 km west of the well-site. It overlies a 0.8 m thick very fine-grained reddish sediment. The drilled succession consists dominantly of compound lava flows of thin flow-units of plagioclase-phyric basalts with vesicular crusts characteristic to pahoehoe lava. 150 complete flow-units have been identified in MBF and 99 in UBF. The mean thickness of the flow-unit is 2.2 m in MBF increasing to a mean thickness of 3.4 m in UBF. Thick flow-units above 10 m are only present in the upper 300 m of the well section. Sediments make up 1.3 % of the drilled succession. Most sediment layers are thin and increase in abundance and thickness upwards. Details on the lava succession in Vestmanna-1 is given in Waagstein and Hald (1984).

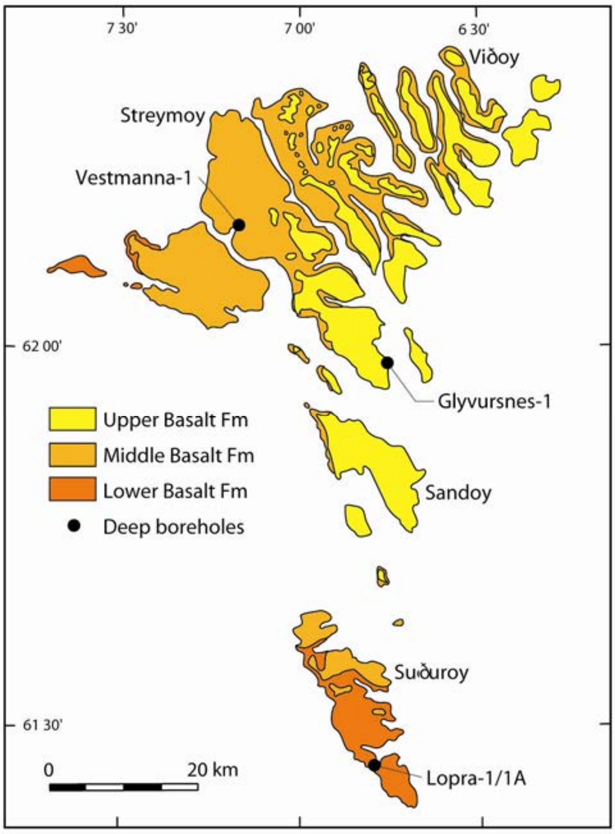

Figure 1. *Geological map of the Faroe Islands showing the location of deep boreholes and the distribution of the three Palaeogene basalt formations (modified from Waagstein 1998; Japsen 2005).*

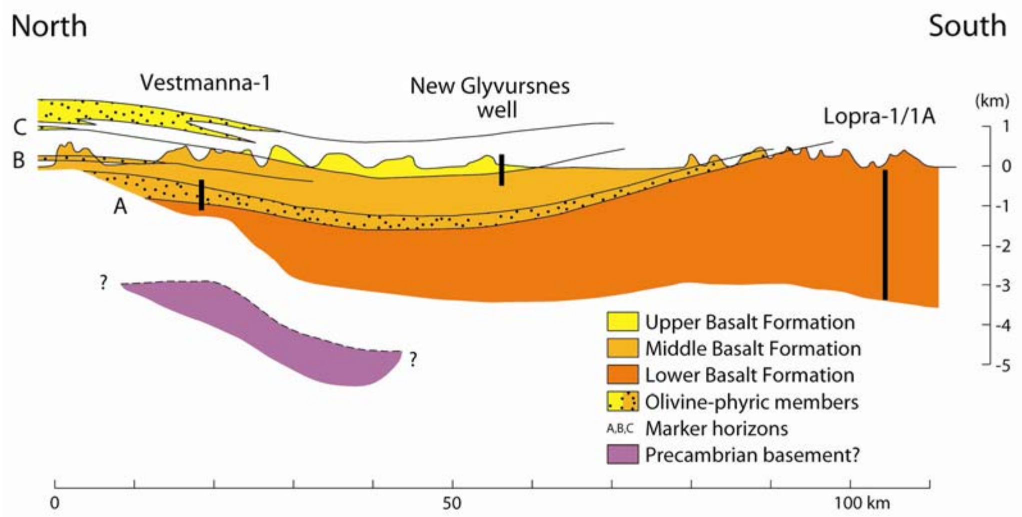

Figure 2. *Stratigraphical position of deep boreholes in the Faroe Islands (modified from Waagstein 1988; Japsen 2005).*

Classification scheme of basaltic rocks

A simple classification scheme of basaltic rocks has been developed to distinguish such rocks from silisiclastic sediments or hard rocks such as rhyolites penetrated by drill holes (Andersen et al. 2005; Andersen & Boldreel 2006). The classification is based on log data supplemented by descriptions of cuttings and sidewall cores. The study is based on wireline logs from 7 UK off-shore exploration wells (UK154/03-01; UK164/07-01; UK164/25-01; UK164/25-01Z; UK205/09-01; UK209/03-01; UK209/04-01; UK209/09-01) and from two research wells on the Faroes Islands (Glyvursnes-1; Vestmanna-1). Completion reports and description of sidewall cores were available for most of the wells (Andersen et al. 2005). Full cores were available from the two research wells (Vestmanna-1 and Glyvursnes-1) and the wireline logs in these wells were correlated to core descriptions (Waagstein & Andersen 2003). Wireline log-based stratigraphy of flood basalts has also been established from the Lopra-1/1A (Boldreel 2006).

A method has been developed for subdivision of basaltic successions into five different classes (Fig. 3). The classification is based on the overall response of natural gamma radiation (GR), neutron porosity (NPHI), bulk density (RHOB), seismic velocity (VP) and resistivity (e.g. MSFL). The five classes are:

1. Simple lavaflows (referred to as low-frequency lava beds in Andersen et al. 2005) are characterised by high-amplitude asymmetric log response on all porosity related logs (NPHI, RHOB, VP and resistivity logs). The typical velocity range is very wide 2–6 km/s at c. 1.5 km depth. Low-frequency lava beds often represent a single, large lava flow, more than 5 m thick. The log response reflects a vertical subdivision of the lava flow in an upper porous crust, a massive core and a thin lower porous crust. In the two cored wells a similar subdivision can be defined by visual inspections. However, significant discrepancies may occur between the subdivision based on wireline logs and the subdivision based on visual core inspection; e.g. where a visually defined compound lavaflow (see below) has a log response similar to a low-frequency lava bed.

2. Compound lavaflows (referred to as high-frequency lava beds in Andersen et al. 2005) are characterised by a log response with a period which generally is less than 5 m on all porosity-related logs. The typical velocity range is 2.5—5.5 km/s at c. 1. 5 km depth. The amplitude of deflections on log traces is generally less than in low-frequency lava beds. In the two cored wells it is seen that the low-porosity intervals of high-frequency lava bed may correlate with individual thin flow units.

3. Volcaniclastic sedimentary units are generally characterised by higher porosity (NPHI) than found in both classes of lava flows. The typical velocity range in a volcaniclastic unit is c. 2–3 km/s at c. 1.5 km depth. Slightly elevated natural gamma radiation is frequently observed in volcaniclastic sedimentary units.

4. Foreset breccias units which may be ascribed as lava deltas (not shown in the figure) are characterised by porosities (NPHI) that generally are higher than in volcaniclastic sediments and amplitude of deflections that are less than in lava beds. Typical velocity range in foreset breccias units is 3—4.5 km/s.

5. Basaltic intrusives (hypabysal) are characterised low porosity (NPHI) and by a symmetric high amplitude log response on the porosity-related logs. Typical velocities are c. 6 km/s at c. 3 km depth. In shaley sediments the response of natural gamma radiation is also symmetric and the intrusives are characterised by low natural gamma radiation.

Furthermore, a detailed characterisation of individual units consisting of basaltic material may be established using log response components (characteristic patterns of one or more log trace within a part of the unit).

A database of physical properties for basaltic rocks estimated from wireline logs has been established and statistical values have been calculated that support the 5 classes mentioned above (Andersen et al. 2005). The range of the porosity-related parameters appear mainly to reflects burial depth and a preliminary linear relation between seismic velocity and depth for basaltic successions has been established using data from the seven UK exploration wells (Andersen & Boldreel 2006). The velocity-depth trend for the UK wells is different from a trend based on data from the Faroese wells.

Seismic attenuation of seismic signals due to stratigraphic filtering in basaltic successions has been modelled in several wells. The results indicate that attenuation due to stratigraphic filtering may reduce the seismic signal considerably at all frequencies. The Q-factor is generally estimated to be above 40 indicating that frequency-dependent attenuation observed in some seismic experiments (Q<40) is caused by other sources than stratigraphic filtering (cf. Shaw et al. 2006). Results of the detailed analysis of seismic attenuation at Glyvursnes and Vestmanna are presented in the section Seismic attenuation.

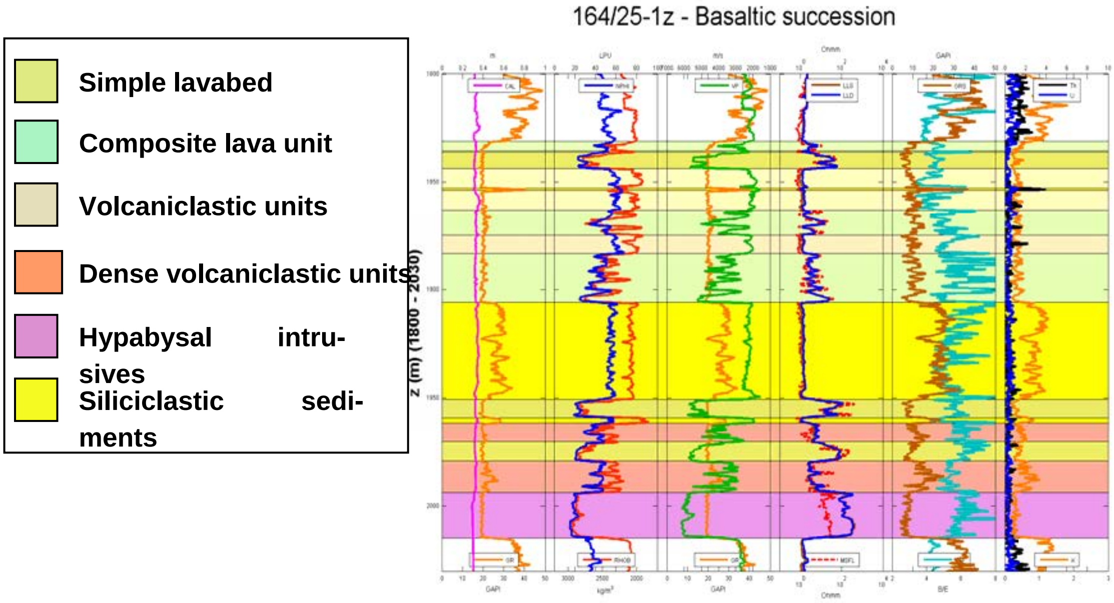

Figure 3. *Classification of volcanic units in 164/25-1z.*

Rock physics analysis of Faroese and Icelandic basalts

The acoustic properties of basalts have been analyzed based on sonic log data from three Faroese and three Icelandic boreholes and ultrasonic laboratory measurements on 43 1.5” core plugs from the three Faroese boreholes (Japsen & Mavko 2006; see Olsen 2005, Olsen et al. 2005). The Faroese boreholes are Lopra-1/1A, Vestmanna-1 and Glyvursnes-1 that penetrate the Palaeogene basalts of the Lower, Middle and Upper Basalt Formations (UBF, MBF and LBF) and these rocks are mainly subaerial flood basalts apart from hyaloclastites below c. 2.5 km depth in Lopra-1. The Icelandic wells penetrate volcanic rocks of Plio-Pleistocene age and cover a mixed environment: HH-1 (95% hyaloclastites), LA-10 (45% submarine and 45% subaerial basalts) and LL-3 (95% subaerial basalts).

We find a tight correlation between sonic Vp and He-porosity based on core data irrespective of basalt facies and well (only data for sediment samples deviate). The core data also reveal a well-defined relation between Vp and Vs, which is to be expected from rocks of broadly similar composition. However, there is a significant scatter in plots of Vp versus density and this scatter is related to the range of grain (matrix) densities from 2.7 to 3.1 g/ccm (Fig. 4). Low grain densities represent altered samples with high content of light minerals such as zeolite and clay.

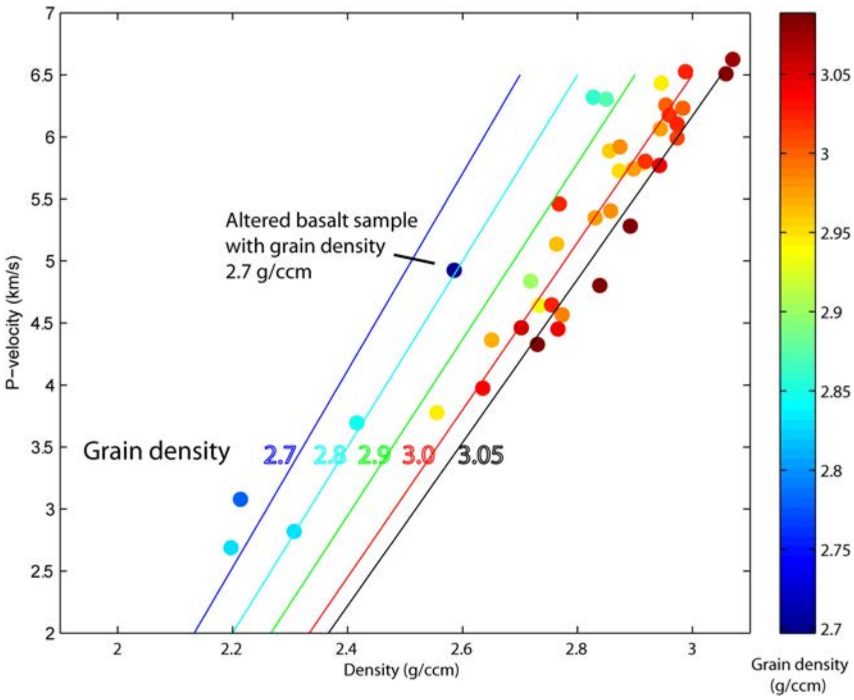

Figure 4. *Plot of ultrasonic data for water saturated core samples from Glyvursnes-1, Lopra-1 and Vestmanna-1 measured at 300 bar: Vp versus density colorcoded by grain density. Straight lines represent different grain densities for a linear velocity-porosity trend given by equation (6) in Japsen & Mavko (2006). Note the general good fit between the datapoints and the model that predict rocks with smaller grain densities to plot to the left in the diagram. Data points for sediments (Vp < 3.5 km/s) do not necessarily have to fit the model.*

Two main Vp-density trends can be distinguished for flood basalts based on the log data (Fig. 5): (1) a trend of relatively low Vp compared to density (the UBF in Glyvursnes-1; the flood basalts in LL-3), and (2) a trend of relatively high Vp compared to density (the LBF in Lopra-1). The properties of the MBF are transitional between the two trends. The Glyvursnes-1 data from this interval represents both the high and the low trend, whereas the Vestmanna-1 data represent a very high trend. The analysis of the Vp-density relation for the core data shows that the outlying samples towards low densities are characterized by low grain density. Hence the relatively high Vp-density trend defined for the log data in these wells for the MBF also must be characterized by low grain densities. This means that the low Vp-density trend represents basalt with unaltered matrix with high grain density and the high trend represents altered basalt with a low grain density.

The transition from the low Vp-density trend of fresh basalts to the high trend of altered basalts within the MBF occurs concurrently with an increase of the sonic velocity and density with depth even though there is no increase in the flow thickness. This indicates that that there probably is a net influx of mass into the altered basalt leading to higher densities (growth of zeolites).

Grain density of the core samples is found to be inversely correlated with Loss on Ignition (LoI) for all rock types and approaches a minimum density of 2.7 g/cm^3 at a maximum Loss on Ignition of 8 Wt.%. (Japsen & Waagstein 2005). LoI is primarily a measure of the water released when the sample is heated to about 1000ºC. The rocks with the highest loss are the most altered ones and consist dominantly of water-bearing secondary minerals as smectite clay and various zeolites. There is a high correlation between neutron porosity (log-value estimated at the depth of the core) minus He-porosity (core) and the volume of water bound in secondary minerals. Neutron porosity measures the amount of hydrogen whether present in pore water or bounded in crystals and it is on average about 8 % too high as compared to gas porosities. The difference between neutron and He-porosity is thus a measure of mineral bound water.

Matrix (or grain) density for the core samples varies systematically with bulk density and alteration of the rocks. A grain density of 3.05 g/ccm is taken as an approximation for unaltered basalt (Japsen & Mavko 2006). For sediments in Faroese wells we assign the mean sample value of 2.8 g/ccm. Measurements on fresh Icelandic basalt lava indicate that 3.05 g/ccm is a reasonable pick (Omar Sigurdsson pers. comm.), and we also apply that value for volcanic sediments in Icelandic wells. Dolerites in Lopra-1 have smaller densities than for the surrounding basalt and we assign a matrix density of 3.02 g/ccm for these rocks. We convert log density to porosity based on these values for the matrix density for different lithologies and a pore water density of 1 g/ccm (and thus overestimate porosity of altered basalts).

The matrix properties of unaltered flood basalts were estimated by comparing acoustic log data from Lopra-1 with the self-consistent formulation of Berryman (1995): bulk modulus, K = 83.4 GPa; shear modulus, G = 40.1 GPa and grain density, ρ = 3.05 g/ccm. Comparison of the model with the log data for Faroese and Icelandic wells reveals a good agreement, but the Glyvursnes-1 data appear to be biased towards relatively high values of Vs.

A modified upper and lower Hashin-Shtrikman model has been estimated to model the velocity-porosity relation for basalt. We have tested a model with the following properties at a maximum porosity of 45%: K = 5.55 GPa, G = 3.2 GPa and the above properties at zero porosity. We find that most data points for all wells fall within the upper and lower bounds defined by this model. There is however, a considerable ambiguity in the relation between velocity and porosity as estimated from bulk density due to the wide range of grain densities. Sonic velocity is thus a proxy for the porosity of basalt and a median model defined by the mean of the upper and lower bounds may thus provide reasonable estimates of basalt porosity from sonic data.

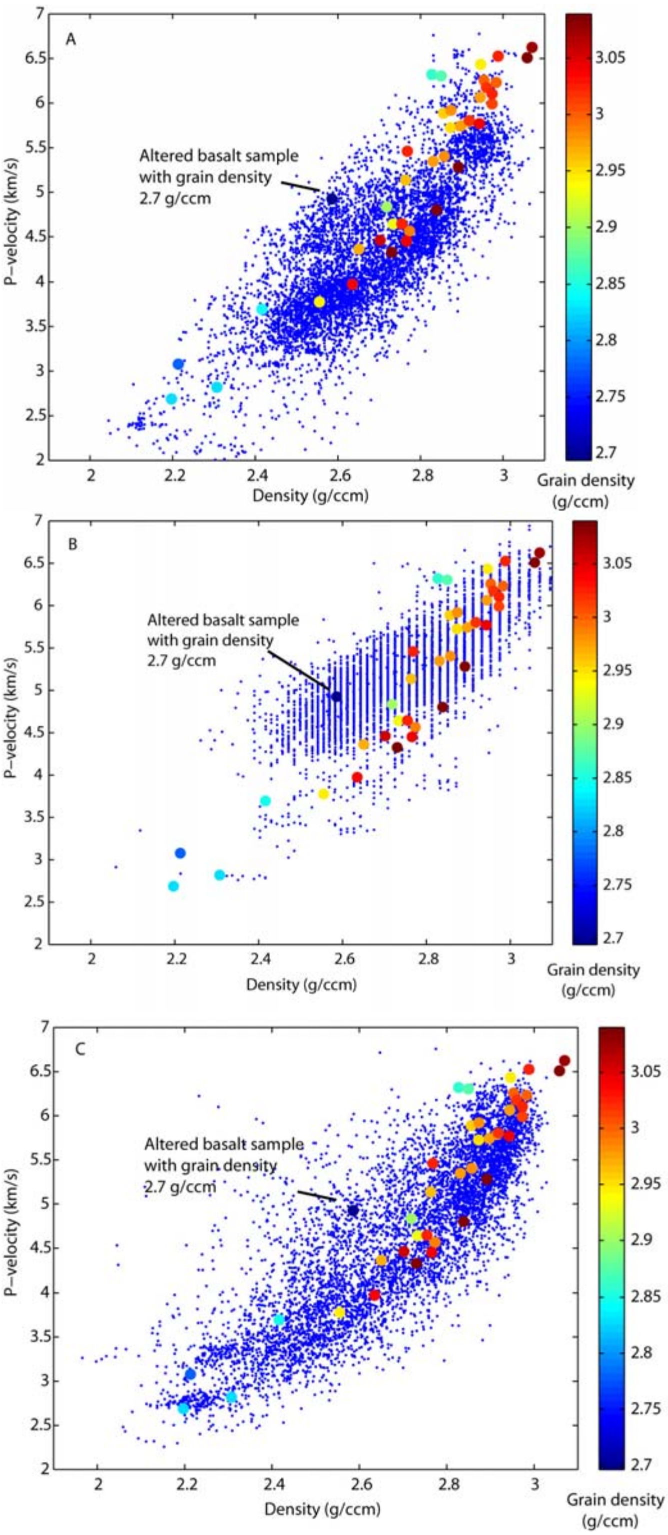

Figure 5. *Plot of Vp versus density for water saturated core data at 300 bar (all samples) and log data for (A) Glyvursnes-1, (B) Vestmanna-1 and (C) LL-3. The low-density part of the relatively high Vp-density trend for the altered MBF in the two Faroese wells is only represented by one sample. The low Vp-density trend represents basalt with unaltered matrix with high grain density (most of the Glyvursnes log data and the LL-3 log data) and the high trend represents altered basalt with a low grain density (the Vestmanna log data). The core data are shifted slightly towards higher Vp values compared to the log data.*

Seismic data acquisition at Glyvursnes and Vestmanna

Four seismic field experiments were carried out as part of the SeiFaBa Project: Two at Glyvursnes (2002, 2003) and two at Vestmanna (2004).

Glyvursnes seismic experiment, 2002

In June 2002, a small experiment was carried out by University of Faeroe Islands and Aarhus University (Petersen et al. 2003). This experiment was mainly aimed at obtaining sufficient data to investigate problems related to acquisition of near-vertical incidence and wide-angle seismic data in the Glyvursnes area. During this survey an external radio source, which induced a high frequency signal of unacceptable amplitude were identified, 500 MHz ground waves originating from the Loran-C transmitter at Eide. New antialias filters were designed in consultation with Geometrix and tested in the field during the winter 2002-2003. The new filters performed as expected and removed the Loran-C noise to a level below detection.

Otherwise the Glyvursnes seismic experiments 2002 showed that data suitable to investigate propagation of seismic waves in the basalts a Glyvursnes could be acquired using near-vertical incidence and wide-angle seismic methods.

Glyvursnes seismic experiments, 2003

In 2003 a two seismic experiments were carried out (Fig. 6a; Andersen et al. 2004). Vertical seismic profiles in Glyvursnes-1 were acquired in June-July and surface seismic data were acquired in September.

Prior to and during the first experiment, a dense array of 45 Guralp (6TD) three component seismometers were deployed. During periods of controlled source seismic shooting all sites maintained a sampling rate of 200 samples/second. For intervening periods when recording earthquakes a sampling rate of 100 samples/second was used. A three component tool was build for the VSP experiment. Three SM-7M 10 Hz geophones were arranged orthogonally and attached to a custom made hydraulic clamping system. The source was a 150 cu. inches Sodera G-gun fired in specially constructed ponds. The data was recorded on CD in SEG-Y format with a Geometrics Geode seismic recording system. Sample interval 0.125 ms. A Vertical VSP, a 242 m offset VSP and a 415 m offset VSP were acquired.

In September 2003 surface seismic data was acquired using three different energy sources 250 g dynamite in 3 m deep holes, 2 x 380 cu. inches Sodera G-gun cluster and a 4 x 40 cu. inches Haliburton slevegun cluster. Data were recorded on a marine streamer, vertical and 3-component geophones. Two vertical component near-vertical seismic incidence profiles at right angles to each other and a grid with pseudo-3D coverage were all acquired with 5 m receiver interval and 10 m shot interval using the dynamite source. Three 400 m profiles at 45° to each other were acquired using both airgun sources and a geophone string with vertical geophones every 5 m and 3-component geophones every 25 m. Two marine near-vertical seismic incidence pseudo-3D grid using the 4 x 40 slevegun clusters recorded on a streamer with 6.5 m group interval and the above mentioned geophone receiver arangement. The three component downhole receiver were clamped permanently at 400 m recording three component data during acquisition of most of the marine shoots.

Figure 6. *Left (A): Overview of part of the survey area. giving an idea of data coverage during Glyvursnes 2003 surface seismic experiment. Key to symbols: Red cross: autonomous seismometers; blue lines (onshore): geophone strings for vertical component reflection seismic profiles; red lines geophone strings for mixed 1C and 3C onshore-offshore seismic profiles; red lines offshore: approximate streamer positions during onshore-off seismic experiments; yellow and green crosses shot positions for two suites of marine reflection profiles with lateral offsets*
Right (B): Multiple shot locations for walk-away and azimuthal profiles at Vestmanna – at 400-, 600- and 800-m-offsets: shot over 26th-29th June 2004. 3 x 40 cu. in. (120 cu. in.) sleeve-guns were used throughout this acquisition.

<u>Vestmanna seismic experiment, 2003</u>

During June and July 2004 various VSP and offset VSP surveys were carried out at the Vestmanna-1 well (Fig. 6b; Petersen et al. 2005).

A 400 metre geophone line was deployed in an easterly direction from the borehole. This consisted of 120 vertical geophones cemented to outcrop at 5 metre intervals and a three component geophone every 4th location. 9 6TD Guralp seismometers were deployed west of the borehole to a maximum offset of 1200 metres. Airgun shots were fired in a natural pond 18 m from the well using a 2 x 40 cu. inches Haliburton slevegun cluster and in the Vestmanna fjord using a 3 x 40 cu. inches Haliburton slevegun cluster. A vertical offset VSP, two offset VSP were acquired with offsets of 230 and 610 m and walkaway azimuthal surveys were acquired. A boomer survey of Vestmanna Fjorð was conducted in order to obtain accurate information on the nature and thickness of sediments in the fjord.

Seismic processing

Processing of the seismic data and further analysis were carried out as ph.d./post.doc. projects at the universities of Cambridge, Faeroe Islands and Oxford. Surface seismic reflections from Glyvursnes were processed in the Faeroe Islands, VSP and offset VSP data in Oxford and azimuthal data from Vestmanna and Glyvursnes in Cambridge (Petersen et al. 2003, 2005). See the following sections.

Seismic attenuation estimated from VSP data acquired at Glyvursnes and Vestmanna

The poor quality of most seismic reflection images within and beneath basalts is likely to be due to a combination of factors whose relative importance varies for different survey locations. The three boreholes at Glyvursnes, Vestmanna and Lopra provide an outstanding source of data for the determination of both the petrophysical and seismic properties of basalts in the Faroe Islands region and how these properties might vary laterally. In addition to estimating the values of seismic attenuation (Q) of the rocks at Glyvursnes and Vestmanna, we have also attempted to deduce the attenuation mechanisms, since this knowledge is required when assessing how the effective Q might vary laterally throughout a survey region (cf. Shaw et al. 2006).

Values of seismic Q determined from VSP data acquired at wells at Lopra, Glyvursnes and Vestmanna in the Faroe Islands are all sufficiently low to be a dominant cause of the poor quality of seismic reflection images. Figure 7 shows histograms of the range of values of effective Q determined at Vestmanna and Glyvursnes.

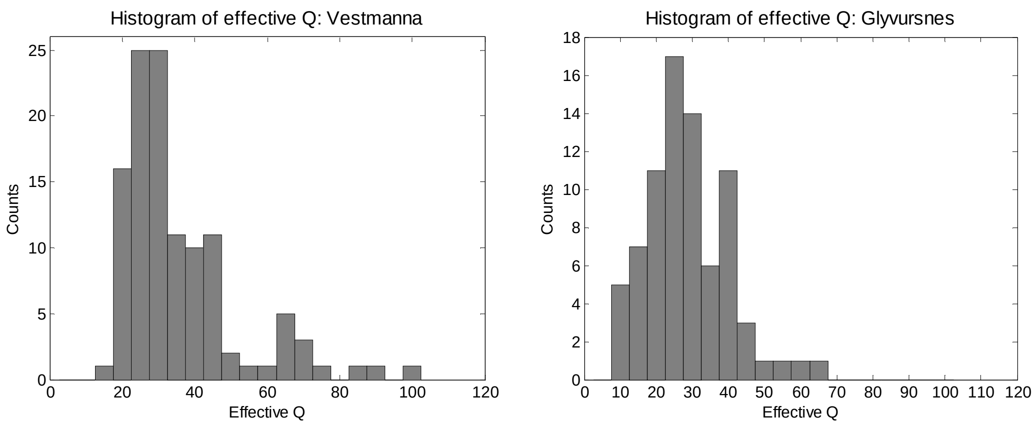

Figure 7. *Histogram of effective Q values determined from VSP data in (a) the Vestmanna borehole and (b) the Glyvursnes borehole.*

However, the possible causes of the low Q have been found to vary between the three borehole localities. Christie *et al*. (2006) concluded that 1-D scattering is the dominant attenuation mechanism at Lopra. It is possible, based on our modelling studies, to come to the same conclusion for the UBF in the top half of the Glyvursnes hole. However, within the MBF in the bottom half of the Glyvursnes hole (360-700 m) and at Vestmanna, very little attenuation can be attributed to 1-D scattering. In Figure 8 it can be seen that the character of the acoustic impedance in the top half of the Glyvursnes hole is markedly different from the remainder of the logs displayed.

Results from 3-D elastic wave numerical modelling with a hypothetical basalt model constructed on the basis of field observations indicate that very little scattering attenuation is caused by lateral variations in basalt structure. However, the low values of effective Q observed at Glyvursnes and Vestmanna can be explained as resulting from a combination of 1-D scattering and intrinsic attenuation due to seismic wave induced fluid flow within pores and micro-cracks.

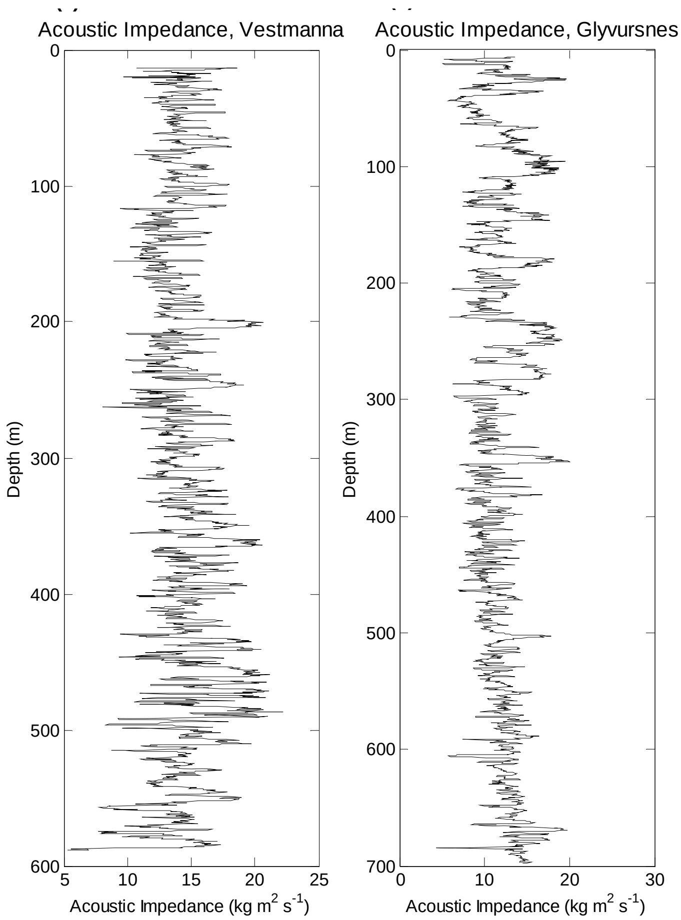

Figure 8. *Acoustic impedance logs from the Glyvursnes and Vestmanna boreholes.*

This study adds to the now substantial number of observations of seismic attenuation within basalt sequences in the North Atlantic region and reinforces the general conclusion that low values of effective Q are to be expected. However, the causes of the high attenuation may vary greatly from one locality to another.

Processing and interpretation of surface seismic data acquired at Glyvursnes

The seismic data acquired around the Glyvursnes-1 borehole makes it possible to compare borehole data (wireline logs) with surface seismic data acquired using different acquisition techniques (Fig. 9). Data were acquired on vertical geophones, 3-component geophones and a marine streamer using two different marine sources and dynamite shots in 3 m deep boreholes (Andersen et al 2004).

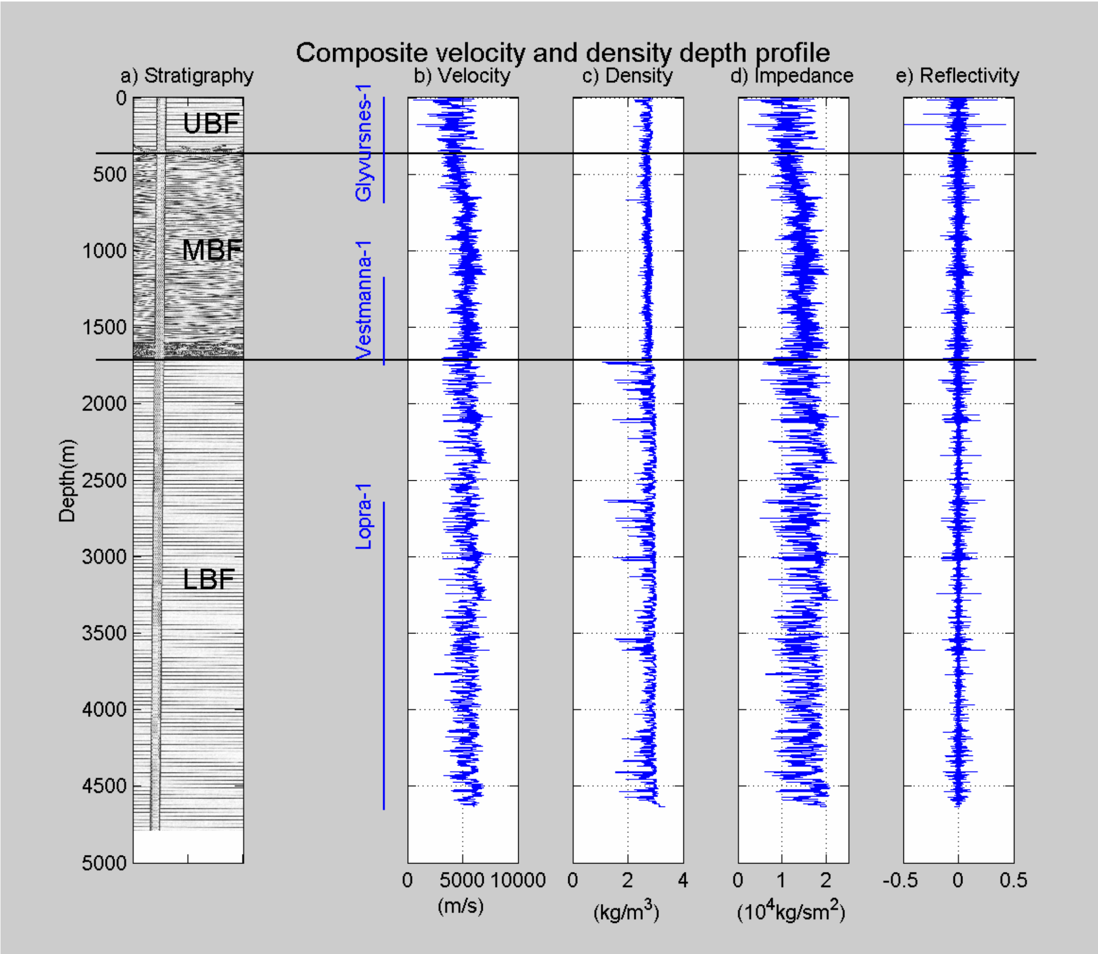

Figure 9. *Composite velocity and density logs for the total stratigraphic sequence below Glyvursnes, constructed using the logs from Glyvursnes-1, Vestmanna-1 and Lopra-1. a) Stratigraphic subdivision (modified from Rasmussen & Noe-Nygaard 1970). The base of the UBF and the base of the MBF are drawn as black horizontal lines across the figure; b) composite velocity log. The uppermost 485 m of Vestmanna-1 are used to represent the missing interval in the MBF and the uppermost 720 m of Lopra-1 are used to represent the missing interval in the LBF; c) composite density log; d) and e) calculated acoustic-impedance and the reflection coefficient series. From Petersen et al. 2006.*

The signal quality of the data recorded by the different combination of source and receivers were compared using time variant frequency analysis of individual traces using a wavelet transform (Figs 10, 11; Petersen *et al.* 2006). This analysis demonstrates a strong time dependent decay for all source-receiver combinations, especially of high frequency seismic data. Qualitatively this is in good agreement with attenuation estimates obtained from analysis of the down-going waves in the zero offset VSP from Glyvursnes-1 (Shaw *et al.* 2004, 2006).

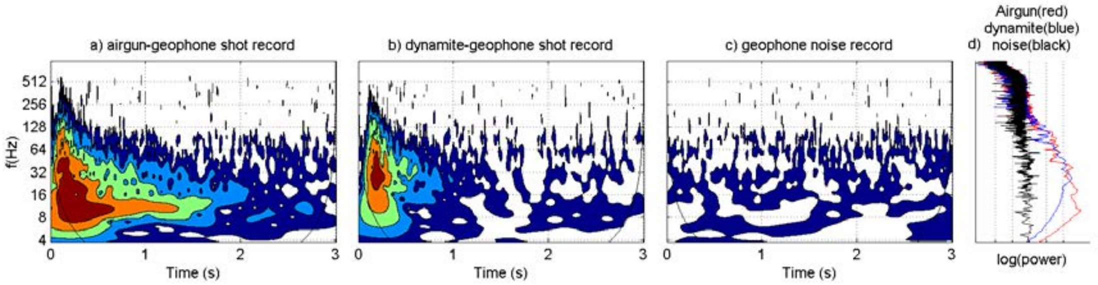

Figure 10. *Plot of the continuous wavelet transforms of geophone channel 110. a) Airgun-geophone, offset 208 m; b) dynamite-geophone, offset 224 m; c) geophone noise record; d) frequency spectra of all three records. Contour levels are increasing exponentially.*

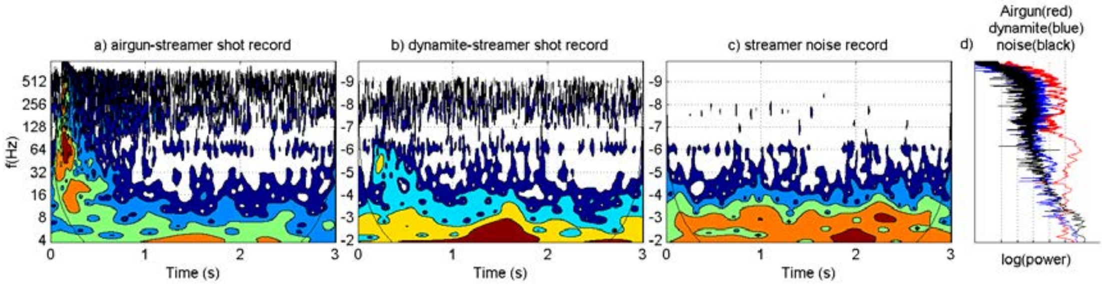

Figure 11. *Plot of the continuous wavelet transforms of streamer channel 130. a) Airgun-streamer, offset 195 m; b) dynamite-streamer, offset 415 m; c) streamer noise record; d) the frequency spectra of all three records. Contour levels are increasing exponentially.*

The time variant frequency analysis indicates that a seismic signal, not necessary primary reflections, should be expected to a recording time of 3 s when 160 cu. inches airgun shots are recorded on geophones (Fig. 10a), but only to about 1 s recording time when recorded on the streamer (Fig. 10b). When dynamite shots are recorded on geophones a seismic signal is expected to ca. 1-1.5 s recording time (Fig. 11a). Due to the higher frequencies in dynamite shots, better resolutions may be achieved at shallow depth. Due to the weak signal (Fig. 11b), dynamite shots were not recorded systematically on the streamer.

Processing and further analysis is focused at highlighting and identifying phases within the time-windows of seismic data for the different source-receiver combinations. Coherent events are seen to a recording time of at least 3 s in the airgun-geophone data, ca. 2 s in the dynamite-geophone data and to ca 1.5 s in the airgun streamer data, highlighting the ability of stacking to enhance weak coherent signal (not obvious in individual traces). Recording time should thus be constrained by stacking tests rather than signal analysis on individual traces.

The stacked sections are characterised by sub-horizontal, almost planar reflections (Fig. 12). Dip is therefore of little help constraining multiple events or other arrivals not being primary P-wave reflections. Two fairly distinct and coherent reflections are picked on the stacked sections from all three acquisition combinations (horizons A' and C'). The succession below horizon A' is characterised by strong continuous internal reflectors and the strength of internal reflectors decreases gradually with depth (recording time). The succession A'-C' is characterised by weak reflectors, which mostly are non-continuous. This is best seen in the dynamite-geophone and airgun-geophone data. The succession above horizon C' is incompletely imaged due to the shallow depth. However, internal reflections are strong and fairly continuous. It is suggested that the contrasting character of the three successions defined by horizon A' and C' replicate the contrasting character of the three exposed basalt formations on the Faeroe Islands. Therefore Horizon A' is interpreted to be approximately equivalent to the LBF-MBF boundary while horizon C' corresponds to the MBF-UBF boundary.

Shaw et al. (2006, in press/this volume) suggest that 1D scattering is one of the main reasons for the low Q-values obtained from the zero offset VSP in Glyvursnes-1 (see the Section Seismic attenuation). We should thus expect short period interbed reverberations to be a significant constituent of the reflected seismic energy. Planke (1994) pointed out that the bed thickness in basalt successions generally is small compared to the wavelength of the seismic signal and concluded that reflections in the seaward dipping reflector sequence around ODP well 642E mostly represented tuning of reflections from individual bed boundaries. Bed thickness in the LBF on the Faroe Islands is on average around 20 m, well below the dominant wavelength in the seismic signal. Coherent events below horizon A' on the stacked sections is thus likely not to represent reflections from individual beds, but at best complex interferences of tuned primaries and short period reverberations. However, even a coherent event constituted by interferences of tuned primaries and short period reverberations carry information about geology corresponding approximately to the TWT time of the event. Coherent events below horizon A' in stacked sections of the dynamite-geophone and airgun-geophone (Fig. 12) is thus likely to contain relevant geophysical information, as we believe long period interbed multiples is scarce.

The processing and interpretation of the surface seismic data acquired at Glyvursnes in 2003 indicate that imaging of the basalt succession encountered at Glyvursnes is possible. Decay of the source signature with depth into the formation and correct stacking velocities are key factors controlling the quality of the final stack of the basalt succession. As proposed by Planke et al. (1999) seismic imaging of basalt thus amounts to the conventional task of separating primary energy from noise.

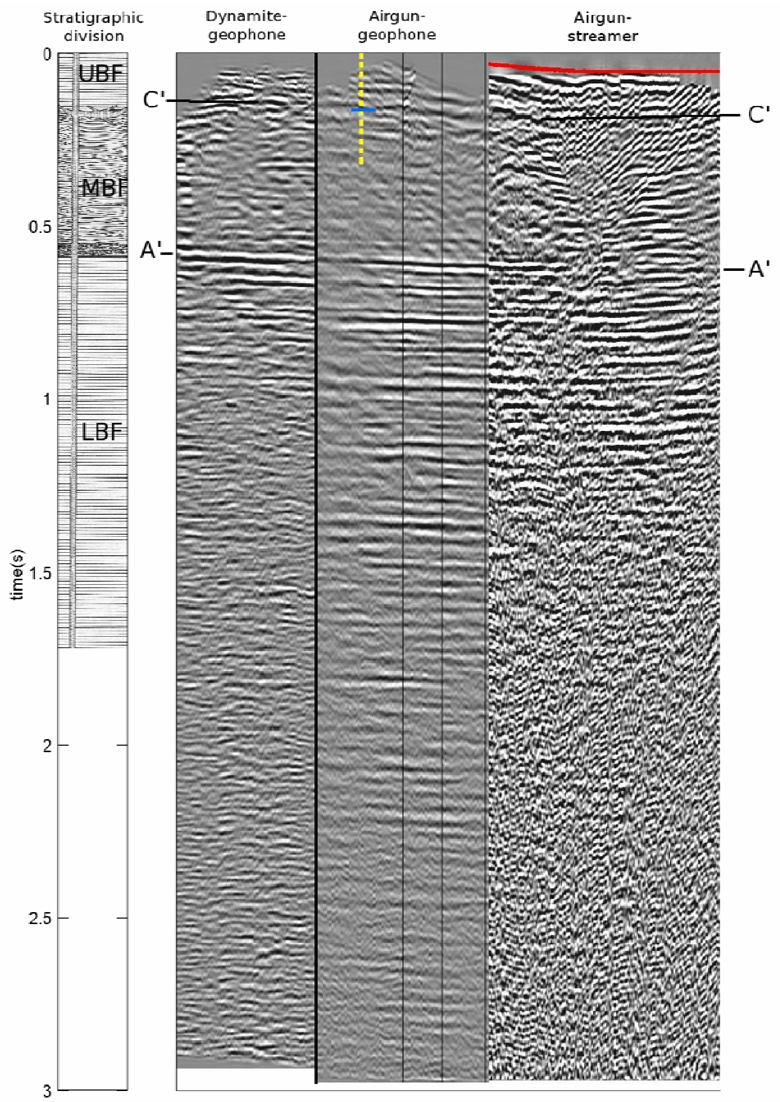

Figure 12. *Combined profile of the total stratigraphic sequence below Glyvursnes (Fig. 1) and the seismic data. A threefold subdivision of the seismic profile is distinct both in the airgun-geophone-streamer and dynamite-streamer data. Two high-amplitude successions (above C' and below A') and a low-amplitude succession (between A' and C') are clearly identified. The red line is the seabed derived from bathymetric information. The blue marker on the yellow line is the UBF-MBF boundary in the well.*

Seismic velocities, anisotropy and seismic imaging of Vestmanna basalts from integrated borehole and wide-angle data

Borehole data, vertical seismic profiles, near-offset and wide-angle seismic reflection data have been used to investigate the velocities, anisotropic properties and internal imaging of layered basalts at Vestmanna harbour (Fig. 13) (Bais et al. 2006). Here the 660 m Vestmanna-1 borehole penetrates the lower 550 m of homogeneous “pahoheoe” lavas of the Middle Basalt Formation (MBF) and into the 10–30 m thick, “aa” lava type flows of the Lower Basalt Formation (LBF). We have correlated the ultrasonic-scale velocity measurements from the borehole with the seismic-scale velocities and reflection images derived from VSP and surface data.

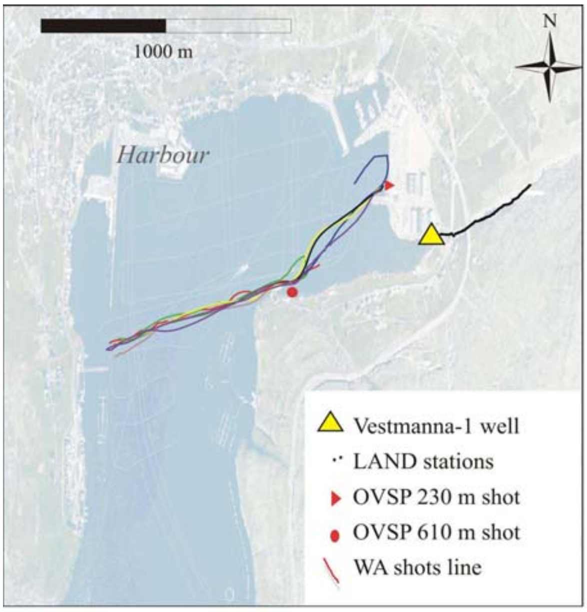

Figure 13. *Location map of the Vestmanna survey. Seismic data were acquired from a 3component sensor in the borehole and from a 120-channel 3-component Geometrics geophone array extending away from the borehole on basalt outcrops. We recorded a vertical seismic profile (VSP), six offset VSPs (OVSP) with borehole sensors at 50 m depth intervals, and six wide-angle (WA) profiles into the borehole receivers and the land array (LAND).*

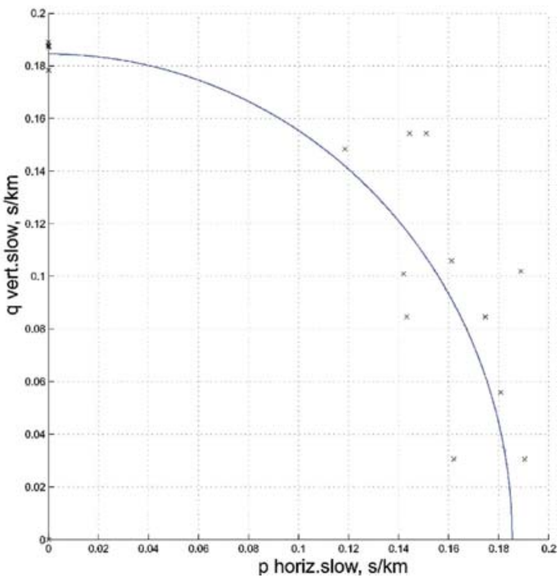

Figure 14. *Plot of vertical versus horizontal slowness. Phase slowness analysis shows a horizontal to vertical slowness ratio of 1.005. This indicates that anisotropy from the layered basalts is less than 0.5%, even smaller than the value of 1% derived by theoretical calculation from the layered structure.*

Using the phase-slowness method of Gaiser (1990) on the first arrivals on OVSP and WA data we find that the observed anisotropy from the layered basalts is less than 0.5%, even smaller than the value of 1% derived by theoretical calculation from the layered structure (Fig. 14).

The geometry of the borehole (WA, VSP, OVSP) plus land acquisition allows rays to be recorded over a wide range of illumination angles: the P wave velocity model calculated from the first arrivals by an isotropic ray tracing code shows average velocities of 5200–5800 m/s with an overall increase with depth. The observed travel-times from borehole and wide-angle P-wave data match well with those predicted from the borehole logging measurements.

Reflection profiles from our data show a strong and continuous intra-basalt reflector at 600 m depth (Fig. 15): This does not correlate exactly with the MBF-LBF boundary but is produced by a 30 m thick basalt flow ~40 m deeper. Synthetic seismogram modelling confirms that 10–30 m thick basalt layers of the LBF are capable of producing strong reflections from individual layers, whereas the thin (average < 2 m) layers of the MBF produce reflectivity from the interference effect of multiple thin layers, as reported by Smallwood *et al.* (1998) from the basalt sequence in eastern Iceland. This highlights the important result that strong and readily identified intra-basalt reflectors may not necessarily be caused by the main stratigraphic horizons or discontinuities, but rather are a seismic response to the particular sequence of layered basalts resulting from an interference pattern.

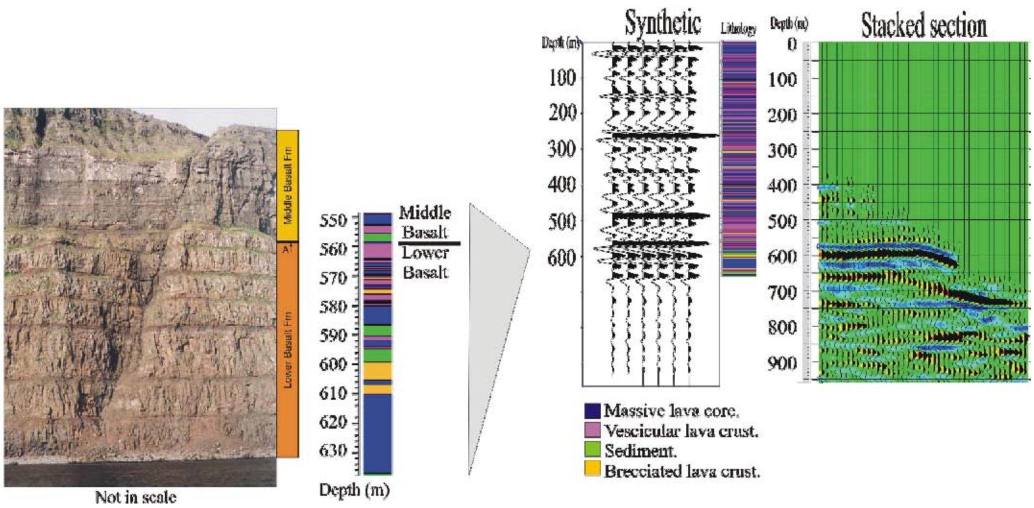

Figure 15. *Correlation between log and seismic stacked data: the strong reflection is immediately below the MBF-LBF boundary.*

References

Andersen, M.S., Worthington, M., Mohammed, N.G., White, R.S., Shaw F. & Petersen, U.K. 2004: Seismic experiments at Glyvursnes June-December 2003, Acquisition report, Contribution to the SeiFaBa project. Funded by the Sindri Group. Danmarks og Grønlands Geologiske Undersøgelse Rapport **2004/37**, 34 pp.

Andersen, M.S., Boldreel, L.O. & Hansen, H.K. 2005: Analysis of wireline logs through basaltic successions in nine wells from the Faroe-Shetland area. Danmarks og Grønlands Geologiske Undersøgelse Rapport Rapport **2005/3**, 170 pp.

Bais G., White R. S., Worthington M. H., Andersen M. S. & SeiFaBa Group 2006: The seismic response of Faroe basalts from integrated borehole and wide-angle seismic data, 68th Meeting European Association of Geoscientists and Engineers, Vienna, 5pp., expanded abstract A033, 4 pp.

Berryman, J.G., 1995: Mixture theories for rock properties, in: A Handbook of Physical Constants, Ahrens, T.J., ed., American Geophysical Union, Washington, 236 pp.

Boldreel, L.O. 2006. Wire-line log-based stratigraphy of flood basalts from the Lopra-1/1A. Geological Survey of Denmark and Greenland Bulletin **9**, 39–53.

Boldreel, L.O. & Andersen, M.S. & the SeiFaBa group 2006: Efffect of burial on in situ properties of flood basalt successions in the Faroe-Shetland Region. The Sindri Conference, Tórshavn, September 2006.

Christie, P., Gollifer, I. & Cowper, D. 2006: Borehole seismic studies of a volcanic succession from the Lopra-1/1A borehole in the Faroe Islands, N.E. Atlantic, Geological Survey of Denmark and Greenland Bulletin **9**, in press.

Gaiser, J.E. 1990: Transversely isotropic phase velocity analysis from slowness estimates, Journal of Geophysical Research **95**, 11241–11254.

Japsen, P. & Mavko, G. 2006: Rock physics analysis of sonic velocities in basalts from Faroes and Icelandic wells. Contribution to the SeiFaBa Project. Funded by the Sindri Group. Danmarks og Grønlands Geologiske Undersøgelse Rapport **2006/28**, 91 pp.

Japsen, P. & Waagstein, R. 2005: Preliminary analysis of ultrasonic and geochemical properties of core samples from Glyvursnes-1 and Vestmanna-1, Faroe Islands. Contribution to the SeiFaBa project. Funded by the Sindri Group. Danmarks og Grønlands Geologiske Undersøgelse Rapport **2005/19**, 39 pp.

Japsen, P., Andersen, C., Andersen, H.L., Andersen, M.S., Boldreel, L.O., Mavko, G., Mohammed, N.G., Pedersen, J.M., Petersen, U.K., Rasmussen, R., Shaw, F., Springer, N., Waagstein, R., White, R.S. & Worthington M. 2005: Preliminary results from investigations of seismic and petrophysical properties of Faroes basalts in the SeiFaBa project. In*:* Doré, A.G. & Vining, B.A. (eds): Petroleum Geology: North-West Europe and Global Perspectives: Proceedings of the 6th Petroleum Geology Conference. Geological Society, London, 1461-1470.

Olsen, D. 2005: Special Core Analysis for the SeiFaBa Project. Ultrasonic velocity measurements on plug samples from the Vestmanna-1 and Glyvursnes-1 wells, Faroe Islands. Danmarks og Grønlands Geologiske Undersøgelse Rapport Rapport **2005/10,** 65 pp (1 cd).

Olsen, D., Jørgensen, M. & Guvad, C. 2005: Special Core Analysis for the SeiFaBa Project. Ultrasonic velocity measurements on 12 plug samples from the Lopra-1, Vestmanna-1 and Glyvursnes-1 wells, Faroe Islands. Danmarks og Grønlands Geologiske Rapport **2005/76**, 32 pp, Appendix (1 cd).

Petersen, U.K., Andersen, M.S. & Andersen, H.L. 2003: Glyvursnes seismic experiment, summer 2002. Field report and preliminary data analysis. A Sindri progress report. University of the Faroe Islands, 24 pp, Appendix.

Petersen, U.K., Andersen, M.S., White, R.S., Worthington, M.H., Mohammed, N.G., Shaw, F., Normark, E. & Trinhammer, P. 2005: Preliminary processing of the seismic data acquired in the vicinity of wells Glyvursnes-1 and Vestmanna-1. Contribution to the SeiFaBa project. Funded by the SINDRI Group. University of the Faroe Islands, 36 pp (1 cd).

Petersen, U.K., Andersen, M.S., & White, R.S., 2006: Seismic imaging of basalts at Glyvursnes, Faroe-Islands – Hunting for future exploration methods in basalt covered areas. First Break **24**, 45–52.

Planke, S. 1994. Geophysical Response of Flood Basalts from Analysis of Wire Line Logs - Ocean Drilling Program Site-642, Voring Volcanic Margin. Journal of Geophysical Research-Solid Earth **99(B5)**, 9279–9296.

Planke, S., Alvestad, E., Eldholm, O. 1999. Seismic characteristics of basaltic extrusive and intrusive rocks. The Leading Edge **March**, 342–348.

Rasmussen, J., Noe-Nyggard, A. 1970. Geology of the Faeroe Islands. C. A. Reitzels Forlag, København.

Shaw, F., Worthington, M.H., White, R.S., Andersen, M.S. & Petersen, U.K. 2005: Seismic attenuation in Faroe Island basalts. EAGE 67th Conference & Exhibition — Madrid, Spain, 13–17 June 2004. 4 pp.

Shaw, F., Worthington, M.H., White, R.S., Andersen, M.S., Petersen, U.K. & the SeiFaBa Group 2006: Seismic attenuation in Faroe Islands basalts. Accepted for Geophysical Prospecting (pending minor revisions).

Smallwood, J.R., White, R.S. and Staples, R.K. 1998. Deep crustal reflectors under Reydarfjördur, eastern Iceland: Crustal accretion above the Iceland mantle plume. *Geo*physical J. Int. **134**, 277–290.

Waagstein, R. 1998: A geological field guide to the Palaeogene flood basalts of Suδeroy, Faroe Islands. Danmarks og Grønlands Geologiske Undersøgelse Rapport **1998/30**, 46 pp.

Waagstein, R. & Andersen, C. 2004: Well completion report: Glyvursnes-1 and Vestmanna-1, Faroe Islands. Contribution to the SeiFaBa project funded by the Sindri Group. Danmarks og Grønlands Geologiske Undersøgelse Rapport **2003/99**, 67 pp (1cd).

Waagstein, R. & Hald, N. 1984: Structure and petrography of a 660m lava sequence from the Vestmanna-1 drill hole, lower and middle basalt series, Faeroe Islands. In: Berthelsen, O., Noe-Nygaard, A. & Rasmussen, J. (eds) The Deep Drilling Project 1980–81 in the Faeroe Islands. Føroya Frodskaparfelag, Torshavn, 39–70.

List of publications

Papers

Japsen, P., Andersen, C., Andersen, H.L., Andersen, M.S., Boldreel, L.O., Mavko, G., Mohammed, N.G., Pedersen, J.M., Petersen, U.K., Rasmussen, R., Shaw, F., Springer, N., Waagstein, R., White, R.S. & Worthington M. 2005: Preliminary results from investigations of seismic and petrophysical properties of Faroes basalts in the SeiFaBa project. In*:* Doré, A.G. & Vining, B.A. (eds): Petroleum Geology: North-West Europe and Global Perspectives: Proceedings of the 6th Petroleum Geology Conference. Geological Society, London, 1461 - 1470.
File name: 2005_Japsen_etal_PGC_Seifaba.pdf

Japsen, P., Andersen, M.S., Boldreel, L.O., Waagstein, R., White, R.S. & Worthington, M. 2004: Seismic and petrophysical properties of Faroes basalts (SeiFaBa project). Geological Survey of Denmark and Greenland Bulletin **4**, 53-65.
File name: 2004_Japsen_etal_ROSA.pdf

Petersen, U.K. 2006: Propagation, decay, phase conversion and recording of seismic waves in the basalt succession at Glyvursnes, the Faroe Islands - Summary of thesis in preparation. In: Japsen, P. , Andersen, M.S., Boldreel, L.O., White, R.S., Waagstein, R., Worthington, M. & the SeiFaBa group. Seismic and petrophysical properties of Faroes basalts (the SeiFaBa project) Final Report. Funded by the Sindri group. Danmarks og Grønlands Geologiske Undersøgelse Rapport **2006/29**.
File name: 2006_Petersen_propagation.pdf

Petersen, U.K., Andersen, M.S., White, R.S. & the SeiFaBa Group 2006: Seismic imaging of basalts at Glyvursnes, Faroe Islands: hunting for future exploration methods in basalt covered areas. First Break **24**, March 2006. In: Japsen, P. , Andersen, M.S., Boldreel, L.O., White, R.S., Waagstein, R., Worthington, M. & the SeiFaBa group. Seismic and petrophysical properties of Faroes basalts (the SeiFaBa project) Final Report. Funded by the Sindri group. Danmarks og Grønlands Geologiske Undersøgelse Rapport **2006/29**.
File name: 2006_Petersen_First_Break24.pdf

Shaw, F. 2006: 1-D heterogeneity and statistical studies of the Faroes wireline logs. 10 pp, 5 tables, 13 figures. In: Japsen, P. , Andersen, M.S., Boldreel, L.O., White, R.S., Waagstein, R., Worthington, M. & the SeiFaBa group. Seismic and petrophysical properties of Faroes basalts (the SeiFaBa project) Final Report. Funded by the Sindri group.
File name: 2006:_Shaw_1D_heterogeneity.pdf

Shaw, F., Worthington, M.H., White, R.S., Andersen, M.S., Petersen, U.K. & the SeiFaBa Group 2006: Seismic attenuation in Faroe Islands basalts. Accepted for Geophysical Prospecting (pending minor revisions).
File name: 2006_Shaw_etal_Geoph_Prosp.pdf

Reports

Andersen, M.S., Boldreel, L.O. & Hansen, H.K. 2005: Analysis of wireline logs through basaltic successions in nine wells from the Faroe-Shetland area. Danmarks og Grønlands Geologiske Undersøgelse Rapport Rapport **2005/3**, 170 pp.
File name: 2005_03_Andersen_etal.pdf

Andersen, M.S., Worthington, M., Mohammed, N.G., White, R.S., Shaw F. & Petersen, U.K. 2004: Seismic experiments at Glyvursnes June-December 2003, Acquisition report, Contribution to the SeiFaBa project. Funded by the Sindri Group. Danmarks og Grønlands Geologiske Undersøgelse Rapport **2004/37**, 34 pp.
File name: 2004_37_Andersen_etal.pdf

Gommesen, L. 2005: SeiFaBa well log analysis, lithology and rock physics. Ødegaard A/S Report 04.26074.01, 23 pp.
File name: 2005_Gommesen_Ødegaard.pdf

Gommesen, L. & Ahmed M. 2005: SeiFaBa log analysis of Icelandic wells, Lithology and Rock Physics. Ødegaard A/S Report 03.24036.02, 29 pp.
File name: 2005_Gommesen_Ahmed_Ødegaard.pdf

Japsen, P. (ed.) 2005: Seismic and petrophysical properties of Faroes basalt. SeiFaBa Workshop September 29 2005. Contribution to the SeiFaBa project. Funded by the Sindri Group. Danmarks og Grønlands Geologiske Undersøgelse Rapport **2005/57**, 24 pp.
File name: 2005_57_Japsen_ed_Workshop.pdf

Japsen, P., Andersen, M.S., Boldreel, L.O., White, R.S., Waagstein, R., Worthington, M. & the SeiFaBa group 2006: Seismic and petrophysical properties of Faroes basalts (the SeiFaBa project) Final Report. Funded by the Sindri group. Danmarks og Grønlands Geologiske Undersøgelse Rapport **2006/29**.
File name: 2006_29_Japsen_etal.pdf

Japsen, P. & Mavko, G. 2006: Rock physics analysis of sonic velocities in basalts from Faroes and Icelandic wells. Contribution to the SeiFaBa Project. Funded by the Sindri Group. Danmarks og Grønlands Geologiske Undersøgelse Rapport **2006/28**, 91 pp.
File name: 2006_28_Japsen_Mavko.pdf

Japsen, P. & Waagstein, R. 2005: Preliminary analysis of ultrasonic and geochemical properties of core samples from Glyvursnes-1 and Vestmanna-1, Faroe Islands. Contribution to the SeiFaBa project. Funded by the Sindri Group. Danmarks og Grønlands Geologiske Undersøgelse Rapport **2005/19**. 39 pp.
File name: 2005_19_Japsen_Waagstein.pdf

Jørgensen, O. 2005: Zeolites and other secondary minerals in the drill core Glyvursnes-1, Faroe Islands. Contribution to the SeiFaBa project. Funded by the Sindri Group. 18 pp, 11 figs.
File name: 2005_Jørgensen_SAMA.pdf

Madsen, T. 2006. The Vágar Tunnel, Faroe Islands. Geological Profile. Result of field work 2002. Jardfeingi. 18 pp, 2 tables, 12 figures, 1 enclosure.
File name: 2006_Madsen_Jardfeingi_Vagar_Tunnel.pdf

Mavko, G. & Japsen, P. 2005: Rock physics analysis of sonic velocities in wells Lopra-1, Glyvursnes-1 and Vestmanna-1. Danmarks og Grønlands Geologiske Undersøgelse Rapport Rapport **2005/17**. 29 pp.
File name: 2005_17_Mavko_Japsen.pdf

Mavko, G., Japsen, P. & Boldreel, L.O. 2004: Preliminary rock physics analysis of basalts in the Lopra-1 well. Danmarks og Grønlands Geologiske Undersøgelse Rapport **2004/96**, 11 pp.
File name: 2004_96_Mavko_etal.pdf

Olsen, D. 2005: Special Core Analysis for the SeiFaBa Project. Ultrasonic velocity measurements on plug samples from the Vestmanna-1 and Glyvursnes-1 wells, Faroe Islands. Danmarks og Grønlands Geologiske Undersøgelse Rapport Rapport **2005/10,** 65 pp (1 cd).
File name: 2005_10_Olsen.pdf

Olsen, D., Jørgensen, M. & Guvad, C. 2005: Special Core Analysis for the SeiFaBa Project. Ultrasonic velocity measurements on 12 plug samples from the Lopra-1, Vestmanna-1 and Glyvursnes-1 wells, Faroe Islands. Danmarks og Grønlands Geologiske Rapport **2005/76**, 32 pp, Appendix A (1 cd).
File name: 2005_76_Olsen_etal.pdf

Passey, S.R. 2005: Geology of Glyvursnes, Streymoy, Faroe Islands. A Contribution to the SeiFaBa project. Funded by the Sindri Group. Jardfrødisavnid, 24 pp, 1 map.
File name: 2005_Passey_Jardfrødisavnid_report.pdf
File name: 2005_Passey_Jardfrødisavnid_map.pdf

Petersen, U.K., Andersen, M.S. & Andersen, H.L. 2003: Glyvursnes seismic experiment, summer 2002. Field report and preliminary data analysis. A Sindri progress report. University of the Faroe Islands, 24 pp, Appendix.
File name: 2003_Petersen_etal_2002_Field_Rep.pdf

Petersen, U.K., Andersen, M.S., White, R.S., Worthington, M.H., Mohammed, N.G., Shaw, F., Normark, E. & Trinhammer, P. 2005: Preliminary processing of the seismic data acquired in the vicinity of wells Glyvursnes-1 and Vestmanna-1. Contribution to the SeiFaBa project. Funded by the SINDRI Group. University of the Faroe Islands, 36 pp (1 cd).
File name: 2005_Petersen_etal_G1_V1.pdf

Waagstein, R. & Andersen, C. 2004: Well completion report: Glyvursnes-1 and Vestmanna-1, Faroe Islands. Contribution to the SeiFaBa project funded by the Sindri Group. Danmarks og Grønlands Geologiske Undersøgelse Rapport **2003/99**, 67 pp (1cd).
File name: 2003_99_Waagstein_Andersen.pdf

Abstracts

Andersen, M.S., Boldreel, L.O. & the SeiFaBa group 2006: Lithological analysis of wireline logs through flood basalts in 8 exploration wells in the Faroe-Shetland Region. The Sindri Conference, Tórshavn, September 2006.
File name: 2006_Andersen_Boldreel_Sindri_Torshavn_Log.pdf

Andersen, M.S., Boldreel, L.O. & the SeiFaBa group 2006: In situ properties to flood basalt successions in 8 exploration wells in the Faroe-Shetland Region. The Sindri Conference, Tórshavn, September 2006.
File name: 2006_Andersen_Boldreel_Sindri_Torshavn_InSitu.pdf

Bais, G., White, R.S., Worthington, M.H. & Andersen, M.S. Submitted to EAGE 2006: The seismic response of Faroe basalts from integrated borehole and wide-angle seismic data. EAGE 68th Conference & Exhibition – Vienna, Austria, 12-15 June 2006.
File name: 2006_Bais_etal_EAGE_Vienna.pdf

Bais, G., White, R.S., Worthington, M.H., Shaw, F., Andersen, M.S. & the SeiFaBa group 2006: Seismic velocities, anisotropy and attenuation of Faroe Islands basalts. The Sindri Conference, Tórshavn, September 2006.
File name: 2006_Bais_etal_Sindri_Torshavn.pdf

Boldreel, L.O. & Andersen, M.S. & the SeiFaBa group 2006: Efffect of burial on in situ properties of flood basalt successions in the Faroe-Shetland Region. The Sindri Conference, Tórshavn, September 2006.
File name: 2006_Boldreel_Andersen_Sindri_Torshavn.pdf

Japsen, P., Waagstein, R., Andersen, C., Andersen, M.S., Djurhuus, J., Mavko, G., Boldreel, L.O., Pedersen, J.M., Petersen, U.K., Rasmussen, R., Springer, N., White, R.S., Worthington, M. & Shaw, F. 2003: Sub-basalt imaging – new insight from investigations of petrophysical and seismic properties of Faroes basalts (SeiFaBa project). Petroleum Geology Conference, London, 1 p.
File name: 2003_Japsen_etal_Petr_Geol_Conf_London.pdf

Japsen, P., Waagstein, R., Andersen, C., Andersen, M.S., Djurhuus, J., Mavko, G., Boldreel, L.O., Pedersen, J.M., Petersen, U.K., Rasmussen, R., Springer, N., White, R.S., Worthington, M. & Shaw, F. 2004: Sub-basalt imaging – new insight from investigations of petrophysical and seismic properties of Faroes basalts (SeiFaBa project). Faroe Islands Exploration Conference, 1 p.
File name: 2004_Japsen_etal_FO_Expl_Conf.pdf

Japsen, P., Mavko, G., Waagstein, R., Olsen, D. & the SeiFaBa group 2006: Rock physics analysis of sonic velocities in basalts from Faroese and Icelandic wells. The Sindri Conference, Tórshavn, September 2006.
File name: 2006_Japsen_etal_Sindri_Torshavn.pdf

Mohammed, N.G., White, R.S., Worthington, M., Andersen, M.S., Shaw, F., Petersen, U.K. & SeiFaBa Group 2004: Seismic properties of Faroese basalts. Faroe Islands Exploration Conference, 1 p.
File name: 2004_Mohammed_etal_FO_Expl_Conf.pdf

Mohammed, N.G., White, R.S., Worthington, M., Andersen, M.S., Shaw, F. & Petersen, U.K. 2004: Seismic properties of Faroese basalts. Geophysical Research Abstracts **6**, 1p.
File name: 2004_Mohammed_etal_Geoph_Res_Abs_6.pdf

Petersen, U.K., Andersen, M.S., Worthington, M., White, R.S., Mohammed, N.G. & Shaw, F. 2004: A small reflection seismic experiment on Faroe Island during summer 2003, preliminary results. Faroe Islands Exploration Conference, 1p.
File name: 2004_Petersen_etal_FO_Expl_Conf.pdf

Petersen, U.K., Andersen, M.S., Worthington, M., White, R.S., Mohammed, N.G. & Shaw, F. 2005: A small reflection seismic experiment on Faroe Islands during summer 2003. EGU General Assembly, Vienna, April 2005, 1 p.
File name: 2005_Petersen_etal_EGU_Vienna.pdf

Shaw, F., Worthington, M., Andersen, M.S. & Petersen, U.K. 2004: A study of seismic attenuation in basalt using VSP data from a Faroe Islands borehole. EAGE Paris 2004, 4 pp.
File name: 2004_Shaw_etal_EAGE_Paris.pdf

Shaw, F., Worthington, M.H., White, R.S., Andersen, M.S. & Petersen, U.K. 2005: Seismic attenuation in Faroe Island basalts. EAGE 67th Conference & Exhibition — Madrid, Spain, 13 - 17 June 2004. 4 pp.
File name: 2005_Shaw_etal_EAGE_Madrid.pdf

Waagstein, R., Boldreel, L.O. & Andersen C. 2003: An integrated petrophysical approach to the sub-basalt imaging problem using well logging data to link measurements from cores and seismic surface experiments. Geophysical Research Abstracts **5**(09388), 2 pp.
File name: 2003_Waggstein_etal_Geoph_Res_Abs_5.pdf

Waagstein, R. & the SeiFaBa group 2006: Integration of wire-line log and core data from Glyvursnes-1 and Vestmanna-1, Faroe Islands. The Sindri Conference, Tórshavn, September 2006.
File name: 2006_Waagstein_etal_Sindri_Torshavn.pdf

Summaries of reports

Andersen, M.S., Boldreel, L.O. & Hansen, H.K. 2005: Analysis of wireline logs through basaltic successions in nine wells from the Faroe-Shetland area. Danmarks og Grønlands Geologiske Undersøgelse Rapport Rapport **2005/3**, 170 pp.

Andersen, M.S., Worthington, M., Mohammed, N.G., White, R.S., Shaw F. & Petersen, U.K. 2004: Seismic experiments at Glyvursnes June-December 2003, Acquisition report, Contribution to the SeiFaBa project. Funded by the Sindri Group. Danmarks og Grønlands Geologiske Undersøgelse Rapport **2004/37**, 34 pp.

Gommesen, L. 2005: SeiFaBa well log analysis, lithology and rock physics. Ødegaard A/S Report 04.26074.01, 23 pp.

Gommesen, L. & Ahmed M. 2005: SeiFaBa log analysis of Icelandic wells, Lithology and Rock Physics. Ødegaard A/S Report 03.24036.02, 29 pp.

Japsen, P. (ed.) 2005: Seismic and petrophysical properties of Faroes basalt. SeiFaBa Workshop September 29 2005. Contribution to the SeiFaBa project. Funded by the Sindri Group. Danmarks og Grønlands Geologiske Undersøgelse Rapport **2005/57**, 24 pp.

Japsen, P., Andersen, M.S., Boldreel, L.O., White, R.S., Waagstein, R., Worthington, M. & the SeiFaBa group 2006: Seismic and petrophysical properties of Faroes basalts (the SeiFaBa project) Final Report. Funded by the Sindri group. Danmarks og Grønlands Geologiske Undersøgelse Rapport **2006/29**.

Japsen, P. & Mavko, G. 2006: Rock physics analysis of sonic velocities in basalts from Faroes and Icelandic wells. Contribution to the SeiFaBa Project. Funded by the Sindri Group. Danmarks og Grønlands Geologiske Undersøgelse Rapport **2006/28**, 91 pp.

Japsen, P. & Waagstein, R. 2005: Preliminary analysis of ultrasonic and geochemical properties of core samples from Glyvursnes-1 and Vestmanna-1, Faroe Islands. Contribution to the SeiFaBa project. Funded by the Sindri Group. Danmarks og Grønlands Geologiske Undersøgelse Rapport **2005/19**. 39 pp.

Jørgensen, O. 2005: Zeolites and other secondary minerals in the drill core Glyvursnes-1, Faroe Islands. Contribution to the SeiFaBa project. Funded by the Sindri Group. 18 pp, 11 figs.

Madsen, T. 2006. The Vágar Tunnel, Faroe Islands. Geological Profile. Result of field work 2002. Jardfeingi. 18 pp, 2 tables, 12 figures, 1 enclosure.

Mavko, G. & Japsen, P. 2005: Rock physics analysis of sonic velocities in wells Lopra-1, Glyvursnes-1 and Vestmanna-1. Danmarks og Grønlands Geologiske Undersøgelse Rapport Rapport **2005/17**. 29 pp.

Mavko, G., Japsen, P. & Boldreel, L.O. 2004: Preliminary rock physics analysis of basalts in the Lopra-1 well. Danmarks og Grønlands Geologiske Undersøgelse Rapport **2004/96**, 11 pp.

Olsen, D. 2005: Special Core Analysis for the SeiFaBa Project. Ultrasonic velocity measurements on plug samples from the Vestmanna-1 and Glyvursnes-1 wells, Faroe Islands. Danmarks og Grønlands Geologiske Undersøgelse Rapport Rapport **2005/10,** 65 pp (1 cd).

Olsen, D., Jørgensen, M. & Guvad, C. 2005: Special Core Analysis for the SeiFaBa Project. Ultrasonic velocity measurements on 12 plug samples from the Lopra-1, Vestmanna-1 and Glyvursnes-1 wells, Faroe Islands. Danmarks og Grønlands Geologiske Rapport **2005/76**, 32 pp, Appendix A (1 cd).

Passey, S.R. 2005: Geology of Glyvursnes, Streymoy, Faroe Islands. A Contribution to the SeiFaBa project. Funded by the Sindri Group. Jardfrødisavnid, 24 pp, 1 map.

Petersen, U.K., Andersen, M.S. & Andersen, H.L. 2003: Glyvursnes seismic experiment, summer 2002. Field report and preliminary data analysis. A Sindri progress report. University of the Faroe Islands, 24 pp, Appendix.

Petersen, U.K., Andersen, M.S., White, R.S., Worthington, M.H., Mohammed, N.G., Shaw, F., Normark, E. & Trinhammer, P. 2005: Preliminary processing of the seismic data acquired in the vicinity of wells Glyvursnes-1 and Vestmanna-1. Contribution to the SeiFaBa project. Funded by the SINDRI Group. University of the Faroe Islands, 36 pp (1 cd).

Waagstein, R. & Andersen, C. 2004: Well completion report: Glyvursnes-1 and Vestmanna-1, Faroe Islands. Contribution to the SeiFaBa project funded by the Sindri Group. Danmarks og Grønlands Geologiske Undersøgelse Rapport **2003/99**, 67 pp (1cd).

Analysis of wireline logs through basaltic successions in nine wells from the Faroe-Shetland area

Andersen, M.S., Boldreel, L.O. & Hansen, H.K.
GEUS Rapport 2005/3

Summary. Wireline logs through basaltic successions in seven exploration wells and two research wells from the Faroe Shetland area have been investigated. The two research wells, the Vestmanna-01 and Glyvursnes-01, were fully cored and the wireline logs are in these wells correlated to core descriptions. Basaltic rocks are characterised by low concentrations of the most common radioactive isotopes, and basaltic successions are thus characterised by low natural gamma radiation compared to most other rock types. In the Faroe Shetland area natural gamma radiation may generally be used to distinguish between siliciclastic sediments and basaltic rock types. The basaltic successions can be divided into units of five different classes based on the overall response of neutron porosity (NPHI), bulk density (RHOB), seismic velocity (VP) and resistivity (e.g. MSFL). These classes are:

1. *Low frequency lava beds*, which are characterised by high amplitude asymmetric log response with a period exceeding 5 meters on all porosity related logs (NPHI, RHOB, VP and resistivity logs). Typical velocity range is ca. 2000-6000 m/s. Low frequency lava beds are frequently representing a single large lava flow of more than 5 meters thickness. The log responses are in these cases reflecting a vertical subdivision of the lava flow in an upper porous crust, a massive core and a thin lower porous crust. In the two cored wells a similar subdivision can be defined by visual inspections. However, significant discrepancies are seen between the subdivisions based on wireline logs and the subdivisions based on visual core inspection. Examples where a fairly complex succession defined by visual core inspection has a log response of a low frequency lava bed are present in Vestmanna-01 and Glyvursnes-01.
2. *High frequency lava beds* are characterised by log response with a period which generally are less than 5 meters on all porosity related logs. The amplitude of deflections on log traces are generally less than in low frequency lava beds. In the two cored wells it is seen that the low porosity intervals of high frequency lava bed units may correlate to individual thin flow units. However, the correlation is not perfect. Typical velocity range in a low frequency lava bed unit is ca. 2500-5500 m/s at ca. 1500 m depth.
3. *Volcaniclastic sediments*, which are generally characterised by higher porosity than found in both classes of lava beds. In addition slightly higher natural gamma radiation is frequently observed in volcaniclastic sediment units. Typical velocity range in a low frequency lava bed unit is ca. 2000-3000 m/s at ca. 1500 m depth.
4. *Foreset breccias* (lava deltas) are characterised by porosities that generally are higher than in volcaniclastic sediments and an amplitude of deflections that are less than in lava beds. Typical velocity range in a low frequency lava bed unit is ca. 3000-4500 m/s.
5. *Basaltic intrusives*, which are characterised by a symmetric high amplitude log response on the porosity related logs and low porosity. In shaley sediments the re-

sponse of natural gamma radiation is also symmetric and the intrusives are characterised by low natural gamma radiation. Typical velocities of basaltic intrusives are ca. 6000 m/s at ca. 3000 m depth.

The ranges of intrinsic values of parameters measured by the logging tools vary from well to well. This may to some extent reflect imperfect calibration of the logging tools as indicated by the large variation of the level of natural gamma radiation measured in the basaltic succession in the different wells (e.g. 3-10 GAPI in UK 154/03-01 and 22-56 GAPI in UK 205/09-01). However, the different ranges of intrinsic values of porosity related parameters measured in the different wells appear mainly to be related to burial/depth. Preliminary linear relation between seismic velocity and burial depth and between bulk density and burial depth for basaltic successions has been estimated using data from the seven exploration wells:

$$z = (\mathrm{VP}\text{-}2499\ \mathrm{m/s}) \cdot 1.06\ \mathrm{s} \quad \text{and}$$

$$z = (\mathrm{RHOB}\text{-}2159\ \mathrm{kg/m^3}) \cdot 5.23\ \mathrm{m^4/kg}.$$

Fractionation in shallow magma chambers may also produce depth related variation of seismic velocity and density, which may be approximated by linear relations. This should be taken into consideration when it is planned to use one of the two burial functions above or similar functions.

Seismic attenuation of seismic signals due to stratigraphic filtering in basaltic successions is modelled. The model responses indicate that attenuation due to stratigraphic filtering may reduce the seismic signal considerably at all frequencies. The Q-factor is generally above 40 indicating that frequency dependent attenuation observed in some seismic experiments (Q<40) is caused by other sources than stratigraphic filtering. In the deviated well (UK164/25-01 and 01z) subtle differences was found in the basalt succession over a short distance (30 m) indicating that continuity in basalt successions may play a role in this context. Statistical values for the properties of basaltic units and a data base containing a synopsis of data related to all picked units are compiled.

Seismic experiments at Glyvursnes June-December 2003. Acquisition report

Andersen, M.S., Worthington, M., Mohammed, N.G., White, R.S., Shaw F. & Petersen, U.K.
GEUS Rapport 2004/37

Summary. In 2003 Cambridge University, Oxford University and the University of the Faroe Islands acquired seismic data on and around Glyvursnes, the Faroe Islands. The data were acquired as part of a larger project addressing the petrophysic and seismic properties of Faroes basalts. The SeiFaBa Project, sponsered by the Sindri Group.
Data were acquired for four different experiments, which in combination with analysis of the logs from the and petrophysical analyses of plugs from the core from the Glyvursnes-1

borehole provide a unique dataset for detailed analysis of seismic wave propagation through the Faroese basalts at different scales. The data acquired are:

- VSP, offset VSP's and multilevel offset VSP's (June-July 2003)
- Surface seismic reflection data (September 2003)
- Wide-angle multi-channel seismic data for investigation of lateral anisotropy using both high resolution geophones and autonomous seismometers for the recording (September 2003)
- Broadband data for seismic tomography (June-December 2003)

This report covers the acquisition of seismic data at Glyvursnes in June-July and September 2003. The main report provides the crucial facts about the VSP experiments carried out in June-July 2003 and the high resolution surface seismic experiments carried out in September 2003. Details concerning recording with the autonomous seimometers (Guralp 6TD's) are provided in a separate report "Sindri: Petrophysical and seismic properties of Faroese basalts, 6TD Technical Field Report" included as an appendix to the main report. Detailed information needed for further work with the data are included in the digital appendixes to this report.

SeiFaBa well log analysis, lithology and rock physics

Gommesen, L.
Ødegaard A/S Report 04.26074.01, 2005

Summary. The objective of the study was to quality-control and analyse the well log suites from three Faroe Islands wells with focus on the elastic properties of the sub-surface basalt formations. This was done in order to obtain knowledge about the rock physics behaviour of the Faroe basalts. The study is based on the recalibrated density log for the Glyvursnes-1 and a Vestmanna-1 well, provided by GEUS in November 2005, and is thus an updated version of a previous Ødegaard report (04.26074.01). The three wells are Lopra-1, Glyvursnes-1, and Vestmanna-1. The study included several phases: 1) loading of data, 2) well log quality control of log data, 3) rock physics analysis, where the elastic properties, petrophysical properties and different lithological and geological units are studied through cross plots analysis. The Lopra-1 only represent Lower Basalt Fm, Glyvursnes-1 represents Middle and Upper Basalt Fms whereas Vestmanna-1 represents Lower and Middle Basalt Fms.

The well log analysis showed that: (1) The quality of the well log data is generally good: However, data that deviates from the general trends observed in Lopra-1 generally correlate to intervals of high rugosity (caliper minus bitsize). Noteworthy is also the strong VP-VS relationship of Glyvursnes-1 which may suggest that the shear velocity log have undergone too intense processing. (2) Flag curves, which flag out different lithologies, were established to ease lithology dependent cross plot analysis. The lithology interpretation was supplied by GEUS for all three wells and were grouped as: "Undefined", "Transition", "Sediments", "Top flows/Crust", "Top Breccia", "Massives/Core", "Dolorites", "Hyaloclastites".

The cross plot analysis showed that: (1) For each well we observe a relatively wide bulk density range (all formations). The compressional velocity is observed to increase with increasing bulk density. (2) Based all three wells and independent of geological formation the Dolorites and Massives/Core are observed to be elastically stiffer than Top Breccia, Top flows/Crust and Sediments and define the upper end member for both acoustic impedance and bulk density. The lower end member is not well defined and Top Breccia, Top flows/Crust and Sediments all show a variation in bulk density acoustic impedance. (3) For a study of both Massives/Core and Top flows/Crust data we observe that the Upper Basalt Fm. for a given bulk density has a significantly lower acoustic impedance relative to the Lower Basalt Fm. The Middle Basalt Fm. separates into two distinct data clouds, where one is following the Upper Basalt Fm. trend and the other follows the Lower Basalt trend. (4). Based all three wells and independent of geological formation the compressional velocity - shear velocity relationship is observed to be robust and independent of basalt class. (5). The Hyaloclastites (Lopra-1 only) follow the overall trends of the three wells. Here bulk density indicates a higher minimum porosity compared to Massives/Cores.

SeiFaBa log analysis of Icelandic wells, Lithology and Rock Physics

Gommesen, L. & Ahmed M.
Ødegaard A/S Report 03.24036.02, 2005.

Summary. The objective of the study was to quality-control and analyse the well log suites from three Icelandic wells with focus on the elastic properties of the sub-surface basalt formations. This was done in order to obtain knowledge about the rock physics behaviour of the Icelandic region and then compare it with the Faroe Islands Wells. The three Icelandic wells are HH-01, LA-10, and LL-03. Log data for these wells were acquired from Orkustofnun and Norsk Hydro and provided by GEUS as part of the SeiFaBa Project. The study included several phases: 1) loading of data, 2) well log quality control of log data, 3) rock physics analysis, where the elastic properties, petrophysical properties and different lithological and geological units are studied through cross plots analysis.

The well log analysis showed that the quality of the well log data is generally good: However, the data that deviates from the general trends is observed in HH-01 and LL-03. Noteworthy is also that there is no resistivity and neutron porosity data available for the three wells. Calliper log is also missing for LA-10. Flag curves, which flag out different lithologies, were established to ease lithology dependent cross plot analysis. The lithology interpretation was supplied by GEUS for all three wells and were grouped as: classes of “Basalts”, classes of “Sediments”, “Tuff”, and “Dolerites”.

The cross plot analysis showed that: 1. For each well we observe a relatively wide bulk density range (all formations). The compressional velocity is observed to increase with increasing bulk density. 2. Based on the three wells and independent of geological formation the dolorites are observed to be elastically stiffer than basalts and Sediments and define the upper end member for both acoustic impedance and bulk density. The lower end member is not well defined as the basalts and sediments all show a variation in bulk density acoustic impedance. 3. Based on the three wells and independent of geological formation

the compressional velocity - shear velocity relationship is observed to be robust and independent of basalt class.

Seismic and petrophysical properties of Faroes basalt. SeiFaBa Workshop September 29 2005

Japsen, P. (ed.)
GEUS Rapport 2005/57

List of abstracts included:

Apparent burial functions of some physical properties in basaltic successions from the Faroe-Shetland region (Morten S. Andersen and Lars Ole Boldreel)

Velocity analysis from VSP and surface data at Vestmanna site (Giovanni Bais, Robert S. White, Michael H. Worthington, Morten Sparre Andersen and Felicia Shaw)

Petrophysical characterisation of basaltic rocks from nine wells from the Faroe-Shetland region (Lars Ole Boldreel and Morten Sparre Andersen)

A comparison between log data from Faroes and Icelandic basalts (Peter Japsen and Lars Gommesen)

New field observations regarding the transitional zone between the middle and upper basalt series around the Faroe Islands (Simon R. Passey)

Characterisation of basalt formation applying time variant frequency analysis (Uni P. Petersen, Morten Sparre Andersen, Robert S. White, Michael H. Worthington and Felicia Shaw)

Heterogeneity and Seismic Properties of Faroe Islands Basalts (Felicia M. J. Shaw)

Comparison of wire-line log and core data from the flood basalt succession of the Faroe Islands (Regin Waagstein and Peter Japsen)

Rock physics analysis of sonic velocities in basalts from Faroes and Icelandic wells

Japsen, P. & Mavko, G.
GEUS Rapport 2006/28

Summary. We have analysed the acoustic properties of basalts based on sonic log data from three Faroese and three Icelandic boreholes and ultrasonic laboratory measurements on 43 1.5” core samples from the three Faroese boreholes. The Faroese boreholes are Lopra-1/1A (LP-1), Vestmanna-1 (VM-1) and Glyvursnes-1 (GL-1) that penetrate the Palaeogene basalts of the Lower, Middle and Upper Basalt Formations (UBF, MBF and LBF) and these rocks are mainly subaerial flood basalts apart from hyaloclastites below c.

2.5 km depth in the LP-1 well. The Icelandic wells penetrate volcanic rocks of Plio-Pleistocene age and cover a mixed environment: HH-1 (95% hyaloclastites), LA-10 (45% submarine and 45% subaerial basalts) and LL-3 (95% subaerial basalts).

We find a tight correlation between sonic Vp and He-porosity based on core data irrespective of basalt facies and well (only data for sediment samples deviate). The core data also reveal a well-defined relation between Vp and Vs, which is to be expected from rocks of broadly similar composition. However, there is a significant scatter in plots of Vp versus density and this scatter is related to the range of grain (matrix) densities from 2.7 to 3.1 g/ccm. Low grain densities represent altered samples with high content of light minerals such as zeolite and clay.

Two main Vp-density trends can be distinguished for flood basalts based on the log data: (1) a trend of relatively low Vp compared to density (the UBF in the GL-1 well; the flood basalts in the LL-3 well), and (2) a trend of relatively high Vp compared to density (the LBF in the LP-1 well). The properties of the MBF are transitional between the two trends. The GL-1 data from this interval represents both the high and the low trend, whereas the VM-1 data represent a very high trend. However, towards the base of VM-1, we observe a 'reversal' of the Vp-density trend within the thin sequence of the LBF penetrated by the well. The analysis of the Vp-density relation for the core data shows that the outlying samples towards low densities are characterized by low grain density. Hence the relatively high Vp-density trend defined for the log data in these wells for the MBF also must be characterized by low grain densities. This means that the low Vp-density trend represents basalt with unaltered matrix with high grain density and the high trend represents altered basalt with a low grain density.

The transition from the low Vp-density trend of fresh basalts to the high trend of altered basalts within the MBF occurs concurrently with an increase of the sonic velocity and density with depth even though there is no increase in the flow thickness. This shows that the transition from fresh to altered basalt is accompanied by an increase in velocity and density and thus probably also by net influx of mass leading to higher densities (growth of zeolites). This means that data points along a high Vp-density trend represents samples with relatively high velocity compared to density, because filling of the pore space with zeolites and clay increases velocity and only changes density of low-porosity basalts slightly.

Maximum values of velocity and density of Icelandic flood basalts are generally higher than for the unaltered Faroese basalts of the UBF, but the two data sets follow the same velocity-density trend. These observations suggest that the smallest porosities are reached in the Icelandic basalts where the flow units are the thicker and that elastic moduli and density of the basalt matrix must be almost identical for these basalts of very different age.

Matrix (or grain) density for the core samples varies systematically with bulk density and alteration of the rocks. A grain density of 3.05 g/ccm is taken as a fair approximation for unaltered basalt with the higher values (almost 3.1 g/ccm) interpreted as outliers related to anomalous content of heavy minerals and lower values (minimum 2.7 g/ccm) corresponding to more altered rock. For sediments in Faroese wells we assign the mean sample value of 2.8 g/ccm. Measurements on fresh Icelandic basalt lava indicate that 3.05 g/ccm is a reasonable pick (Omar Sigurdsson pers. comm.), and we also apply that value for volcanic sediments in Icelandic wells. Dolerites in Lopra-1 have smaller densities than for the surrounding basalt and we assign a matrix density of 3.02 g/ccm for these rocks. We convert log density to porosity based on these values for the matrix density for different lithologies and a pore water density of 1 g/ccm.

We estimate the mineral end-point properties of flood basalt with zero porosity by comparing log data from the Lopra-1 well with the self-consistent formulation of Berryman (1995) where the models represents the pore space as a collection of ellipsoidal inclusions. We find that the following matrix properties yield consistent values of aspect ratios based on both Vp and Vs data: bulk modulus, K = 83.4 GPa; shear modulus, G = 40.1 GPa and grain density, ρ = 3.05 g/ccm. Comparison of the inclusion model with the log data for Faroese and Icelandic wells reveals good agreement between the mineral end-point and the data points with porosities close to zero and that the predicted aspect ratios are similar for both Vp and Vs. However, the Glyvursnes-1 data appear to be biased towards relatively high values of Vs.

A modified upper and lower Hashin-Shtrikman model has been estimated to model the velocity-porosity relation for basalt. The model describes how the dry bulk and shear moduli, K and G increase as porosity is reduced along either a lower or an upper bound from a maximum value, ϕmax, to mineral end-point properties at zero porosity. We have tested a model with the following properties at the maximum porosity of 45%: K = 5.55 GPa, G = 3.2 GPa and the above properties at zero porosity. We find that most data points for all wells fall within the upper and lower bounds defined by this model. There is however, a considerable ambiguity in the relation between velocity and porosity as estimated from bulk density due to the wide range of grain densities. Sonic velocity is thus a proxy for the porosity of basalt and a median model defined by the mean of the upper and lower bounds may thus provide reasonable estimates of basalt porosity from sonic data.

Preliminary analysis of ultrasonic and geochemical properties of core samples from Glyvursnes-1 and Vestmanna-1, Faroe Islands

Japsen, P. & Waagstein, R.
Rapport 2005/19

Summary. The relations between physical properties, petrography and chemical composition of core samples from the Glyvursnes and Vestmanna wells have been studied. The acoustic properties of the 28 water saturated core samples were analysed at the highest confining pressure available for all samples, 300 bar. The data reveal a general trend of increasing velocity, both P and S, as porosity is reduced and only one data point deviate from the trend. Porosity ranges from almost 0% to c. 33%, Vp range from 2.8 to 6.6 km/s and Vs from 1.4 to 3.7 km/s. Vp-Vs ratios are typical around 1.8 to 1.85, but two sediment samples have Vp/Vs around 2 and one core sample has a very deviating value, also at 2. The data for samples of lava core, crust and breccia and sediment follow the same velocity-porosity trend, but two high-porosity sediment samples have significantly higher Vp-Vs ratio

than the lava samples. There is no systematic difference between the velocity-porosity and Vp-Vs relations Glyvursnes and Vestmanna samples.

We compare the core data with a modified upper Hashin-Shtrikman bound (MUHS) that describes the properties of the water-saturated rock as porosity varies between 0% and the critical porosity (the total porosity at the point when the rock would fall apart). We obtain a first-order fit with the core data and the MUHS bound by assuming a critical porosity of 30% and the following mineral properties: bulk modulus, K = 85 GPa; shear modulus, G = 42 GPa and matrix density, ρ = 3.07 g/ccm.

The log measurements in the Glyvursnes-1 and the Vestmanna-1 wells have been estimated at the same depths as where the core samples were taken: density, neutron porosity, Vp and Vs. The comparison of core and log density shows a good correlation, but for high core densities all core plugs have significantly higher densities than the log readings. The comparison of core porosity and the neutron porosity log shows that the neutron porosity overestimates porosity significantly (mean difference -8%). The comparison of Vp and Vs for core and log data shows a very good correlation. There is no difference in the correlation between the core and log data between Glyvursnes and Vestmanna.

Sixty core samples from the Glyvursnes-1 well have been chemically analysed and examined in thin section. The sediments are all tuffs, that is altered volcanic ash. Most basalts are glomerophyric. The glomerocrystic aggregates consist mainly of phenocrysts of plagioclase. However, they are often intergrown with phenocrysts of olivine and sometimes also with small phenocrysts of pyroxene.

The fine groundmass of the basalts consists mainly of plagioclase and pyroxene, but contains small amounts of Fe-Ti-oxides and usually also some olivine. The groundmass contains variable amounts of mesostasis, which consists of clay, zeolites or other secondary minerals replacing interstitial glass or filling interstitial voids. The olivine in the basalts is completely replaced by clay or other secondary minerals in all but two samples. The plagioclase is generally fresh although often showing incipient alteration. The pyroxene is almost always completely unaltered. The basalts contain variable amounts of gas vesicles or tiny pores. The vesicles or pores are usually partly or completely filled with secondary minerals, mostly clay or zeolites. The gas porosity measurements are generally considerably higher than those estimated from thin sections. This suggests that many pores are thinner than the thickness of the thin section (c. 0.03 mm). The basalts are quartz tholeiites and olivine tholeiites.

Grain density is positively correlated with the content of total iron, which is residing mainly in Fe-Ti-oxides, pyroxene and olivine in fresh basalts. The grain density is systematically lower in lava crust than in lava core for the same iron content and this suggests that a larger part of the iron is residing in clay in the lava crust than in lava core and is in keeping with the higher degree of alteration of lava crusts.

Grain density is inversely correlated with Loss on Ignition (LoI) for all rock types and approaches a minimum density of 2.7 g/cm^3 at a maximum Loss on Ignition of 8 Wt.%. LoI is primarily a measure of the water released when the sample is heated to about 1000ºC. The rocks with the highest loss are the most altered ones and consist dominantly of water-bearing secondary minerals as smectite clay and various zeolites.

There is a high correlation between neutron porosity (log-value estimated at the depth of the core) minus He-porosity (core) and the volume of water bound in secondary minerals. Neutron porosity measures the amount of hydrogen whether present in pore water or bounded in crystals and it is on average about 8 % too high as compared to gas porosities. The difference between neutron and He-porosity is thus a measure of mineral bound water. When neutron porosity is corrected for fixed water the correlation between Vp and porosity measured by wire-line logging is very similar to that measured on plugs in the laboratory.

There is a good correlation between K_2O content and natural gamma-ray response (log), and the potassium content increases more rapidly than the gamma-ray intensity. This shows that the relative contribution from Th and U is lower in the high-K than in the low-K rocks and suggests that the potassium in the former rocks has been increased by secondary alteration processes. Potassium is known to be highly mobile during such processes, while Th is considered relatively immobile.

Zeolites and other secondary minerals in the drill core Glyvursnes-1, Faroe Islands

Jørgensen, O.
Scandinavian Asbetos & Mineral Analysis (SAMA) Report 2005

Summary. The report describes the zeolites and other secondary minerals deposited in veins and vesicles of the core from the borehole Glyvursnes-1, Faroe Islands. The zeolite assemblages have been used to estimate that the mineralization of the basalt took place at temperatures between 50 and 100° C, corresponding to temperatures of the mesolite zone. The palaeothermal gradient is estimated to have been 46 ± 16°C/km and a linear extrapolation of the gradient places the palaeosurface of the Upper Basalt Formation at an altitude of 1430 ± 767 m above present-day sea level. The degree of mineralization of the vesicles in the basalt varies from nearly empty to completely mineralized and a continuous transition has been found between these two end points. All types of mineralized vesicles (amygdales) exist side by side within the basalt. The degree of mineralization has been classified into the three classes of empty, partially- and completely-filled vesicles. The amount of filling shows no consistent variation with depth, so the degree of mineralization must reflect local variations in the permeability of the rock or in the flow of hydrothermal solutions through the basalt. Two different types of amygdales are found in the drill core. Most frequent are one-chamber amygdales with an onion-like texture of concentric mineral layers. Less frequent are two chamber amygdales divided into an upper and a lower chamber by a horizontal floor that are filled by different minerals. Analysis of the physical conditions for formation of amygdales shows that the two-chamber amygdales are formed when the hydrostatic pressure of the mineral forming solutions was low compared to the internal gas pressure within the vesicle.The existence of two-chamber amygdales shows that the mineralization of the vesicles started when the lava was solidified, the temperature was below

the critical temperature of water (374°C) and a system of hydrothermal water streams had been established.

The Vágar Tunnel, Faroe Islands. Geological profile. Result of field work 2002

Madsen, T.
Jardfeingi Report 2006

The result of field work in the Vágar Tunnel performed immediately after the tunnel was drilled through is presented. A geological profile along the tunnel track is constructed based on this field work, geological logging by the engineering company Landsbyggifelagið and reports produced in connection with the Vágar Tunnel Project. The Vágar Tunnel drilled through the central part of the middle basalt series. The basalts show all characteristics of compound lava flows. The compound lava flows are sometimes separated by thin (10-20 cm) volcaniclastic sediments. 20 fracture zones were identified in the tunnel. Surprisingly the density of fracture zones is lower in the fiord section compared to the onshore sections. There does not seem to be a clear correlation between fracture zones and 'low velocity zones' defined from refraction seismics.

Rock physics analysis of sonic velocities in wells Lopra-1, Glyvursnes-1 and Vestmanna-1

Mavko, G. & Japsen, P.
GEUS Rapport **2005/17**

Summary. We have examined the sonic behaviour of basalts as estimated from log data from wells Lopra-1, Glyvursnes-1, and Vestmanna-1. In general we observe that the sediment facies have the highest gamma ray and the lowest velocities, while the basalt facies have the highest velocities. Data from Lopra-1 and Vestmanna-1 have similar velocities and Vp/Vs ratios, while Glyvursnes-1 indicates smaller Vp/Vs ratios. Comparison of the sonic data and porosity estimated from the neutron porosity log with rock physics ellipsoidal inclusion models suggests that there are slight mineralogical difference among the three wells, indicated by different mineral elastic moduli required for model consistency. It is not obvious how the introduction of quartz, calcite, clay, or zeolites can account for these differences in average mineral moduli. In the future analysis of the data, a correction of the neutron porosity values should be attempted to give a better estimate of the true porosity. Well Lopra-1 showed little correlation of velocity or pore stiffness with depth, though wells Glyvursnes-1 and Vestmanna-1 show a fairly systematic stiffening of the pore space with depth although Vestmanna-1 shows an abrupt change in the lower 100 m of the well.

Preliminary rock physics analysis of basalts in the Lopra-1 well

Mavko, G., Japsen, P. & Boldreel, L.O.
GEUS Rapport 2004/96

Summary. A preliminary investigation of the rock physics properties of flood basalt on the Faroes has been carried out based on the extensive logging data from the Lopra-1/1A well. Data from the extensive logging program have been used to establish a detailed stratigraphy for the flood basalt sequence between 200 m and 2500 m by dividing the lava flows into massive and porous parts. In addition several intervals with >1% potassium were mapped at the flow boundaries and interpreted as altered basalt or tuffaceous sediments. Two dolerite dikes intruding the basalt column were identified by having the highest values of density, P- and S-velocities and lowest values of the neutron porosity.

The high-density limit of the density log is nearly constant with depth, while the low density values are wildly fluctuating. We believe that the high bulk densities are asymptotically approaching the mineral density as the porosity approaches zero, while the low density values vary with porosity. The P-wave velocities have wide fluctuations between about 3000 m/s and 7000 m/s, though there are systematic differences among the various facies. The sediments have the lowest velocities; the topflows have slightly higher velocities; the massive basalts are higher still; and the dolerites have the highest velocities. Empirical upper bounds on density and velocity are taken as estimates of the mineral properties. The velocities and densities should asymptotically approach values appropriate for the minerals, as the porosity approaches zero.

We superimpose effective medium models for velocity vs. neutron porosity, computed using Berryman's (1980) formulation of the self-consistent approximation. For each of the four curves, the pores are assumed to take the shape of oblate spheroids, having aspect ratios 1, 0.3, 0.1, and 0.03, respectively. The mineral is assumed to have properties similar to pyroxene and the pores are assumed to be filled with water. The overall trends of the various lithological facies in the Lopra-1 well can be represented with pores that are nearly spherical (aspect ratio 1) or slightly flattened (0.3), as one might expect for vesicular basalts. Those data that fall at velocities significantly below these trends are consistent with the occurrence of micro or macro fractures, which can be represented with very low aspect ratios.

Crossplots of Vp vs. Vs for the four facies of the Lopra-1 well show that Vp and Vs are highly correlated. All facies have a nearly constant Poisson's ratio of 0.3. High-velocity points can be interpreted as approaching the mineral values, while porosity increases along the trend to the lower left. Empirical upper bounds on P- and S-wave velocities are taken as estimates of the mineral properties.

The preliminary analysis of log data from the flood basalts in the Lopra-1 well presented here suggests that the acoustic properties of these basalt flows are mainly controlled by

porosity and the high correlation between P- and S-velocities may be indicative of a constant mineralogical composition for the Lower Basalt Formation.

Special Core Analysis for the SeiFaBa Project. Ultrasonic velocity measurements on plug samples from the Vestmanna-1 and Glyvursnes-1 wells, Faroe Islands

Olsen, D.
Rapport 2005/10

Summary. GEUS Core Laboratory has carried out ultrasonic velocity measurements on a total of 31 plug samples from the Faroe Islands. 12 of the samples come from the Vestmanna-1 well and 19 from the Glyvursnes-1 well. 19 of the samples are classified as lava core, 6 as lava crust, 1 as lava breccia, and 5 as sediment. The porosity ranges from 0.8 to 34.0% for the lava samples and from 24.1 to 33.5% for the sediment samples. Permeability ranges from 0.003 to 5.8 mD for the lava samples and from 0.06 to 10.2 mD for the sediment samples.

For all samples the P- and S-wave velocities were measured at three different stress conditions, i.e. at hydrostatic confining pressures 100 bar, 200 bar and 300 bar. In addition, two of the samples from Vestmanna-1 were measured at a confining pressure of 500 bar. The measurement at the highest pressure step was repeated after 15 hours as an equilibrium check. All samples were measured in a water-saturated state. The Glyversnes-1 samples and two of the Vestmanna-1 samples were also measured in a gas saturated state.

For measurements in the water-saturated state, estimates of pore volume compression and length reduction were obtained by quantification of the amount of water expelled during sample loading.

Ultrasonic measurements were conducted with a centre frequency of 700 kHz at a temperature of 23°C.

The precision of the ultrasonic velocity determinations are considered to be 1% (1 σ level) for a large majority of the samples. This is based on control measurements on a velocity standard and uncertainty evaluation of the ultrasonic signals. For 5% of the measurements, however, the signal evaluation indicates that the precision is between 1 and 3%.

Well-defined negative correlations are present for V_P vs. porosity and V_S vs. porosity for both water-saturated and gas-saturated samples. Similarly, well-defined positive correlations are present for V_P vs. V_S for both water-saturated and gas-saturated samples. A weak positive correlation is present for V_P/V_S ratio vs. porosity for samples in water-saturated state, while a weak negative correlation is present for samples in gas-saturated state. V_P for water-saturated samples vs. V_P for gas-saturated samples shows a well-defined positive correlation shifted towards higher velocities for water-saturated samples. Similarly, V_S for water-saturated samples vs. V_S for gas-saturated samples shows a well-defined positive correlation but now clustered tightly around a 1:1 correlation, i.e. the saturation state of the samples has little effect on the S-velocity. In several of the correlations sample V10 behaves as an outlier, though the cause of this behaviour is not known.

The mean porosity reduction from 0 bar to 300 bar hydrostatic stress is 0.4 percent unit (p.u.) ranging from 0.03 p.u. for low-porosity lava samples to 2.5 p.u. for high-porosity sediment. Positive correlations of ultrasonic velocity with hydrostatic stress are present for most of the samples.

Special Core Analysis for the SeiFaBa Project. Ultrasonic velocity measurements on 12 plug samples from the Lopra-1, Vestmanna-1 and Glyvursnes-1 wells, Faroe Islands

Olsen, D., Jørgensen, M. & Guvad, C.
Rapport 2005/76

Summary. GEUS Core Laboratory has carried out ultrasonic velocity measurements on a total of 12 plug samples from the Faroe Islands. 5 of the samples come from the Lopra-1 well, 1 comes from the Vestmanna-1 well and 6 come from the Glyvursnes-1 well. 8 of the samples are classified as massive lava, 3 as vuggy lava, and 1 as tuff. The porosity ranges from 0.9 to 16.1% for the lava samples. The tuff sample has a porosity of 34.4%. Permeability ranges from 0.005 to 2.8 mD for the lava samples. The tuff sample has a permeability of 17.4 mD.

The present study is a supplement to the study reported in Danmarks og Grønlands Geologiske Undersøgelse Rapport 2005/76 and identical analytical procedures were used.

For all samples, the P- and S-wave velocities were measured at three different stress conditions, i.e. at hydrostatic confining pressures 100 bar, 200 bar and 300 bar. The measurement at 300 bar was repeated after 15 hours as an equilibrium check. All samples were measured in a water-saturated state. Four of the Lopra-1 samples were also measured in a gas-saturated state.

Ultrasonic measurements were conducted with a centre frequency of 700 kHz at a temperature of 23°C. For measurements in the water-saturated state, estimates of pore volume compression and length reduction were obtained by quantification of the amount of water expelled during sample loading.

The precision of the ultrasonic velocity determinations on the lava samples is considered to be better than 1% (1 σ level). This is based on control measurements on a velocity standard and uncertainty evaluation of the ultrasonic signals. For the tuff sample the uncertainty evaluation of the ultrasonic signals indicate an inferior precision between 1 and 3%.

Well-defined negative correlations are present for V_P vs. porosity and V_S vs. porosity for water-saturated. For the gas-saturated samples the porosity range is only 1.2% but a negative correlation is present. Similarly, positive correlations are present for V_P vs. V_S for both water-saturated and gas-saturated samples. Disregarding the tuff sample, the V_P/V_S ratio vs. porosity relationship does not show any clear correlation for neither the water-saturated sample nor the gas-saturated samples. V_P for water-saturated samples vs. V_P for gas-saturated samples shows a distinct shift towards higher velocities for water-saturated samples. Similarly, V_S for water-saturated samples vs. V_S for gas-saturated samples shows a shift towards higher velocities for the water-saturated samples, though the effect is less than for V_P.

The mean porosity reduction for the lava samples when increasing the hydrostatic stress from 0 to 300 bar is 0.2 percent unit (p.u.) with a range from 0.02 to 0.8 p.u. The tuff sample shows a large porosity reduction of 4.2 p.u. Positive correlations of ultrasonic velocity with hydrostatic stress are present for most of the samples.

Geology of Glyvursnes, Streymoy, Faroe Islands

Passey, S.R.
Jardfrødisavnid 2005

Summary. A geological map of the Glyvursnes area has been compiled in scale 1 : 10 000. Furthermore, a generalized stratigraphic column and a cross section showing the general relations of rocks along a WSW-ENE trending line across the area has been produced. Within the Glyvursnes area six lineaments have been identified from orthophotographs and from mapping in the field. The lineaments are characterised by being extremely straight and are commonly constrained to streams that transect the area. Only the Glyvursgil lineament is exposed where it meets the sea. Here it can be seen that there is little or no movement along the lineament and that it has not been subsequently infilled with a basaltic dyke.

Glyvursnes seismic experiment, summer 2002. Field report and preliminary data analysis

Petersen, U.K., Andersen, M.S. & Andersen, H.L.
University of the Faroe Islands 2003

Summary. In June 2002, a small experiment was carried out by University of Faeroe Islands and Aarhus University (Petersen et al. 2003). This experiment was mainly aimed at obtaining sufficient data to investigate problems related to acquisition of near-vertical incidence and wide-angle seismic data in the Glyvursnes area. Four different data sets were acquired.

- A 500 m long profile with 5 m geophone interval and 10 m shot interval using a 10 g dynamite source placed in 1.8 m deep holes.
- Two wide-angle seismic profiles with maximum offsets around 1400 m with a 375 m geophone string (5-m geophone interval) using a 130 cu. inches Halliburton slevegun cluster.
- A wide-angle seismic profile perpendicular to geophone string using the slevegun energy source.

During acquisition of all three data sets, an external radio source induced a high frequency signal of unacceptable amplitude. The radio source was identified as 500 MHz ground waves originating from the Loran-C transmitter at Eide. These waves occurred in a notch on the analog antialias filters on the Geometrix acquisition system. The further analysis of the data was severely hampered by this noise source.

During the near-vertical incidence experiment most coherent energy in both shot and receiver gathers was related to the direct arrivals and reverberations of direct arrivals. Refractions through the basalt were also evident. However, due to the low signal/noise ratio caused by the noise from the Loran-C transmitter at Eide, the near-vertical incidence data were not of sufficient quality to study reflections from the basalts. A larger source and removal of the radio noise was deemed necessary to provide data suitable for the study of reflections from the basalts below Glyvursnes.

The slevegun data recorded a good, repeatable signal with significant penetration, and it was considered suitable as the source for a P-wave azimuthal VSP-survey in Glyvursnes. However, a larger energy source was considered preferable. New antialias filters were designed in consultation with Geometrix and tested in the field during the winter 2002-2003. The new filters performed as expected and removed the Loran-C noise to a level below detection.

Preliminary processing of the seismic data acquired in the vicinity of wells Glyvursnes-1 and Vestmanna-1

Petersen, U.K., Andersen, M.S., White, R.S., Worthington, M.H., Mohammed, N.G., Shaw, F., Normark, E. & Trinhammer, P.
University of the Faroe Islands 2005

Summary. Following the drilling of well Glyvursnes-1, an array of 45 Guralp (6TD) seismometers, various lines of geophones and a hydrophone streamer were deployed within the immediate vicinity of the well. A large number of air-gun shots at sea and dynamite shots on land were fired. 2-D and 3-D reflection seismic images were obtained from these data. In addition, a VSP and two offset VSP surveys were carried out, using a three component clamped downhole geophone. Up-going wavefields have been extracted from the vertical VSP data. Earthquake data have been acquired with the Guralp array over a six month period from June to December 2003.

A geophone receiver line and a line of Guralp seismometers were also deployed within the vicinity of the Vestmanna-1 well. Air-gun shots were fired in a stream and from a small vessel in a nearby harbour. Walkaway and azimuthal surveys were carried out with a downhole geophone fixed at 100, 200, 300, 400 and 500 metres depth. In addition, one zero offset and two offset VSP surveys were performed. A boomer survey was carried out in the harbour to obtain accurate information on the nature and thickness of the sediments. Preliminary processing of these data includes the extraction of the up-going wavefield from the vertical VSP data.

All these data have been sorted, edited, documented and safely archived in the Universities of The Faroe Islands, Cambridge, Oxford and Aarhus. The analysis and interpretation of these processed data will be described in the final project report.

Well completion report: Glyvursnes-1 and Vestmanna-1, Faroe Islands

Regin Waagstein (GEUS) and Claus Andersen (JFS)
Rapport 2003/99

Summary. A new 700 m deep scientific well (*Glyvursnes-1)* with continuous coring was successfully drilled autumn 2002 near Tórshavn through the Upper and Middle Basalt Formation boundary and the existing *Vestmanna-1* well was reamed prior to running an extensive logging programme.

The Glyvursnes-1 well, located on the headland 2 km southeast of Tórshavn with the top of the surface casing at 16.56 m above sea level, was drilled by the Finnish drilling contractor SMOY. The drilling method was diamond core drilling with fresh water flushing. The 51.5 mm diameter core was partly described visually on-site and later fully using a set of high quality digital core photos. The observed structural and petrographic features allowed the drilled succession to be subdivided into flow-units based on abundance and size of vesicles and presence of chilled surfaces and sediments.
The existing 660 m deep Vestmanna-1 borehole penetrating the lower part of the Middle Basalt Formation with TD 100 m into the Lower Basalt Formation was originally drilled in 1980. It had to be reamed prior to logging due to partly blocking by precipitation of white tufa along the wellbore. The reaming operation was terminated at 615 m due to stuck pipe.

An extensive suite of slim hole wire-line logs was run in both wells by Robertson Geologging (RG). The logging programme comprised acquisition of the following logs: optical televiewer (OPTV), three arm caliper (3ACS), formation density ((FDGS), dual neutron (DNNS), focussed electric (GLOG), full waveform/compensated sonic (FWVS), natural gamma spectroscopy (SGAM) and temperature/conductivity (TCDF). The log quality is generally acceptable except for the spectral gamma logs due to lack of proper calibration. The full wave logs recorded with a tool with only two receivers are affected by high frequency noise causing difficulties to pick the shear waves. As the processing results from RG of the full wave sonic logs were considered unsatisfactory time-consuming additional processing passes to enhance results were undertaken both by the Norwegian company Logtek and by GEUS.
The logging runs were made with only one tool at a time. As a good integration of wire-line log and core data is paramount to the project a tedious task of depth matching was carried out. It was carried out in two steps. First the formation density runs were chosen as the master run to which the depths of all other runs were compared. Afterwards the wire-line log runs were compared and adjusted with the drill cores. The depth shifts have been applied to the composite logs and composite LAS-files.

A full documentation of the work-flow during and after the field operations is given in the report with four fold-out enclosures containing composite logs and full wave sonic logs, and a data DVD. The DVD contains the complete report in electronic format including core descriptions, core photos and all raw and processed logs from both wells.

The well results are highlighted in the composite logs in the scale 1:500 showing all log runs together general lithology and petrography of the cores. For simplicity only a distinc-

tion between sediments, brecciated lava crust, vesicular lava crust and massive lava core is made in the lithology column. The wire-line logs reflect clearly the bedding and other features seen in the core. For example the massive core of thicker flow-units comes out clearly with high bulk density, high sonic velocities, high resistivity and low neutron porosity. Details on the lava succession in Vestmanna-1 wells are given in Waagstein and Hald (1984). Therefore only the preliminary results from the new Glyvursnes-1 well is summarized. The boundary between the Upper (UBF)and Middle Basalt formations (MBF) was picked at a depth of 355 m. It is picked at the base of 9 m simple flow of aphyric basalt with a very low gamma ray response morphologically and lithological similar to the so-called C-horizon exposed some 6 km west of the well-site. It overlies a 0.8 m thick very fine-grained reddish sediment. The drilled succession consists dominantly of compound lava flows of thin flow-units of plagioclase-phyric basalts with vesicular crusts characteristic to pahoehoe lava. 150 complete flow-units have been identified in MBF and 99 in UBF. The mean thickness of the flow-unit is 2.2 m in MBF increasing to a mean thickness of 3.4 m in UBF. Thick flow-units above 10 m are only present in the upper 300 m of the well section. Sediments make up 1.3 % of the drilled succession. Most sediment layers are thin and increase in

Extended abstracts and abstracts for the Sindri Conference, Tórshavn 2006

Andersen, M.S., Boldreel, L.O. & the SeiFaBa group 2006: Lithological analysis of wireline logs through flood basalts in 8 exploration wells in the Faroe-Shetland Region. The Sindri Conference, Tórshavn, September 2006.

Andersen, M.S., Boldreel, L.O. & the SeiFaBa group 2006: In situ properties to flood basalt successions in 8 exploration wells in the Faroe-Shetland Region. The Sindri Conference, Tórshavn, September 2006.

Bais, G., White, R.S., Worthington, M.H., Andersen, M.S.& the SeiFaBa group 2006: The seismic response of Faroe basalts from integrated borehole and wide-angle seismic data. EAGE 68th Conference & Exhibition – Vienna, Austria, 12-15 June 2006.

Bais, G., White, R.S., Worthington, M.H., Shaw, F., Andersen, M.S. & the SeiFaBa group 2006: Seismic velocities, anisotropy and attenuation of Faroe Islands basalts. The Sindri Conference, Tórshavn, September 2006.

Boldreel, L.O. & Andersen, M.S. & the SeiFaBa group 2006: Efffect of burial on in situ properties of flood basalt successions in the Faroe-Shetland Region. The Sindri Conference, Tórshavn, September 2006.

Japsen, P., Mavko, G., Waagstein, R., Olsen, D. & the SeiFaBa group 2006: Rock physics analysis of sonic velocities in basalts from Faroese and Icelandic wells. The Sindri Conference, Tórshavn, September 2006.

Shaw, F., Worthington, M., Andersen, M.S. & Petersen, U.K. 2004: A study of seismic attenuation in basalt using VSP data from a Faroe Islands borehole. EAGE Paris 2004.

Shaw, F., Worthington, M.H., White, R.S., Andersen, M.S. & Petersen, U.K. 2005: Seismic attenuation in Faroe Island basalts. EAGE 67th Conference & Exhibition — Madrid, Spain, 13 - 17 June 2004.

Waagstein, R. & the SeiFaBa group 2006: Integration of wire-line log and core data from Glyvursnes-1 and Vestmanna-1, Faroe Islands. The Sindri Conference, Tórshavn, September 2006.

Lithological analysis of wireline logs through flood basalts in 8 exploration wells in the Faroe-Shetland Region

Morten Sparre Andersen, University of Faroe Islands, msa@geus.dk
Lars Ole Boldreel, Geological Institute, Copenhagen University
and the SeiFaBa group

Basaltic successions of various thicknesses and characters have been penetrated in a number of exploration wells in the British sector of the Faroe-Shetland Channel and around the Northeast Rockall Basin. The wireline logs through basaltic successions in eight released wells were selected for a systematic study of the log-response of basaltic rocks in this region.

We propose a simple classification scheme of basaltic rocks, which is based on the log data from these wells and the well site descriptions of cuttings and sidewall cores.

All of the basaltic successions in the studied wells can be sub-divided into five major classes, *simple lava beds*, *compound lava units*, *volcaniclastic units*, *hyaloclastic units*, and *hypabysal intrusive units* characterized by distinct log responses. Further characterisation of the individual basaltic unit is easily carried out using a small number of *response components*, which mostly reflect the porosity distribution within the units

The response components used in this study are selected in such a way that they as far as possible can be considered diagnostic of typical lava morphological features of basaltic eruptives. In the studied wells, the classification and characterisation of log responses allowed a description of the eruptive style and the environment of lava emplacement, which is in good agreement with descriptions based on palynological and petrological investigations of the successions. Examples illustrating the use of log response components in basaltic rocks will be presented.

Wireline logs, as well as any other investigation of borehole data, provide data along one dimension only. However, the log response may frequently be related to general (or local/regional) lava morphologic facies, especially if supported by studies of cuttings from crucial intervals. In addition to environmental parameters, the wireline logs provide in situ measurements of physical properties. Elaborate models for forward and inverse studies of 3D distribution of physical properties in basaltic successions should thus as far as possible be linked to interpretation on wireline logs, which provide a basis for a feasible lateral extrapolation of the physical properties in the vicinity of the well.

This study was funded by the Sindri Group (oil companies with exploration licences in the Faroese sector).

In situ properties of flood basalt successions in 8 exploration wells in the Faroe-Shetland Region

Morten Sparre Andersen, University of Faroe Islands, msa@geus.dk
Lars Ole Boldreel, Geological Institute, Copenhagen University
and the SeiFaBa group

Basaltic successions of various thicknesses and characters have been penetrated in a number of exploration wells in the British sector of the Faroe-Shetland Channel and around the Northeast Rockall Basin. Wireline logs through the basaltic successions in eight released wells were selected for a systematic study of physical properties of basaltic rocks from this region. In these wells in situ measurements of physical properties were carried out through ca. 4000 m of extrusive and ca. 1100 m of hypabysal intrusive basaltic rocks buried to a depth of 1172-5089 m below sea-level . It is thus one of the largest databases of physical parameters in a basalt province buried in a sediment basin.

The physical properties measured in the wells from the Faeroe-Shetland flood basalt province are as variable as the properties of sediments from the same wells, and large variation in property distributions is seen both within the individual wells and among the wells.

In cross plots of bulk density and seismic velocity versus neutron porosity, the basaltic rocks from the Faeroe-Shetland region are characterised by very large apparent matrix densities and velocities (typically above 3100 kg/m^3 and 7000 m/s). These apparent values are considerably higher than those reported from fresh un-altered basalt matrix. However, neutron porosity measures not only pore water; but also hydrogen in the matrix. Diagenetic alteration of basalts is mainly a hydration process. If allowance are made for hydration of basaltic rocks, the three porosity logs provide information about of true porosity, degree of hydration and matrix properties. Using the log classification and characterisation proposed by Andersen & Boldreel[1], a clear distinction is seen between on the one hand lava flows emplaced in a dry environment and on the other hand and lava lava flows emplaced in a wet environment, possibly sub-aquatic. The lava beds emplaced in dry environment is characterised by a relatively constant hydration throughout the beds and simple well defined trends in cross plots of bulk density and seismic velocity versus neutron porosity. Lava beds emplaced in wet environments are characterised by variable degree of hydration, "poorly" defined trends, and frequently the lower part of these lava beds are characterised by a low degree of hydration.

This study was funded by the Sindri Group (oil companies with exploration licences in the Faroese sector).

[1] Andersen, M.S. & Boldreel, L.O. and the SeiFaBa group, 2006. Lithological analysis of wireline logs through flood basalts in 8 explorations wells in the Faroe-Shetland Region, **This volume**.

The seismic response of Faroe basalts from integrated borehole and wide-angle seismic data

BAIS G.[1], WHITE R.S.[1], WORTHINGTON M.H.[2],ANDERSEN M.S. & SEIFABA GROUP

[1] *Department of Earth Sciences, Bullard Laboratories, Madingley Rd. Cambridge , UK, CB3 OEZ, UK*

[2] *Department of Earth Sciences, Oxford University, Parks Road, Oxford, OX1 3PR, UK*

[3] *Geological Survey of Denmark and Greenland Ostervold Gade 10, Copenhagen DK-1350, Denmark*

Summary

We study the seismic response of layered basalts in the Faroe Islands using borehole data and vertical seismic profiles from the Vestmanna borehole, combined with reflection and wide-angle seismic data recorded into arrays of both borehole and land multicomponent receivers. Imaging through the basalt cover in the Faroe-Shetland Basin is a challenge for conventional seismic surveys: scattering caused by the high reflectivity of the basalt as well as intra-basalt multiples and high attenuation from the layered sequence make it difficult to image within and beneath the basalts. This project allows us to correlate ultrasonic-scale velocity and density measurements from the borehole together with ground-truthing from borehole logs and core samples with the seismic-scale velocities and reflection images derived from VSP and surface data. We find a good match of observed travel-times of borehole and wide-angle P-wave data with those predicted from the borehole measurements, suggesting lateral homogeneity over horizontal distances on the kilometre scale, and restricted transverse anisotropy of the layered basalts. A pronounced intra-basalt reflector identified on the multichannel surface seismic can be correlated with lithostratigraphic interpretation of the borehole logs as caused by thick flows near the top of the Lower Basalt formation.

Introduction

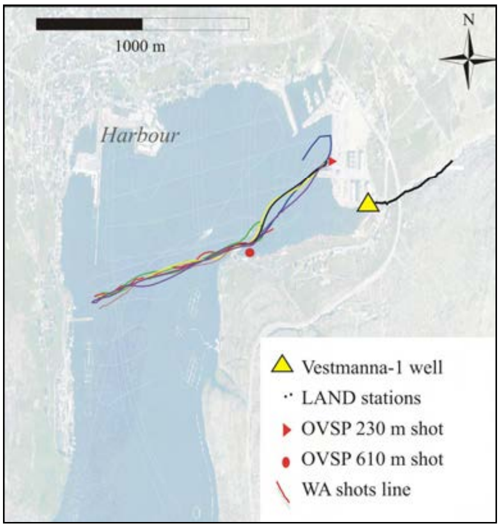

Figure 1: Location map

Massive extrusion of basalt flows accompanied the early Tertiary breakup of the northern North Atlantic, producing an estimated 1 million km^3 of extrusive basalt. The pile of extrusive lavas reaches more than 7 km thick on the Faroe Islands which lay near the hottest part of the underlying mantle thermal anomaly at the time of continental break-up (White *et al.* 2003). The basalts on the Faroe Islands have been divided into three series. From the older to the younger they are: the Lower Basalt Formation (LBF), the Middle Basalt Formation (MBF) and the Upper Basalt Formation (UBF). The 660 m deep Vestmanna-1 well sampled the lower 550 m of the MBF characterized by pahoheoe flows of thickness < 2 m, while the deeper part crossed the MBF–LBF boundary and sampled the aa lava type with 10–30 m thick flows of the LBF. Both facies are locally parallel bedded. However the aa flows of the LBF are thicker and develop massive interiors with highly variable porosity at the weathered and often vesicular margins of the flows, in contrast to the pahoheoe lavas of the MBF which produce less internal physical variation (Japsen *et al.* 2005).

Data acquisition

The seismic experiments in the harbour around the Vestmanna borehole (Fig. 1) include an 'onshore-offshore' configuration with walk-away (WA), zero offset VSP (VSP) and offset-VSP (OVSP) profiles shot into four-component receivers in the Vestmanna borehole and a 120-channel Geometrics geophone array with 3 component data in a marine-land geometry (LAND). The seismic source consisted of three 0.7 litre (40 cu. in.) sleeve guns, towed behind a small boat. Marine reflection profiles with a 100 joule source (BOOMER) were shot to map sediment thickness variations along the offshore profiles.

In total we recorded eight WA profiles (200 to 1500 m offset, 0.5 ms sampling rate), two fixed-offset VSPs (OVSP) (at 230 m and 610 m offset, 0.5 ms), and one zero offset VSP (consisting of records at 5 m depth intervals from 50–500 m depth, with two 0.7 litre sleeve guns). Redundant shots were fired during the OVSP acquisition, which has allowed stacking and, consequently, a significant increase in the signal-to-noise (S/N) ratio. In the same way it has been possible to stack redundant data acquired on the 120 channel land array during the wide-angle shooting.

A 400-m-long (120-channel, 5 m spacing) land array of 3-component Geometrics geophones was set up to record the shots made for the OVSP and WA data. A combination of one- and three-component geophones was utilised with the following pattern to optimise both the spread and the 3-component data: a single three-component geophone alternated with three one-component geophone in a profile extending away from the Vestmanna-1 borehole, in an area where basalt outcrops. The geophones were cemented into holes drilled in the basalt outcrop.

Transverse anisotropy of layered basalts

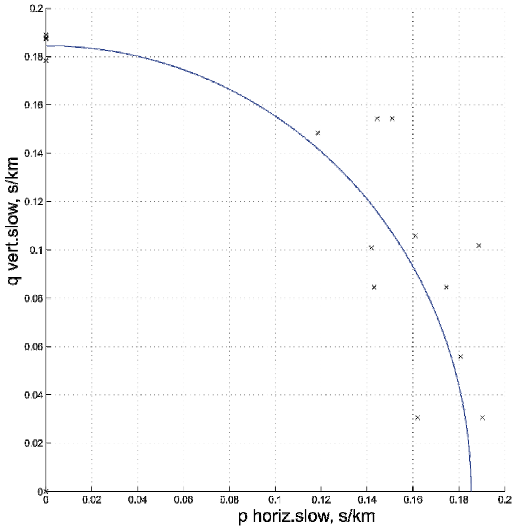

Figure 2: Phase slowness analysis shows a horizontal:vertical slowness ratio of 1.005 .

One purpose of this study is to investigate whether there is significant transverse anisotropy with a vertical symmetry axis produced by the horizontally layered basalts. Using the procedure proposed by Backus (1962) suggests from the borehole logs that such P-wave anisotropy should average about 1%.

Using the phase-slowness method proposed by Geiser (1990), we find that the observed anisotropy from the VSPs is less than 0.5% (Fig. 2), but the resolution of our measurements is insufficient to measure smaller degrees of anisotropy than this. As we show below, the wide-angle data is consistent with isotropic velocities within the basalt sector.

Ray tracing of borehole and surface data

Since we find the anisotropy to be small, we are able to use an isotropic ray tracing method to model the arrival times and thus construct a P-wave velocity model. First arrival travel times picked on the vertical component of the WA, VSP, OVSP and LAND data were used to construct a velocity model. The average picking misfit 5 ms. The geometry of the borehole plus land acquisition allows different rays to be recorded over a wide range of illumination angles (Fig. 3). The 1D velocity profile from the borehole sonic log shows average velocities of 5200–5800 m/s with an overall increase with depth, but some local velocity inversion due to the presence of ‘softer’ lithologies inter-bedded between massive lava flows (Fig. 3). A starting velocity model for the ray-tracing was constructed from well log Vp data which was sampled every 0.2 m, and averaged every 10 m in the slowness domain. The sonic velocities obtained by the well log were calibrated using the zero-offset VSP first arrivals obtained using an airgun source.

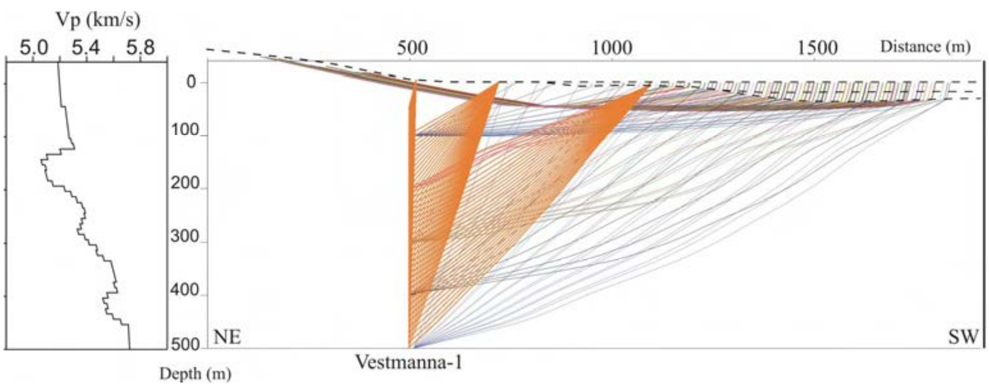

Figure 3: Ray tracing of WA , OVSP, VSP and LAND data through the Vp isotropic model. On the left is shown the Vp profile matching the first arrivals. For WA and LAND the figure shows only tenth ray.

In the shallow section, a vertical velocity gradient of 0.1 /s was introduced for tracing the rays recorded by the LAND array. In order to model the irregular sedimentary coverage in the harbour beneath the shooting lines, the sedimentary thickness was calculated from the travel times picks read on the BOOMER data: it varied from 0–35 m. Two-point ray tracing was performed for WA, VSP and LAND first arrivals on the vertical component (Fig. 3). The model allows us to trace rays from different angles with the following average misfits: VSP & OVSP 4.9 ms (173 traveltime picks); WA 5.1 ms (601 picks); LAND 3.5 ms (2520 picks). We did not need to introduce lateral heterogeneity, suggesting that not only is the degree of transverse anisotropy small, but that the velocities in the lava sequence sampled by the borehole do not vary laterally over distances of at least 2000 m sampled by our data.

Multichannel seismic data

The land multichannel seismic recordings from offshore airgun shotpoints were processed using conventional techniques in order to image intra-basalt reflections in the vicinity of the borehole. The redundancy of the shots obtained from the VSP data and the huge coverage for the LAND data allowed us to bin and sum the traces in common offset gathers for each channel, allowing considerable improvement of the S/N ratio on the prestack data. This was followed by f-k filtering and muting to remove ground roll and refracted arrivals, with spiking deconvolution. We used the Vp velocity model derived from the raytracing for depths < 660 m (sampled by the borehole), and semblance analyses for the deeper portion down to 2.5 s two-way time. The final stacked and depth-converted section is shown in Fig. 4: there is no data from the upper 400 m because the geometry of the acquisition and shallow water immediately adjacent to the borehole meant that the minimum source-receiver offset is 500 m.

The most notable feature of the reflection data is a strong, laterally continuous, horizontal reflection at 600 m depth. This is near the top of the Lower Basalt formation, although interestingly it does not correlate exactly with the boundary between the Middle and Lower Basalts. Full waveform synthetic seismogram reflectivity modelling shows that it is caused by the thick basalt flows which occur about 40 m below the Middle-Lower Basalt boundary.

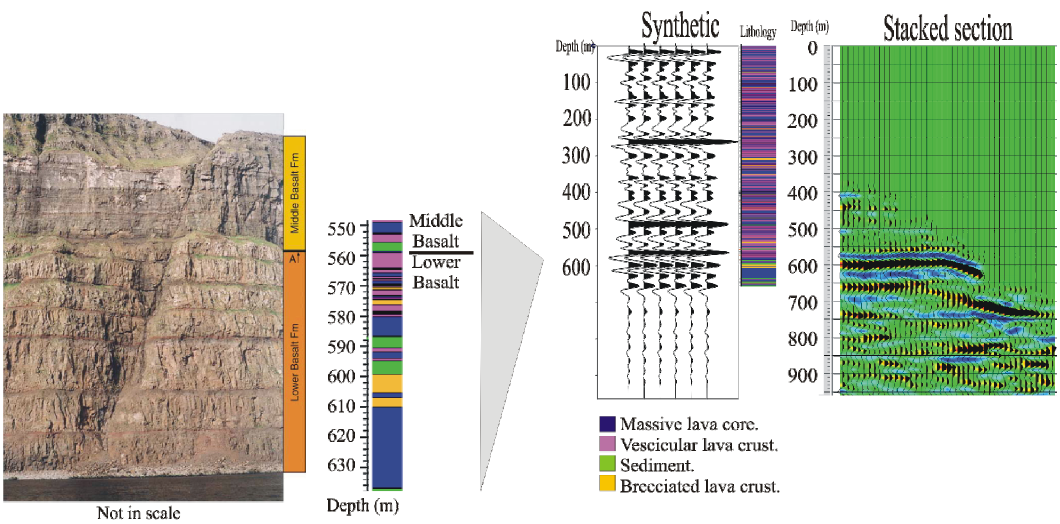

Figure 4: Correlation between log and seismic stacked data: the strong reflection is immediately below the Middle-Lower Basalt formation boundary.

As Smallwood *et al.* (1998) show, reflections within layered basalt sequences are formed by interference effects of multiple thin layers that are usually much thinner than the seismic wavelength. The dominant frequency of our seismic data is reduced to 45 Hz by attenuation in the basalts (Maresh and White 2005). The wavelength at the top of the LBF is therefore about 125 m. So the thick (10–30 m) basalt layers of the LBF are capable of producing strong reflections from individual layers, whereas the thin (average < 2 m) layers of the MBF produce reflectivity from the interference effect of multiple layers. This difference in reflection character enables the MBF and LBF to be differentiated on seismic reflection profiles, but even so, it is important to note that the strong reflection from near the top of the LBF does not correspond exactly to the MBF–LBF stratigraphic boundary, but comes from c.50 m deeper.

Acknowledgments

The SeiFaBa project (Seismic and petrophysical properties of Faroe Basalt) is funded by the Sindri Group (www.sindri.fo), who have given permission for publication of this paper. The SeiFaBa Working Group comprises P. Japsen, C. Andersen, H.L. Andersen, M.S. Andersen, G. Bais, L.O. Boldreel, G. Mavko, J.M. Pedersen, U.K. Petersen, R. Rasmussen, F. Shaw, N. Springer, R. Waagstein, R.S. White and M. Worthington. Acquisition of seismic data used equipment from the Department of Earth Science, University of Aarhus, the Universities of Oxford and Cambridge and the NERC Geophysical Equipment Pool. We thank N. Mohammed and F. Shaw for their help in the field collecting the data. The views expressed here are those of the authors, who are solely responsible for any errors.

References

Backus G.E. [1962] Long-wave elastic anisotropy produced by horizontal layering, Journal of Geophysical Research, **67**, 4427–4440.

Gaiser, J.E. [1990] Transversely isotropic phase velocity analysis from slowness estimates, Journal of Geophysical Research, **95**, 11241–11254.

Japsen, P. et al. [2005] Preliminary results from investigations of seismic and petrophysical properties of Faroes basalts in the SeiFaBa project. In: Doré, A.G. and Vining, B.A. (eds) Petroleum Geology: North-West Europe and Global Perspectives –Proceedings of the 6th Petroleum Geology Conference, 1461–1470. Geological Society, London.

Maresh, J. and White, R.S. [2005] Seeing through a glass, darkly: strategies for imaging through basalt, First Break, **23**, 27–33.

Smallwood, J.R., White, R.S. and Staples, R.K. [1998]. Deep crustal reflectors under Reydarfjördur, eastern Iceland: Crustal accretion above the Iceland mantle plume. Geophysical Journal International, **134**, 277–290.

White, R.S., Smallwood, J.R., Fliedner, M.M., Boslaugh, B., Maresh, J. and Fruehn, J. [2003] Imaging and regional distribution of basalt flows in the Faroe-Shetland Basin. Geophysical Prospecting, **51,** 215–231.

Seismic velocities, anisotropy and attenuation of Faroe Islands basalts

Bais G., Bullard Laboratories, Madingley Rd, Cambridge, CB3 0EZ, UK: gb327@cam.ac.uk
White, R. S., Bullard Laboratories, Madingley Rd, Cambridge CB3 0EZ
Worthington M.H., Dept Earth Sciences, Oxford University, Parks Road, Oxford, OX1 3PR, UK
Shaw F. Dept Earth Sciences, Oxford University, Parks Road, Oxford, OX1 3PR, UK
Andersen M.S. GEUS, Oster Voldgade 10, DK-1350, Kobenhavn, Denmark
& the SeiFaBa Group

Borehole data, vertical seismic profiles, near-offset and wide-angle seismic reflection data have been used to investigate the velocities, anisotropic and attenuation properties of seismic waves in layered basalts on the Faroe Islands. We present the first results from studies at Vestmanna harbour, where the 660 m Vestmanna-1 borehole penetrates the lower 550 m of homogeneous “pahoheoe” lavas of the Middle Basalt Formation (MBF) and into the 10–30 m thick, “aa” lava type flows of the Lower Basalt formations (LBF). We have correlated the ultrasonic-scale velocity measurements from the borehole with the seismic-scale velocities and reflection images derived from VSP and surface data.

Sesismic data were acquired from a 3-component sensor in the borehole and from a 120-channel 3-component Geometrics geophone array extending away from the borehole on basalt outcrop. We recorded a vertical seismic profile (VSP), six offset VSPs (OVSP) with borehole sensors at 50 m depth intervals, and six wide-angle (WA) profiles into the borehole receovers and the land array (LAND). Using the phase-slowness method on the first arrivals on OVSP and WA data we find that the observed anisotropy from the layered basalts is less than 0.5%, even smaller than the value of 1% derived by theoretical calculation from the layered structure. The geometry of the borehole (WA, VSP, OVSP) plus land acquisition allows rays to be recorded over a wide range of illumination angles: the P wave velocity model calculated from the first arrivals by an isotropic ray tracing code shows average velocities of 5200–5800 m/s with an overall increase with depth. The observed travel-times from borehole and wide-angle P-wave data match well with those predicted from the borehole logging measurements.

Reflection profiles from our data show a strong and continuous intra-basalt reflector at 600 m depth: This does not correlate exactly with the MBF-LBF boundary but is produced by a 30 m thick basalt flow ~40 m deeper. Synthetic seimogram modelling confirms that 10–30 m thick basalt layers of the LBF are capable of producing strong reflections from individual layers, whereas the thin (average < 2 m) layers of the MBF produce reflectivity from the interference effect of multiple thin layers, as reported by Smallwood *et al.* (1998) from the basalt sequence in eastern Iceland.

Measured values of apparent Quality Factor (Q) are ~30, similar to values elsewhere in basaltic sequences (Maresh & White, 2005). We demonstrate that the most likely cause of the low values of Q is a combination of 1D scattering by the layered basalt sequence and intrinsic attenuation due to seismic wave induced fluid flow within pores and micro-cracks.

References

Maresh, J. and White, R.S. [2005] Seeing through a glass, darkly: strategies for imaging through basalt, *First Break*, **23**, 27–33.

Smallwood, J.R., White, R.S. and Staples, R.K. [1998]. Deep crustal reflectors under Reydarfjördur, eastern Iceland: Crustal accretion above the Iceland mantle plume. *Geophysical J. Int.*, **134**, 277–290.

Effect of burial on in situ properties of flood basalt successions in the Faroe-Shetland Region

Lars Ole Boldreel, Geological Institute, Copenhagen University, lob@geol.ku.dk
Morten Sparre Andersen, University of Faroe Islands,
and the SeiFaBa group

Early Cenozoic flood basalts are found throughout most of the Faroe-Shetland region. We have investigated burial related variation of logged properties using data from eight exploration wells where the flood basalts apparently are at their maximum burial depth. The basalt successions represent basalts buried to depths varying from ca. 1100 to 3500 m. In addition, burial related variations of logged properties have been studied in the Lopra-1/1A well drilled into the Lower Basalt Series, Faeroe Islands. The basalt in this well represents the depth interval 200-2489 m below sea-level. Overall neutron porosity decreases with depth while seismic P-wave velocity and density increase. In the Lopra-1/1A well, also seismic S-wave velocity is recorded and increases with depth. Using all data from the eight offshore wells, crude trends are established representing porosity reduction and seismic velocity and density increase as functions of burial depth. The variation around the general trend is large and related to lithology[1]. Trends specific to the individual lithologies are thus better suited for predicting property changes with depth.

Overall porosity reduction, velocity and density increase with depth is also observed in the Lopra-1/1A well. The trend from Lopra-1/1A is offset towards lower porosities and higher velocities and densities relatively to the offshore wells. However, Lopra-1/1A is not at its maximum burial depth. It is thus suggested that the depth dependent change of the porosity related properties is mainly due to porosity reduction during burial and that the offset of the trends observed in Lopra-1/1A is caused by denudation of the basalt succession at Lopra.

This study was funded by the Sindri Group (oil companies with exploration licences in the Faroese sector).

[1] Andersen, M.S. & Boldreel, L.O. and the SeiFaBa group, 2006. Lithological analysis of wireline logs through flood basalts in 8 explorations wells in the Faroe-Shetland Region, **This volume**.

Rock physics analysis of sonic velocities in basalts from Faroese and Icelandic wells

Peter Japsen, GEUS, pj@geus.dk
Gary Mavko, Stanford University
Regin Waagstein, GEUS
Dan Olsen, GEUS

We have analysed the acoustic properties of basalts based on sonic log data from three Faroese and three Icelandic boreholes and ultrasonic laboratory measurements on 43 1.5” core samples from the three Faroese boreholes. The Faroese boreholes are Lopra-1/1A (LP-1), Vestmanna-1 (VM-1) and Glyvursnes-1 (GL-1) that penetrate the Palaeogene basalts of the Lower, Middle and Upper Basalt Formations (UBF, MBF and LBF) and these rocks are mainly subaerial flood basalts apart from hyaloclastites below c. 2.5 km depth in the LP-1 well. The Icelandic wells penetrate volcanic rocks of Plio-Pleistocene age and cover a mixed environment: HH-1 (95% hyaloclastites), LA-10 (45% submarine and 45% subaerial basalts) and LL-3 (95% subaerial basalts).

We find a tight correlation between sonic Vp and He-porosity based on core data irrespective of basalt facies and well (only data for sediment samples deviate). The core data also reveal a well-defined relation between Vp and Vs, which is to be expected from rocks of broadly similar composition. However, there is a significant scatter in plots of Vp versus density and this scatter is related to the range of grain (matrix) densities from 2.7 to 3.1 g/ccm. Low grain densities represent altered samples with high content of light minerals such as zeolite and clay.

We can distinguish two main Vp-density trends for flood basalts based on the log data: (1) a trend of relatively low Vp compared to density (the UBF in the GL-1 well; the flood basalts in the LL-3 well), and (2) a trend of relatively high Vp compared to density (the LBF in the LP-1 well). The properties of the MBF are transitional between the two trends. The GL-1 data from this interval represents both the high and the low trend, whereas the VM-1 data represent a very high trend. However, towards the base of VM-1, we observe a ‘reversal’ of the Vp-density trend within the thin sequence of the LBF penetrated by the well. The analysis of the Vp-density relation for the core data shows that the outlying samples towards low densities are characterized by low grain density. Hence the relatively high Vp-density trend defined for the log data in these wells for the MBF also must be characterized by low grain densities. This means that the low Vp-density trend represents basalt with unaltered matrix with high grain density and the high trend represents altered basalt with a low grain density.

The transition from the low Vp-density trend of fresh basalts to the high trend of altered basalts within the MBF occurs concurrently with an increase of the sonic velocity and density with depth even though there is no increase in the flow thickness. This shows that the transition from fresh to altered basalt is accompanied by an increase in velocity and density and thus probably also by net influx of mass leading to higher densities (growth of zeolites). This means that data points along a high Vp-density trend represents samples with relatively high velocity compared to density, because filling of the pore space with zeolites and clay increases velocity and only changes density of low-porosity basalts slightly.

P015 A STUDY OF SEISMIC ATTENUATION IN BASALT USING VSP DATA FROM A FAROE ISLANDS BOREHOLE.

F.SHAW[1], M.H.WORTHINGTON[1], M.S.ANDERSEN[2] & U.K.PETERSEN[2]

1 Department of Earth Sciences, Oxford University, Parks Road, Oxford, OX1 3PR, UK
2 University of the Faroe Islands, Faculty of Science and Technology, Box 2109, FO-165 Argir,Faroe Islands.

Summary

We describe an investigation of the magnitude and mechanisms of seismic attenuation in basaltic sequences. Using near-zero-offset vertical seismic profile (VSP) data collected from the Faroe Islands, measurements of effective seismic attenuation have been obtained using the spectral ratio method. A change of Q occurs between the Faroes Upper and Middle basalt series, but with Q values that are similar to those of other investigations of basalt in the North Atlantic region. The upgoing wave derived from the VSP data is approximately modelled with 1-D synthetic seismograms. However, disparities between the spectra of vertical and horizontal components suggest that 3-D scattering effects may be a dominant cause of seismic attenuation.

Introduction

A vertical seismic profile (VSP) survey has been carried out at Glyvursnes, on the Faroe Islands. The 700 metre deep Glyvursnes borehole passes through two major basalt formations (the Middle Series and Upper Series). Very little sediment occurs within the sampled sequence (less than 5%), allowing us to examine basalt properties in isolation of basalt-sediment interaction. The near-zero-offset survey was conducted from 50 - 600 metres depth, with a spatial interval of 10 metres. The receiver was a three component, clamped geophone. The source was a 150 cu. in. air gun fired in a pit with an approximate water depth of 2 metres. A hydrophone was placed in a slim hole 10 metres beneath the air-gun pit to monitor the near-field source signature.

Seismic Q estimation using the spectral ratio method

For a constant seismic quality factor over a certain bandwidth, the amplitude of a seismic signal in relation to the source amplitude is given by:

$$\mathbf{A = A_o . exp(-\pi\, fx/Qc)} \qquad (1)$$

A= amplitude at depth x, $A_{o=}$ source amplitude, f= frequency, x= depth, Q= seismic quality factor, c= wave propagation velocity.

Comparing traces from two depths,

$$\mathbf{A_2 / A_1 = A_{o2}.exp(-\pi\, fx_2 / Qc) / A_{o1}.exp(-\pi\, fx_1 / Qc)} \qquad (2)$$

To compensate for any variations in the source signature (such as changes in water depth of the airgun pit), the source amplitudes (estimated using the near-field hydrophone) are retained as a correction factor in equations (2) and (3).

$$\ln (A_2 / A_1) - \ln (A_{o2} / A_{o1}) = - \pi f \delta t_{2\text{-}1} / Q \quad (3)$$

$\delta t_{2\text{-}1}$is the difference in travel times and $\ln(A_{o2} / A_{o1})$ is the source variation correction factor.

Figure 1 illustrates how Q estimates are obtained using a linear regression based on equation 3. Figure 1a shows the amplitude spectra of the first arriving wavelet on the vertical component at two depths. Figure 1b shows the importance of restricting the application of equation 3 to a frequency range with good signal to noise ratio.

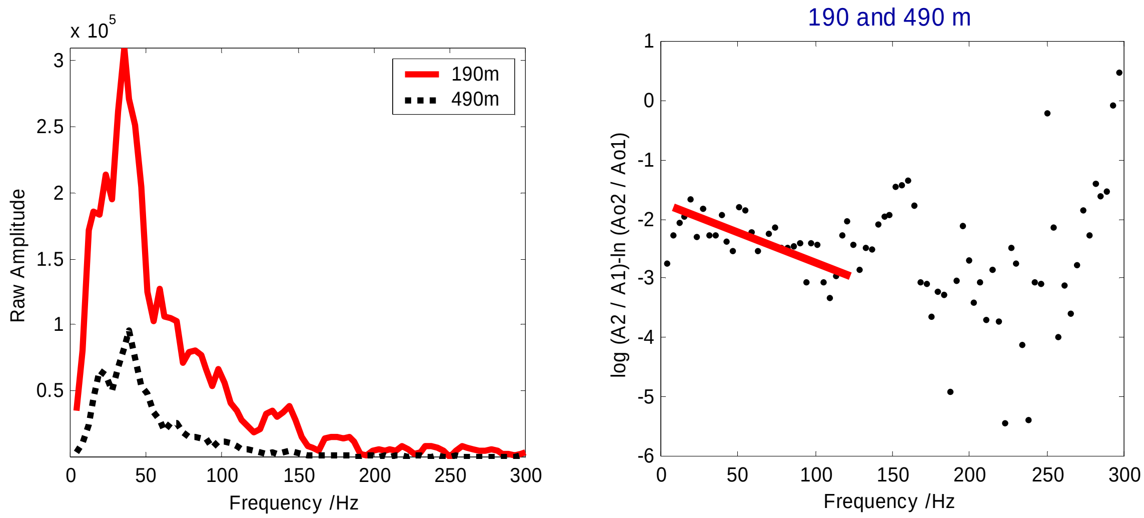

Fig 1 a: Comparison between amplitude at depth 190 m (solid red line) and depth 490 m (dashed black line). b: The spectral ratio is stable between frequency of ~ 10 - 150 Hz, hence line is fitted to that region only.

The choice of receiver separation (spacing) is also important. A larger spacing improves the accuracy of the estimate by increasing the magnitude of the effect that is being measured but at the expense of the spatial resolution. For a frequency window between ~10 and 150 Hz, Q was calculated with a trace receiver separation of 300 metres. This was then repeated for four other spacings of 280, 290, 310 and 320 metres. The spread of values obtained with these five slightly different spacings provides a measure of the error of the Q estimates (error bars in figure 2).

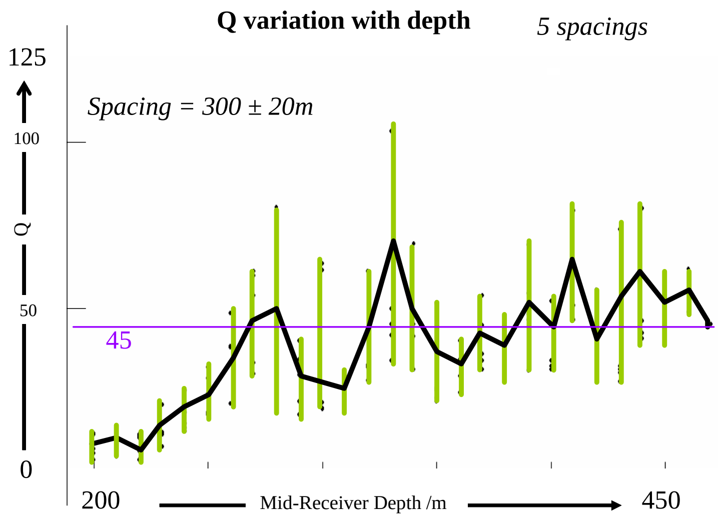

Fig 2: Q variation plotted against approximate mid-point. A mid-point of 200 m represents comparisons between ~ 50 m and ~ 350 m.

Q was found to be ~ 10 at shallow depth, increasing with some fluctuations to ~ 45 at deeper levels (fig 3). The change in Q across the 300 metre level appears fairly abrupt, approximately matching the transition between the Upper Series and Middle Series Basalts. The results are similar to those of other recent Q investigations from the North Atlantic region. (Table 1).

Rutledge & Winkler	**1987**	***Upper Basalt Series, Vøring Plateau, E. Norwegian Sea***	**Effective Q~40, Intrinsic Q>100**
Christie, Gollifer & Cowper	**2001**	***Lopra-1/1A Borehole, Suđuroy, Faroe Islands***	**Q~35, mostly from scattering**
Maresh, Hobbs, White & Ringwood	**2003**	***Northern Rockall Trough, North Atlantic Margin***	**Q~15-35**
This survey	**2003**	***Glyvursnes, Streymoy, Faroe Islands***	**Q~10-45**

Table 1: Investigations of seismic quality factor from the North Atlantic Region.

Study of attenuation mechanisms

Using the vertical VSP component, the upgoing wave was derived and compared with 1-D synthetic seismograms (with and without multiples) generated from the logs (fig 3). Although pronounced interfaces are adequately modeled, the mismatch between synthetic and real data suggests that a solely 1-D model of the basalt sequence insufficiently accounts for the observed seismic signature.

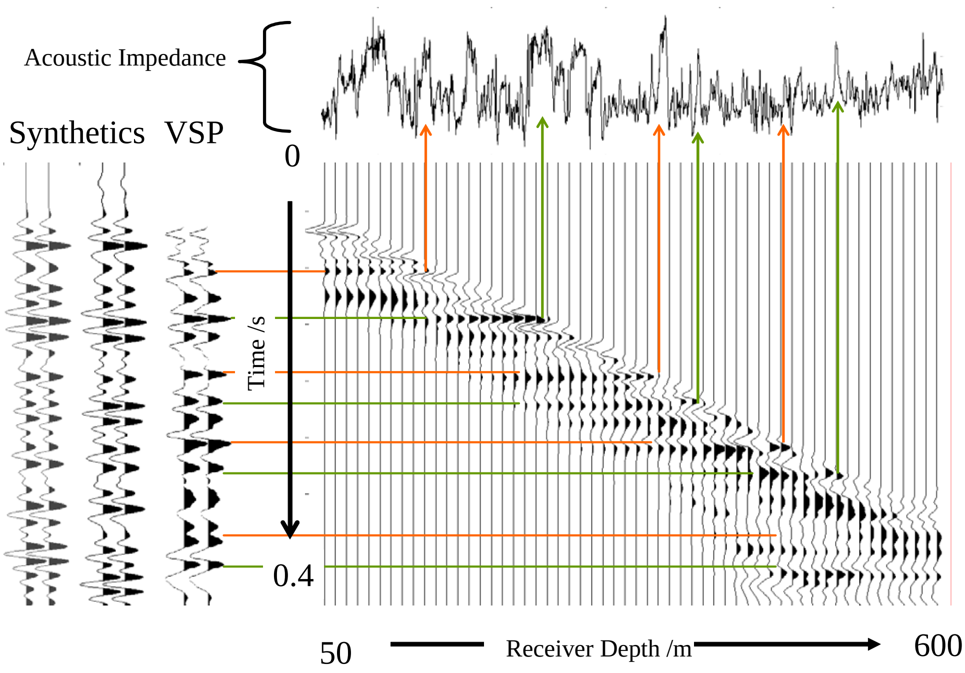

Fig 3: The VSP upgoing wave compared with synthetic seismograms generated from borehole logs (primaries only, and with multiples). Significant events are picked out by the arrows and correlated with acoustic impedance.

Amplitude spectra for the first arrival wavelet averaged over two depth intervals (60-160 metres and 500 - 600 metres) are shown in figure 4. Note the expected low-pass filtering effect with depth in the vertical component data from which the Q estimates arise. However the spectra of the averaged horizontal component data remains relatively broad band for both depth intervals. This suggests that much of the high frequency seismic energy is scattered in 3-D and is not permanently lost through intrinsic attenuation. This effect has previously been observed in VSP data by Worthington and Hudson (2000).

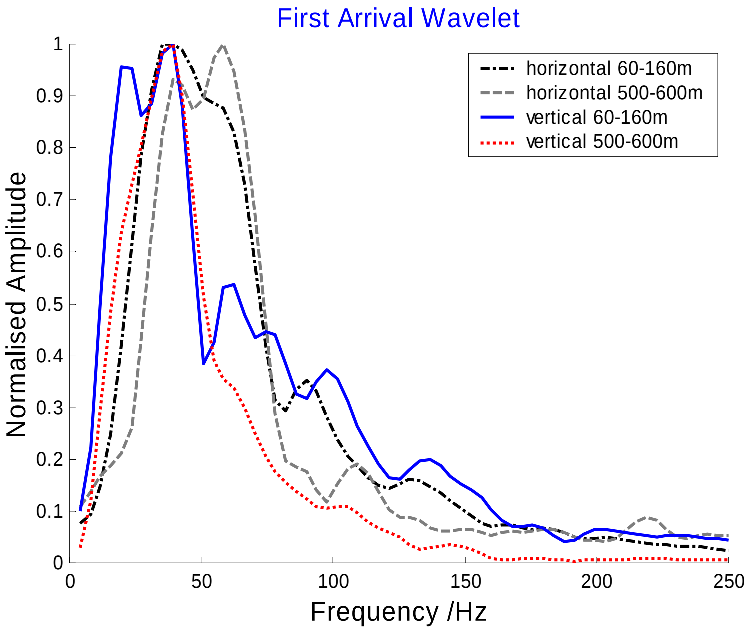

Fig 4 : Amplitude spectra for the first arrival wavelet only. Amplitudes are averaged over 10 traces in the range 60 - 160 m and 500 - 600 m, then normalized. Vertical component 60-160 m (solid blue); vertical component 500-600 m (dotted red). Horizontal components 60-160 m (dashed black); horizontal components 500-600 m (dashed grey).

Conclusions

1) A range of Q ≈ 10 – 45, comparable to other values obtained from the North Atlantic region, was obtained using the spectral ratio method. A significant increase occurs at approximately 300 metres depth, which coincides with the transition between the Upper Series and Middle Series Basalts.

2) The degree of mismatch between 1-D synthetic seismograms and the VSP upgoing wave indicates that 1-D scattering cannot solely account for the observed seismic data. Changes in the frequency content between horizontal and vertical components, over depth and time, suggest that 3-D scattering could be a dominant mechanism of attenuation in basalt.

Acknowledgements

This research was funded by Atlanticom Sp/f as part of the SINDRI programme project *Petrophysical and seismic properties of Faroes basalts.*

References

Worthington,M.H. and Hudson J.A., 2000. Fault properties from seismic Q. Geophysical Journal Int., **143**, 937-944.

P502 Seismic attenuation in Faroe Island basalts

F.SHAW[1], M.H.WORTHINGTON[1], R.S.WHITE[2], M.S.ANDERSEN[3] U.K. PETERSEN[4] and SEIFABA GROUP
1 Department of Earth Sciences, Oxford University, Parks Rd., Oxford, OX1 3PR, UK
2 Department of Earth Sciences, Cambridge University
3 The Danish Geological Survey
4 The University of the Faroe Islands

Introduction

Basaltic rocks are often seismically opaque, but the mechanisms of attenuation are not well understood. The Faroe Islands has three outcropping basalt formations (Lower, Middle and Upper Series), and is thus an ideal laboratory for comparing geological facies, borehole data and seismic data. Vertical seismic profiling (VSP) experiments were conducted in boreholes at Glyvursnes (intersecting Upper and Middle Series Basalts) and Vestmanna (intersecting Middle and Lower Series Basalts) in 2003/2004, as part of the ongoing SeiFaBa project on the Faroe Islands. We describe studies of the effective seismic quality factor (Q) in relation to well logs, and to basaltic internal architecture.

Seismic Attenuation Observed From Faroe Islands VSP Experiments

Time domain methods were used to estimate effective seismic Q as the spectral ratio method was found to be less robust when S/N ratio was poor and the bandwidth was relatively narrow. Data were first corrected for geometrical spreading, and a series of Q values was derived for VSP traces at two different depth levels. By varying the vertical distance between the pairs ('spacing'), scatter plots were obtained over the entire VSP interval. The time domain method estimates at Vestmanna show a gradual decrease in attenuation (Fig. 1) with depth. The dominant frequency of the seismic wave varied from 250 to 150 Hz. The majority of the measurements of effective Q fall between 9 and 55 (1/Q =0.018−0.11) when 'spacing' is between 100 and 300 m.

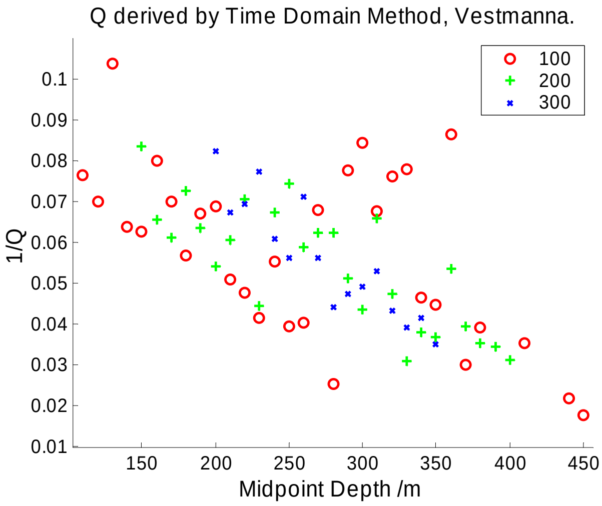

Fig. 1: 1/Q estimates from the time domain method, Vestmanna

The above methods of analysis were repeated for the Glyvursnes VSP data. Here, the time domain method again shows a gradual decrease in attenuation with depth (Fig. 2). The bulk of the estimates of effective Q fall between 7 and 60 (1/Q = 0.015–0.14). The dominant frequency of these data was 80 to 100 Hz.

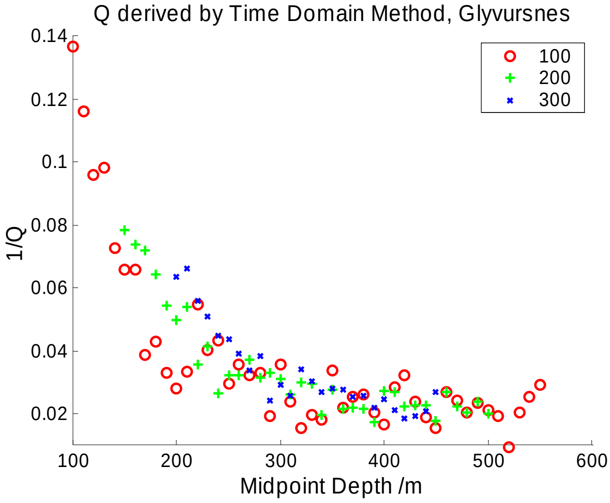

Fig. 2: 1/Q estimates from the time domain method, Glyvursnes

Q estimates have also been reported from the Lopra-1/1A well on the Faroese island of Suđuroy by Christie *et al.* (2005). This hole only intersects the Lower Basalt series. Q estimates were obtained, also using a time domain method, with values between 32 and 40 from 1350 m to 2450 m depth, and > 100 from 2450 m to 3510 m depth. It is also worth noting that Maresh *et al.* (2003) obtained values of Q of 15−35 in a 1200 metre thick basalt sequence in the northern Rockall Trough, NE Atlantic Margin. Hence there is now strong evidence that values of seismic Q of less than 50 are to be expected in basaltic sequences in the North Atlantic region.

Modelled Seismic Attenuation due to 1-D Layering

Possible mechanisms for apparent or actual energy loss in basalt include intrinsic attenuation, apparent attenuation due to inter bed multiples within a 1-D medium, scattering within a 3-D medium and the effects of frequency dependent transmission coefficients at partially sealed interfaces (cracks).

Synthetic traces were produced using an algorithm after Kennett (1979), to model 1-D multiple attenuation. Earth models were obtained from the sonic and density logs from the two wells, with depth sampling interval of 0.2 m. A zero phase input wavelet was used with the same bandwidth as the corresponding VSP first arrivals. Q values were derived using the spectral ratio method. A seismic wave travelling from 50 m to 600 m depth in the Glyvursnes borehole would be attenuated with an apparent Q due to 1-D scattering of 80–180. For 50 m to 500 m depth in the Vestmanna borehole, an apparent Q of 80–200 was obtained. When modelling shorter depth intervals, no clear correlation with the real data of change in Q with depth was obtained.

Determining Crustal Heterogeneity From Borehole Logs

In modelling experiments by Martini *et al*. (2004), energy loss from 3-D scattering is linked to internal complexity and the presence of fractal interfaces. The cyclicity of basalt emplacement gives rise to fractal lava lobes (Bruno *et al*., 1992). The above observations are supported by detailed geological mapping in Skye by Single et al (2004), which shows that heterogeneities are complex and widespread at sub-seismic-wavelength or 'intra-facies' scale. Lava conduits, volcanic break-outs, injection and loading structures, small lobes, sills and dykes cause high lateral complexity. Within the flows, there can be pahoehoe textures with alternating bands of high and low vesiculation. Therefore a key question is whether seismic response (i.e. acoustic impedance) matches the fractal character of the intra-flow architecture of ancient basalts. In unbounded fractal scaling, the medium has no characteristic scale, and is self-similar over zero to infinite lengths. Here, we analyse the power spectra of Glyvursnes and Vestmanna log data, following the approach of Dolan *et al.* (1998), to determine whether there is any evidence of fractal character in the Faroes basalt sequences.

The power spectra of the log data were derived. In each case a best straight line was fitted by least squares linear regression in $\log_{10}$ - $\log_{10}$ space. Its slope β is related to the Hurst exponent H by:

$$\beta = 2H + 1$$

H is commonly used as index to describe self-similarity, and is directly related to the fractal dimension D (Turcotte, 1992). A fractal medium is characterised by a good straight line fit. Figure 3 shows the Glyvursnes density data. Density (ρ) logs for both boreholes have a Hurst number close to 0.5, equivalent to a fractal dimension D of 1.5. indicating a Gaussian random walk. V_p and acoustic impedance in Glyvursnes were found to have an H of < 0.4. For Vestmanna log data, the power spectra also gave H values of < 0.4, but showed greater scatter for higher wavenumbers. These relatively low values of H are indicative of sequences that are more prone to reversal than random series, and large values are likely to be followed by small values over varying scales (a pattern known as anti-persistence).

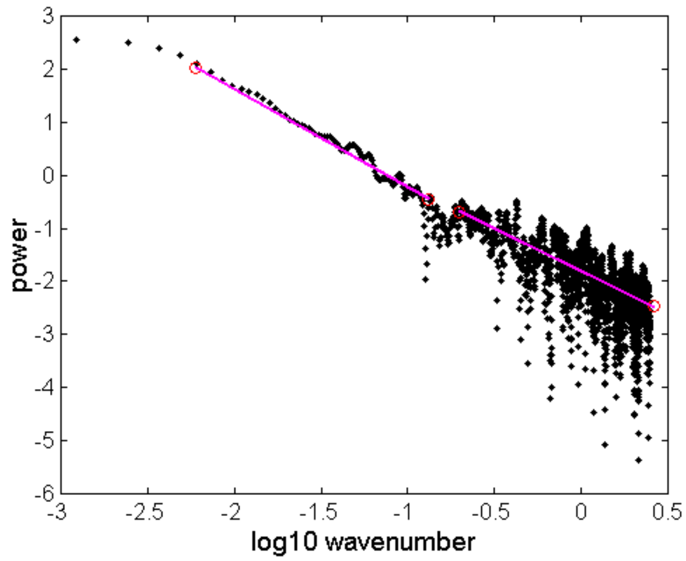

Fig. 3: Best straight line of slope β (magenta) fitted to acoustic impedance log power spectrum from Glyvursnes (black). H ~ 0.39.

The general conclusion from this analysis is that no significant difference was observed between the data from the two wells. The results obtained are broadly consistent with values quoted by Dolan *et al.* (1998).

Conclusions

Using a robust time domain method we have observed a gradual decrease in seismic attenuation in the Faroe Island basalts over the first 500−600 metres depth beneath the surface. Q values are low throughout, ranging from 5 to 55 in both Vestmanna and Glyvursnes. No significant difference is observed between the statistical character of the sequences at the two well sites.

Analysis of synthetic VSP data generated with a model based on the wireline log data has revealed that the observed Q values at Vestmanna and Glyvursnes cannot be due to 1-D scattering alone. This is in contrast to results obtained by Christie *et al*. (2005) and Maresh (2004) who conclude that seismic attenuation can largely be modelled by geometrical spreading and 1-D scattering loss. Consequently, we believe that the relative importance of different attenuation mechanisms can vary considerably within apparently quite similar geological sequences. 2-D scattering attenuation modelling and intrinsic attenuation modelling is work that is yet to be completed.

Acknowledgements

We thank the Sindri Group for permission to publish these results and for financial support. The *SeiFaBa* project, of which this work is a part, is funded collectively by oil companies operating in the Faroe Islands sector (the Sindri Group).

References

Bruno, B.C., Taylor, G.J., Rowland, S.K., Lucey, P.G., Self, S. (1992) Lava flows are fractals. *Geophysical Research Letters, v. 19, no. 3, p. 305–308.*

Christie, P., Gollifer, I., and Cowper, D., 2005. Borehole seismic studies of a volcanic succession from the Lopra-1/1A borehole in the Faroe Islands, NE Atlantic. *In press, Geology of Denmark Survey.*

Dolan, S.S., Bean, C.J. and Riollet, B. (1998) The broad-band fractal nature of heterogeneity in the upper crust from petrophysical logs. *Geophysical Journal International, v. 132, p. 489−507.*

Kennett, B.L.N. (1979) Theoretical reflection seismograms for elastic media. *Geophysical Prospecting, v. 27, p. 301−32.1*

Maresh, J., 2004. The seismic expression of Paleogene Basalts on the Atlantic Margin, *PhD thesis, Cambridge University.*

Maresh, J., Hobbs, R.W., White, R. S. & Smallwood, J.R. (2003). Attenuation of Atlantic margin basalts using downhole VSP (extended abstract), *73rd Annual International Meeting: Society of Exploration Geophysicists, Dallas, pp. 1310–1313.*

Martini, F., Bean, C.J., and Hobbs, R. (2004) Building a complex 3-D volume for sub-basalt imaging. *Abstract, EAGE 66th Conference & Exhibition, Paris 2004.*

Single, R., Jerram, D.A. & Pearson, D.G. (2004) The 3D facies architecture of flood basalt provinces and their internal heterogeneity: examples from the Palaeogene Skye Lava Field. *Journal of the Geological Society, v. 161, no. 6, p. 911−926.*

Turcotte, D. (1992) Fractals and Chaos in Geology and Geophysics, *Cambridge University Press.*

Integration of wire-line log and core data from Glyvursnes-1 and Vestmanna-1, Faroe Islands

Regin Waagstein, Geological Survey of Denmark and Greenland (GEUS), rw@geus

The Glyvursnes-1 and Vestmanna-1 boreholes form part of the Sindri project called 'SeiFaBa', which purpose was to examine the seismic properties of basalts by combining seismic experiments carried out around the two boreholes with studies of wire-line logs and cores. Results from the latter studies are presented here. The 700-m Glyvursnes-1 borehole was drilled in 2002 at the tip of the flat Glyvursnes peninsula near Tórshavn with wire-line coring technique (recovery >99.9%). The 3-inch diameter borehole was located such that it could serve as a focal point of seismic experiments at both land and sea. The 660-m Vestmanna-1 well was drilled in 1980 with the same technique 30 km farther north as part of the Faroes Deep Drilling Project. It was reamed (cleaned) in 2002 removing thick deposits of tufa to a final depth of 590 m. After drilling, both holes were wire-line logged with eight different slim-hole tools including optical televiewer, caliper, formation density, dual neutron porosity, focussed electric, full-wave sonic, spectral gamma and temperature/ conductivity. The logs were run one by one mounted with a gamma-ray unit for depth correlation.

Glyvursnes-1 starts in the lower part of the Upper Basalt Formation (UBF) and extends 345 m into the 1.4 km thick Middle Basalt Formation (MBF). The formation boundary is characterised by a 0.78-m tuffaceous bed overlain by a 9-m low-Ti basalt flow forming part of the so-called C-horizon. The old Vestmanna-1 borehole begins in MBF and extends 100 m into the Lower Basalt Formation (LBF) separated by a 0.7-m bed of basaltic conglomerate belonging to the coal-bearing formation (A-horizon). MBF is dominated by thin-bedded compound flows. These are mainly olivine-phyric in Vestmanna-1, but plagioclase-phyric in Glyvursnes-1. Tuffaceous beds are rare. UBF in Glyvursnes-1 is likewise dominated by plagioclase-phyric compound flows, but flow-units are generally thicker and tuffaceous beds (<6 m) more abundant.

The Glyvursnes and Vestmanna cores have been divided into >2000 units of massive, vesicular and brecciated lava, chilled lava skin and sediment beds. The wire-line logs were carefully depth-shifted to fit the detailed core descriptions. Sixty core samples from Glyvursnes-1 were selected for rock chemistry and 38 samples from both boreholes for measurements of bulk density, porosity, permeability, Vp and Vs (up to 300 kb confined pressure, dry or brine saturated). The two-receiver full-wave sonic log was processed several times at two service companies and GEUS to obtain Vp and Vs. The final results show excellent correlation with the velocities measured in GEUS Corelab. The density logs, on the other hand, show systematic differences from core data because of poor calibration and have been adjusted accordingly.

Measured physical properties show clear correlation with lithology. Examples are shown of the log response of the different volcanic lithologies and mean values are given. The prime parameter is porosity. Porosity measured by the neutron porosity tool is systematically higher than the gas porosity measured on cores. The reason is that the neutron tool measures the hydrogen content of the formation, which is assumed to be contained in free water. However, some water is bound in secondary minerals of the volcanic matrix. The degree of alteration of the rocks is therefore the second most important parameter. The matrix water have been either analysed or estimated from loss of ignition and subtracted from the neutron porosity to give true porosity. This results in a fine correlation with Vp and suggests that Vp can be used as a proxy for true porosity.

Papers

Japsen, P., Andersen, C., Andersen, H.L., Andersen, M.S., Boldreel, L.O., Mavko, G., Mohammed, N.G., Pedersen, J.M., Petersen, U.K., Rasmussen, R., Shaw, F., Springer, N., Waagstein, R., White, R.S. & Worthington M. 2005: Preliminary results from investigations of seismic and petrophysical properties of Faroes basalts in the SeiFaBa project. In*:* Doré, A.G. & Vining, B.A. (eds): Petroleum Geology: North-West Europe and Global Perspectives: Proceedings of the 6th Petroleum Geology Conference. Geological Society, London, 1461 - 1470.

Japsen, P., Andersen, M.S., Boldreel, L.O., Waagstein, R., White, R.S. & Worthington, M. 2004: Seismic and petrophysical properties of Faroes basalts (SeiFaBa project). Geological Survey of Denmark and Greenland Bulletin **4**, 53-65.

Petersen, U.K. 2006: Propagation, decay, phase conversion and recording of seismic waves in the basalt succession at Glyvursnes, the Faroe Islands - Summary of thesis in preparation. In: Japsen, P. , Andersen, M.S., Boldreel, L.O., White, R.S., Waagstein, R., Worthington, M. & the SeiFaBa group. Seismic and petrophysical properties of Faroes basalts (the SeiFaBa project) Final Report. Funded by the Sindri group. Danmarks og Grønlands Geologiske Undersøgelse Rapport **2006/29**.

Petersen, U.K., Andersen, M.S., White, R.S. & the SeiFaBa Group 2006: Seismic imaging of basalts at Glyvursnes, Faroe Islands: hunting for future exploration methods in basalt covered areas. First Break **24**, March 2006.

Shaw, F. 2006: 1-D heterogeneity and statistical studies of the Faroes wireline logs. In: Japsen, P. , Andersen, M.S., Boldreel, L.O., White, R.S., Waagstein, R., Worthington, M. & the SeiFaBa group. Seismic and petrophysical properties of Faroes basalts (the SeiFaBa project) Final Report. Funded by the Sindri group. Danmarks og Grønlands Geologiske Undersøgelse Rapport **2006/29**.

Shaw, F., Worthington, M.H., White, R.S., Andersen, M.S., Petersen, U.K. & the SeiFaBa Group 2006: Seismic attenuation in Faroe Islands basalts. Accepted for Geophysical Prospecting (pending minor revisions).

Preliminary results from investigations of seismic and petrophysical properties of Faroes basalts in the SeiFaBa project

P. JAPSEN,[1] C. ANDERSEN,[2] H. L. ANDERSEN,[3] M. S. ANDERSEN,[4]
L. O. BOLDREEL,[5] G. MAVKO,[6] N. G. MOHAMMED,[7] J. M. PEDERSEN,[8]
U. K. PETERSEN,[4] R. RASMUSSEN,[1] F. SHAW,[9] N. SPRINGER,[1] R. WAAGSTEIN,[1]
R. S. WHITE[7] and M. WORTHINGTON[9]

[1] *Geological Survey of Denmark and Greenland (GEUS), Øster Voldgade 10, DK-1350 Copenhagen K, Denmark (e-mail: pj@geus.dk)*
[2] *Geological Survey of the Faroes (JFS), Postbox 3169, Brekkutún 1, FO-188 Hoyvík, Faroe Islands (Present address: GEUS)*
[3] *Geological Institute, University of Aarhus, DK-Aarhus C, Denmark*
[4] *University of the Faroe Islands, Noatún 3, FO-100 Tórshavn, Faroe Islands*
[5] *Geological Institute, University of Copenhagen, Øster Voldgade 10, DK-1350 Copenhagen K, Denmark*
[6] *Department of Geophysics, Stanford University, California 94305-2215, USA*
[7] *Bullard Laboratories, University of Cambridge, Madingly Road, Cambridge CB3 0EZ, UK*
[8] *Ødegaard A/S, Titangade 15, DK-2200 Copenhagen N, Denmark*
[9] *Department of Earth Sciences, University of Oxford, Parks Road, Oxford OX1 3PR, UK*

Abstract: The development of methods of seismic imaging beneath basalts is still hindered by a lack of knowledge about the elastic properties of basaltic sequences and the degree of three-dimensional heterogeneity. The SeiFaBa project (2002–2005) is funded by the Sindri Group as part of the programmes for licensees within the Faroese area and will attempt to address these issues.

The Glyvursnes-1 well was drilled by SeiFaBa through the Upper Basalt Formation outside Tórshavn in 2002. A full core and numerous wireline logs were acquired from the 700 m deep well. During the same operations, the existing 660 m deep Vestmanna-1 well drilled mainly into the Middle Basalt Formation was reamed and logged. The two wells are central to a number of closely co-ordinated experiments, which are all targeted at creating models for seismic wave propagation through a succession of basalt by combining detailed analysis at core, log and seismic scales. Data from these two wells, in combination with the data for the Lopra-1 well drilled into the Lower Basalt Formation, will give new stratigraphic and petrophysical control of the Lower, Middle and Upper Basalt formations on the Faroes.

The seismic programme was initiated in 2002 and the main acquisition was carried out during 2003. The well site at Glyvursnes gives optimal conditions for combining VSP, offset-VSP and surface seismic experiments both onshore and offshore and the seismic effects of a nearby near-vertical shear zone can be studied in detail. Preliminary analysis of log data from the Lopra-1 well suggests that the acoustic properties of these basalt flows are mainly controlled by porosity of a stiff matrix filled with clay minerals and water. Further studies will allow for explanations of the sonic response of basalt in terms of physical and compositional properties and a better understanding of the seismic signatures of flood basalt successions.

Keywords: basalts, drill holes, Faroe Islands, petrophysics, seismic methods, sonic waves

DVD: Core display G2 is relevant to this chapter and can be viewed on the accompany DVD.

Flood basalt-covered basins exist world-wide along continental margins and are now targets for future hydrocarbon exploration. One such area is the Northwest European margin covering Norwegian, UK, Irish and Faroese waters, but similar cases include areas offshore Namibia, India, Brazil and West Greenland. Exploration strategies in Faroese waters are largely driven by the nearby British Foinaven Field, which is covered in the western part by basalt entering from the Faroese side (Roberts *et al.* 1999).

Offshore from the Faroe Islands it is generally difficult to image through the basalt cover by conventional seismic reflection methods. Alternative strategies include the use of wide-angle data from super-long offset profiles acquired with two seismic vessels (e.g. White *et al.* 1999, 2003), or, increasingly, with single 12 km long streamers; the use of seismic sources tuned to low frequencies (White *et al.* 2002; Ziolkowski *et al.* 2003); deployment of ocean bottom receivers (e.g. Scrutton 1970); and the possibility of utilizing converted waves (Purnell 1992) (although the latter seems not to be viable according to work by Hanssen *et al.* 2003).

Surprisingly, it is, however, possible to image through kilometre-thick basalts on some conventional profiles; details of basalt stratigraphy are revealed on old, reprocessed seismic profiles as well as on recently acquired profiles even though the imaging may be unsuccessful on near-by profiles (Fig. 1; e.g. Boldreel & Andersen 1993; Roberts *et al.* 1999). This stresses the need for a better understanding of the acoustic and other physical properties of basalt as well as of the degree of three-dimensional heterogeneity (cf. Kern & Richter 1979). The SeiFaBa project (‘Seismic

JAPSEN, P. *ET AL.* 2005. Preliminary results from investigations of seismic and petrophysical properties of Faroes basalts in the SeiFaBa project. *In*: DORÉ, A. G. & VINING, B. A. (eds) *Petroleum Geology: North-West Europe and Global Perspectives—Proceedings of the 6th Petroleum Geology Conference*, 1461–1470. © Petroleum Geology Conferences Ltd. Published by the Geological Society, London.

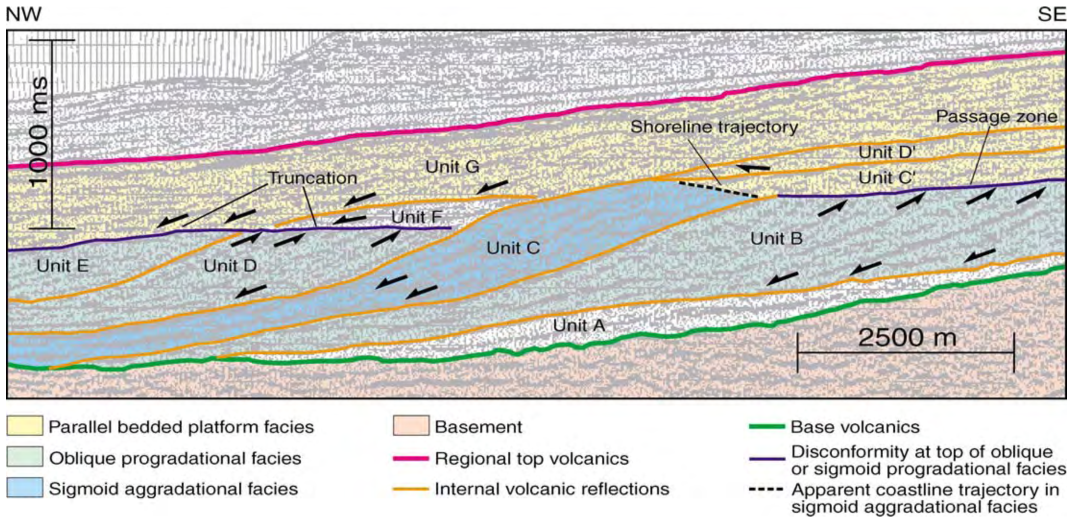

Fig. 1. Multi-channel reflection seismic profile across a basalt succession east of the Faroe Islands. Seismic stratigraphical principles can be applied in reflection seismic interpretation of the basalt succession and various units can be mapped. However, correlation between the seismic profiles of thick basalt offshore and the basalt formations onshore has proven difficult. With permission of BP. Originally published by Musgrove & Mitchener (1996), re-interpretation by M. S. Andersen (GEUS) and K. Hitchen (British Geological Survey).

and petrophysical properties of Faroes Basalt', 2002–2005) is funded by the Sindri Group as part of the programmes for licensees within the Faroese area and will address these issues with special focus on the subaerially extruded flood basalts.

The Glyvursnes-1 well was drilled to 700 m by SeiFaBa outside Tórshavn in 2002 (Fig. 2; Waagstein *et al.* 2003). During the same operations, the existing 660 m deep Vestmanna-1 well was reamed and logged. The purpose of the experiments at these wells is to provide a link from the hand-specimen scale of the core–log, through the slightly larger averaging of borehole logs to seismic scales. The seismic scales will range from high-resolution VSPs and multi-channel land arrays, to onshore–offshore shooting using wide-band airguns, to the truly long-period response of the basalt flows using teleseismic arrivals recorded by a tight array of broad-band (0.03–100 Hz) seismometers. Glyvursnes is suited for combining VSP and surface seismic experiments: the terrain is

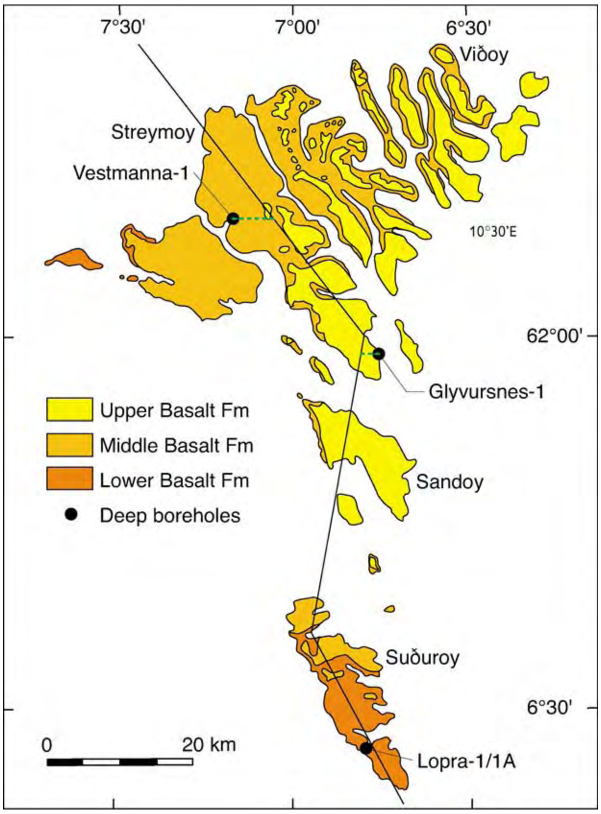

Fig. 2. Geological map of the Faroe Islands showing the location of deep boreholes, distribution of the three Palaeogene basalt formations and the line of section in Fig. 4 (modified after Waagstein 1998).

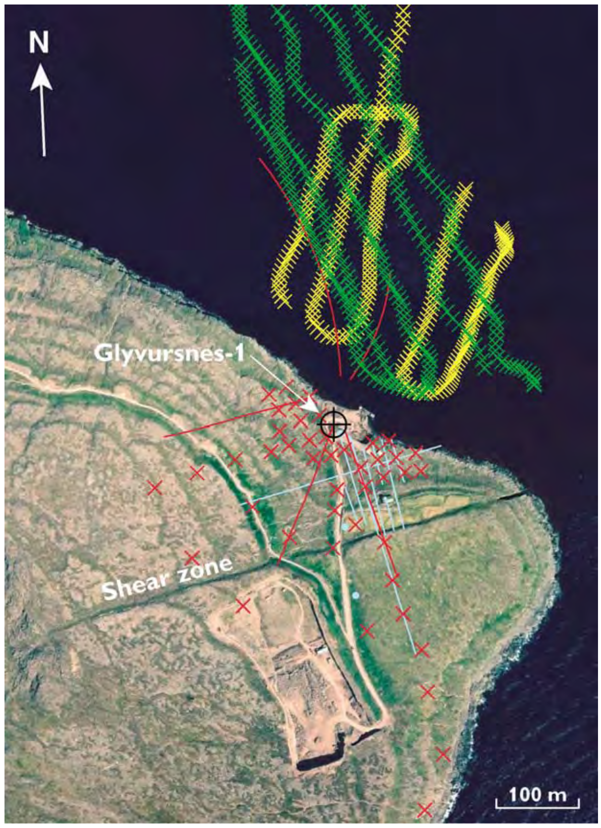

Fig. 3. Airphoto of Glyvursnes with well location and outline of seismic data recording on Glyvursnes in 2003. Red crosses indicate the locations of permanent seismometers during the experiments. Blue dots mark the positions of the three airgun pits for the VSP experiments. Blue lines mark the locations of the 14 Hz geophone strings used for the onshore reflection profiles. Red lines show the locations of onshore geophone strings and the tethered streamer during the offshore–onshore experiments and marine reflection experiment. Yellow and green crosses mark shotpoints for the marine reflection experiment.

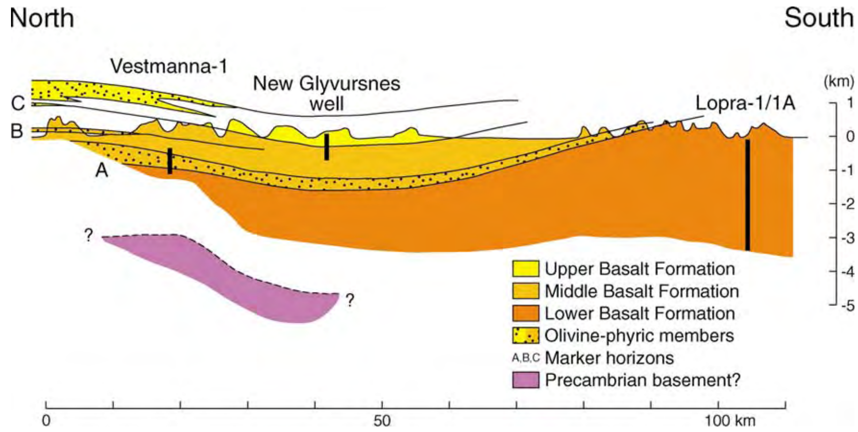

Fig. 4. North–South section through the Faroe Islands along the line in Fig. 2. The strata in the northern Faroes are partly extrapolated from exposures far west and east of the line of section. Projection of exposures and well stratigraphy (dashed lines) is due east–west along the regional dip. The top of the drilled section in the Vestmanna well thus projects below sea level (modified after Waagstein 1988).

relatively flat and the seismic effects of a nearby near-vertical shear zone can be studied in detail (Fig. 3).

The investigations will provide a unique dataset and new understanding of the petrophysical and seismic properties of Faroes basalt. The relations of sonic velocities of basalt to porosity, composition, stress, burial depth and fluid content will be studied through analysis of well logs and core material. This will allow for explanations of the sonic response of basalt in terms of physical and compositional properties and a better understanding of the seismic signatures of flood basalt successions.

Regional outline

Break-up of the North Atlantic in the Palaeogene was accompanied by widespread magmatism caused by interaction of the Iceland mantle plume with lithospheric rifting (White & McKenzie 1989). Massive lava flows extend away from the rifted margin across the hydrocarbon-bearing basins along much of the northern North Atlantic margin (Barton & White 1997). The Faroe Islands comprise a fragment of continental crust capped by up to 7 km of Palaeogene lavas produced during continental break-up and underlain by an underplated or heavily intruded lower-crustal region (Richardson *et al.* 1998, 1999).

Extrusive igneous rocks dominate the northwestern flank of the Faroes–Shetland Basin. Flood basalts created at the time of break-up between the Faroe Islands and East Greenland extend over >200 000 km^2 (Roberts *et al.* 1984; Andersen 1988; Waagstein 1988; Larsen *et al.* 1999), at least 40 000 km^2 of which lie in the Faroe–Shetland Basin (Naylor *et al.* 1999). The lavas flowed *c.* 150 km eastward away from the Faroes Islands, feathering out in the Faroes–Shetland Trough (White *et al.* 2003). The lavas are 59–55 Ma old and are divided into the Lower, Middle and Upper Basalt formations (Fig. 4; Rasmussen & Noe-Nygaard 1970; Waagstein 1988; Larsen *et al.* 1999; Waagstein *et al.* 2002).

The extensive cover of basaltic rocks around the Faroes is characterized by densities and seismic velocities that are high compared to sedimentary successions. Seismic facies analysis of a large dataset from the region show that the dominant lithology is parallel-bedded basalts that are comparable to the basalts exposed on the Faroe Islands where two contrasting lava morphologies are dominant (Figs 5 and 6).

- Aa flows are generally thick (10–50 m), with sediments and tuffaceous deposits in between. These thick-bedded basalts are characterized by systematic porosity variations within individual basalt beds and they dominate the Lower Basalt Formation. This lithologic succession is characterized by large, systematic, internal variations of most physical properties (e.g. Planke & Eldholm 1994; Boldreel 2003).
- Pahoehoe flows are often of compound type, being made up of fairly thin basalt beds (about 2 m on average). The compound flows may be separated by thin beds of tuff. Thin-bedded basalts are dominant in the Middle Basalt Formation and part of the Upper Basalt Formation. The variation of physical properties, such as density and velocity, is moderate in this type of lava flow, but it is still significant compared to that of most sediments (e.g. Nielsen *et al.* 1984).

No systematic studies have been carried out on the elastic properties of thin-bedded basalts in the Faroe region and

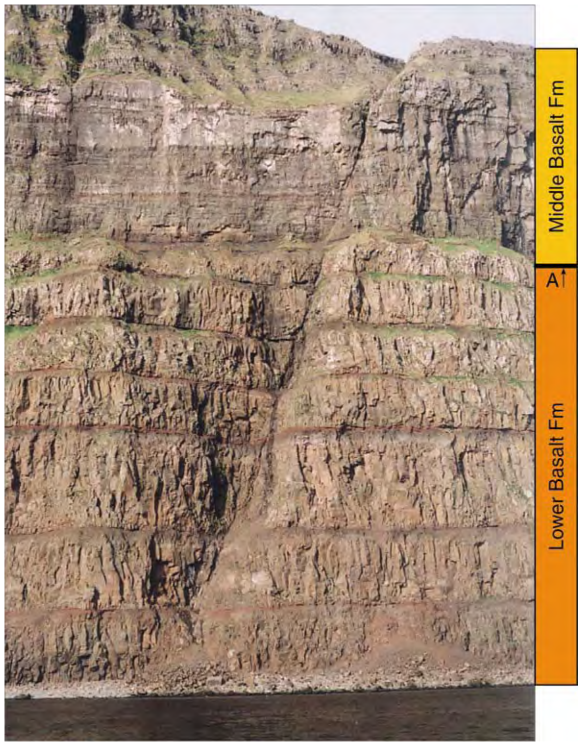

Fig. 5. Photo of contrasting lava morphologies exposed on a 400 m high cliff, Prestfjall, west coast of Suduroy (from Waagstein 1998). Thick simple aa flows (Lower Basalt Formation) overlain by compound thin-bedded pahoehoe flows (Middle Basalt Formation) with the coal-bearing A-horizon in between. The flows of the Lower Basalt Formation have a massive centre or core overlain by a thick purple to red rubbly crust and red tuffaceous clay.

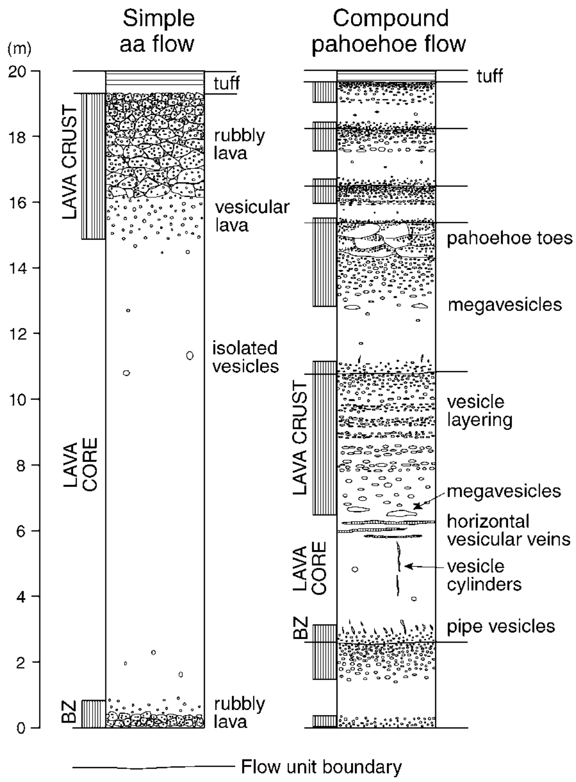

Fig. 6. Sketch of typical lava morphologies of the Faroes (from Waagstein 1998). Thick aa flows have non-vesicular cores grading into a rubbly top and base. Pahoehoe flows have smooth undulating tops and are typically compound, consisting of thin beds of variable thickness, vesicle abundance and mineralization.

understanding of the distribution of elastic properties in thick-bedded basalts is based on only a few studies (e.g. Kern & Richter 1979).

Drilling and logging at Glyvursnes and Vestmanna

The Lower, Middle and Upper Basalt formations are all exposed on the Faroe Islands due to late Cenozoic uplift and erosion (Andersen *et al.* 2002). Thick sections of each formation have been drilled by three deep onshore wells (Figs 2 and 4).

- The Vestmanna-1 well was drilled to 660 m in 1980 (Waagstein & Hald 1984) and re-opened to 590 m in 2002 and logged as part of the SeiFaBa project (Fig. 7). The hole is located 30 km northwest of Glyvursnes-1 in the lower part of the Middle Basalt Formation and extends 100 m into the Lower Basalt Formation. A full core was taken.
- The Lopra-1/1A well was drilled through the Lower Basalt Formation to 2.2 km in 1981 and deepened to 3.6 km in 1996 without reaching the base of the volcanics (Fig. 8) (Hald & Waagstein 1984; Nielsen *et al.* 1984; Kiørboe & Petersen 1995; Christie *et al.* 2002; Boldreel 2003). The upper 2.5 km are flood basalts and the remaining section is dominated by subaqueous hyaloclastites (Waagstein 2002). Six short cores of basalt were taken from this well.
- The Glyvursnes-1 well was drilled to 700 m in autumn 2002 as a slim borehole with wireline coring technique around the boundary between the Middle and Upper Basalt formations on the shore of Glyvursnes (Fig. 9). The drilling was carried out by the Finnish company Suomen Malmi (SMOY). A full core was taken (Fig. 10).

An extensive logging programme was run in the Glyvursnes and Vestmanna boreholes by Robertson Geologging in 2002, comparable to that previously run in the Lopra well (1981, 1996). It included optical televiewer, caliper, natural gamma, resistivity,

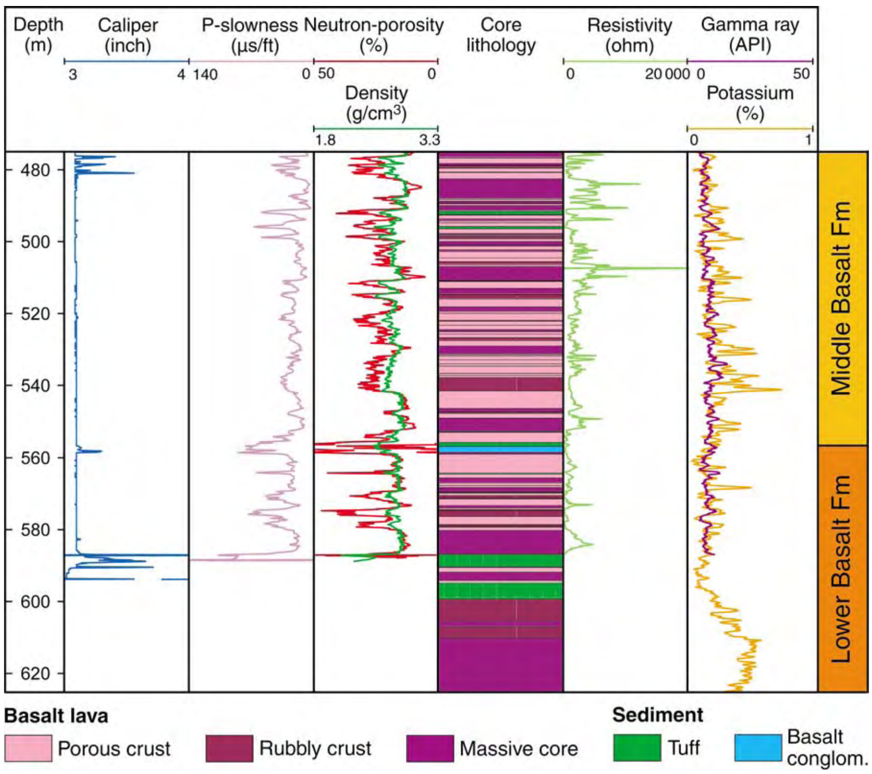

Fig. 7. Composite log from the lowermost part of the Middle Basalt Formation and the uppermost part of the Lower Basalt Formation in the Vestmanna-1 well measured after the re-opening of the well.

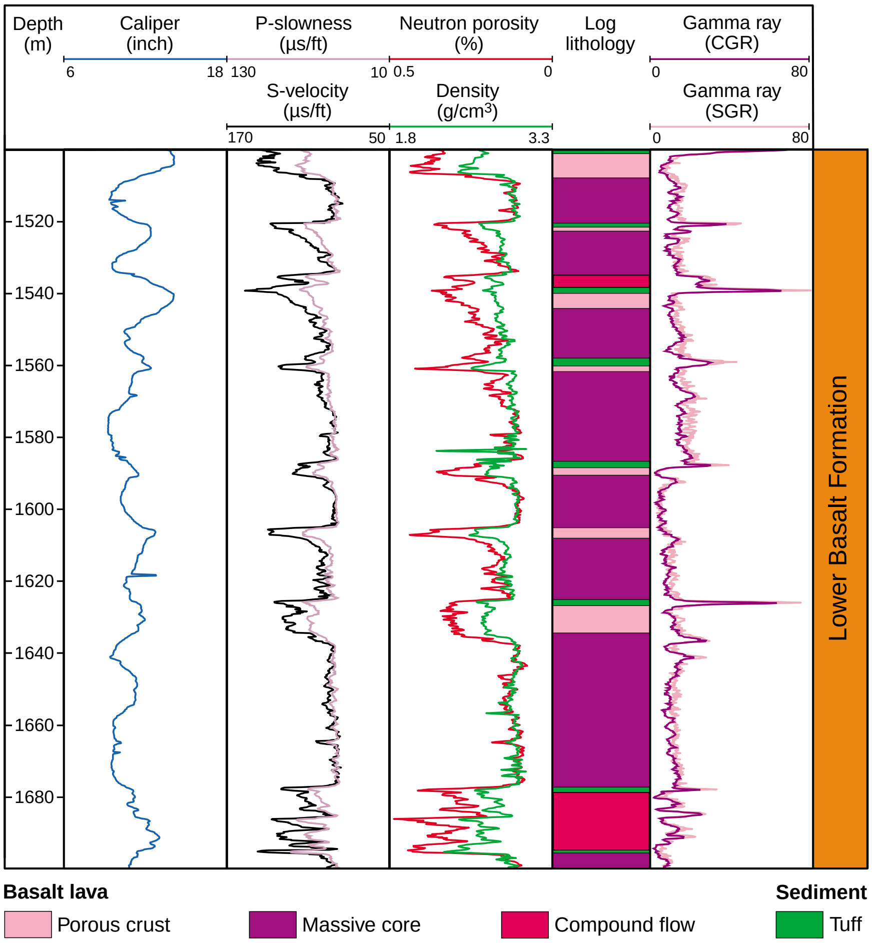

Fig. 8. Composite log from the Lopra-1/1A well. Note the variations in the physical properties within the individual lava flows. CGR, calculated (clay) gamma ray (Th+K); SGR, spectral gamma ray (Th+K+U). After Boldreel (2003).

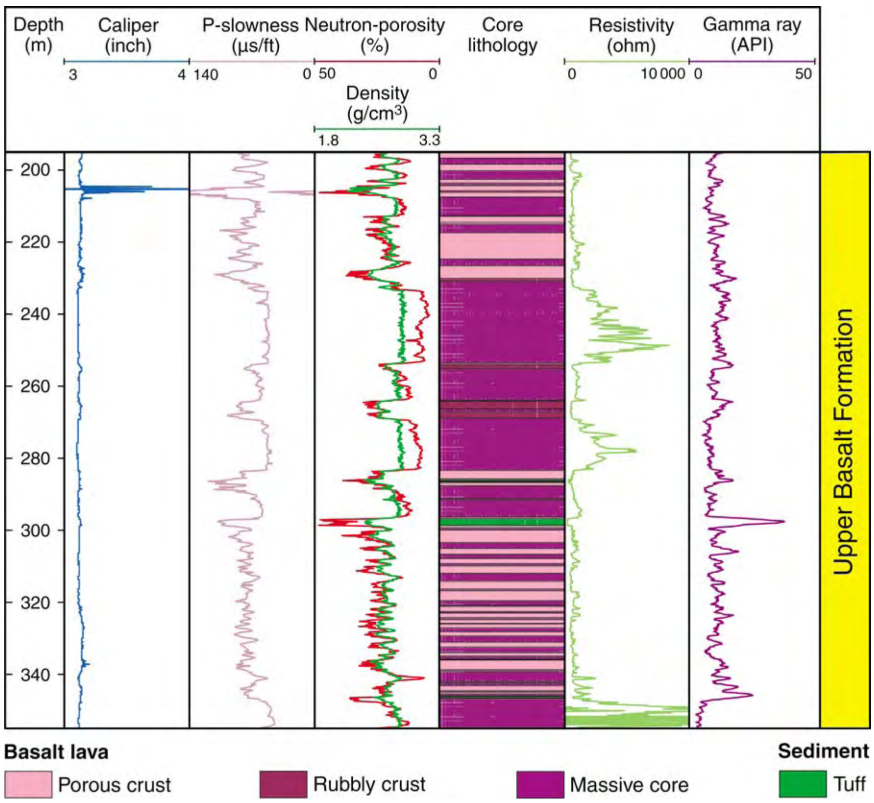

Fig. 9. Composite log from the Glyvursnes-1 well. Note the correlation between P-slowness (P-velocity) and density/neutron porosity that reflects the porosity contrast between the porous crust and the massive core of the basalt flows.

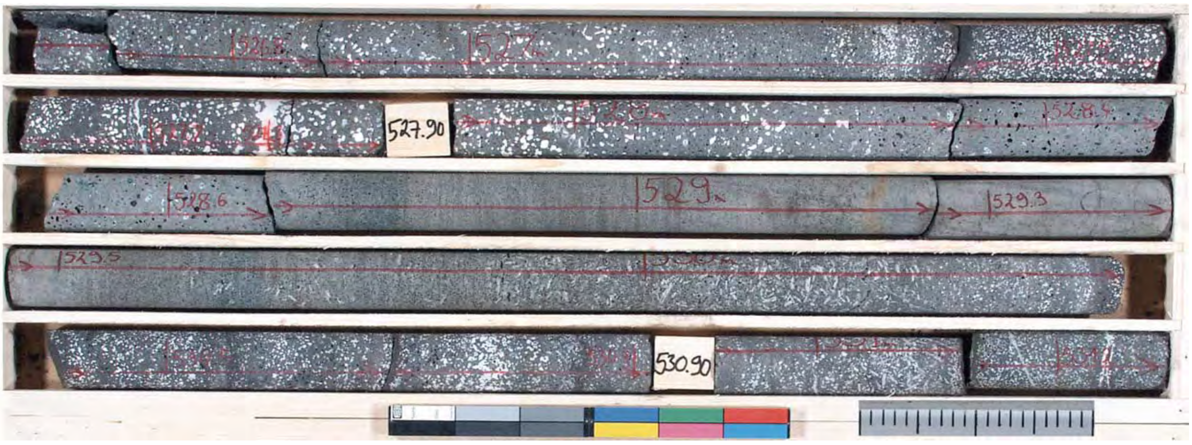

Fig. 10. Photo of the Glyvursnes-1 core in the interval 526.64–531.29 m (box 115), displaying strong variations in vesicularity and mineralogy of the lava flows. 526.64–527.41 m: vesicular, aphyric basalt (almost one complete flow-unit); 527.41–528.63 m: lava crust of vesicular, aphyric basalt with 1 cm thick dark top of altered glass (chill); 528.63–530.25 m: lava core of massive (i.e. non-vesicular), aphyric to plagioclase-phyric basalt; 530.25–530.69 m: basal zone of vesicular, sparsely plagioclase-phyric to aphyric basalt; 530.69–530.85 m, 530.85–531.12 m and 531.12–534.39 m: three vesicular flow-units of aphyric to plagioclase-phyric basalt, with 1 cm thick dark tops of altered glass (only 0.17 m of the lower unit shown). The vesicles are mainly filled with zeolites.

neutron porosity, density, full wave sonic, spectral gamma (of poor quality) and temperature/conductivity.

The Vestmanna and Glyvursnes boreholes penetrate the lowermost 550 m and the uppermost 450 m of the 1400 m thick Middle Basalt Formation, respectively. In both sections the Middle Basalt Formation is characterized by the presence of plagioclase-phyric compound flows composed of thin flow-units of variable porosity and by rare thin beds of tuff. The lowermost part of the Middle Basalt Formation in Vestmanna (Fig. 7) and the lowermost 70 m of the Upper Basalt Formation in the Glyvursnes borehole are very similar (Fig. 9). The overlying section between 230 and 285 m in Glyvursnes-1 consists of a few relatively thick plagioclase-phyric flow-units forming two (?) compound flows (the Tórshavn flows), which are morphologically more similar to the flows of the Lower Basalt Formation, although the latter are near-aphyric.

The Glyvursnes, Vestmanna and Lopra boreholes represent sections of increasing age and depth of burial. The Glyvursnes core displays variable degrees of mineralization of vesicles and voids, while the Vestmanna core is more completely mineralized (Jørgensen 1984). The depth of burial is clearly reflected by increasing palaeotemperatures as estimated from the zeolite parageneses found in Vestmanna and Lopra (Jørgensen 1984; Waagstein *et al.* 2002).

Rock physics properties of Faroes basalts

A preliminary investigation of the rock physics properties of flood basalt on the Faroes has been carried out based on the extensive logging data from the Lopra-1/1A well. A detailed stratigraphy of basalt flows, sediment/tuff layers and dolerite dykes was established for the hole drilled in 1981 based on drill cuttings and cores and compared with the density, porosity, resistivity and gamma-ray log-response (Hald & Waagstein 1984; Nielsen *et al.* 1984).

A more extensive logging programme, including a full wave sonic log was run in the deepened hole from 200 m to TD. The new logs have been used to establish a detailed stratigraphy for the flood basalt sequence between 200 m and 2500 m by dividing the lava flows into massive and porous parts (Boldreel 2003). The porous upper part of a flow is characterized by high values of the neutron porosity log, low values of density, low P- and S-velocities and intermediate values of the caliper. This, in contrast, to the rather massive part characterized by high values of density, high P- and S-wave velocities and low values of the neutron porosity. The basal zone is seldom identified due to the small vertical extent of the zone. In addition, 52 intervals with >1% potassium were mapped at the flow boundaries and interpreted as altered basalt or tuffaceous sediments. These intervals were also identified from the high values of neutron porosity and caliper, in combination with low values of density, P- and S-velocity. Two dolerite dykes intruding the basalt column were identified by having the highest values of density, P- and S-velocities and lowest values of the neutron porosity. The logs show that large differences exist in acoustic properties within the basalt column and these are attributed to significant variations in porosity – both in the form of vesicles and fractures – across each flow unit.

The gamma-ray log for flood basalts in the Lopra-1 well reveals intermediate values for the porous crust (red curve in Fig. 11) and the massive basalt facies (blue). Systematically lower values are observed for the dolerite (magenta) and higher values for the tuffaceous sediments (green) in accordance with how this unit was defined. The bulk density log shows large fluctuations ($1.2–3.1\ \mathrm{g\,cm^{-3}}$), but the high-density limit of the curve increases only slightly with depth, while the low-density values are wildly fluctuating. It is believed that the high bulk densities are asymptotically approaching the mineral density as the porosity approaches zero, while the low density values vary with porosity, as well as caliper anomalies. The P-wave velocities have wide fluctuations ($3–7\ \mathrm{km\,s^{-1}}$), though there are systematic differences among the various facies: the tuffaceous sediments have the lowest velocities; the porous crusts have slightly higher velocities, the massive basalts are higher still, and the dolerites have the highest velocities.

P-velocities increase consistently with bulk density (and, therefore, decreasing porosity), with all four facies falling roughly along the same trend (Fig. 12). The sediments and crusts, being most porous, have the lowest velocities and densities. The massive basalts span a large range of velocity and density, while the dolerites seismically resemble the lowest porosity basalts. Superimposed on Figure 12 are empirical upper bounds on density and velocity (black lines), which are taken as estimates of the mineral properties. These values are consistent with a mineral having properties similar to a mixture of plagioclase and pyroxene (Table 1). Note that the upper density limit for the dolerite is slightly below the limit for the massive basalt. This is in agreement with the relatively low iron content of the dolerite observed from rock chemistry of cuttings from the well (Hald & Waagstein 1984).

P-velocities decrease consistently with increasing neutron porosity, with all four facies falling approximately along the same trend (Fig. 13). This supports the idea that porosity is the dominant parameter controlling the velocity, even though neutron porosity depends on both the free water in the pore space and the

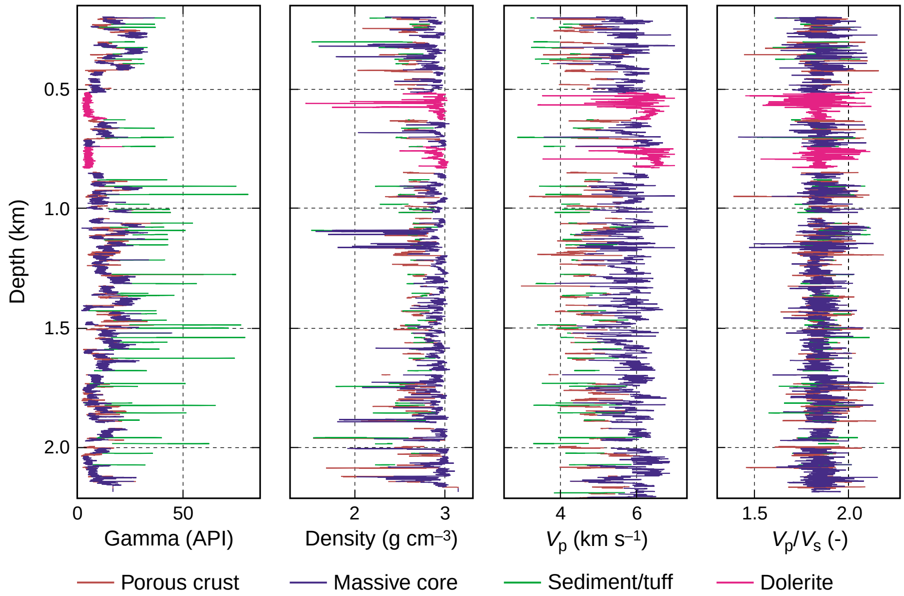

Fig. 11. Log data for the flood basalt sequence in well Lopra-1 above 2.2 km. The colour-coded lithological facies were interpreted by integrated log analysis (after Boldreel 2003). Sediment/tuff interbeds are intervals with >1% potassium.

water bound in clay minerals. The Lopra-1 data can be compared with effective medium models for velocity vs. porosity, computed using Berryman's (1980) formulation of the self-consistent approximation where the pores are assumed to take the shape of oblate spheroids, having varying aspect ratios. While spheroidal inclusion models are idealized, the trends of decreasing pore stiffness with decreasing aspect ratio make physical sense. The overall trends of the various facies can be represented with pores that are nearly spherical (aspect ratio 1) or slightly flattened (aspect ratio 0.3), as one might expect for vesicular basalts. Those data that fall at velocities significantly below these trends are consistent with the occurrence of fractures, which can be represented with very low aspect ratios.

V_p and V_s are highly correlated as one would expect for a fixed mineral composition and it is observed that all four facies fall along the same narrow trend (nearly constant Poisson's ratio of 0.3; Fig. 14). High-velocity points lying to the upper right are dominated by the mineralogy, while porosity increases along the trend to the lower left, where the low-velocity points are dominated by the pore fluid.

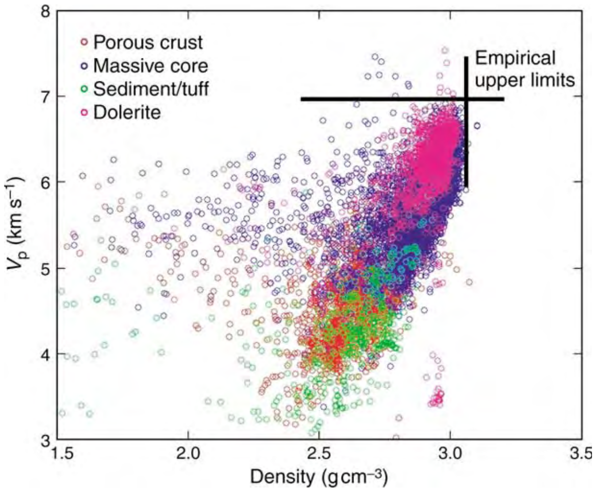

Fig. 12. Cross-plot of V_p vs. density for flood basalts in well Lopra-1. The black lines are empirical upper limits which are taken as rough estimates of the mineral properties (cf. Fig. 14; Table 1).

The seismic experiments at Glyvursnes

Although the extrusive basalt flows in the Faroes–Shetland Basin are generally sub-horizontal on a large scale, there are often large physical property variations (largely governed by porosity) within individual flows and sometimes locally rugged small-scale relief on the tops of flows. The strong layering and local rugged relief may cause some or all of the following: internal multiples, forward-and backscattering of the incident energy, multiple mode conversion, anisotropy, absorption and geometric spreading and low-pass filtering of the energy that propagates through a stacked layer of basalt flows.

Since flow thicknesses are an order of magnitude or more smaller than the seismic wavelength, reflections are rarely seen from individual flows: the seismic response depends on the complex interactions of reflections off multiple flow units (e.g. Planke & Eldholm 1994; Smallwood *et al.* 1998). In the specific case of the Faroe basalts, synthetic sections representing multiple flows show that the reflectivity pattern and average velocities vary between the Lower, Middle and Upper Basalt formations, which each have distinctively different average flow thicknesses and properties. To study these effects, three experiments were carried out around the Glyvursnes-1 borehole in 2003.

(1) Three VSP surveys with source offsets of 14 m, 242 m and 415 m. The source was a 150 in^3 (2.46 l) air gun deployed in water-filled pits. The two offset locations were on either side of a well-defined dyke/fracture zone.

Table 1. Physical properties of typical rock-forming minerals and empirical upper limit for flood basalts estimated from log data, Lopra-1 well (Figs 12 and 14; Mavko *et al.* 1998)

	Density (g cm^{-3})	V_p (km s^{-1})	V_s (km s^{-1})	Bulk modulus (GPa)	Shear modulus (GPa)
Pyroxene (Augite)	3.26	7.22	4.18	94	57
Plagioclase (Albite)	2.63	6.46	3.12	76	26
Olivine	3.32	8.45	0.49	130	80
Flood basalts, Lopra-1	3.07	6.95	3.75	91	43

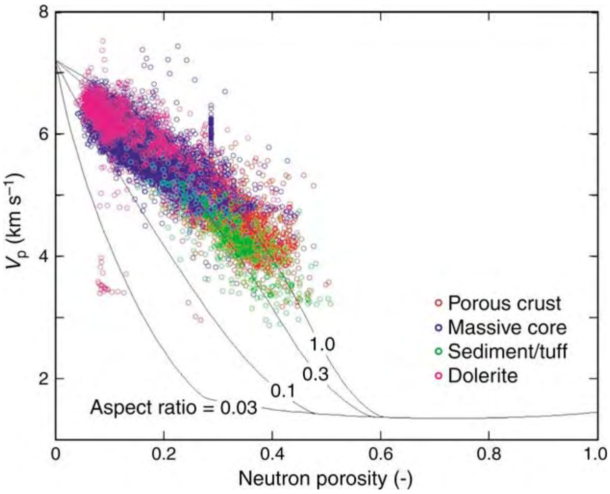

Fig. 13. Cross-plot of V_p vs. neutron porosity for flood basalts in Lopra-1 well. The overall trend of the lithological facies can be represented by pores that are nearly spherical (aspect ratio 1) or slightly flattened (aspect ratio 0.3). Solid black curves are effective medium models assuming ellipsoidal inclusions of four different aspect ratios based on mineral properties similar to pyroxene (Table 1; Berryman 1980).

(2) Onshore and offshore high-resolution reflection data acquisition along the lines shown in Figure 3 (0.5 ms sample interval and 3 s recording length). All of the onshore reflection seismic data were acquired with 10 m shot spacing (250 g charges) and 5 m geophone spacing using 14 Hz 1-component geophones. The two 625 m lines were shot with the charges along the line, while the short profiles were acquired with the source displaced laterally with 25 m, 50 m or 75 m offset relative to the geophone string. The marine seismic reflection data were acquired on a tethered streamer using a moving 160 in^3 (2.62 l) air-gun cluster. Additional data were acquired at longer offsets, using both the 160 in^3 (2.62 l) source and a 860 in^3 (14.09 l) source.

(3) A dense array of 45 autonomous Guralp (6TD) seismometers was deployed for a six-month period around the site of the borehole. During the periods of controlled source seismic shooting, all sites maintained a sampling rate of 200 samples s^{-1}. For intervening periods when they were recording earthquakes, a sampling rate of 100 samples s^{-1} was used. In addition, three 400 m long (120 channel) independent temporary land arrays were set up in September 2003 using a mixture of one- and three-component geophones.

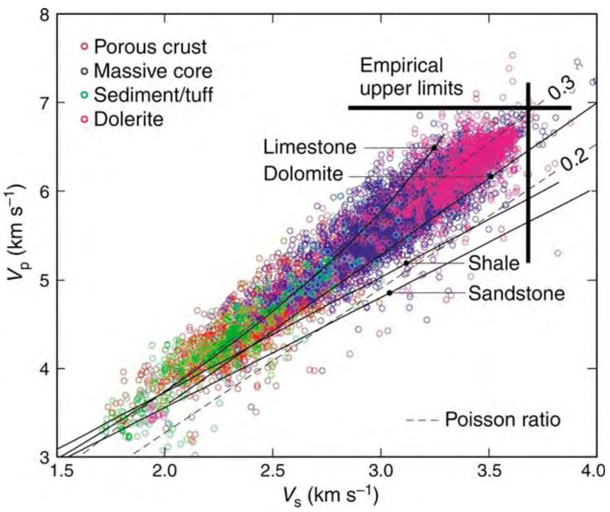

Fig. 14. Cross-plot of V_p vs. V_s for flood basalts in Lopra-1 well. Empirical lines for different sediments are shown for reference (solid lines; Greenberg & Castagna 1992). Dashed lines represent constant Poisson's ratio. Thick lines are empirical upper limits which are estimates of the mineral properties (cf. Fig. 12; Table 1).

Throughout acquisition of the marine reflection seismic and the offshore–onshore, wide-angle seismic data, a three-component borehole seismometer was held clamped at 400 m in the Middle Basalt Formation in the Glyvursnes borehole.

The three experiments are closely integrated. During analysis, it will be possible to combine data recorded by the three-component borehole seismometer with sub-critical reflection gathers, measured by the streamer, and post-critical events, measured by both the temporary and autonomous array. The characteristics of wave propagation, including P- and S-wave response, anisotropy, absorption and scattering may be investigated in detail and at different scales. Recording of teleseismic phases by the autonomous array will make it possible to explore the response of the layered basalt flows to a wider spectrum of frequencies than that provided by the air-gun sources alone. It will thus potentially be possible to measure the crustal thickness and evaluate evidence for underplating from receiver function analysis.

Future work

Ultrasonic velocities and other parameters will be measured on core samples from drill holes in the Faroe Islands. The samples will be investigated under varying pressure for both dry and saturated samples. The investigations of the velocity–porosity relations of basalts will focus on matrix properties but will also take into account variations in magma type, secondary mineralization, pore shapes and fractures.

Lithostratigraphic interpretation of logs will be carried out and the results correlated with petrography, rock chemistry and rock physical lab measurements of core samples for scaling of the core and log data to a seismic scale for data from flood basalts of all three formations. Well log data will be examined to find how magma type and secondary mineralization influence the relation between velocity and porosity of basalt. Supplementary analysis of well logs from commercial wells in the Faroe–Shetland Basin will be carried out to provide additional data concerning the distribution of elastic properties of the basalts around the Faroes.

Future work on seismic field data will include:

- VSP data processing to extract up and downgoing wave fields at both sites and matching with synthetic seismograms derived from log data;
- analysis of offset VSP data at the sites of Glyvursnes-1 and Vestmanna-1 to investigate evidence for velocity and attenuation anisotropy;
- investigation of causes of noise and aberrations in the images;
- investigation of causes of P- to S-mode conversion, anisotropy and shear wave imaging at both sites;
- specific investigation of causes of seismic attenuation (intrinsic, scattering) in core, log and VSP data;
- investigation of seismic characteristics of a well-defined fracture zone exposed at the Glyvursnes locality in VSP and surface seismic data. Reflection, transmission, attenuation and scattering as a function of azimuth and incidence angle;
- seismic modelling of attenuation and the seismic signatures of flood basalt successions for typical variations in thickness and internal structure of individual lava flows and volcaniclastic beds.

Summary

Drilling of the new borehole at Glyvursnes and re-logging of Vestmanna-1, in combination with the extensive dataset for the Lopra-1 well, will give valuable new stratigraphic and petrophysical control of the Lower, Middle and Upper Basalt formations on the Faroes.

Preliminary analysis of log data from the flood basalts in the Lopra-1 well suggests that the acoustic properties of these basalt flows are mainly controlled by porosity and the high correlation between P- and S-velocities may be indicative of a constant mineralogical composition for the Lower Basalt Formation. The new data acquired for the Upper and Middle Basalt formations may reveal how the acoustic properties of these formations differ from those of the Lower Basalt Formation.

The planned experiments will provide a link from the hand-specimen scale, through the slightly larger averaging of borehole logs, to seismic scales ranging from high-resolution VSPs and multi-channel land arrays, to onshore–offshore shooting using wide-band air guns, to the truly long-period response of the basalt flows using teleseismic arrivals.

Thanks to the Sindri group for permission to publish results from the Glyvursnes-1 well. SeiFaBa is funded collectively by oil companies operating in the Faroe sector (the Sindri Group): Agip Denmark; Amerada Hess (Faroes) Limited; Anadarko Faroese Company; BG International; BP Amoco Exploration (Faroes) Limited; DONG Efterforskning og produktion A/S; Enterprise Oil Exploration Limited; Føroya Kolvetni P/K; P/F Atlantic Petroleum; Philips Petroleum Europe Exploration Limited; Shell UK Limited; Statoil Færøyene AS; Veba Oil & Gas GmbH. The paper is published with permission of the Geological Survey of Denmark and Greenland.

References

Andersen, M. S. 1988. Late Cretaceous and Palaeogene extension and volcanism around the Faeroe Islands. *In*: Morton, A. C. & Parson, L. M. (eds) *Early Tertiary Volcanism and the Opening of the NE Atlantic*. Geological Society, London, Special Publications, **39**, 115–122.

Andersen, M. S., Sørensen, A. B., Boldreel, L. O. & Nielsen, T. 2002. Cenozoic evolution of the Faroe Platform: comparing denudation and deposition. *In*: Doré, A. G., Cartwright, J. A., Stoker, M. S., Turner, J. P. & White, N. (eds) *Exhumation of the North Atlantic Margin: Timing, Mechanisms and Implications for Petroleum Exploration*. Geological Society, London, Special Publications, **196**, 291–311.

Barton, A. J. & White, R. S. 1997. Crustal structure of the Edoras Bank continental margin and mantle thermal anomalies beneath the North Atlantic. *Journal of Geophysical Research*, **102**, 3109–3129.

Berryman, J. G. 1980. Long-wavelength propagation in composite elastic media, I and II. *Journal Acoustical Society America*, **68**, 1809–1831.

Boldreel, L. O. 2003. Identification and characterization of basalt and sediment units based on wireline logs from the Lopra deep well, Faroe Islands, NE-Atlantic Ocean. Abstract EGS02-A-05330, presented at the EGS General Assembly XXVII Nice, France.

Boldreel, L. O. & Andersen, M. S. 1993. Late Paleocene to Miocene compression in the Faroe–Rockall area. *In*: Parker, J. R. (ed.) *Petroleum Geology of Northwest Europe: Proceedings of the 4th Conference*. Geological Society, London, 1025–1034.

Christie, P., Gollifer, I. & Cowper, D. 2002. Borehole seismic results from the Lopra deepening project. *Journal of Conference Abstracts*, **7**, 138.

Greenberg, M. & Castagna, J. 1992. Shear wave velocity estimation in porous rocks: Theoretical formulation, preliminary verification and applications. *Geophysical Prospecting*, **40**, 195–209.

Hald, N. & Waagstein, R. 1984. Lithology and chemistry of a 2-km sequence of Lower Tertiary tholeiitic lavas drilled on Suduroy, Faroe Islands (Lopra-1). *In*: Berthelsen, O., Noe-Nygaard, A. & Rasmussen, J. (eds) *The deep drilling project 1980–1981 in the Faeroe Islands*. Føroya Frodskaparfelag, Torshavn, 15–38.

Hanssen, P., Ziolkowski, A. & Li, X.-Y. 2003. A quantitative study on the use of converted waves for sub-basalt imaging. *Geophysical Prospecting*, **51**, 183–193.

Jørgensen, O. 1984. Zeolite zones in the basaltic lavas of the Faroe Islands – A quantitative description of the secondary minerals in the deep wells of Vestmanna-1 and Lopra-1. *In*: Berthelsen, O., Noe-Nygaard, A. & Rasmussen, J. (eds) *The Deep Drilling Project 1980–1981 in the Faeroe Islands*. Føroya Frodskaparfelag, Torshavn, 71–91.

Kern, H. & Richter, A. 1979. Compressional and shear wave velocities at high temperature and confining pressure in basalts from the Faroe Islands. *Tectonophysics*, **54**, 231–252.

Kiørboe, L. & Petersen, S. A. 1995. Seismic investigation of the Faroe basalts and their substratum. *In*: Scrutton, R. A., Stoker, M. S., Shimmield, G. B. & Tudhope, A. W. (eds) *The Tectonics Sedimentation and Palaeoceanography of the North Atlantic Region*. Geological Society, London, Special Publications, **90**, 111–123.

Larsen, L. M., Waagstein, R., Pedersen, A. K. & Storey, M. 1999. Trans-Atlantic correlation of the Palaeogene volcanic successions in the Faeroe Islands and East Greenland. *Journal of the Geological Society, London*, **156**, 1081–1095.

Mavko, G., Mukerji, T. & Dvorkin, J. 1998. *The Rock Physics Handbook*. Cambridge University Press.

Musgrove, F. M. & Mitchener, B. 1996. A structural history of the Rockall Trough, west of Britain. *Petroleum Geoscience*, **2**, 353–360.

Naylor, P. H., Bell, B. R., Jolley, D. W., Durnall, P. & Fredsted, R. 1999. Palaeogene magmatism in the Faeroe–Shetland Basin: influences on uplift history and sedimentation. *In*: Fleet, A. J. & Boldy, S. A. R. (eds) *Petroleum Geology of Northwest Europe: Proceedings of the 5th Conference*. Geological Society, London, 545–558.

Nielsen, P. H., Stefánsson, V. & Tulinius, H. 1984. Geophysical logs from Lopra-1 and Vestmanna-1. *In*: Berthelsen, O., Noe-Nygaard, A. & Rasmussen, J. (eds) *The Deep Drilling Project 1980–1981 in the Faeroe Islands*. Føroya Frodskaparfelag, Torshavn.

Planke, S. & Eldholm, O. 1994. Seismic response and construction of seaward dipping reflectors in flood basalts: Vøring volcanic margin. *Journal of Geophysical Research*, **99**, 9263–9278.

Purnell, G. W. 1992. Imaging beneath a high-velocity layer using converted waves. *Geophysics*, **57**, 1444–1452.

Rasmussen, J. & Noe-Nygaard, A. 1970. *Geology of the Faroe Islands*. Danmarks Geologiske Undersøgelse, 1. Rekke, **25**.

Richardson, K. R., Smallwood, J. R., White, R. S., Snyder, D. & Maguire, P. K. H. 1998. Crustal structure beneath the Faroe Islands and the Faroe-Iceland Ridge. *Tectonophysics*, **300**, 159–180.

Richardson, K. R., White, R. S., England, R. W. & Fruehn, J. 1999. Crustal structure east of the Faroe Islands. *Petroleum Geoscience*, **5**, 161–172.

Roberts, D. G., Backman, J., Morton, A. C., Murry, J. W. & Keene, J. B. 1984. US Government Printing Office, Washington, D.C., Evolution of volcanic rifted margins: synthesis of Leg 81 results on the west margin of Rockall Plateau. *Initial Reports of the Deep Sea Drilling Project*, **81**, 883–911.

Roberts, D. G., Thompson, M., Mitchener, B., Hossack, J., Carmichael, S. M. M. & Bjørnseth, H. M. 1999. Palaeozoic to Tertiary rift and basin dynamics; mid-Norway to Bay of Biscay; a new context for hydrocarbon prospectivity in deep water frontier. *In*: Fleet, A. J. & Boldy, S. A. R. (eds) *Petroleum Geology of Northwest Europe: Proceedings of the 5th Conference*. Geological Society, London, 7–40.

Scrutton, R. A. 1970. Results of a seismic refraction experiment on Rockall Bank. *Nature*, **227**, 826–827.

Smallwood, J. R., White, R. S. & Staples, R. K. 1998. Deep crustal reflectors under Reydarfjördur, eastern Iceland: Crustal accretion above the Iceland mantle plume. *Geophysical Journal International*, **134**, 277–290.

Waagstein, R. 1988. Structure, composition and age of the Faeroe basalt plateau. *In*: Morton, A. C. & Parson, L. M. (eds) *Early Tertiary Volcanism and the Opening of the NE Atlantic*. Geological Society, London, Special Publications, **39**, 225–238.

Waagstein, R. 1998. *A geological field guide to the Palaeogene flood basalts of Suderoy Faroe Islands*. Danmarks og Grønlands Geologiske Undersøgelse Rapport **1998/30**.

Waagstein, R. 2002. Basaltic lavas and hyaloclastites from the submerged part of the Palaeogene Faroes flood basalt province: stratigraphy, lithology and chemistry of the volcanic succession of the Lopra re-entry well. Abstract presented at the Frontier Exploration of Volcanic Continental Margins conference, Geological Society, London, 17–18 September.

Waagstein, R. & Hald, N. 1984. Structure and petrography of a 660 m lava sequence from the Vestmanna-1 drill hole, lower and middle basalt series, Faeroe Islands. *In*: Berthelsen, O., Noe-Nygaard, A. & Rasmussen, J. (eds) *The Deep Drilling Project 1980–81 in the Faeroe Islands*. Føroya Frodskaparfelag, Torsharn, 39–70.

Waagstein, R., Guise, P. & Rex, D. 2002. K/Ar and 39Ar/40Ar whole-rock dating of zeolite facies metamorphosed flood basalts: the upper Paleocene basalts of the Faroe Islands, NE Atlantic. *In*: Jolley, D. W. & Bell, B. R. (eds) *The North Atlantic Igneous Province:*

Stratigraphy, Tectonic, Volcanic and Magmatic Processes. Geological Society, London, Special Publications, **197**, 219–252.

Waagstein, R., Boldreel, L. O. & Andersen, C. 2003. An integrated petrophysical approach to the sub-basalt imaging problem using well logging data to link measurements from cores and seismic surface experiments. *Geophysical Research Abstracts*, **5** no. 09388.

White, R. & McKenzie, D. 1989. Magmatism at rift zones: The generation of volcanic continental margins and flood basalts. *Journal of Geophysical Research*, **94**, 7685–7729.

White, R. S., Fruehn, J., Richardson, K. R., Cullen, E., Kirk, W., Smallwood, J. R. & Latkiewicz, C. 1999. Faroes Large Aperture Research Experiment (FLARE): Imaging through basalts. *In*: Fleet, A. J. & Boldy, S. A. R. (eds) *Petroleum Geology of Northwest Europe: Proceedings of the 5th Conference*. Geological Society, London, 1243–1252.

White, R. S., Christie, P. A. F., Kusznir, N. J. *et al.* 2002. iSIMM pushes frontiers of marine seismic acquisition. *First Break*, **20**, 782–786.

White, R. S., Smallwood, J. R., Fliedner, M. M., Boslaugh, B., Maresh, J. & Fruehn, J. 2003. Imaging and regional distribution of basalt flows in the Faroe–Shetland Basin. *Geophysical Prospecting*, **51**, 215–231.

Ziolkowski, A., Hanssen, P., Gatliff, R. *et al.* 2003. Use of low frequencies for sub-basalt imaging. *Geophysical Prospecting*, **51**, 169–182.

Seismic and petrophysical properties of Faroe Islands basalts: the *SeiFaBa* project

Peter Japsen, Morten Sparre Andersen, Lars Ole Boldreel, Regin Waagstein, Robert S. White and Michael Worthington

Flood basalt-covered basins exist worldwide along continental margins and are now in focus as targets for future hydrocarbon exploration. It is generally difficult to image through the basalt cover by conventional seismic reflection methods, and this is a major challenge to future petroleum exploration offshore the Faroe Islands. Long-offset profiling has proven very successful (White *et al*. 2003). Surprisingly, however, it is possible to image through kilometre-thick basalt sequences on some conventional profiles. Details of basalt stratigraphy are revealed on old, reprocessed seismic profiles as well as on recently acquired profiles, even though the imaging may be unsuccessful on nearby profiles (e.g. Boldreel & Andersen 1993). This stresses the need for a better understanding of the acoustic and other physical properties of basalt as well as of the degree of three-dimensional heterogeneity. The *SeiFaBa* project (**Sei**smic and petrophysical properties of **Fa**roes **Ba**salt, 2002–2005) is funded by the Sindri Group as part of the programmes for licensees within the Faroese offshore area, and addresses these issues with special focus on the subaerially extruded flood basalts of the Faroe Islands (cf. Japsen *et al*. in press).

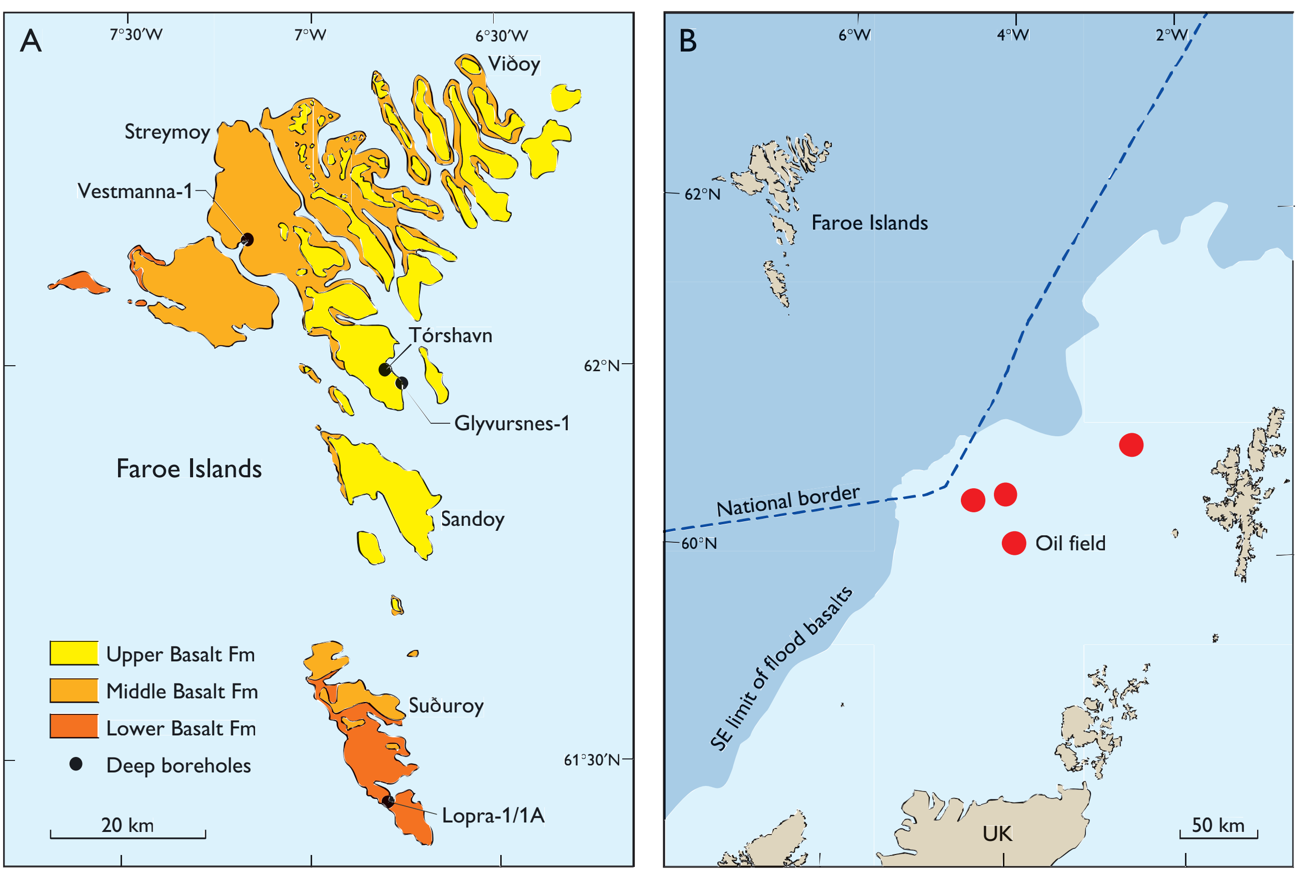

Fig. 1. **A**: Geological map of the Faroe Islands showing the location of deep boreholes and the distribution of the three Palaeogene basalt formations (modified from Waagstein 1998). **B**: Location of the Faroe Islands relative to the extent of flood basalts and producing oil fields (modified from Grant *et al.* 1999; Sørensen 2003).

© GEUS, 2004

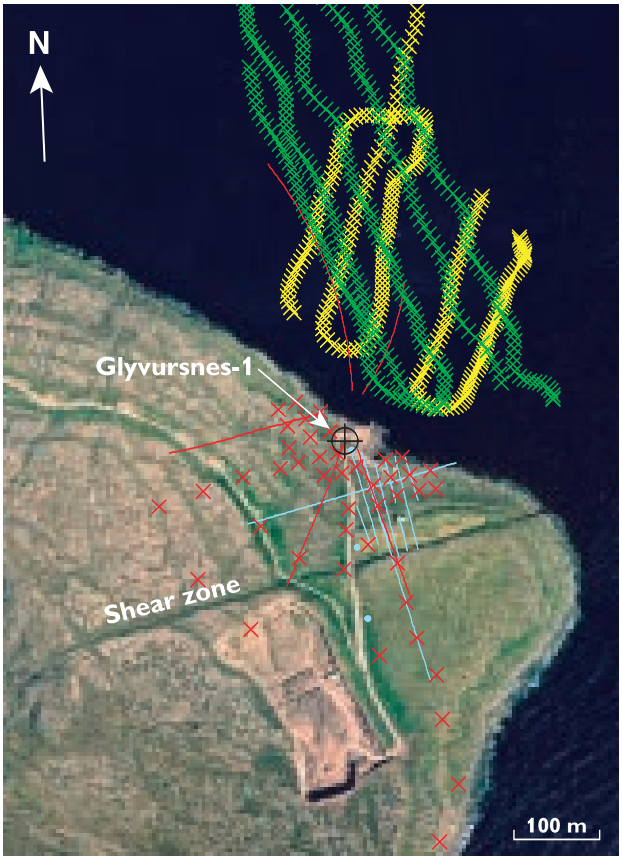

Fig. 2. Aerial photograph of Glyvursnes with well location and outline of seismic data recording on Glyvursnes in 2003. **Red crosses** indicate the locations of permanent seismometers during the experiments. **Blue dots** mark the positions of the three airgun pits for the VSP experiments. **Blue lines** mark the locations of the 14 Hz geophone strings used for the onshore reflection profiles. **Red lines** show the locations of onshore geophone strings and the tethered streamer during the offshore–onshore experiments and marine reflection experiment. **Yellow** and **green crosses** mark shotpoints for the marine reflection experiment (from Japsen *et al.* in press).

Drilling and logging at Glyvursnes and Vestmanna

The Glyvursnes-1 well was drilled outside Tórshavn to 700 m as a slim borehole with wire-line coring technique as part of the *SeiFaBa* project in 2002 (Fig. 1; Waagstein *et al.* 2003). Glyvursnes is well suited for combining vertical seismic profiles (VSP) and surface seismic experiments (onshore and offshore): the terrain is relatively flat and the seismic effects of a nearby near-vertical shear zone can be studied in detail (Fig. 2). During the same operations, the existing 660 m deep Vestmanna-1 well was reamed and logged. Three deep wells on the Faroe Islands have drilled thick sections of the Lower, Middle and Upper Basalt Formations (Fig. 3; Rasmussen & Noe-Nygaard 1970):

1. The Vestmanna-1 well was drilled to 660 m in 1980 and reopened to 590 m in 2002 and logged. The hole was drilled in the lower part of the Middle Basalt Formation and extends 100 m into the Lower Basalt Formation. A full core was taken.
2. The Lopra-1/1A well was drilled through the Lower Basalt Formation to 2.2 km in 1981, and deepened to 3.6 km in 1996 without reaching the base of the volcanic succession. One short core of basalt was taken from this well.
3. The Glyvursnes-1 well was drilled to 700 m in 2002 to around the boundary between the Middle and Upper Basalt Formations (Fig. 4). A full core was taken.

An extensive logging programme was run in the Glyvursnes and Vestmanna boreholes, comparable to that previously run in the Lopra well in 1981 and 1996. The programme includes optical televiewer, caliper, natural gamma ray, resistivity, neutron porosity, density, full wave sonic, spectral gamma (of poor quality) and temperature/conductivity measurements.

The Vestmanna and Glyvursnes boreholes penetrate, respectively, the lowermost 550 m and the uppermost 450 m of the 1400 m thick Middle Basalt Formation. In both sections the Middle Basalt Formation is characterised by the presence of plagioclase-phyric compound flows composed of thin flow-units of variable porosity, and by rare thin beds of tuff. The lowermost part of the Middle Basalt Formation in the Vestmanna borehole and the lowermost 70 m of the Upper Basalt Formation in the Glyvursnes borehole are very similar. The overlying section at about 230 to 285 m in Glyvursnes-1 consists of a few relatively thick plagioclase-phyric flow-units possibly forming two compound flows (the Tórshavn flows), that are morphologically very similar to the flows of the Lower Basalt Formation (except that the latter are near-aphyric).

Future work

Ultrasonic velocities and other parameters will be measured on core samples from selected drill holes. The samples will be investigated under varying pressure for both dry and saturated samples. Studies of the velocity–porosity relationships of basalts will focus on matrix properties, but will also take into account variations in magma type, secondary mineralisation, pore shapes and fractures.

A lithostratigraphic interpretation of the borehole logs will be carried out, and the results will be correlated with petrography, rock chemistry and ultrasonic properties of core samples. This comparison of data acquired at core and log scale will be extended to data of seismic scale acquired from flood basalts of all three formations. Well log and core data

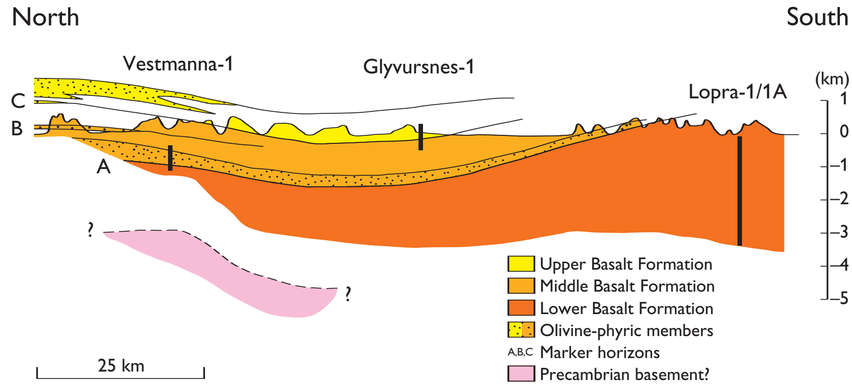

Fig. 3. Stratigraphical position of deep boreholes in the Faroe Islands (modified from Waagstein 1988). See Fig. 1 for location of wells.

will be examined to evaluate how magma type and secondary mineralisation influence the relationships between velocity and porosity of basalt. Supplementary analysis of well logs from exploration wells in the Faroe–Shetland Basin will be carried out to provide additional data concerning the distribution of elastic properties of the basalts around the Faroe Islands.

Seismic experiments at Glyvursnes

The extrusive basalt flows in the Faroe–Shetland Basin are generally sub-horizontal on a regional scale, although there are often large physical property variations (largely governed by porosity) within individual flows, and locally rugged small-scale relief on the tops of flows. The strong layering and local relief may cause internal multiples, forward- and back-scattering of the incident energy, multiple-mode conversion, anisotropy, absorption and geometric spreading, and low-pass filtering of the energy that propagates through a stacked layer of basalt flows.

Since flow thicknesses are at least an order of magnitude smaller than the seismic wavelength, reflections are rarely seen from individual flows: the seismic response depends on the complex interactions of reflections from multiple flow units. To study these effects, three closely integrated seismic experiments were carried out around the Glyvursnes-1 borehole in 2003 (Fig. 2).

Three VSP surveys were undertaken with source offsets of 14, 242 and 415 m. The two offset locations were on either side of a well-defined shear zone.

Onshore and offshore high resolution data were acquired along the lines shown in Fig. 2. Two 625 m lines were shot with the charges along the line, while short profiles were acquired with the source displaced laterally. The marine seismic reflection data were acquired on a tethered streamer using a moving airgun cluster. Additional data were obtained at longer offsets.

A dense array of 45 autonomous seismometers was deployed for a six-month period around the site of the borehole. During periods of controlled source seismic shooting, all sites maintained a sampling rate of 200 samples/sec. For intervening periods, when recording earthquakes, a sampling rate of 100 samples/sec was used. In addition, three 400 m long independent temporary land arrays were set up in September 2003 using a mixture of one- and three-component geophones.

Throughout acquisition of the marine reflection seismic and the offshore–onshore, wide-angle seismic data, a three-component borehole seismometer was held clamped at a depth of 400 m in the Middle Basalt Formation in the Glyvursnes borehole.

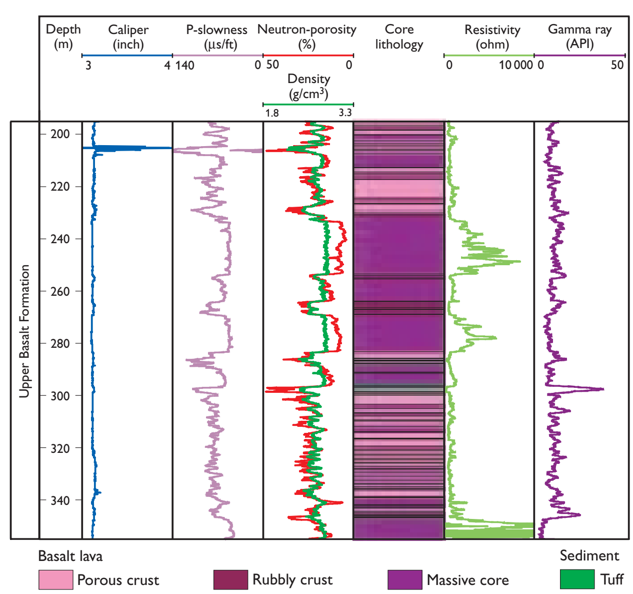

Fig. 4. Composite log from the Glyvursnes-1 well. Note the correlation between P-slowness (P-wave velocity) and density/neutron porosity that reflects the porosity-contrast between the porous crust and the massive core of the basalt flows (from Japsen *et al.* in press).

Future work

A detailed analysis of seismic wave propagation through a typical Faroese basalt succession will be carried out using the logging carried out in 2002, ongoing laboratory work on the core and the seismic data acquired during the summer of 2003. With the sonic logging and the vertical VSP, a detailed vertical velocity profile will be obtained in the Glyvursnes-1 borehole and determine intrinsic and extrinsic attenuation/scattering of seismic waves in one dimension. By combining the two detailed fixed offset VSPs and variable offset with data registered at fixed depth, it is planned to address attenuation/scattering in two (three) dimensions. Using the multichannel seismic data and the autonomous seismic array it is planned to obtain two-dimensional and three-dimensional velocity distribution in a small area around the borehole. The multichannel surface seismic experiment is designed to analyse sub-critical and post-critical reflections from the basalt succession drilled at Glyvursnes, providing an image of structural continuity in the area.

Perspectives

Drilling of the new borehole at Glyvursnes and re-logging of Vestmanna-1 in combination with the extensive data set for the Lopra-1 well will give valuable new stratigraphic and petrophysical control of the Lower, Middle and Upper Basalt Formations on the Faroe Islands. The planned experiments will provide a link from hand-specimen scale, through the slightly larger averaging of borehole logs, to seismic scales ranging from high-resolution VSPs and multi-channel land arrays, to onshore–offshore shooting using wide-band air-guns, to the truly long-period response of the basalt flows using teleseismic arrivals. The investigations will provide a unique data set and, hopefully, new understanding of the seismic and petrophysical properties of Faroe Islands basalts.

Acknowledgements

Thanks are due to the Sindri Group for permission to publish results from the Glyvursnes-1 well. *SeiFaBa* is funded collectively by all oil companies operating in the Faroe Islands sector (the Sindri Group).

References

Boldreel, L.O. & Andersen, M.S. 1993: Late Paleocene to Miocene compression in the Faroe–Rockall area. In: Parker, J.R. (ed.): Petroleum geology of Northwest Europe: Proceedings of the 4th Conference, 1025–1034. London: Geological Society.

Grant, N., Bouma, A. & McIntyre, A. 1999: The Turonian play in the Faroe-Shetland Basin. In: Fleet, A.J. & Boldy, S.A.R. (eds): Petroleum geology of Northwest Europe: Proceedings of the 5th Conference, 661–673. London: Geological Society.

Japsen, P. *et al.* in press: Preliminary results of petrophysical and seismic properties of Faroes basalts (SeiFaBa project). In: Doré, A.G. & Vining, B. (eds): Petroleum geology: North-West Europe and global perspectives: Proceedings of the 6th Petroleum Geology Conference. London: Geological Society.

Rasmussen, J. & Noe-Nygaard, A. 1970: Geology of the Faroe Islands. Danmarks Geologiske Undersøgelse, I. Række **25**, 142 pp.

Sørensen, A.B. 2003: Cenozoic basin development and stratigraphy of the Faroes area. Petroleum Geoscience **9**, 189–207.

Waagstein, R. 1988: Structure, composition and age of the Faeroe basalt plateau. In: Morton, A.C. & Parson, L.M. (eds): Early Tertiary volcanism and the opening of the NE Atlantic. Geological Society Special Publication (London) **39**, 225–238.

Waagstein, R. 1998: A geological field guide to the Palaeogene flood basalts of Suðeroy, Faroe Islands. Danmarks og Grønlands Geologiske Undersøgelse Rapport **1998/30**, 46 pp.

Waagstein, R., Boldreel, L.O. & Andersen, C. 2003: An integrated petrophysical approach to the sub-basalt imaging problem using well logging data to link measurements from cores and seismic surface experiments. Geophysical Research Abstracts **5**(09388), 2 pp.

White, R.S., Smallwood, J.R., Fliedner, M.M., Boslaugh, B., Maresh, J. & Fruehn, J. 2003: Imaging and regional distribution of basalt flows in the Faroe-Shetland Basin. Geophysical Prospecting **51**, 215–231.

Authors' addresses

P.J. & R.W., *Geological Survey of Denmark and Greenland, Øster Voldgade 10, DK-1350 Copenhagen K.* E-mail*: pj@geus.dk*

M.S.A., *University of the Faroe Islands, Noatún 3, FO-100 Tórshavn, Faroe Islands.* Present address: *Geological Survey of Denmark and Greenland, Øster Voldgade 10, DK-1350 Copenhagen K.*

L.O.B., *Geological Institute, University of Copenhagen, Øster Voldgade 10, DK-1350 Copenhagen K, Denmark.*

R.S.W., *Bullard Laboratories, University of Cambridge, Madingly Road, Cambridge CB3 0EZ, UK.*

M.W., *Department of Earth Sciences, University of Oxford, Parks Road, Oxford OX1 3PR, UK.*

Propagation, decay, phase conversion and recording of seismic waves in the basalt succession at Glyvursnes, the Faroe Islands - Summary of thesis in preparation

Uni K. Petersen

Introduction

The seismic data acquired around the Glyvursnes-1 borehole in the summer 2003 makes it possible to compare borehole data (wireline logs) with surface seismic data acquired using different acquisition techniques. Data were acquired on vertical geophones, 3-component geophones and a marine streamer using two different marine sources 760 cu. inches and 160 cu. inches and 250 g dynamite shots in 3 m deep boreholes (Andersen et al 2004).

Prediction of imaged geology from borehole and exposure data

By combining wireline logs from the Glyvursnes-1 well (Waagstein & Andersen 2004) with wireline logs from Vestmanna-1 and Lopra-1 (e.g. Boldreel 2006; Christie et al. 2006) an almost complete composite density and velocity (V_P and V_S) logs can be constructed for the known stratigraphic sequence of basalts below the Glyvursnes (Petersen *et al.* 2006). Data is only missing for ca. 150 m in the middle part of the Middle Basalt Formation, in the Glyvursnes area, and for ca. 910 m in the upper part of the Lower Basalt Formation. The surface geology is well known and the general behaviour of both the Middle Basalt Formation and the Lower Basalt Formation remains the same throughout the Faroe Islands (Rasmussen and Noe-Nyggard 1970). It is thus feasible to represent the general elastic behaviour of the un-logged stratigraphic intervals by log data from similar intervals in the Vestmanna-1 and Lopra-1 well thus and construct a detailed (15-20 cm resolution) 1D seismic and elastic model of the lower 4500 m of the ideal stratigraphic profile of the Faroe Islands (Figure 1). This 1D model (or suitable modifications) is used as the basis for a number of full waveform simulations of the seismic signal recorded at Glyvursnes.

Data quality - band width and signal/noise

The character of the data recorded by the different combination of source and receivers were compared visually using gathers, stacked sections, and numerically using time variant frequency analysis of individual traces using a wavelet transform (Petersen *et al.* 2006). Ambient noise recorded on the streamer is very strong but variable at frequencies below ca. 20 Hz (swell noise) and moderate at higher frequencies (Figure 2; Figure 3). On vertical geophones the ambient noise are low and mostly present at frequency band 0-64 Hz. A narrow, weak noise band around 60 Hz is seen with both detectors and presumably inherent to the recording system. The specific source of the 60 Hz noise was not located during acquisition.

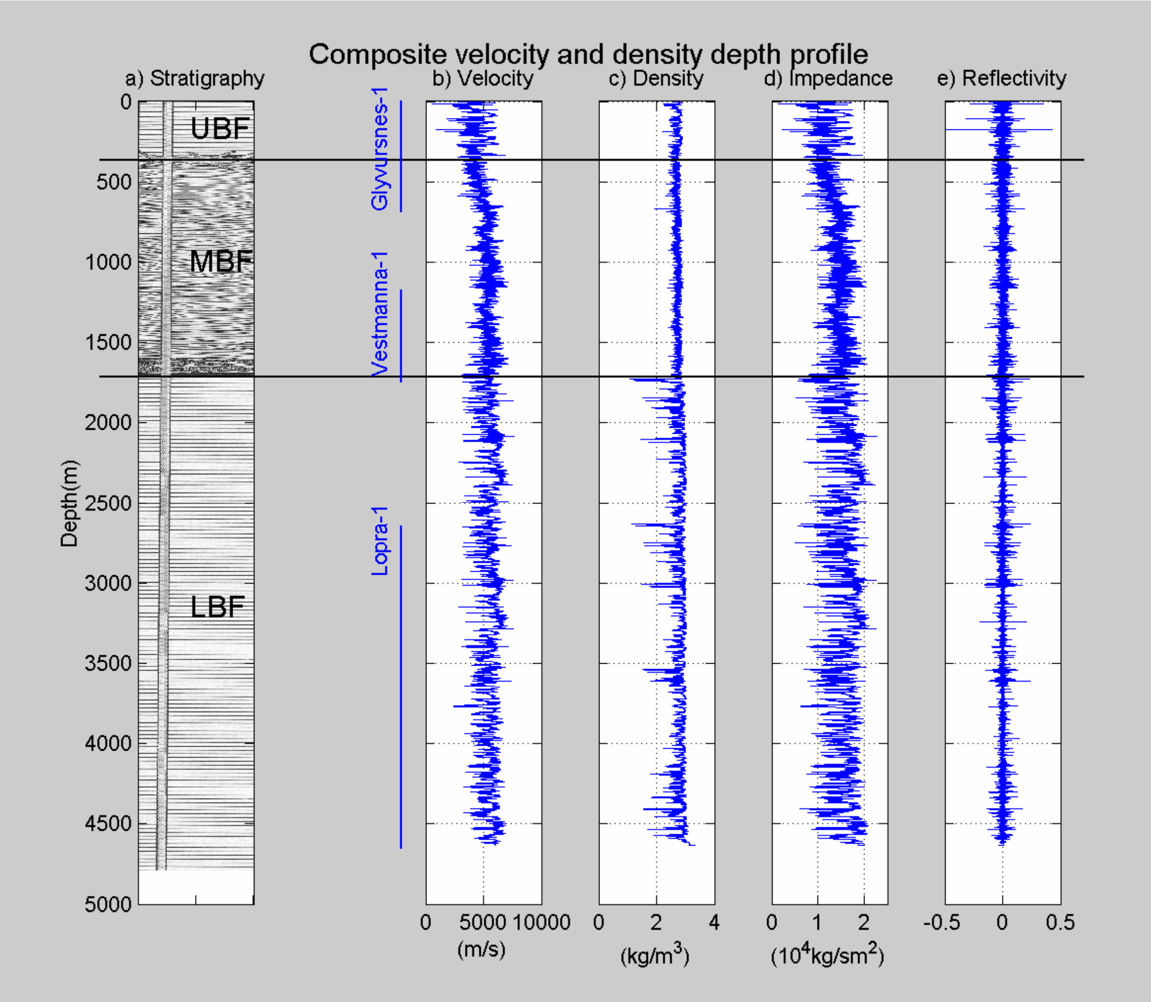

Figure 1. *Composite velocity and density logs for the total stratigraphic sequence below Glyvursnes, constructed using the logs from Glyvursnes-1, Vestmanna-1 and Lopra-1 (the actual well segments are labelled between a) and b), see also figure 1). a) The stratigraphic division mapping the boundaries of various stages of volcanism (modified from Rasmussen and Noe-Nygaard, 1970). The base of the UBF and the base of the MBF are drawn as black horizontal lines across the figure; b) composite velocity log. The uppermost 485 m of Vestmanna-1 are used to represent the missing interval in the MBF and the uppermost 720 m of Lopra-1 are used to represent the missing interval in the LBF; c) composite density log; d) and e) show the calculated acoustic-impedance and the reflection coefficient series. The repeated log sequences can be identified on the composite logs*.

The numerical analysis of individual shot traces provide approximate effective far field signatures measured on the first arrival. When recorded on geophones, the 160 cu. inches airgun source has a central frequency of ca. 16 Hz and a band width of about 4-128 Hz (Figure #FB5.a). However, the frequency band of seismic energy narrows with depth (recording time). At 1.5 seconds, it is around 5-20 Hz and still dominating over ambient noise. At later arrival times, the effective bandwidth of seismic decreases further and from around 3 seconds recording time the seismic energy apparently vanishes in ambient noise. Qualitatively this is in good agreement with attenuation estimates obtained from analysis of the down-going waves in the zero offset VSP from Glyvursnes-1 (Shaw et al. 2004, 2006).

When 160 cu. inches airgun shots are recorded on the streamer, the centre frequency is considerably higher, ca. 60 Hz, than that recorded on geophones (Figure 3.a). The reason for this apparent change in signature is to some extent found in the tow depth of the streamer (3 m). At this depth, the ghost causes considerable attenuation of low frequencies. The higher frequency content of the signal recorded on the streamer is reflected in a significantly faster decay of recorded seismic signal. At around 1 second recording time, the seismic signal recorded on the streamer is effectively hidden in low frequency swell noise. At high frequencies around 128-512 Hz reverberations in the water column adds to the noise problem in the streamer data (Figure #FB6.a, b).

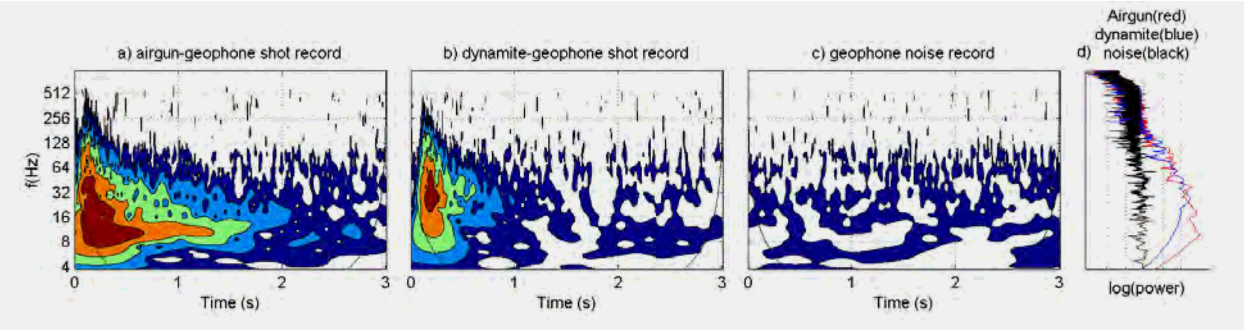

Figure 2 *Shows the continuous wavelet transforms of geophone channel 110 (station 74). a) Airgun-geophone, offset 208 m; b) dynamite-geophone, offset 224 m; c) geophone noise record; d) frequency spectra of all three records. Values are not scaled. Contour levels are increasing exponentially and are the same for a), b) and c).*

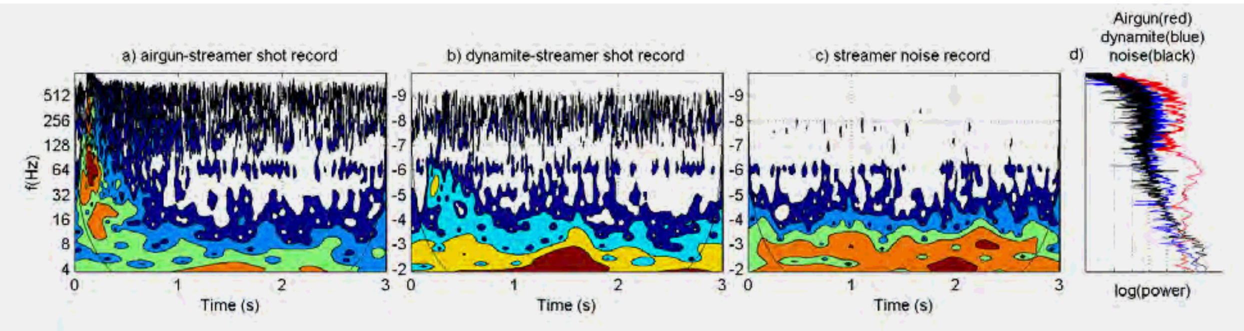

Figure 3 *Shows the continuous wavelet transforms of streamer channel 130 (station 90). a) Airgun-streamer, offset 195 m; b) dynamite-streamer, offset 415 m; c) streamer noise record; d) is the frequency spectra of all three records. Values are not scaled. Contour levels are increasing exponentially and are the same for a), b) and c).*

The dynamite source used during the 2003 acquisition at Glyvursnes produced a considerably weaker and more high-frequent signal than the airgun sources (compare Figure 2.a, b and Figure 3.a, b). On geophones the signal from the dynamite shots to a recording time of ca. 1 second on the time-frequency plot. On the streamer, hardly any seismic energy is apparent above the noise (Figure 3.b).

Overall, the time variant frequency analysis indicate that seismic signal, not necessary primary reflections, should be expected to a recording time of 3 seconds when 160 cu. inches airgun shots are recorded on geophones, but only to about 1 second recording time when recorded on the streamer. When dynamite shots are recorded on geophones seismic signal is expected to ca. 1-1.5 seconds recording time. Due to the higher frequencies in dynamite shots, better resolutions may be achieved. Due to the weak signal, dynamite shots were not recorded systematically on the streamer.

Processing

Processing and further analysis is focused at highlighting and identifying phases within the time windows of seismic data for the different source-receiver combinations. The processing sequence used is simple (Petersen *et al.* 2005). 2D or 3D processing is used as required by the geometry of the individual data sets. Stacking velocities is obtained by careful velocity picking of contoured semblance plots. RMS velocities obtained from the geological model (see below) were used as tool guiding picking to primary reflections. However, complete removal of multiples may not be achieved due to the high stacking velocities and relatively short offsets. Identification of multiples and other arrivals not being primary P-wave reflections should thus be carried out during interpretation.

Coherent events are seen to a recording time of at least three seconds in the airgun-geophone data, ca. 2 seconds in the dynamite-geophone data and to ca 1.5 seconds in the airgun streamer data, highlighting the ability of stacking to enhance weak coherent signal (not obvious in individual traces). Recording time should thus be constrained by stacking tests rather than signal analysis on individual traces.

Interpretation of stacked sections

The stacked sections are characterised by sub-horizontal, almost planar reflections (Figure 4). Dip is therefore of little help constraining multiple events or other arrivals not being primary P-wave reflections.

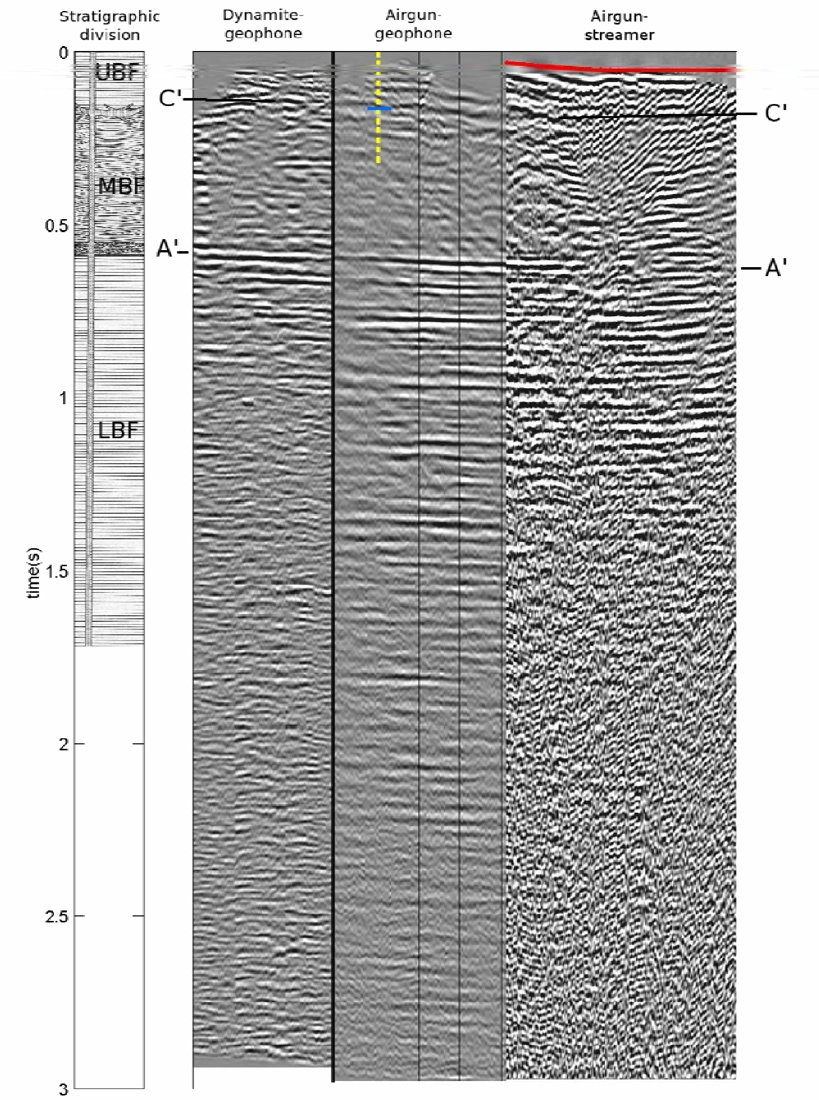

Figure 4 *shows the combined profile. See figure 7 for location. An adjusted stratigraphic model is plotted to the left. A threefold subdivision of the seismic profile is distinct both in the airgun-geophone/streamer and dynamite-streamer data. Two high-amplitude successions (0-0.16 s and 0.59 s to end of record) and a low-amplitude succession (0.16-0.59 s) are clearly identified. By comparing this figure to figure 3b (synthetic from composite logs), we see that the low-amplitude succession is characterised by a frequency content that is comparable to that of the synthetic seismogram through the MBF, while the frequency content of the lower high-amplitude succession is comparable to that of the LBF. Horizon C' ties well to the UBF-MBF boundary in the well (blue marker on yellow line). A' is interpreted to be the MBF-LBF boundary. The red line is the seabed derived from bathymetric information.*

Two fairly distinct and coherent reflections are picked on the stacked sections from all three acquisition combinations. The lower, found at a depth of ca. 0.6 seconds TWT is called horizon A' and the upper, found at ca. 0.15 seconds TWT is called horizon C'. The succession below horizon A' is characterised by strong continuous internal reflectors. The strength of internal reflectors below horizon A' decreases gradually with depth (recording time). The succession A'-C' is characterised by weak reflectors, which mostly are non-continuous. This is best seen in the dynamite-geophone and airgun-geophone data (Figure 4). The succession above horizon C' is incompletely imaged due to the shallow depth. However, internal reflections are strong and fairly continuous.

It is suggested that the contrasting character of the three successions defined by horizon A' and C' replicate the contrasting character of the three exposed basalt formations on the Faeroe Islands. Lower and Upper basalt formations are dominated by laterally continuous tabular lava flows, while Middle Basalt Formation is characterised by compound braided basalts of little lateral continuity (Passey 2005). Therefore Horizon A' is interpreted to be approximately equivalent to the boundary between the Lower Basalt and Middle Basalt formations while horizon C' is interpreted as approximately equivalent to the boundary between the Middle Basalt and Upper Basalt formations.

Seabed multiples?

Potentially seabed multiples and peg-legs generated at the seabed could be a problem in the data acquired with an airgun source, and seabed multiples is known to be a serious problem within the Faroese continental shelf. In the data acquired at Glyvursnes in 2003 we can use the dynamite-geophone data to identify events as not being multiples and peg-legs generated at the seabed and thus indirectly identify these events in the data acquired with an airgun source. It is clear that removal of seabed multiples not have been very successful in the airgun streamer data (Figure 4). However, in the data recorded with geophones multiples and peg-legs generated at the seabed are apparently removed efficiently. The larger offsets present in the airgun-geophone data is the main reason for this.

Interbed multiples and other arrivals not being primary P-wave reflections.

Although, multiples and peg-legs generated at the seabed apparently not is a problem in the data recorded with geophones, interbed multiples and other arrivals not being primary P-wave reflections may be present in the stacked data. Shaw et al. (2006, in press/this volume) suggest that 1D scattering is one of the main reasons for the low Q-values obtained from the zero offset VSP in Glyvursnes-1. We should thus expect short period interbed reverberations to be a significant constituent of the reflected seismic energy. Planke (1994) pointed out that the bed thickness in basalt successions generally is small compared to the wavelength of the seismic signal and concluded that reflections in the seaward dipping reflector sequence around ODP well 642E mostly represented tuning of reflections from individual bed boundaries. Bed thickness in the Lower Basalt Formation on the Faroe Islands is on average around 20 m, well below the dominant wavelength in the seismic signal. Coherent events below horizon A' on the stacked sections is thus likely not to represent reflections from individual beds, but at best complex interferences of tuned primaries and short period reverberations. However, even a coherent event constituted by interferences of tuned primaries and short period reverberations carry information about geology corresponding approximately to the TWT time of the event. Coherent events below horizon A' in stacked sections of the dynamite-geophone and airgun-geophone (Figure #FB8) is thus likely to contain relevant geological information.

The dynamite source used during the 2003 acquisition at Glyvursnes produced a considerably weaker and more high-frequent signal than the airgun sources (compare Figure 2.a, b and Figure 3.a, b). On geophones the signal from the dynamite shots to a recording time of ca. 1 second on the time-frequency plot. On the streamer, hardly any seismic energy is apparent above the noise (Figure 3.b).

Overall, the time variant frequency analysis indicate that seismic signal, not necessary primary reflections, should be expected to a recording time of 3 seconds when 160 cu. inches airgun shots are recorded on geophones, but only to about 1 second recording time when recorded on the streamer. When dynamite shots are recorded on geophones seismic signal is expected to ca. 1-1.5 seconds recording time. Due to the higher frequencies in dynamite shots, better resolutions may be achieved. Due to the weak signal, dynamite shots were not recorded systematically on the streamer.

In addition to multiples, peg-legs and short period reverberations phase conversions may constitute a problem for imaging in and below basalts. Possible S-wave conversions of reflections from horizon A' are observed in gathers (Figure 5). They are quite strong events at intermediate to long offsets. Full elastic forward modelling succeeds in simulate these events, and they are also identified as S-wave arrivals on the 3-component geophones. However, the converted reflections from horizon A' is not present in the stack. Their moveout are large compared to the stacking velocities used to generate the stack and at short offsets, their amplitudes are low.

As long as we are within the basalt succession and we use the correct P-wave stacking velocity converted waves may be a problem that can be resolved by fairly routine processing. If sediments is present below the basalts (or believed to be present), it is possible that converted reflections from within the basalts are misinterpreted as sub-basaltic sediments. However, analysis of amplitude variations as a function of offset should allow distinction between low velocity arrivals from sediments and converted reflections from within the basalts.

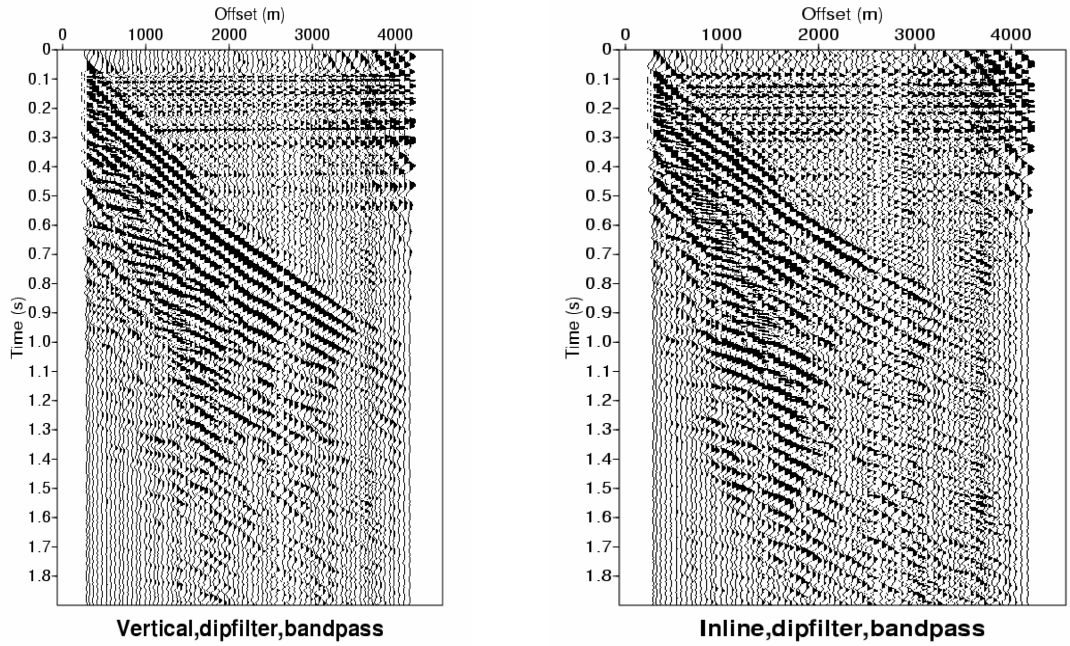

Figure 5. *Vertical an inline component of shot gather. Converted arrivals is clearly seen at intermediate offsets in the inline gather. Although not dramatically significant at short offsets in the vertical gather, converted arrivals are present at intermediate offsets.*

Comparison of ideal stratigraphic profile and interpretation of Glyvursnes-2003 seismic data

According to the interpretation presented above, the Middle Basalt Formation below Glyvursnes is ca. 1050 m thick. This is less than stratigraphic thickness of the formation in the northern part of the islands, 1350 m, (Rasmussen and Noe-Nyggard 1970) and the 1400 m thickness of the formation reported for the area around Vestmanna (Waagstein 1988). It is thus suggested that the Middle Basalt Formation thins from the northern and western part of the Faeroe Islands towards Glyvursnes (Petersen *et al.* 2006). The reason for the apparent south- and eastwards thinning of the Middle Basalt Formation could be that lava available during emplacement of the MBF was not sufficient to allow all the flows to reach Glyvursnes if their source was to the northwest. However, gradual south- and eastward thinning of the Middle basalt formation was not observed during mapping of the Faeroe Islands (Rasmussen and Noe-Nyggard 1970). Alternatively, the Glyvursnes area may have been uplifted relative to the Vestmanna area after the emplacement of the LBF. Additional data are needed to confirm the south- and eastward thinning of the Middle Basalt Formation and to allow us to chose among the two above-mentioned or other possible hypotheses for the thinning of the formation.

Conclusion

The processing and interpretation of the surface seismic data acquired at Glyvursnes in 2003 indicates that imaging within the basalt succession encountered at Glyvursnes is possible. Decay of the source signature with depth into the formation and correct stacking velocities are key factors controlling the quality of seismic stack of the basalt succession. As proposed by Planke et al. (Planke *et al.* 1999) seismic imaging of basalt thus amounts to the conventional task of separating primary energy from noise.

Sub-basaltic sediments were not identified in the processed data from Glyvursnes. However, wide-angle seismic data indicate they possibly could be present (Richardson et al. 1999). The data from Glyvursnes indicate that fairly strong converted reflections can be generated within the basalt succession. Based only on the stacking velocity, these converted reflections could be misinterpreted as representing a velocity inversion below the basalt. Although Hansen et al (2003) correctly pointed out that pure P-modes provide the best chance of sub-basalt imaging, it may still be necessary to take converted waves into consideration - waves converted within the basalts. When/if they are present the task is to avoid enhancing them together with primary P-waves. Offset dependent processing is an obvious choice for this task.

References

ANDERSEN, M.S, BOLDREEL, L.O., HANSEN. H.K. 2003. Analysis of wireline logs through basaltic successions from the Faroe-Shetland Area. *GEUS Report* **2005/3***,* 1-170.

BOLDREEL, L.O. 2006. Wire-line log-based stratigraphy of flood basalts from the Lopra-1/1. *Geological Survey of Denmark and Greenland Bulletin* ***9****,* 39-53.

CHRISTIE, P., GOLLIFER, I., COWPER, D. 2006. Borehole Seismic Studies of a Volcanic Succession from the Lopra-1/1A Borehole in the Faroe Islands, NE Atlantic. *Geological Survey of Denmark and Greenland Bulletin* ***9****,* In press.

HANSSEN, P., ZIOLKOWSKI, A., LI, X. Y. 2003. A quantitative study on the use of converted waves for sub-basalt imaging. *Geophysical Prospecting* **51**(3), 183-193.

Passey, S. R. Geology of Glyvursnes, Streymoy, Faroe Islands. A contribution to the SeiFaBa project. Funded by the Sindri Group. 20-6-2005.
Ref Type: Report

PETERSEN, U. K., ANDERSEN, M. S., WHITE, R. S. 2006. Seismic imaging of basalts at Glyvursnes, Faroe-Islands – Hunting for future exploration methods in basalt covered areas. *First Break* **24**(March 2006).

PETERSEN, U. K., ANDERSEN, M. S., WORTHINGTON, M., WHITE, R. S., MOHAMMED, N. G., SHAW, F. 2005. A small reflection seismic experiment on the Faroe Islands during summer 2003. European Geopscience Union, 2nd general assembly, Vienna, April 2005.

PLANKE, S. 1994. Geophysical Response of Flood Basalts from Analysis of Wire Line Logs - Ocean Drilling Program Site-642, Voring Volcanic Margin. *Journal of Geophysical Research-Solid Earth* **99**(B5), 9279-9296.

PLANKE, S., ALVESTAD, E., ELDHOLM, O. 1999. Seismic characteristics of basaltic extrusive and intrusive rocks. *The Leading Edge* **March** 342-348.

Rasmussen, J., Noe-Nyggard, A. 1970. Geology of the Faeroe Islands. C. A. Reitzels Forlag, København.

RICHARDSON, K.R., WHITE, R.S., ENGLAND, R.W, FRUEHN, J. 2006. Crustal structure east of Faeroe Islands: mapping sub-basalt sediments using wide-angle seismic data. *Petroelum Geoscience* ***5**,* 161-172.

SHAW, F., WORTHINGTON, M. H., WHITE, R. S., ANDERSEN, M. S., PETERSEN, U. K., SEIFABA GROUP 2004. A study of seismic attenuation in basalt using VSP data from a Faroe Islands borehole. 66th Meeting European Association of Geoscientists and Engineers.

SHAW, F., WORTHINGTON, M. H., WHITE, R. S., ANDERSEN, M. S., PETERSEN, U. K., SEIFABA GROUP 2006. Seismic attenuation in Faroe Islands basalts. SUBMITTED FOR: *Geophysical Prospecting*.

WAAGSTEIN, R. 1988. Structure, composition and age of the Faeroe Basalt plateau, Early Tertiary Volcanism and the opening of the NE Atlantic. *Geological Society Special Publication* **39** 225-238.

WAAGSTEIN, R., ANDERSEN, C. 2003: Well completion report: Glyvursnes-1 and Vestmanna-1, Faroe Islands. Contribution to the SeiFaBa project funded by the Sindri Group. *Danmarks og Grønlands Geologiske Undersøgelse Rapport,* **2003/99.**

Seismic imaging of basalts at Glyvursnes, Faroe Islands: hunting for future exploration methods in basalt covered areas

U.K Petersen,[1*] M.S. Andersen,[1,2] R.S. White,[3] and SeiFaBa Group

Introduction

Obtaining good sub-basalt seismic images is known to be problematic (Ziolkowski et al., 2003; White et al., 2003). Although the properties of basalts are quite different from those of most sediments Planke (1999) suggested that seismic energy is transmitted through basalt in much the same way as through sediments so the problem of seismic imaging through basalts amounts to the conventional task of separating primary energy from noise, even though the noise including multiples may be considerable. The physical properties of basalt are markedly different from those of the overlying and underlying sediments. Strong reflections due to high impedance contrasts at the top (and bottom) of the basalts leads to significant loss of transmitted seismic energy (Fruehn et al., 2001). Large variations of intrinsic properties along vertical cross-sections of basalt flows have been demonstrated and quantified by analyses of well-logs from wells penetrating successions of flood basalts (Planke, 1994) and from surface mapping (e.g., Self et al., 1998; Thordarson and Self, 1998). This causes the stratigraphic filtering effects of basalt successions to be more severe than that of sediments (Maresh and White, 2005; Shaw et al., 2004). Lateral variations in the thicknesses of sediments interbedded between basalt flows and in the thickness of the upper porous part of basalt flows have been demonstrated by detailed investigations in exposed flood basalts (Self et al., 1998; Thordarson and Self, 1998). The roughness of inter-beds causes 3D scattering of seismic energy, as demonstrated in studies comparing stratigraphic filtering and the effective quality factor, Q, of basalt successions (e.g., White et al., 2005; Shaw et al., 2005; Shaw et al., 2004).

Taking these problems into consideration, experiments have been performed in the last decade using: longer offsets (both synthetic aperture, and longer streamers) to improve the signal-to-noise ratio and NMO resolution and to allow processing of post-critical reflections; larger energy sources to increase the general energy level; low-frequency tuning to allow for better penetration through basalts (characterised by low Q values); and shot-by-shot recording of the source signature and combination of OBS and seismic reflection data to improve velocity estimates. In one experiment all of the above-mentioned techniques were applied, providing considerable improvements in sub-basalt imaging relative to previous work (Spitzer and White, 2005; White et al., 2005). An other parameter for seismic acquisition is the orientation of the seismic line relative to the flow direction of the basalt flows (Reshef et al., 2003). However, poor effective transmission of seismic energy, scattering, strong multiple reflections, multiple mode conversions, and low-pass filtering of the energy that propagates through a layer of stacked basalt flows are still hampering routine imaging for petroleum exploration in sediment basins covered by basalts (Maresh and White, 2005). This was demonstrated by the UK164/07-01 well where the base of a basaltic succession was found 700 m deeper than anticipated from interpretation of seismic reflection data (Archer et al., 2005). In order to obtain imaging quality and detail comparable to those obtained in other sedimentary basins, further improvements are necessary.

The SeiFaBa Project (Seismic and petrophysical properties of Faroes Basalts), sponsored by the Sindri group, aims to create data-derived models for the propagation of seismic energy in basalt to provide a basis for better sub-basalt imaging. The project comprises drilling of the Glyvursnes-1 wells near Tórshavn on the Faroe Islands (Figure 1), core analysis for intrinsic physical parameters, recording of VSP and offset-VSP data in the Glyvursnes-1 and Vestmanna-1 wells, and surface seismic wide-angle and reflection data around the Glyvursnes-1 and Vestmanna-1 wells (Japsen et al., 2005). At both sites these investigations of the elastic properties of basalts are made at a number of different scales. In this paper we present surface seismic reflection data from SeiFaBa experiment at Glyvursnes in the summer of 2003 illustrating that basalts can be imaged effectively using relatively small energy sources (250 g dynamite; 2.6-litre airgun cluster) and that stratigraphic details of flood-basalt constructions can be identified and characterized based on analysis of seismic data and then correlated to well data. We also demonstrate how different acquisition and processing techniques influence the effective frequency content of seismic reflection data and thus the effective propagation through and imaging of the basalts.

[1] *University of the Faroe Islands, Noatún 3, FO-100 Tórshavn, Faroe Islands.*
[2] *Geological Survey of Denmark and Greenland, Østervold Gade 10, Copenhagen C, DK-1350, Denmark.*
[3] *University of Cambridge, Bullard Laboratories, Madingley Road, Cambridge CB30EZ, UK.*
[*] *uni@setur.fo.*

© 2006 EAGE

Geological setting

A lava pile about 3 km thick with minor intercalations of volcaniclastic sediments is exposed on the Faroe Islands (Rasmussen and Noe-Nyggard, 1970). Below the exposed section a further 3 km or so of basalt was penetrated in the Lopra-1/1A well without reaching the base of the volcanic succession (Hald and Waagstein, 1984). Andersen (2002) suggested that about 1 km of basalt could have been present above the section exposed on the Faroes. The total stratigraphic thickness of basalt on the Faroe Block would thus be about 7 km, possibly more. Deep seismic results from wide angle experiments confirm this estimate (e.g., Richardson et al., 1999).

Rasmussen and Noe-Nygaard (1970) divide the exposed basalt into three series (Figure 1) representing different stages and ages of volcanism. Although Rasmussen and Noe-Nygaard's stratigraphy has been retained, their three series have informally been treated as formations in recent literature (e.g., Waagstein, 1988). In this paper we follow this tradition: the lower basalt formation (LBF), the middle basalt formation (MBF), and the upper basalt formation (UBF). The LBF (stratigraphic thickness about 900 m, (3000 m when including the lower part found in the Lopra-1A well) and the UBF (stratigraphic thickness about 675 m) consist of thick basaltic lava beds. The lava flows are typically 10-30 m thick in the LBF and 5-10 m thick in the UBF with thin beds of interbasaltic tuff-clay sediments. The MBF (stratigraphic thickness about 1350 m) consists of thin (about 1-2 m) pahoehoe flow units, often forming flowfields up to about 20 m thick. Sediment/tuff beds are of minor importance in the MBF. The base of the LBF sub-aerial basalts is found at about 2450 m in Lopra-1A (Boldreel, in press) and the lowermost 1000 m of the drilled basalt succession on the Faroes comprises mostly hyaloclastic basaltic rocks commonly with massive basalt toward the bottom of the Lopra-1A (Waagstein personal communication, September 2005).

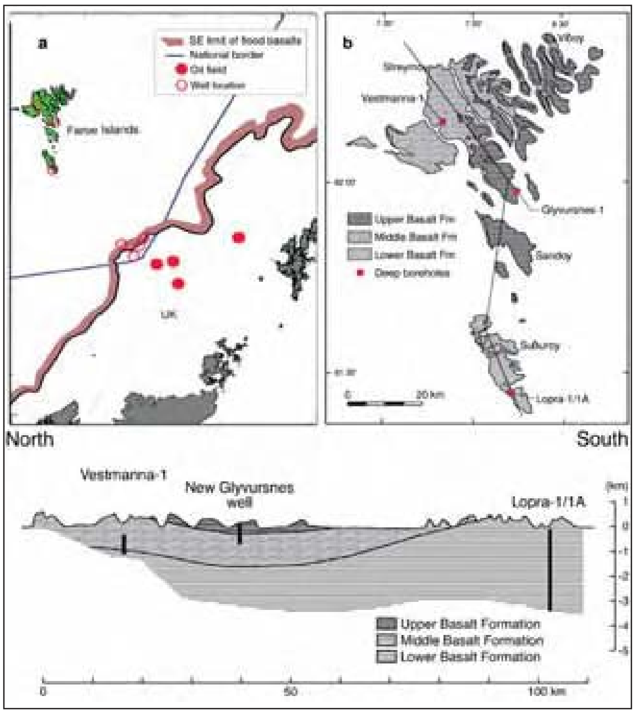

Figure 1 *Upper* **a**, *Location of the Faroe Islands relative to the extent of flood basalts. Drilled wells in the Faroes are shown as red open circles, producing oil wells are shown as red filled circles and the international border of the Faroes territory is shown as a blue line (modified from Sørensen, 2003). Upper* **b**: *Geological map of the Faroe Islands showing the locations of deep boreholes (Vestmanna-1, Glyvursnes-1 and Lopra-1/1A) and the distribution of the three Palaeogene basalt formations (modified from Waagstein, 1988). Lower: Geological section through the Faroe Islands and the three wells shown (modified from Waagstein, 1988). Location of profile is shown on upper figure* **b**.

Well logs

Full-waveform sonic and bulk-density logs in Vestmanna-1 and Glyvursnes-1 boreholes were acquired as part of the SeiFaBa project (Japsen et al., 2005). Details of the physical properties of the Vestmanna-1 and Glyvursnes-1 will be published elsewhere. The Lopra-1/1A well was logged in 1996 and P-wave sonic and bulk-density logs are available from the depth interval 200-3100 m in this well. The Vestmanna-1 and Lopra-1 well are displaced about 28 and 55 km, respectively, from Glyvursnes. However, lateral continuity of all three lava formations on the Faroe Islands is well documented (e.g., Rasmussen and Noe-Nyggard, 1970; Waagstein, 1988). It is thus likely that Vestmanna-1 and Lopra-1/1A represent the general character of the MBF and LBF below Glyvursnes.

Composite velocity and density logs corresponding to the ideal stratigraphic profile (Rasmussen and Noe-Nyggard, 1970) were constructed for the sequence below Glyvursnes using logs from Glyvursnes-1, Vestmanna-1, and Lopra-1 (Figure 2). Velocities and densities in intervals of the MBF and LBF that have not been logged are represented by logged intervals in the Vestmanna-1 and Lopra-1 that are similar based on the description of the wells (Hald and Waagstein, 1984) and on the regional mapping of the Faroes (Rasmussen and Noe-Nyggard, 1970).

Synthetic seismic data

A synthetic seismogram (without correction for geometrical spreading and other attenuation) was generated from the composite logs corresponding to the ideal stratigraphic profile using a source signature extracted from stacked airgun-geophone data (Figure 3b). Note the distinct changes in character at the UBF-MBF and MBF-LBF boundaries. The synthetic seismogram shows that the signals returning from the UBF and LBF are characterized by higher amplitude and more internal character than the signal from the MBF.

Joint time-frequency analysis carried out by means of wavelet transforms (Torrence and Compo, 1998), both of the

 © 2006 EAGE

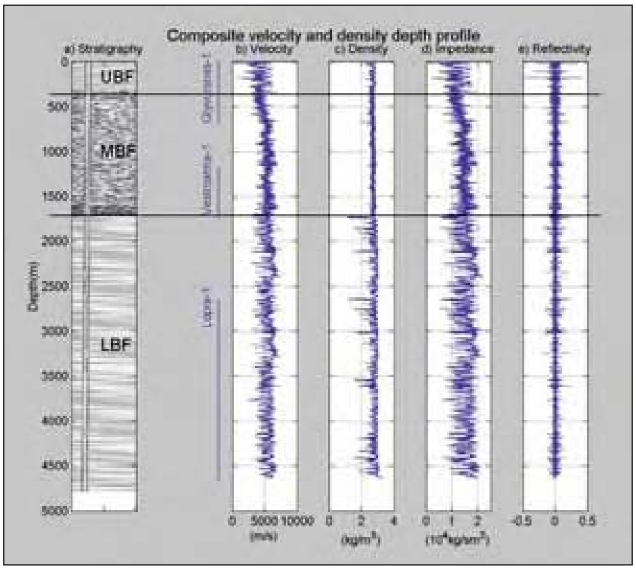

Figure 2 *Composite velocity and density logs for the total stratigraphic sequence below Glyvursnes, constructed using the logs from Glyvursnes-1, Vestmanna-1 and Lopra-1 (the actual well segments are labelled between a) and b), see also Figure 1).* **a**) *The stratigraphic division mapping the boundaries of various stages of volcanism (modified from Rasmussen and Noe-Nygaard, 1970). The base of the UBF and the base of the MBF are drawn as black horizontal lines across the figure;* **b**) *composite velocity log. The uppermost part of Vestmanna-1 log is used to represent the missing interval in the MBF and the uppermost part of the Lopra-1 log is used to represent the missing interval in the LBF;* **c**) *composite density log;* **d**) *and* **e**) *show the calculated acoustic-impedance and the reflection coefficient series. The repeated log sequences can be identified on the composite logs.*

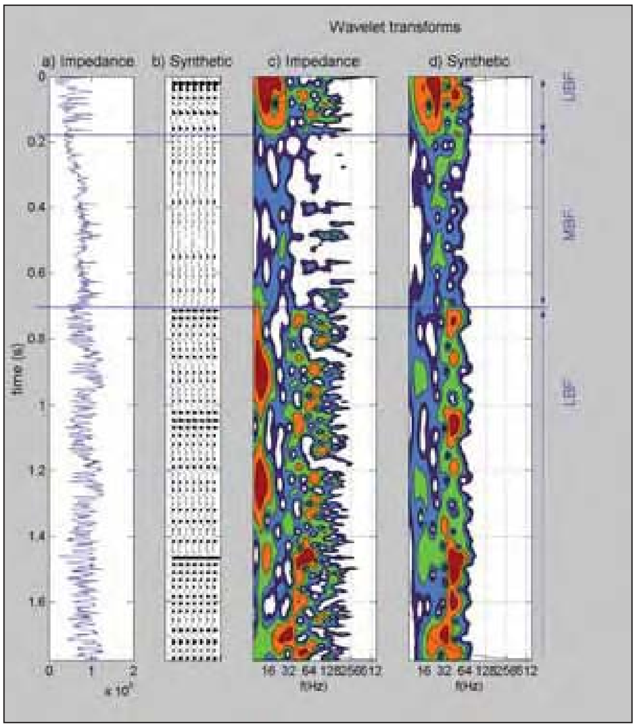

Figure 3 **a**) *Acoustic impedance from composite logs in time domain;* **b**) *Synthetic seismogram generated by means of the acoustic impedance and a source signature extracted from stacked airgun-geophone data (bandwidth 12-60 Hz) without correction for geometrical spreading or other attenuation;* **c**) *Wavelet transform of acoustic impedance. The acoustic impedance and synthetic seismogram traces are normalized by standard deviation (Torrence and Compo, 1998). Contour levels in c) and d). Contour levels are increasing exponentially.*

acoustic impedance series and synthetic seismogram, show that the MBF is characterised by generally lower amplitudes and a different frequency distribution than that of the UBF or LBF (Figure 3c and d).

Seismic data

In the summer of 2003 we acquired a composite seismic data set at Glyvursnes, on the Faroe Islands, including near-vertical-incidence seismic data using six different combinations of energy source and receiver: airgun-geophone and airgun-streamer, each with two different airgun sources; dynamite-geophone and dynamite-streamer. The layout for a selected part of the survey used for the data presented in this paper is shown in Figure 4.

Acquisition

The airgun-geophone/streamer data were acquired on a 96-channel streamer moored between a small jack-up rig near the shoreline and a tugboat at the other end (group interval 6.25 m, depth 3 m) and a line of 80 geophone stations (station interval 5 m, every fourth station had 3-component geophones, the remainder had only vertical geophones). The deployment of the streamer was very sensitive to weather conditions and tidal current and parts of the acquisition were done only with airgun-geophone recordings. The seismic sources used were a 4x40 in^3 (2.6-litre) sleeve-gun cluster and a 560 in^3 (9.2-litre) Solera-Ggun

The dynamite-geophone/streamer data comprised only a few shot-points. The seismic source was 250 g of standard dynamite (burning velocity 3000 m/s) placed in 3 m deep holes, cemented and packed. The dynamite-geophone data were acquired with a line of 120 stations (station interval 5 m) and shot-points at 10 m intervals along the line with the same source parameters as above. In the following discussion we will refer only to data acquired with the 4x40 in^3 sleeve-gun cluster and with dynamite.

Pre-stack noise analysis

Initial comparisons of shot gathers indicate that the streamer data are characterized by considerable noise deriving from a number of different sources while geophone gathers recorded with the same source are characterized by significantly less

© 2006 EAGE

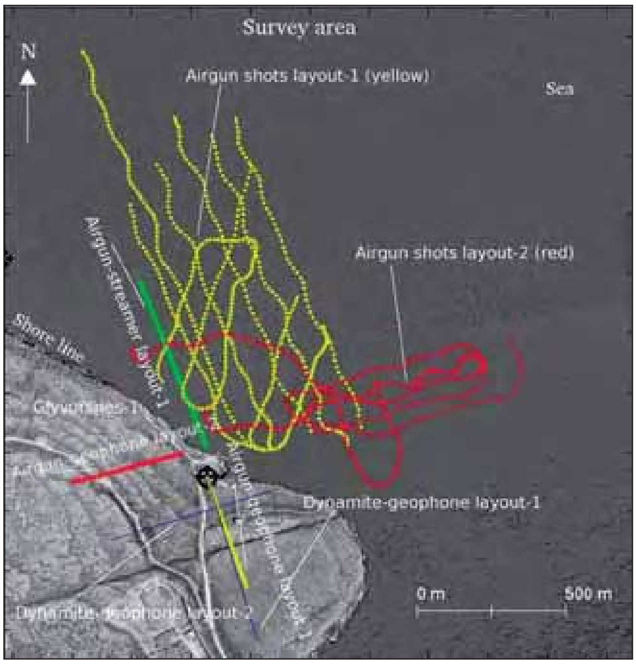

Figure 4 *Air photo of the Glyvursnes survey area showing the layout of a selected part of the survey to be presented in this paper. The airgun-geophone/streamer data were acquired with a 96-channel moored streamer (green line offshore; group interval 6.25 m, depth 3 m) and a line of 80 geophone stations (yellow and red line onshore; station interval 5 m). Layout-1 recorded at the same time on streamer and geophones (yellow geophone line and green streamer line) while during layout-2 recorded only on geophones (red geophone line). Shot-points are plotted with colours respective to the recording geophone layout. The dynamite-geophone/streamer data were recorded on layout-1 (green and yellow line). For the dynamite-*geophone *data there were two layouts (blue lines). Position of Glyvursnes-1 well is shown (black circle with plus sign).*

noise. Time-variant frequency analysis of single raw unprocessed traces based on a continuous wavelet transformation [using a Morlet wavelet with centre frequency 0.995 Hz (Addison 2002)] provides additional information about the composition of the signal and noise (Figures 5 and 6). For short recording times, and at frequencies below 256 Hz, the ambient noise on the geophones is small compared to the seismic signal (Figure 5). The bandwidth of the seismic signal from both sources decays with time reflecting the relatively low effective Q value in the basalts below Glyvursnes (Shaw et al. 2004; Shaw et al. 2005).

Although the dynamite charge used has much higher (5 times) initial chemical energy than the potential energy in the airgun, the airgun produces a better and stronger seismic signal. Most of the energy in the dynamite shot is presumably lost due to non-elastic deformation at the shot site. The centre frequency of the dynamite shots is slightly higher than that of the airgun shots (Figure 5 and Figure 6).

For logistic reasons the streamer was moored at a shallow depth (3 m). Thus the surface ghost gives rise to strong attenuation of the seismic signal at frequencies below about 60 Hz. At the same time the background noise is very strong at frequencies below about 30 Hz (Figure 6c). In addition to ambient noise, the streamer data are characterized by high-frequency noise (~128-512 Hz) caused by reverberations of the seismic signal in the water column. The combined effect of ambient noise, the ghost and reverberations in the water column is to reduce the effective bandwidth, and thus the penetration of the seismic signal recorded on the streamer relative to the signal recorded on the geophones (cf. Figure 5a and Figure 6a). However, the streamer still records a useful seismic signal for recording times up to around 1 s.

The low-frequency background noise on the streamer that we experienced during the data acquisition at Glyvursnes was to a large extent related to the special deployment of the moored streamer during this experiment. In more standard marine operations, the background noise is generally lower. Furthermore, in deep water the source and streamer depths may be adjusted to create the optimum bandwidth at the target depth using signal analysis such as that embodied in Figure 5 and Figure 6 and knowledge of the source signature and the frequency decay in the formation to be penetrated by the seismic signal. However, in the streamer data from the Glyvursnes 2003 experiment, our data has a relatively low effective bandwidth.

Preliminary processing

Generally all the recorded geophone data are dominated by refractions from shallow depths. Refractions in the dynamite-geophone data were removed by top mutes while *f-k* filtering was used for the airgun-geophone data. On the streamer data, refractions and low-frequency coherent noise from an unknown source were removed with surgical mutes.

Although the noise analysis indicates that time-variant filtering before stack is a relevant process, time-invariant filtering was preferred for the preliminary processing presented here. The airgun data were bandpass filtered at 12-14-50-60 Hz (Ormsby) while the dynamite data were filtered at 12-14-100-120 Hz (Ormsby). The dynamite-geophone data and airgun-streamer data were processed assuming a 2D geometry. A 2D filter was applied to the stacked airgun-streamer data (mixing three samples and 11 traces). Airgun-geophone data were processed with 3D geometry. Velocity analysis was performed on selected supergathers. Picked stacking velocities compare well with RMS velocities calculated from the composite velocity log of the ideal stratigraphic profile of the Faroes. Before display, automatic gain control (AGC) was applied with two different windows at 100 ms and 500 ms; traces were blended at a ratio of 1:1. A composite profile along the transect (Figure 7) illustrates the quality of the processed data obtained with the combinations dynamite-geophone, airgun-geophone and airgun-streamer (Figure 8). Although stacking improves the coherency of

© 2006 EAGE

primary reflections, the frequency content of the signal and the signal-to-noise ratio seen on the pre-stack data (Figure 5 and Figure 6) are clearly reflected in the quality of the final stack (Figure 8). The UBF-MBF boundary, which was penetrated in Glyvursnes-1, is not clear in any of the three data sets. However, horizon C' located at about 0.2 s in the dynamite-geophone and dynamite-airgun data ties well to the UBF-MBF boundary in the well. A prominent reflection at about 0.6 s, horizon A', is interpreted as the MBF-LBF boundary. The general character of the successions above and below horizon A' compares well with the character of the UBF and MBF respectively in the synthetic seismogram of the ideal profile (Figure 3b). Although the earth filter and stacking modify the frequency content of the reflected signal, the narrower frequency range of the MBF compared to the UBF and LBF observed on synthetic data is replicated in the stacked and scaled data from Glyvursnes (Figure 9). We consider this further support that horizon-A' represents the MBF-LBF boundary.

Results and discussion

Joint time-frequency analysis in the form of continuous wavelet transformation on unprocessed pre-stack data shows that the higher frequencies of the seismic data trace are reduced drastically with depth below the surface (Figure 5 and Figure 6). The overall best signal-to-noise ratio is obtained with the airgun-geophone combination.

A zero-offset VSP survey recorded in the Glyvursnes-1 borehole by Shaw (2004) demonstrated strong attenuation of the higher frequencies of the seismic signal (low Q value) below Glyvursnes. In accordance with these observations, we see that the effective bandwidth of the surface seismic data is reduced dramatically with time (Figure 5b). From an original bandwidth of about 4-128 Hz, the bandwidth is reduced to 5-20 Hz at a depth of 1.6 s (about 5300 m). This explains the supremacy of the airgun to the dynamite as a seismic source. The airgun generates a lower-frequency signal (centred at approximately 16 Hz; Figure 5a), than the dynamite (centred at approximately 32 Hz; Figure 5b) and is thus better suited for transmitting seismic signals through the basalt.

A composite profile consisting of data acquired with three different acquisition methods (Figure 8) shows that the frequency content of the signal and the signal-to-noise ratio seen in the unprocessed pre-stack data (Figure 5 and Figure 6) are reflected in the quality of the final stack. Simple stacking improves the imaging of the primary reflections.

A threefold subdivision of the seismic profile is distinct in the airgun-streamer, airgun-geophone and dynamite-geophone data. Two high-amplitude successions, one above horizon C' (0-0.16 s) and one below horizon A' (0.59 s) and

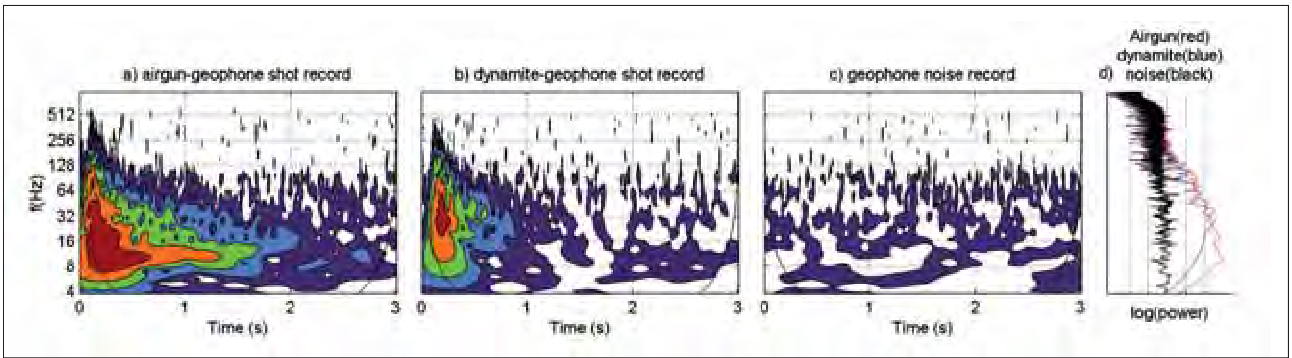

Figure 5 *Shows the continuous wavelet transforms of geophone channel 110 (station 74). a) Airgun-geophone, offset 208 m; b) Dynamite-geophone, offset 224 m; c) Geophone noise record; d) Frequency spectra of all three records. Values are not scaled. Contour levels are increasing exponentially and are the same for a), b) and c).*

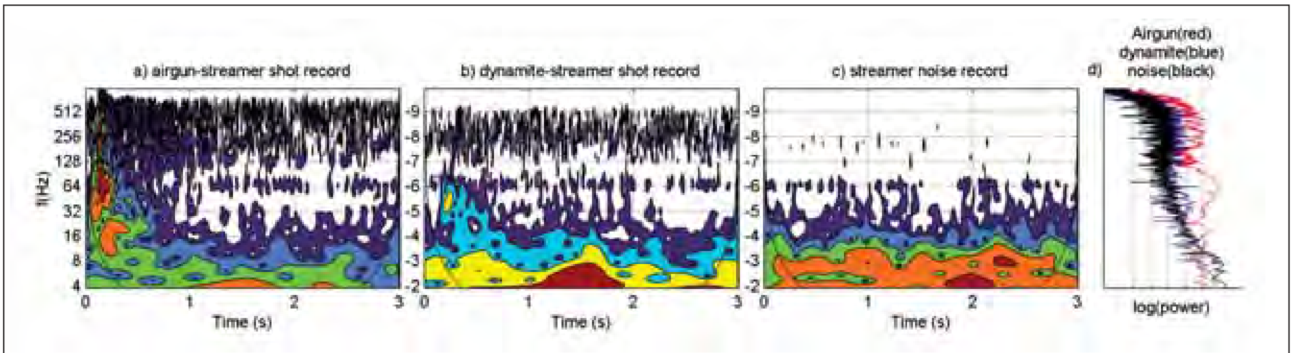

Figure 6 *Shows the continuous wavelet transforms of streamer channel 130 (station 90). a) Airgun-streamer, offset 195 m; b) Dynamite-streamer, offset 415 m; c) Streamer noise record; d) Is the frequency spectra of all three records. Values are not scaled. Contour levels are increasing exponentially and are the same for a), b), and c).*

© 2006 EAGE

a low amplitude succession (between 0.16 and 0.59 s) are clearly identified. By comparing synthetic data of the ideal profile (Figure 3b) with stacked data (Figure 8), it appears plausible that horizon A' is a reflection from (or close to) the boundary between the MBF and LBF. Furthermore, with data comparable to those acquired at Glyvursnes it might be realistic to identify the MBF by its reflection character. Multiples appear to be of minor importance above horizon A'. Although we expect multiples might be important below horizon A', we have not addressed this topic during the preliminary processing, which was aimed at understanding the nature of horizon A' below Glyvursnes.

The UBF-MBF boundary was found at about 340 m (from mean sea level) in the Glyvursnes-1 borehole (Waagstein, personal communication). Depth conversion of the seismic reflection data places the MBF-LBF boundary at a depth of 1390 m, and we thus estimate the total thickness of the MBF to be about 1050 m below Glyvursnes.

This is less than the 1350 m for the total thickness of the MBF found by Rasmussen and Noe-Nygaard (1970) in the northern part of the Faroes and the 1400 m reported from around Vestmanna (Waagstein 1988). It thus appears that the MBF thins towards the south and east. This is in general accordance with Waagstein (1988), who found that the thickness of the MBF is less between Sandoy and Suðuroy than at Vestmanna. The reason for the apparent south- and eastward thinning of the MBF could be that the amount of lava available during emplacement of the MBF was not sufficient to allow all the flows to reach Glyvursnes if their source was to the northwest. However, gradual eastward thinning of the MBF was not observed during mapping of the Faroe Islands (Rasmussen and Noe-Nyggard, 1970). Alternatively the Glyvursnes area may have been uplifted relative to the Vestmanna area after emplacement of the LBF possibly giving rise to faulting. Unfortunately, the present data do not allow us to choose among the two above-mentioned or other feasible hypotheses for the thinning of the MBF.

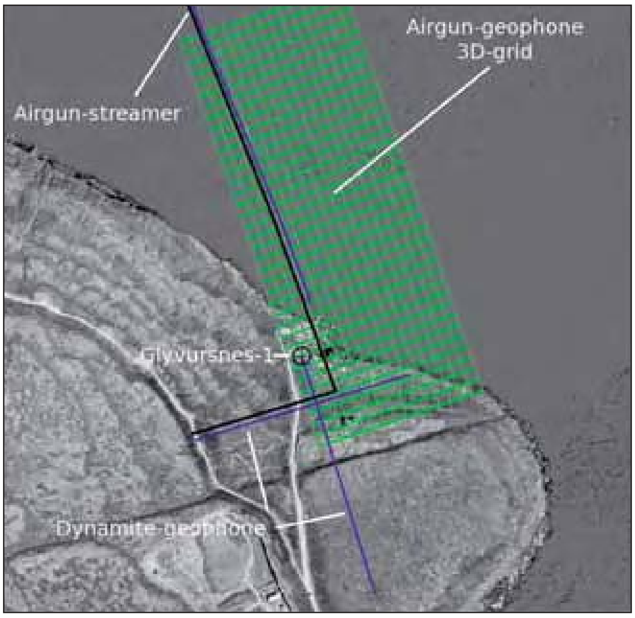

Figure 7 *Air photo of Glyvursnes survey area showing CDP positions of the 2D-processed airgun-streamer and dynamite-geophone data (blue lines), and grid for the 3D processed airgun-geophone data (green lines). The grid shows every inline and every 5th crossline. The black line shows the approximate position of combined dynamite-geophone, airgun-geophone and airgun-streamer profile in Figure 8. Position of Glyvursnes-1 borehole is also shown.*

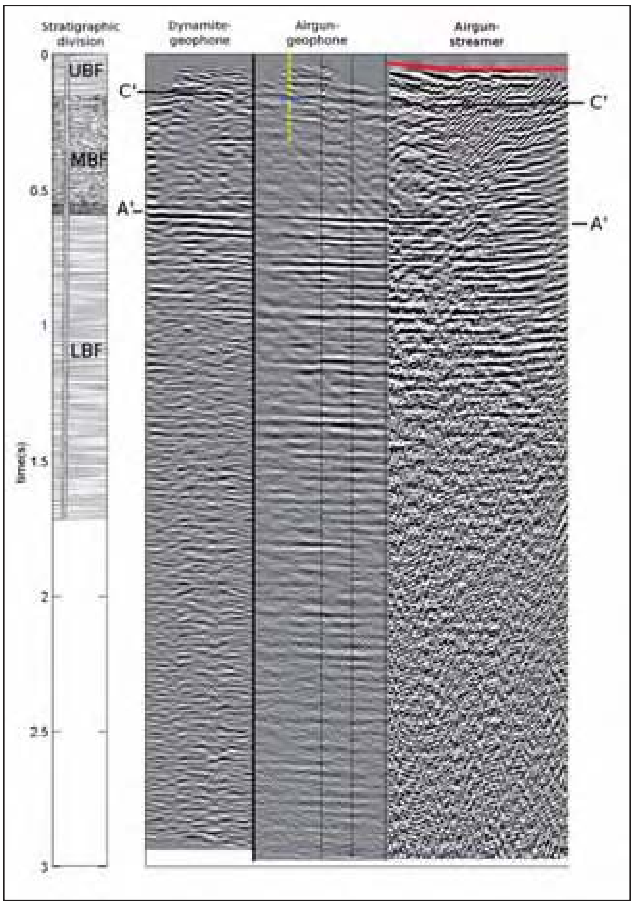

Figure 8 *shows the combined profile. See Figure 7 for location. An adjusted stratigraphic model is plotted to the left. A threefold subdivision of the seismic profile is distinct both in the airgun-geophone/streamer and dynamite-streamer data. Two high-amplitude successions (0-0.16 s and 0.59 s to end of record) and a low-amplitude succession (0.16-0.59 s) are clearly identified. By comparing this figure to Figure 3b (synthetic from composite logs), we see that the low-amplitude succession is characterised by a frequency content that is comparable to that of the synthetic seismogram through the MBF, while the frequency content of the lower high-amplitude succession is comparable to that of the LBF. Horizon C' ties well to the UBF-MBF boundary in the well (blue marker on yellow line). A' is interpreted to be the MBF-LBF boundary. The red line is the seabed derived from bathymetric information.*

© 2006 EAGE

When considering possible errors in the estimate of the thickness of the MBF below Glyvursnes, one has to bear in mind that the Glyvursnes-1 well had a check-shot at 600 m depth, which constrains the time-depth relation down to this depth. Any significant error in the estimated thickness is thus due to erroneous velocities below 600 m. From 600 m to horizon A', a variation of the interval velocities of ± 10% affects the depth of horizon A' by ± 80 m. It is thus unlikely that the thickness of the MBF at Glyvursnes is comparable to the thickness at Vestmanna, unless an unrealistic average velocity around 7000 m/s is considered likely, or the interpretation of horizon A' as the MBF-UBF boundary is rejected.

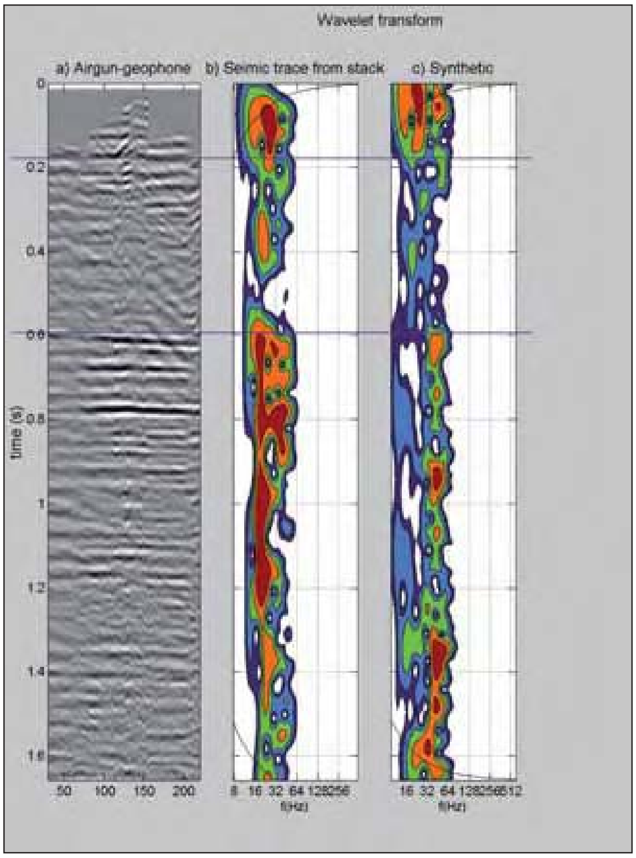

Figure 9 a) *Inline-2 from airgun-geophone stacked data;* **b**) *Wavelet transform of trace from the stack; c) Wavelet transform of the synthetic seismogram generated from the adjusted model. The seismic trace and the synthetic seismogram are normalized by standard deviation (Torrence and Compo, 1998). Contour levels are increasing exponentially. By comparing with Figure 3, we see the same generally lower amplitude and different frequency content for the signal arriving from the MBF than for the signal arriving from the UBF or LBF. This is thus a further verification of the interpretation of the base of MBF (horizon A') and adjustment of the thickness of the MBF. AGC has been applied to the seismic data, resulting in a higher amplitude level for the MBF.*

Acknowledgements

The SeiFaBa project is founded by the Sindri Group (www.sindri.fo). Acquisition of reflection seismic data was done with equipment from the Department of Earth Science, University of Aarhus. Processing with Promax was done at the Department of Earth Science, University of Aarhus. A special thanks to Sjúrður Patursson, farmer on acquisition site for goodwill during fieldwork. We are grateful to students from University of Cambridge, Aarhus University, and University of Faroe Islands for assistance during fieldwork. We thank Robert James Brown, University of Faroe Islands, for proof reading.

Reference List

Addison, P. [2002] *The Illustrated Wavelet Transform Handbook*. Institute of Physics Publishing, London.

Andersen, M. S., Sorensen, A. B., Boldreel, L. O., and Nielsen, T. [2002] Cenozoic evolution of the Faroe Platform: comparing denution and deposition. *Geological Society, London, Special Publications,* **196**, 291-311.

Archer, S. G., Bergman, S. C., Iliffe, J., Murphy, C. M., and Thornton, M. [2005] Palaeogene igneous rocks reveal new insights into the geodynamic evolution and petroleum potential of the Rockall Trough, NE Atlantic Margin. *Basin Research,* **17**, 1, 171-201.

Boldreel, L. O. Wire-line log-based stratigraphy of flood basalts from the Lopra-1/1A well, Faroe Islands. *Geological Survey of Denmark and Greenland Bulletin,* København.

Fruehn, J., Fliedner, M. M., and White, R. S. [2001] Integrated wide-angle and near-vertical subbasalt study using large-aperture seismic data from the Faeroe-Shetland region. *Geophysics,* **66**, 5, 1340-1348.

Hald, N. and Waagstein, R. [1984] Lithology and chemistry of a 2-km sequence of Lower Tertiary tholeiitic lavas drilled on suðuroy, Faeroe Islands, (Lopra-1). The deep drilling project [1980-1981] in the Faeroe Islands 15-38. *Føroya Fróðskaparfelag*, Tórshavn.

Japsen, P., Andersen, C., Andersen, H. L., Andersen, M. S., Boldreel, L. O., Mayko, G., Mohammed, N. G., Pedersen, J. M., Petersen, U. K., Rasmussen, R., Shaw, F., Springer, N., Waagstein, R., White, R. S., and Worthington, M. [2005] Preliminary results from investigations of seismic and petrophysical properties of Faroes basalts in the SeiFaBa project. Petroleum Geology: North-West Europe and Global Perspectives. *Proceedings of the 6th Petroleum Geology Conference,* 1461-1470.

Maresh, J. and White, R. S. [2005] Seeing through a glass, darkly: strategies for imaging through basalt. *First Break* **23**, 27-33.

Planke, S. [1994] Geophysical Response of Flood Basalts from Analysis of Wire Line Logs - Ocean Drilling Program Site-642, Voring Volcanic Margin. *Journal of Geophysical Research-Solid Earth,* **99** (B5), 9279-9296.

Planke, S., Alvestad, E., and Eldholm, O. [1999] Seismic characteristics of basaltic extrusive and intrusive rocks. *The Leading Edge,* **March,** 342-348.

© 2006 EAGE

Rasmussen, J. and Noe-Nyggard, A. [1970] *Geology of the Faeroe Islands*. C. A. Reitzels Forlag, København.
Reshef, M., Shulman, H., and Ben-Avraham, Z. [2003] A case study of sub-basalt imaging in land region covered with basalt flows. *Geophysical Prospecting*, **51**, 3, 247-260.
Richardson, K. R., White, R. S., England, R. W. and Fruehn, J., [1999] Crustal structure east of the Faroe Islands: mapping sub-basalt sediments using wide-angle seismic data. *Petroleum Geoscience,* **5**, 2, 161-172.
Self, S., Keszthelyi, L. and Thordarson, T. [1998] The importance of pahoehoe. *Annual Review of Earth and Planetary Sciences,* **26**, 81-110.
Shaw, F., Worthington, M. H., White, R. S., Andersen, M. S., Petersen, U. K., and SeiFaBa Group [2004] A study of seismic attenuation in basalt using VSP data from a Faroe Islands borehole. *66th Meeting European Association of Geoscientists and Engineers*. Expanded abstract P015.
Shaw, F., Worthington, M. H., White, R. S., Andersen, M. S., Petersen, U. K., and SeiFaBa Group [2005] Seismic attenuation in Faroe Island basalts. *67th Meeting European Association of Geoscientists and Engineers*. Expanded abstract P502.
Sørensen, A. B. [2003] Cenozoic basin development and stratigraphy of the Faroes area. *Petroleum Geoscience* **9**, 189-207.
Spitzer, R. and White, R. S. [2005] Advances in seismic imaging through basalts: A case study from the Faroe-Shetland Basin. *Petroleum Geoscience,* **11**, 2, 147-156.
Thordarson, T. and Self, S. [1998] The Roza Member, Columbia River Basalt Group: A gigantic pahoehoe lava flow field formed by endogenous processes? *Journal of Geophysical Research-Solid Earth* **103**(B11), 27411-27445.
Torrence, C. and Compo, G. P. [1998] A practical guide to wavelet analysis. *Bulletin of the American Meteorological Society* **79**(1), 61-78.
Waagstein, R. [1988] Structure, composition and age of the Faeroe Basalt plateau, Early Tertiary Volcanism and the opening of the NE Atlantic. *Geological Society Special Publication* **39** 225-238.
White, R. S., Smallwood, J. R., Fliedner, M. M., Boslaugh, B., Maresh, J. and Fruehn, J. [2003] Imaging and regional distribution of basalt flows in the Faeroe-Shetland Basin. *Geophysical Prospecting* **51**(3), 215-231.
White, R. S., Spitzer, R., Christie, P. A. F., Roberts, A., Lunnon, Z., Maresh, J., and iSimm Working Group [2005] Seismic Imaging through Basalt Flows on the Faroes Shelf. Faroe Islands Exploration Conference, Proceedings of the 1st Conference. *Føroya Fróðskaparfelag*, Suplementum **43**, Tórshavn, 11-31.
Ziolkowski, A., Hanssen, P., Gatliff, R., Jakubowicz, H., Dobson, A., Hampson, G., Li, X. Y., and Liu, E. R. [2003] Use of low frequencies for sub-basalt imaging. *Geophysical Prospecting,* **51**, 3, 169-182.

 © 2006 EAGE

1-D heterogeneity and statistical studies of the Faroes wireline logs

Felicia Shaw

Introduction

Acoustic modelling has shown that the style of 1-D attenuation varies between the Faroes boreholes. In synthetic seismograms from the Vestmanna log data, the attenuation from 1-D multiple interference occurs at frequencies > 125 Hz, while the Glyvursnes synthetic seismograms exhibit scattering behaviour at a range of frequencies. Alternating two-velocity models demonstrate that strong periodic layering produces localised notches in the spectrum, but this phenomenon cannot fully account for the low Q estimates from real logs. In order to study the effects of multiple interference, log characteristics must first be rigorously described.

Scale invariance has been widely observed in wireline logs from the upper crust of the Earth, such as at Cajon Pass (California), KTB (Germany), Stenberg (Sweden), Sudbury (Canada) and the Abitibi (Canada) boreholes, despite their differing chronology, petrology and tectonic structure (Marsan and Bean, 2002).

In this report, the statistics of 1-D wireline logs at Glyvursnes and Vestmanna are measured, and evidence of fractal behaviour is assessed. The relationship between perceived fractal characteristics and 1-D synthetic seismic response is examined using the spectral ratio method of Q analysis and scalograms.

Monofractal analysis

Fractals are geometrical objects satisfying two criteria: fractional dimensionality (as opposed to the integer dimensions of Euclidean objects) and self-similarity. Self-similarity is satsified when sub-units on multiple levels statistically resemble the structure of the object as a whole. (Mandelbrot, 1989).

One commonly used descriptor of self-similarity is the Hurst exponent, which was first formulated to assess fluctuations in reservoirs (Hurst et al, 1965). Estimating the Hurst exponent for a data set provides a measure of whether the data is a pure random walk or has underlying trends. Over a certain range of time or space, the autocorrelation decays over time according to a power law. A Hurst exponent of exactly 0.5 indicates a random or Brownian walk. In a random walk there is no correlation between any element and a future element. A Hurst exponent value of between 0.5 and 1 indicates persistence, or positive autocorrelation over a certain range, where the succeeding values are influenced by preceding values. A Hurst exponent of between 0 and 0.5 indicates anti-persistence, or negative autocorrelation over a certain range, where succeeding values tend to be the reverse of preceding behaviour. The Hurst exponent is thus directly related to the roughness of a signal, and to its fractal dimension by:

$$H = 2 - D$$

Power spectral method

A typical first step in analysing logs is to de-trend the data, in order to separate deterministic components (e.g. depth-velocity trends, known structural trends) from the residual, stochastic components. Dolan et al (1998) and Holliger (1996) note that this imposes arbitrary scale lengths on the data and may skew the H values. In this analysis, de-trending has been avoided in favour of choosing log intervals which do not cross known formation boundaries such as the Middle to Upper Series transition at approximately 355 m in the Glyvursnes borehole, or Lower Series sediments/lavas at approximately 550 m in Vestmanna. No detailed petrographic description of the Lopra borehole was available, so two sections with contrasting visual characteristics were chosen arbitrarily. Table 1 lists the borehole intervals analysed.

The power spectrum of each dataset was derived by squaring the magnitude of the Fourier transformed data. Power-law dependence, or 1/wavenumber decay, is indicative of a fractal medium. The slope β of the spectrum in $\log_{10}$ wavenumber - $\log_{10}$ power space is related to the Hurst exponent H by:

$$\beta = 2H + 1$$

(Turcotte, 1997).

Results

Power spectral plots of the acoustic impedance logs are shown in Figures 1 to 3. Linear trends occurred in all the datasets, but breaks in slope occur at different scales. This may be due to the averaging effect of the sonic tool, which acts like a boxcar window of the data in the frequency domain and skews the gradient of 1/wavenumber decay (Dolan et al, 1998). At Vestmanna and Glyvursnes the maximum source-to-receiver distance of the sonde was 1.1 m in length, and at Lopra the maximum source-to-receiver distance was 3 m, corresponding to a $\log_{10}$ wavenumber of approximately -0.1. For reference, the scales corresponding to 1.1 m and 3 m are indicated as dashed lines in Figures 1 – 3 b, c.

Table 2 lists Hurst exponents of acoustic impedance from the three boreholes and the spatial scales over which they were derived. Varied statistical behaviour in the three localities is revealed. The Vestmanna log from 296 – 500 m is shown to be anti-persistent. The Glyvursnes log from 396 – 600 m has the characteristics of a random walk, and the Glyvursnes log from 50 – 255 m and the Lopra log from 1250 – 1562 m show persistence.

The power spectral analysis clearly shows fractal behaviour in the Faroes basalt logs. The extent of fractal behaviour, as described by the Hurst exponents, varies between the datasets. The sections of Glyvursnes corresponding to the Upper and Middle Basalt Series do not appear to exhibit differing characteristics. However, the anomalous results from Vestmanna and Lopra suggest that the power spectral method is not capable of fully describing the fractal character of the datasets.

The Hurst exponent is the scaling exponent for a second order statistical measure, and can only characterise monofractal behaviour of order 2. The level of intermittency of the fluctuations cannot be retrieved by this method. This is a major pitfall, as the acoustic impedance structures seen in Figures 1a, 2a and 3a evolve with depth; *a priori* geological knowledge about the Faroes Basalt Series boundaries may not be directly related to actual fractal behaviour.

Variations in the signal's degree of fluctuation require a location-dependent scaling exponent, itself distributed in a scale-invariant way (Marsan and Bean, 2002).

Multifractal analysis

Advances in the study of fractal turbulence (Mandelbrot, 1990, Bacry et al, 1993) have extended the concept of fractal dimensions to multifractal measures. In the latter, the higher order statistical measures of the signal are taken into account and analysed for scale-invariant behaviour. At each level, a different fractal exponent and power law decay behaviour may be exhibited, allowing intermittency and roughness of a signal to be characterised. These levels of detail are vital in understanding the complexity of basalt log data.

The Wavelet Transform Modolus Maxima Method (WTMM)

A natural diagnostic tool for multifractals is the wavelet transform. A method pioneered by Bacry, Muzry and Arnéodo (1993) uses wavelet transform modulus maxima (WTMM) to derive fractal dimensions and has been tested by Herrmann (1998) on borehole log and seismic data. This technique has been used in the following analyses and is outlined below.

A borehole log can be treated as a function which fluctuates with depth, and the irregularity of the function described by how it behaves under differentiation. At any point where the function cannot be differentiated, it is termed a singularity and its type characterised by the Lipschitz exponent α (also referred to as the Hölder exponent). More negative α values indicate a greater abruptness (tending towards a Dirac delta function) while smoother discontinuities take positive α values, as seen in Figure.4 (Herrmann, 1998).

The wavelet transform allows simultaneous analysis of a signal's temporal / spatial and frequency properties. Based on the dilation and translation of elementary wavelets, it possesses greater versatility over Fourier analysis and related transforms, especially when zooming into and out of signal structures. Unlike in Fourier analysis, the wavelets used in the wavelet transform are well localised in time / space. Therefore it is possible to use the wavelet transform to measure Lipschitz exponents over both intervals and points (Mallat, 2001).

Figures 5a and b show the real, continuous wavelet transforms of the Vestmanna acoustic impedance log between 50 and 255 m, under two different analysing wavelets. The local maxima correspond to singularities, with small scale features mapped at the top of the transform and larger scale features mapped at the base. The log data are self-similar in the wavelet transform domain, therefore demonstrating that they are self-similar in the spatial domain. In order to ignore spurious structures, the modulus maxima are chained (Bacry et al, 1993). The small scale maxima are contiguous with the large scale maxima (Figure 5c).

The log data can be considered to be a statistical distribution with moment q. The chained modulus maxima of the wavelet transform are spatially averaged to produce fractal partition functions, for a range of moment q values, and if straight line trends are observed, power-law dependence is indicated (Figure 5d). Whereas a power spectral analysis only calculates a power-law dependence value for the second moment, q=2, the WTMM calculates values for any given range of moments within the data. The gradients of the lines of best fit are used to derive the mass exponents τ (q) (Figure 5e), which is then converted to a singularity spectrum f(α) by a Legendre transform (Mandelbrot, 1989).

The singularity spectrum describes the complexity of the borehole data in several important ways. Firstly, it gives the proportion of α singularities that appear at any scale. In monofractal data all singularities would have the same α value, whereas a multifractal signal has a distribution of different singularity styles, and hence a convex singularity spectrum. Figure 6 relates the mass exponents τ (q) to the shape of the singularity spectrum of a theoretical multifractal (after Mandelbrot, 1989). The intensity and intermittency of the signal can thus be quantified.

Routines based on the WTMM technique have been incorporated into Stanford's freeware program WAVELAB, which has been used extensively in the analyses of the Faroes datasets.

Precautions in multifractal analysis

The WTMM method was applied to the acoustic impedance and S-velocity logs, over the same six depth sections as in the power spectral analyses. Neutron porosity logs from Vestmanna and Glyvursnes were also analysed. The logs analysed have widely varying maximum amplitudes, but the presence or addition of a DC component does not affect the statistical calculations (Bacry et al, 1993). This was verified by testing and no normalisation of the different datasets was needed.

Real wavelets (as opposed to complex analytic wavelets) are used for detecting sharp signal transitions (Mallat, 2001) and have been used in this study. It was vital to choose an analysing wavelet that would resolve all the fluctuations in the signal. The wavelet's number of vanishing moments is related to its rate of decay and thus its differentiability. In theory, the analysing wavelet must have at least as many vanishing moments and the same differentiability as the signal under study (Herrmann, 1998). In practice, a satisfactory analysing wavelet is able to detect fluctuations down to the smallest scale, a property which can be easily seen in the wavelet transform space. A range of different wavelet types was tested against this criterion and the Morlet and ‘Mexican Hat’ wavelets subsequently used.

The real Morlet wavelet is a sinusoid modulated by a Gaussian envelope, and was implemented in the form:

$$\hat{\psi}(\omega) = \frac{1}{\sqrt{s}}\left[\exp\left(-\frac{(\omega-\omega_0)^2}{2}\right) - \exp\left(-\frac{\left(\omega^2+\omega_0{}^2\right)}{2}\right)\right]$$

The Mexican Hat is the second derivative of a Gaussian wavelet and was implemented in the form:

$$\hat{\psi}(\omega) = \frac{1}{\sqrt{s}}\left(\omega^2\right)\exp\left(-\frac{\omega^2}{2}\right)$$

where *s* is the wavelet scale and *ω* the frequency. The Morlet wavelet has better frequency localisation, while the Mexican Hat wavelet has better localisation properties in time or space (Torrence et al, 1998).

Figures 5a and b illustrate the differences between the two wavelet transforms. Both analysing wavelets capture details at the finest scale. At intermediate scales, the Mexican Hat wavelet senses the structures more efficiently due to its quicker time decay.
(e.g. the high amplitude event at ~ 200 m). The Morlet wavelet, which has more peaks and troughs, clouds the transform with extraneous maxima which may adversely affect interpretation. When deriving the fractal partition functions, inflexions are seen at scales corresponding to where the scales interfere (Figure 5c). However, taking the gradients of the partition functions suppresses the instabilities, and the resulting singularity spectra are not affected.

Results

The singularity spectra for acoustic impedance logs of the six borehole intervals are shown in Figure 7. All six are distributions of singularities, and have the convex spectra expected of multifractal signals. The lower Lopra interval produces the narrowest spectrum of the six. This is in accordance with visual inspection of the log; comparatively simple fluctuation style is seen (Figure 3a).

Table 3 summarises the findings from the sixteen logs analysed. For easy interpretation, the minimum α, maximum α and $<\alpha>$ values of the spectra are plotted in three-dimensional space. The results from the Mexican Hat analyses are shown in Figure 8a. They were judged to be more reliable than the Morlet wavelet analyses, as their continuous wavelet transforms contained fewer artefacts or extraneous maxima. Data from the Vestmanna and Lopra boreholes cluster separately, with further differentiation between their respective upper and lower depth intervals. The Glyvursnes data, interestingly, show the largest range in their singularity spectra. The lower 396 – 600m data plot more diffusely in a region spanning the Lopra and Vestmanna clusters, while the upper 50 – 255 data have distinctly larger α values than the other five depth sections.

The results from the Morlet wavelet analyses (Figure 8b) have been included for comparison. The Vestmanna data are once again shown to have the greatest affinity, and the data from the lower Glyvursnes interval overlap into the Vestmanna cluster. Data from the upper Glyvursnes interval are once again distinct. The main deviation from the Mexican Hat analysis comes from the behaviour of the Lopra logs.

Relationship between 1-D scattering attenuation and multifractal character

Using the wavelet transform modulus maxima method (WTMM), it has been established that the borehole logs of Faroes basalts exhibit a range of multifractal characteristics. A change in multifractal character could be analogous to a real world scenario where the lava emplacement mechanisms are self-similar throughout the evolution of a volcanic terrane, but deviations in physical attributes such as viscosity and / or lava chemistry alter the extent of self-similarity. A complex pattern of frequency interference arises, which is not adequately modelled as random noise superimposed on low-frequency sinusoids or square-waves. In this section, self-similar methods of model generation are explored, and synthetic seismic responses are analysed.

Synthesis of multifractal logs

Multiplicative cascades are iterative processes that fragment a given set into smaller and smaller sections according to a geometric rule, distributing the total mass of the given set according to another rule (e.g. a random fraction of mass at the previous step). If the redistribution preserves the total mass of the initial set at each stage of the construction, the cascade is 'conservative' (Mandelbrot, 1989).

Conservative multifractals can be created by the inverse Fourier transform of a random signal (Mandelbrot, 1987), or by the inverse wavelet transform of a random distribution (Arnéodo, 1993). A conservative multifractal thus has the same scaling statistics in all directions. In preliminary tests, it was found that Arnéodo's wavelet cascade scheme was difficult to implement: the statistics of the synthetic datasets could not be easily varied, and the method produced poor results when converting from the wavelet domain to the spatial domain. Furthermore, the criterion of statistical isotropy is also easily justified for models of crustal heterogeneity, where datasets are frequently self-affine rather than self-similar (Marsan and Bean, 2003).

A more suitable model is the non-conservative multifractal model, where the redistribution of mass from one scale to another is not rigidly conserved. (The concept of 'conservative / non-conservative' is thus related to, but cannot be used interchangeably with, the geostatistical concept of 'stationarity / non-stationarity'.) Non-conservative multifractals can be created by modifying the statistical measures of a conservative multifractal, and existing approaches include the fractional integration method (Schertzer and Lovejoy, 1987); the multifractal operational time method (Mandelbrot, 1997); and a hybrid two-step integration scheme by Marsan and Bean (2003).

Schertzer and Lovejoy's fractional integration method employs two parameters, C1 and χ to control the apparent 'roughness' of the surface. The C1 parameter adjusts the mass of the measure, and is related to the mass exponent $\tau(q)$ described in section 2.1. As C1 increases, the amplitude of the strongest fluctuations increases, creating 'intermittency'. The χ parameter adjusts the slope of the power relations, and as the χ parameter increases, the relative intensity of the fluctuations decreases, producing 'smoothness'. Figure 9 displays the change in the shape of the signal as C1 and χ are modified.

Fifty-six synthetic multifractals with a C1 value of between 0.01 and 0.08 and χ value of between 0.1 and 0.7 were generated using a scheme adapted for Matlab® by Marsan and Bean (2003), and then analysed via the WTMM method. In Figure 10, the α exponents of the fifty-six multifractals are presented as a surface, on which the α exponents of the real log data are overlaid. This shows that the fractional integration method produces statistical measures which are closest to that of the real data, and also confirms that the Faroes logs span a range of intermittent, fluctuant behaviour. In parallel tests, the two-step integration method did not produce datasets with either the visual characteristics or the statistical behaviour of real Faroes borehole logs. Synthetic logs from the multifractal operational time method only superficially resembled the real data, and when analysed by the WTMM, did not approach the statistics of the real data closely enough.

Seismic response of synthetic multifractal logs

Ten synthetic logs which most closely approached the statistics of the real data were investigated for their seismic response. The models, described in Table 4, were at first adjusted to a range of actual Vestmanna P-velocity and density log values to create synthetic borehole logs. Typical mean velocity was 5.1 km/s, and typical mean density was 2.7 g/cc. It has been confirmed in this work and other studies (Herrmann, 1998) that such adjustments, and the addition of DC components, do not affect the singularity spectra. The synthetic logs were built to 102.4 m, the same length as the Vestmanna and Glyvursnes data previously analysed.

The intrinsic Q was set at a value of 1000, and a broadband zero-phase wavelet with frequency content up to 800 Hz was propagated through the synthetic logs using an algorithm by Kennett (1973). The transmitted wave from each model was then submitted to analysis by the spectral ratio method, giving effective Q and 1-D scattering Q estimates.

Initial findings were that there was little or no attenuation in the synthetic multifractals. Despite high Q estimates exceeding 250, there was strong indication that as the χ (smoothness) parameter increased, Q increased, while higher C1 (intermittency) parameters did not appear to lower the Q value significantly.

Table 5 lists mean values and standard deviation of the P-velocity and density for Vestmanna and Glyvursnes data. To test if such differences in the first-order statistics affected the Q estimation, models with the same multifractality but different mean velocities were generated. These were based on the upper section Glyvursnes data, from which synthetic seismograms had exhibited the greatest amount of 1-D scattering attenuation.

Figure 11 shows a scalogram of a synthetic seismogram normalised to Vestmanna velocity and density values. Figure 12 shows a scalogram of the response for the same multifractal log, normalised to Glyvursnes velocity and density values. While the multifractal statistics characterised by α remained unchanged, the increased P-velocity and density ranges led to noticeable effects in time and frequency. There is a relatively longer coda, with increased energy between scales 2 and 4 (250 - 500 Hz), between 10 and 50 milliseconds. Stronger interference minima are created which impinge on the primary wavelet.

When a 100 Hz centre frequency wave was propagated through the same log, the seismogram had a truncated spectral response (Figure 13). This is an expected outcome, but the lack of information below scale 4 (i.e. less than 250 Hz) masks the behaviour exhibited in Figures 11 and 12.

Conclusions

The Faroes log datasets have been shown to exhibit fractal behaviour, which varies not only across the three locations but also with depth. Based on plots of the exponent α, the clustering of data points was found to be compatible with geological interpretations of basalt formations intersected by the boreholes.

Synthetic logs were generated from Faroes multifractal statistics. In order to determine if multifractal character was the cause of low Q values, acoustic modelling was performed on the logs and the resulting traces analysed in time and frequency. Impingement of multiple energy on the primary wavelet, especially at small scales (high frequencies) would lead to significantly lower Q estimates. Findings show that the pattern of interference in the theoretical seismograms is controlled by the intensity and scale of fluctuation. However, the multifractals modelled do not produce enough interference at small scales.

Interference at all scales causes spectral ratios TO vary locally, re-emphasizing the importance of the propagating wavelet's bandwidth and also time-gating of the output primary wavelet. Time-frequency analysis via scalograms is a useful tool in monitoring these parameters.

Rererences

Bacry E., Muzy, J.-F., & Arneodo, A. 1993. *Singularity spectrum of fractal signals from wavelet analysis: Exact results.* Journal of Statistical Physics. v.70, p. 635-674.

Dolan, Sean, S., Bean, Christopher J., & Riollet, Bruno (1998). *The broad-band fractal nature of heterogeneity in the upper crust from petrophysical logs.* Geophys. J. Int v.132, p. 489-507.

Herrmann, Felix. 1998. *Multiscale analysis of well and seismic data.* Mathematical Methods in Geophysical Imaging V, Proceedings of SPIE v.3453. p. 180-208.

Holliger, K. 1996. *Upper-crustal seismic velocity hetereogeneity as derived from a variety of P-wave sonic logs.* Geophysical Journal International, vol. 115, p. 813-829

Hurst, H.E., R. P. Black, and Y. M. Simaika, 1965, *Long Term Storage; An Experimental Study* (Constable, London).

Mallat, Stéphane. 2001. A wavelet tour of signal processing, 2nd edn. Academic Press.

Mandelbrot, Benoit 1989. *Multifractal measures, especially for the geophysicist.* PAGEOPH. v. 131, p. 5-42.

Marsan, David & Bean, Christopher J. 1999. *Multiscaling nature of sonic velocities and lithology in the upper crystalline crust: evidence from the KTB Main Borehole.* Geophysical Research Letters, vol. 26, no. 2, p. 275-278

Marsan, David & Bean, Christopher J., 2002. *Multifractal modeling and analyses of crustal heterogeneity,* Ch 8 Heterogeneity in the Crust and Upper Mantle : Nature, Scaling and Seismic Properties, eds. J. A. Goff and K. Holliger, Kluwer Academics.

Torrence,C. & Compo,G. 1998. Practical Guide to Wavelet Analysis. Bulletin of the American Meteorological Society, vol.79, no.1, p.61-78.

WaveLab802 software
http://www-stat.stanford.edu/~wavelab/

Borehole	**Glyvursnes**	**Vestmanna**	**Lopra**
	Depth range /m (sampling interval /m)	Depth range /m (sampling interval /m)	Depth range /m (sampling interval /m)
Borehole Intervals	**50.13 – 254.73 (0.2)** *Upper Basalt Series* **395.53 – 600.13 (0.2)** *Middle Basalt Series* **50.13 – 600.13 (0.2)** *VSP Interval*	**50.1 – 254.7 (0.2)** *Middle Basalt Series* **295.5 – 500.1 (0.2)** *Middle Basalt Series* **50.1 – 500.1 (0.2)** *VSP Interval*	**1250.1 – 1562.1** (0.1524) **2600.1 – 2912.1** (0.1524) *Lower Basalt Series with varied lithological changes. Detailed interpretation unavailable*

Table 1. *Depth range of borehole log datasets analysed*.

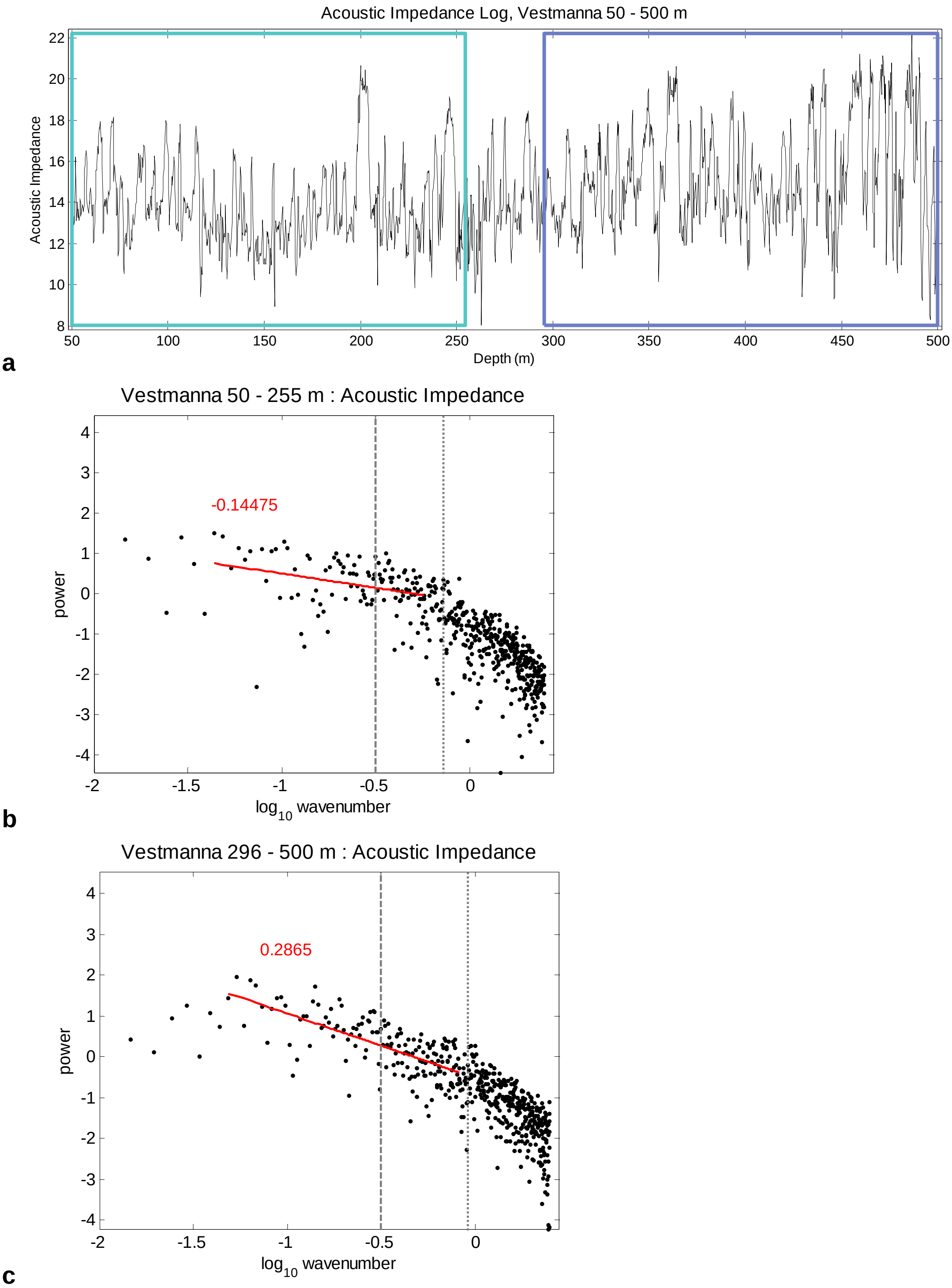

Figure 1

a. *Acoustic impedance log of the Vestmanna borehole***.**

b. *Power spectral analysis of the upper interval, 50 – 255 m.*

c. *Power spectral analysis of the lower interval, 296 – 500 m.*

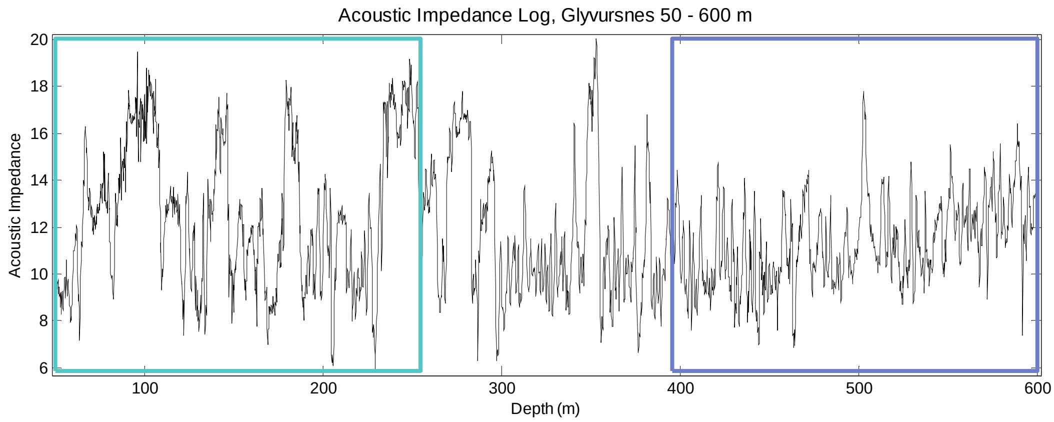

a

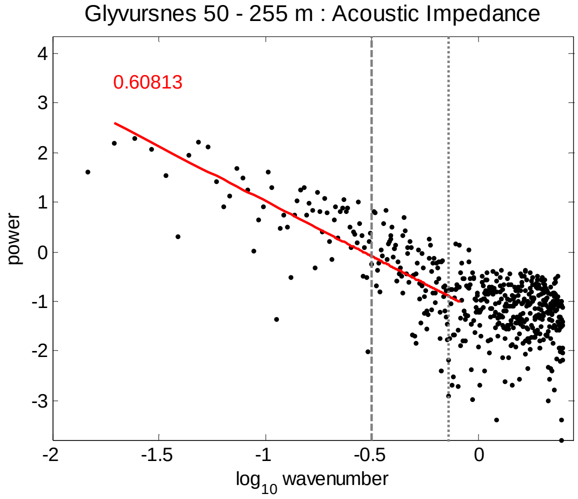

b

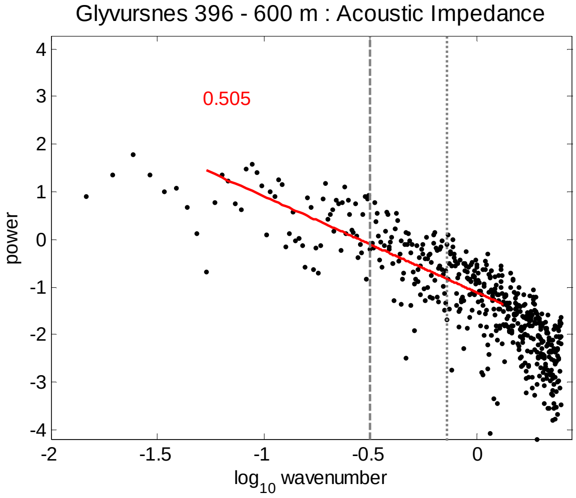

c

Figure 2

a. *Acoustic impedance log of the Glyvursnes borehole*.

b. *Power spectral analysis of the upper interval, 50 – 255 m.*

c. *Power spectral analysis of the lower interval, 396 – 600 m.*

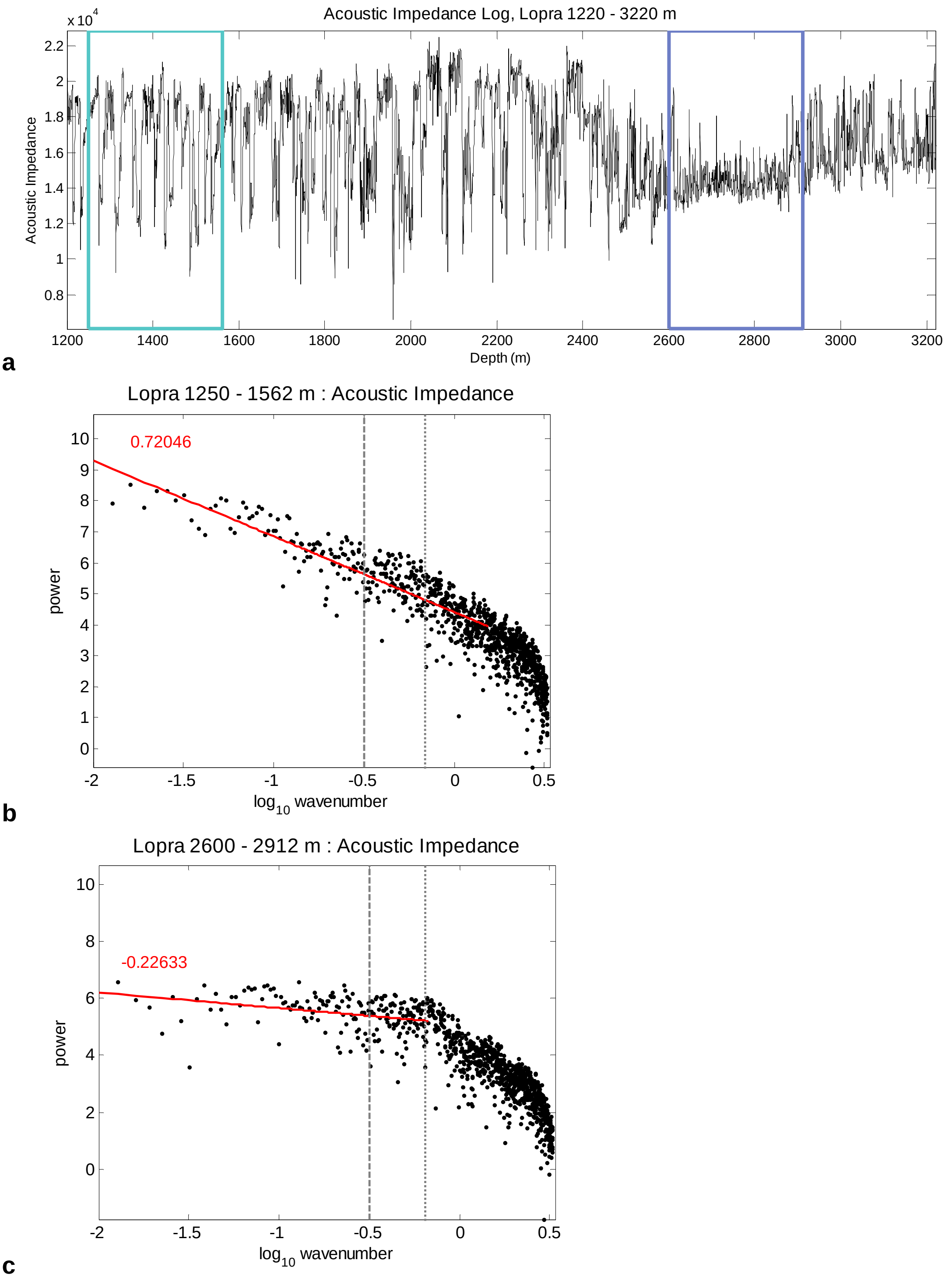

Figure 3

a. *Acoustic impedance log of the Lopra borehole.*

b. *Power spectral analysis of the upper interval, 1250 – 1562 m.*

c. *Power spectral analysis of the lower interval, 2600 – 2912 m.*

Borehole and depth interval	Hurst Exponent	Scales over which linear trend persists
Vestmanna 50 – 255 m	Negative	2 - 20
Vestmanna 296 – 500 m	**0.3**	1 - 20
Glyvursnes 50 – 255 m	**0.6**	1 - 50
Glyvursnes 396 – 600 m	**0.5**	1 - 20
Lopra 1250 – 1562 m	**0.7**	1 - 150
Lopra 2600 – 2912 m	Negative	1 - 150

Table 2. *Hurst exponents over four borehole intervals derived from the power spectral method.*

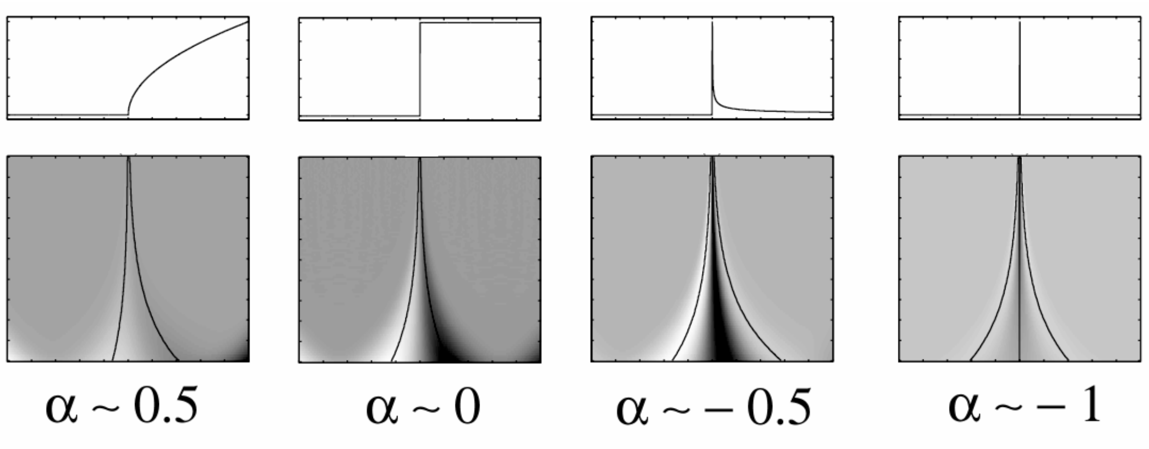

Figure 4. *Synthetic discontinuities (top row), their expression in wavelet transform space, and corresponding alpha values (from Hermann, 1997). Abrupt discontinuities take on negative values.*

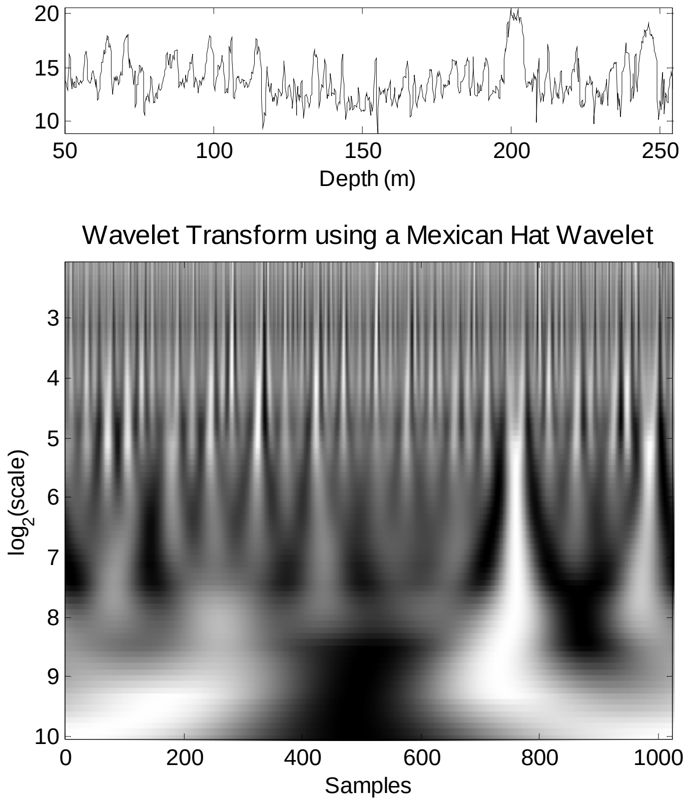

Figure 5a. *Vestmanna acoustic impedance log (50 – 255 m) with its continuous wavelet transform using the Mexican Hat wavelet.*

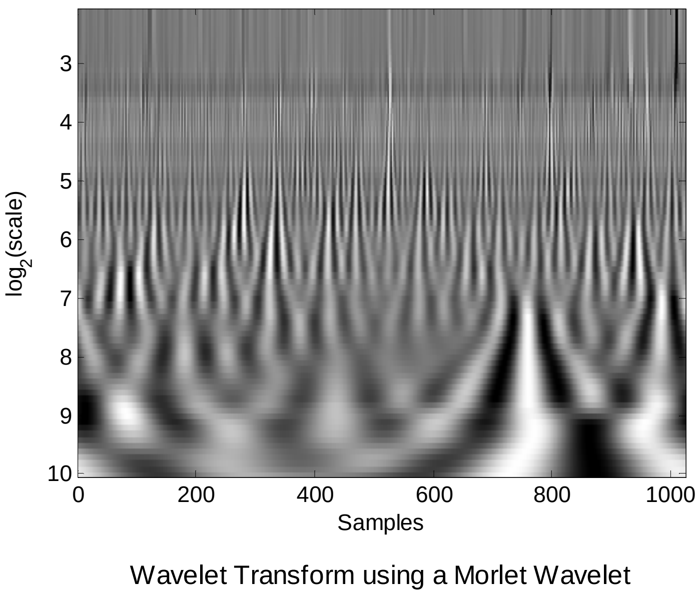

Figure 5b. *The continuous wavelet transform of the same data as above, using a Morlet wavelet.*

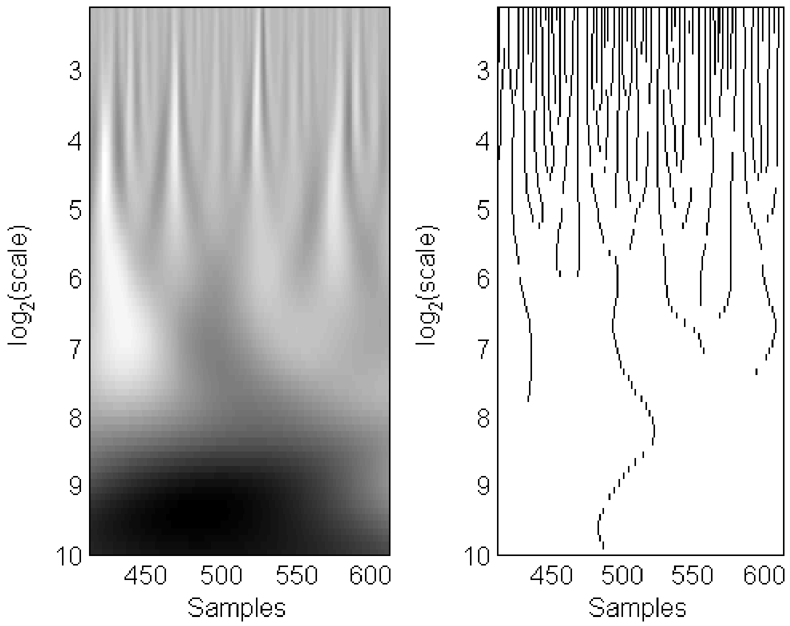

Figure 5c. *Detail of the wavelet transform and its corresponding modulus maxima or 'skeleton'. Energy occurs at a continuum of scales.*

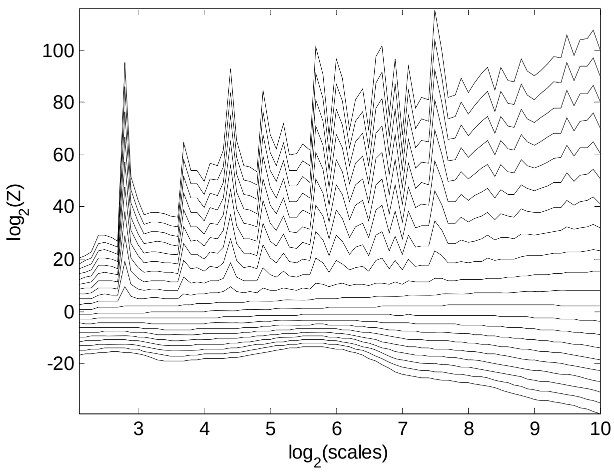

Figure 5d. *Log partition function vs log scales.*

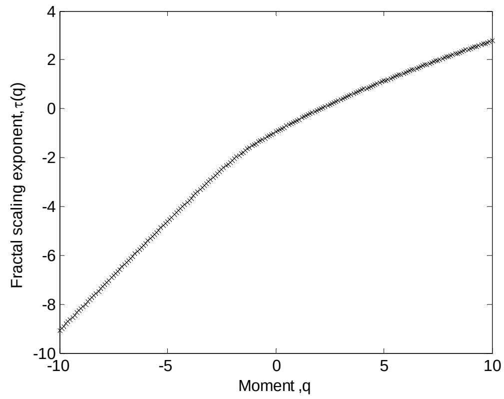

Figure 5e. *The fractal scaling exponent τ(q) as a function of moment q.*

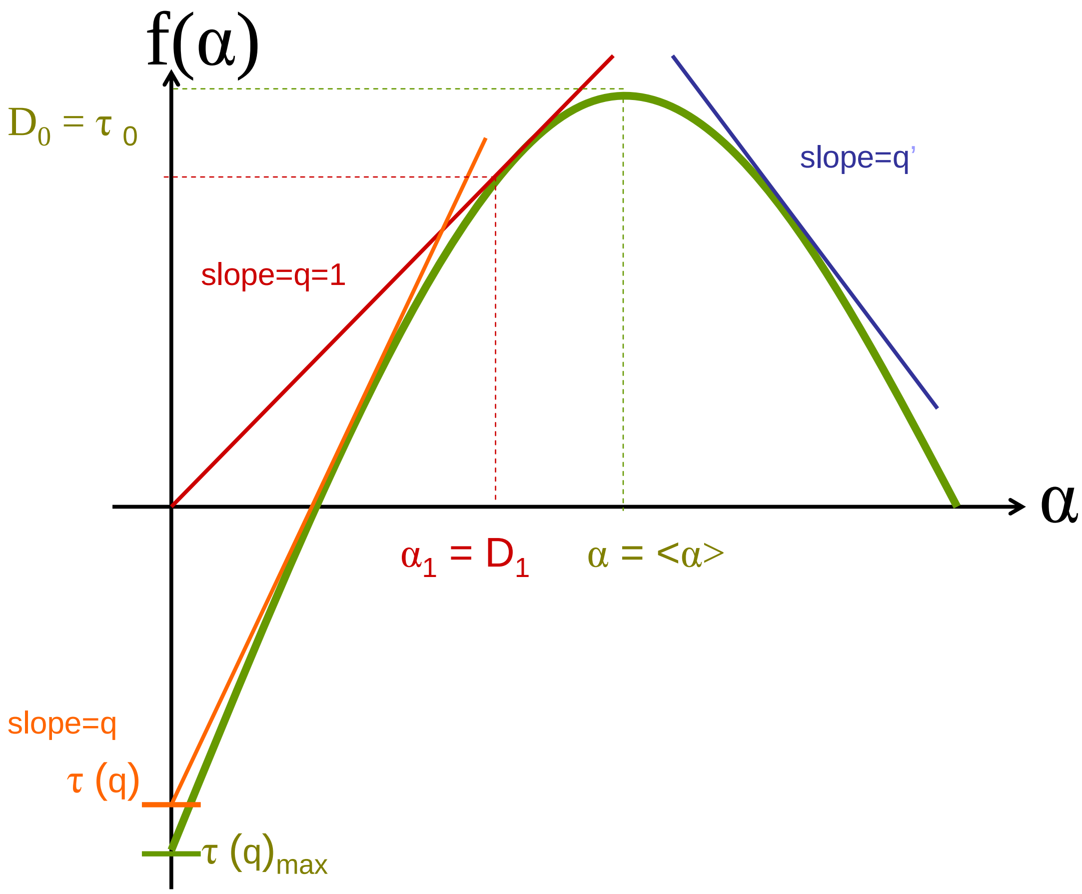

Figure 6. *A theoretical multifractal singularity spectrum, after Mandelbrot, 1989*.

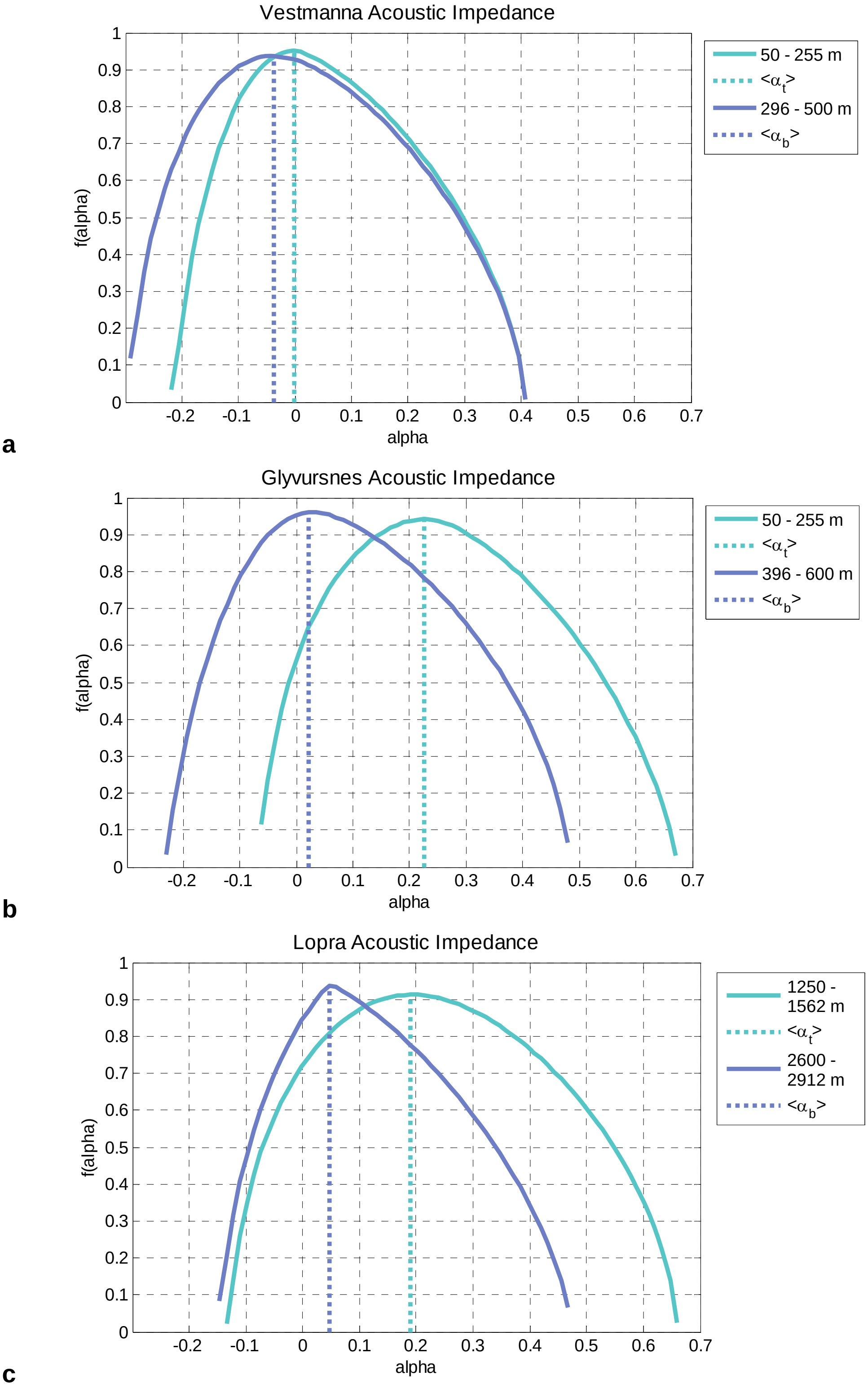

Figure 7. *Experimental singularity spectra, derived from the WTMM method, of acoustic impedance logs from three Faroes boreholes.* **a**. *Vestmanna*. **b**. *Glyvursnes***.** **c**. *Lopra*

Borehole Interval	**Lipschitz / Hölder Exponents**			
	α_{min}		**< α >**	**α_{max}**
Vestmanna 50 – 255 m	AI	-0.23	0	0.41
	V_s	-0.24	0.02	0.47
	Φ_n	-0.18	0.02	0.45
Vestmanna 296 – 500 m	AI	-0.3	-0.04	0.41
	V_s	-0.39	-0.09	0.42
	Φ_n	-0.37	-0.16	0.29
Glyvursnes 50 – 255 m	AI	-0.07	0.23	0.67
	V_s	-0.09	0.21	0.88
	Φ_n	-0.11	0.31	0.89
Glyvursnes 396 – 600 m	AI	-0.24	0.02	0.58
	V_s	-0.18	0.08	0.48
	Φ_n	-0.33	0	0.42
Lopra 1250 – 1562 m	AI	-0.14	0.19	0.66
	V_s	-0.1	0.24	0.68
Lopra 2600 – 2912 m	AI	-0.15	0.05	0.47
	V_s	-0.13	0.08	0.53

Table 3. *Alpha values for singularity spectra derived from WTMM analysis using the Mexican Hat wavelet.*

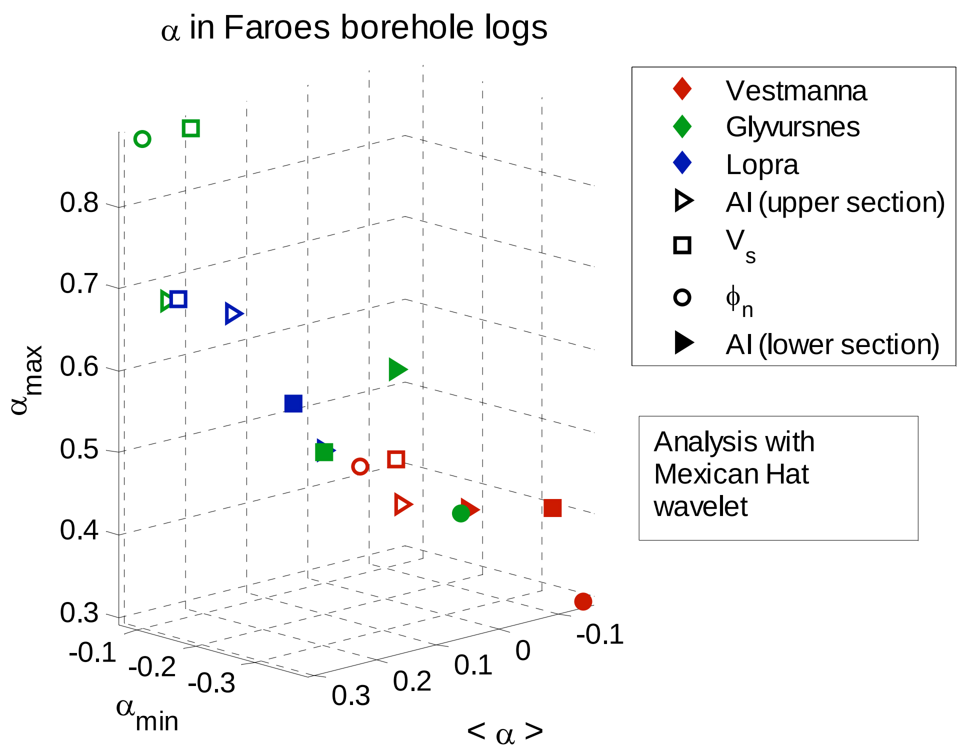

a

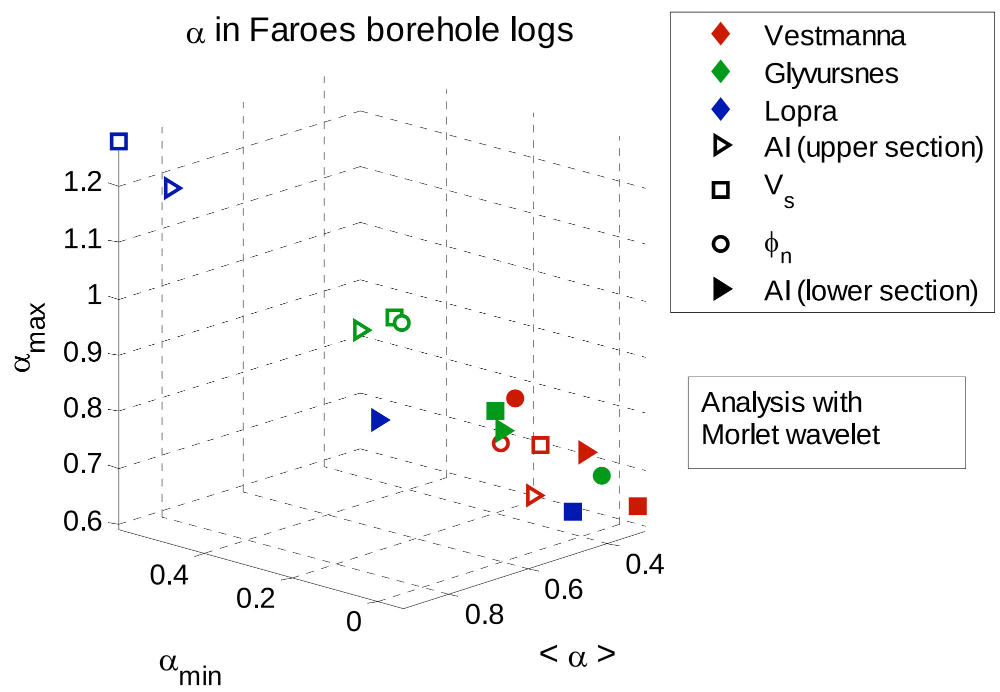

b

Figure 8

a. α exponents of acoustic impedance, S-velocity and neutron porosity logs from the Faroes boreholes. The analyses used a Mexican Hat wavelet.

b. *α exponents of the same Faroes borehole logs using a Morlet wavelet in analyses.*

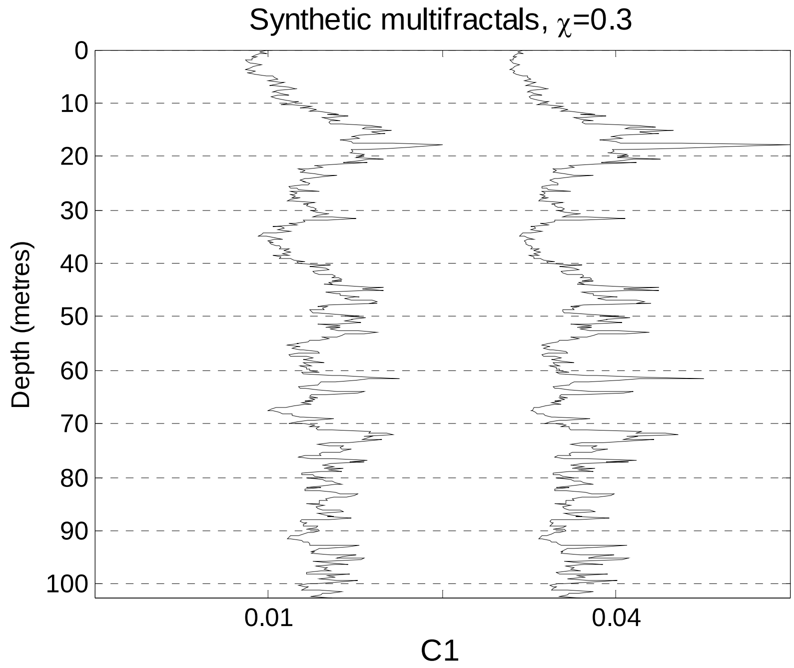

a

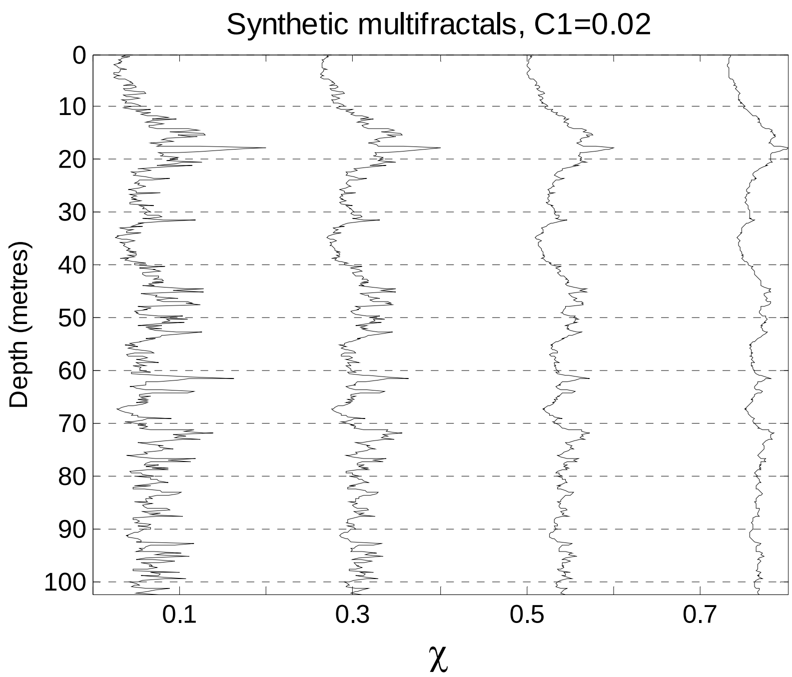

b

Figure 9. *Normalised synthetic multifractals.*

a. *Higher C1 values indicate greater intermittency.*

b. *Lower χ values indicate greater fluctuation.*

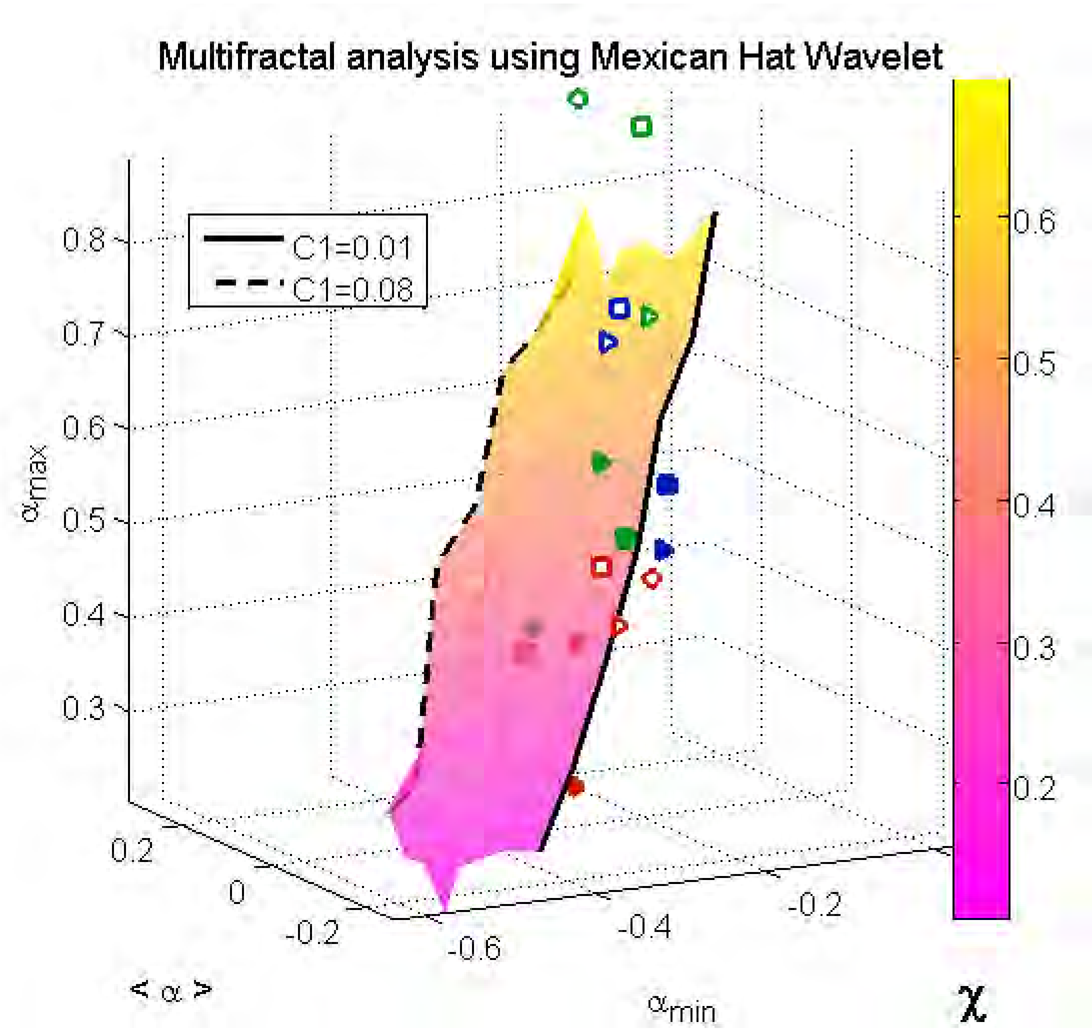

Figure 10. *Real data points (legend as in Figure 8) plotted against the spread of exponents from synthetic multifractals (translucent surface).*

Model	Closest real data analogue	Multifractal parameters		Estimated 1-D Scattering Q
		C1	χ	
1	Vestmanna lower porosity	0.01	0.2	250
2	Vestmanna upper AI, Lopra lower AI	“	0.4	800
3	Vestmanna lower AI	0.015	0.3	450
4	Vestmanna upper Vs	“	0.4	650
5	Vestmanna lower Vs	0.02	0.3	500
6	Vestmanna upper Vs, Glyvursnes lower AI, Vs	“	0.45	1300
7	Glyvursnes upper Vs	“	0.6	>2500
8	Glyvursnes lower porosity	0.04	0.35	800
9	Lopra upper AI	“	0.6	>3000
10	Lopra upper Vs, Glyvursnes upper AI	“	0.7	infinite

Table 4. *All the datasets above were normalised to the Vestmanna Vp and density logs.*

Borehole Interval	Log	Absolute values	
		mean	standard deviation
Vestmanna 50 – 255 m	P-velocity (km/s)	5.12	0.49
	Density (g/cc)	2.70	0.14
Vestmanna 296 – 500 m	P-velocity	5.46	0.64
	Density	2.77	0.14
Glyvursnes 50 – 255 m	P-velocity	4.49	0.86
	Density	2.74	0.18
Glyvursnes 396 – 600 m	P-velocity	4.26	0.63
	Density	2.63	0.13

Table 5. *First order statistics seen in Vestmanna and Glyvursnes P-velocity and density logs.*

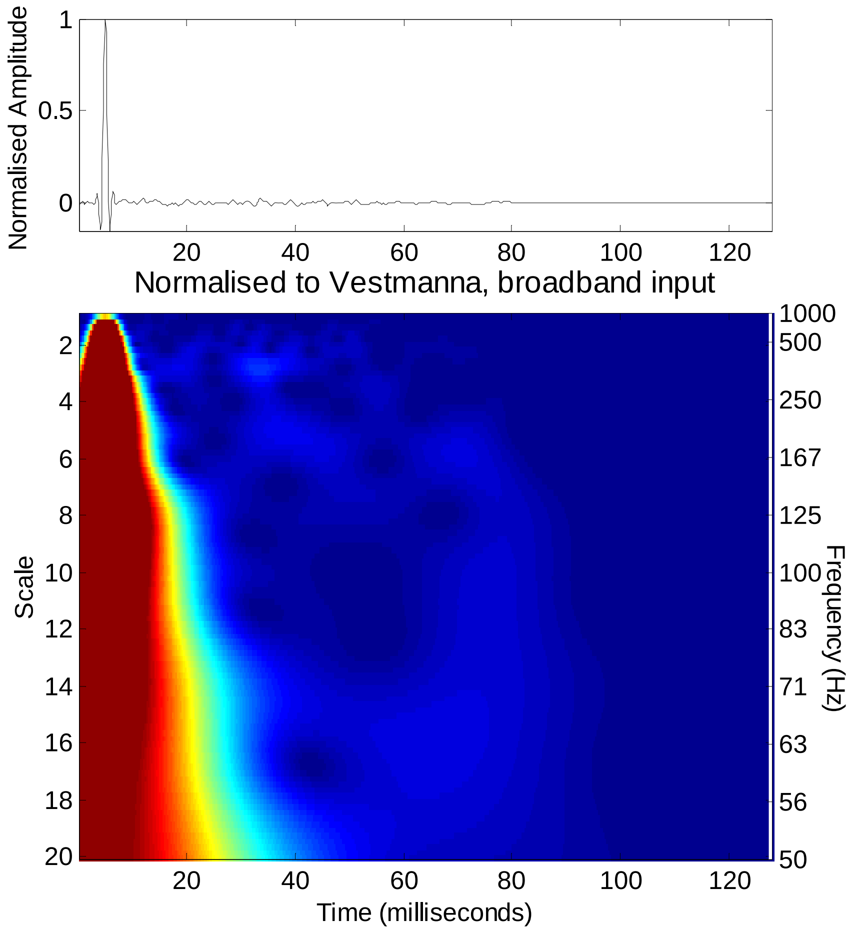

Figure 11. *Scalogram from synthetic seismic response of multifractal with C1 = 0.04, χ = 0.7. Log was normalised to the velocity and density ranges of the upper section of Vestmanna. Input was a broadband wavelet with frequency content to 800 Hz. Estimated Q ~ 1500. The contrast in this figure has been increased.*

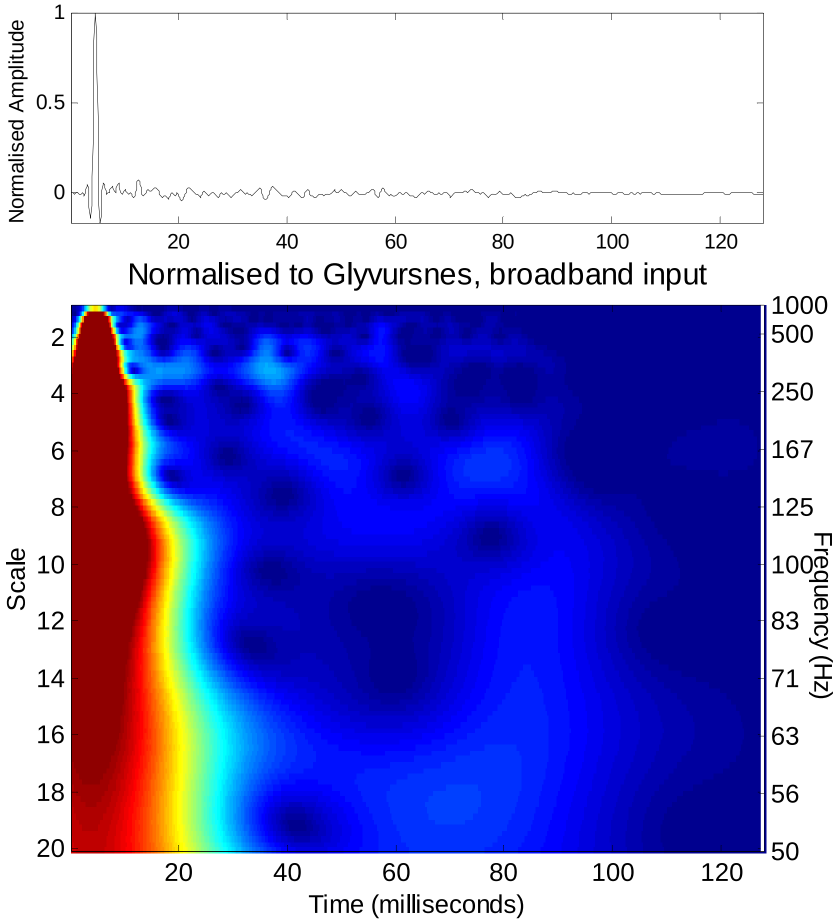

Figure 12. *Scalogram from synthetic seismic response of multifractal with C1 = 0.04, χ = 0.7. Log was normalised to the velocity and density ranges of the upper section of Glyvursnes. Input was a broadband wavelet with frequency content to 800 Hz. The contrast in this figure has been increased.*

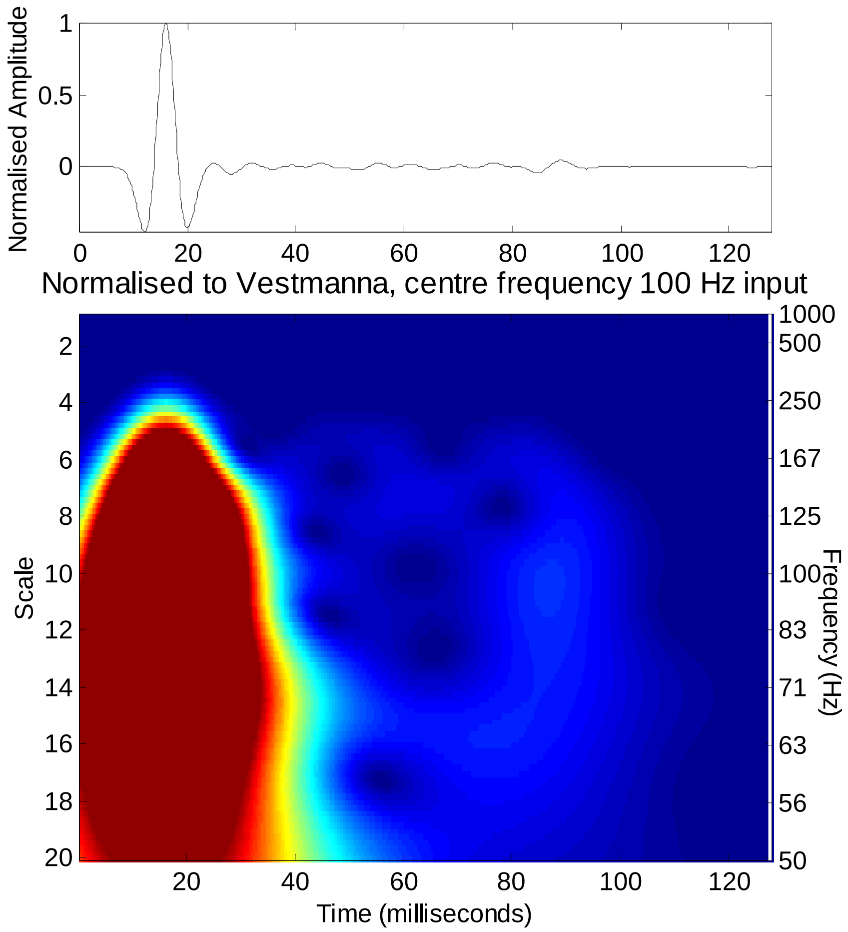

Figure 13. *Scalogram from synthetic seismic response of multifractal with C1 = 0.04, χ = 0.7. Log was normalised to the upper section of Vestmanna. Input was a wavelet with a centre frequency of 100 Hz and maximum frequency of ~ 250 Hz. Estimated Q ~ 270. The contrast in this figure has been increased.*

Accepted for Geophysical Prospecting

Seismic attenuation in Faroe Islands basalts

Shaw F.[1], Worthington M.H.[1], White R.S.[2], Andersen M.S.[3], Petersen U.K.[4]
& the Seifaba Group[5]

1. Department of Earth Sciences, Oxford University, Parks Road, Oxford, OX1 3PR, UK
2. Bullard Laboratories, University of Cambridge, Madingley Road, Cambridge, CB3 0EZ, UK
3. Geological Survey of Denmark and Greenland (GEUS), Oster Voldgade 10, DK-1350, København, Denmark
4. University of the Faroe Islands, Noatun 3, FO-100, Torshavn, the Faroe Islands
5. See acknowledgements for list of names

ABSTRACT

The analysis of VSP data from two boreholes at Glyvursnes and Vestmanna on the island of Streymoy, Faroe Islands, to determine the magnitude and causes of seismic attenuation is described. The work is part of a major project involving offset VSP and surface seismic surveys and the analysis of core samples and wireline log data from the two boreholes. Results from VSP and log data from a third Faroes hole at Lopra on the island of Suduroy already exist. These three boreholes provide an outstanding source of data for the determination of both the petrophysical and seismic properties of basalts in the Faroe Islands region and how these properties might vary laterally. Values of effective seismic quality factor (Q) obtained at Glyvursnes and Vestmanna are sufficiently low to significantly degrade the quality of a surface reflection seismic image. This observation is consistent with results both from the Lopra hole and from other VSP experiments in the North Atlantic region. We demonstrate that the most likely cause of the low values of Q at Glyvursnes and Vestmanna is a combination of 1-D scattering and intrinsic attenuation due to seismic wave induced fluid flow within pores and micro-cracks. Tests involving 3-D elastic wave numerical modelling with a hypothetical basalt model based on field observations indicate that little scattering attenuation is caused by lateral variations in basalt structure.

INTRODUCTION

The poor quality of most seismic reflection images within and beneath basalts is most likely to be due to a combination of factors whose relative importance varies for different survey locations. In the Columbia Plateau, USA, 6 to 120 metre thick basalt flows are interbedded with clay layers which are up to 30 m thick. Pujol *et al.* (1989) concluded that there is nothing unusual about the energy transmission characteristics of these basalts but attributed the observed poor seismic reflection data quality to reverberations caused by the large contrast in the elastic properties of the interbedded clay and basalt. Martini and Bean (2002) investigated, by numerical modelling, the seismic wave scattering due to internal velocity heterogeneity within a basalt sequence and roughness of the boundary surfaces at a scale similar to the seismic wavelength. They concluded that, of two possible causes investigated with their models, interface scattering had the most detrimental effect on imaging at depth beneath a basalt succession. Fliedner and White (2001) have drawn attention to the detrimental effect of multiples produced between the sea-surface and the top of a basalt layer on two profiles from the Faroe-Shetland Basin.

Pujol and Smithson (1991) obtained an estimate of , Q for the Columbia Plateau basalts of 50. This is of the same order as many estimates of Q from localities in sedimentary basins where seismic reflection techniques are usually highly effective. However, other workers have obtained significantly lower values. Rutledge and Winkler (1987) obtained a Q value of approximately 40 for a basalt series beneath the eastern Norwegian Sea. Q values from 15 to 35 were obtained by Maresh *et al.* (2005, 2006) for a basalt series in the Rockall Trough. The work of Christie *et al.* (2006) is of particular relevance to our study. They analysed VSP data from the Lopra well 1/1A situated on the Faroes island of Suduroy and obtained a Q value of approximately 35. The practical significance of these numbers is only appreciated if it is recalled that the amplitude of a seismic wave varies exponentially with the inverse of the quality factor, Q. The amplitude of a seismic wave of frequency 100 Hz will be reduced by a factor of 0.28 after transmission through 2 km of basalt with a velocity of 5000 m/s and a Q of 100. For Q values of 50 and 25, the amplitude is reduced by 0.08 and 0.006 respectively. Hence, the signal to noise ratio of seismic reflection data for reflector depths of 1 km or more will be seriously diminished if the Q of the rocks is less than about 30.

In addition to estimating the value of Q of a basaltic sequence of interest, it is equally useful to know the attenuation mechanism, since this knowledge is required when assessing how the effective Q might vary laterally throughout a survey region. The measured or effective Q is a combination of the intrinsic Q of the rocks and apparent Q caused by elastic scattering. $1/Q_{eff} = 1/Q_{intrinsic} + 1/Q_{scattering}$ (Lerche and Menke, 1986). The most frequently used method for separating these two processes is to obtain synthetic seismic data from a 1-dimensional elastic model based on well log velocities and densities. Analysis of these synthetic data provides an estimate of $Q_{scattering}$. Rutledge and Winkler (1987), Christie *et al.* (2006) and Maresh *et al.* (2006) all use this approach when concluding that 1-D scattering is the dominant attenuation mechanism and that intrinsic attenuation is relatively insignificant. In contrast, Holliger (1996) analysed ten P-wave sonic logs from six igneous and metamorphic rock drill sites in Europe and North America and concluded that velocity fluctuations in the upper crystalline crust are remarkably uniform. He then used 2-dimensional numerical modelling to obtain the general conclusion that scattering attenuation is one to two orders of magnitude lower than the total seismic attenuation inferred from field data and hence anelastic effects must dominate the attenuation of seismic waves in the upper crystalline crust (Holliger, 1997).

In this paper, we describe an investigation of the magnitude and possible mechanisms of seismic attenuation in basalts in the Faroe Islands. The work is part of a major project (from 2002-2006) involving the analysis of core samples and wireline log data from two boreholes on the island of Streymoy, combined with VSP, offset VSP surveys, and extensive surface reflection and refraction seismic surveys. Preliminary results of this project are described in

Japsen *et al.* (2005). The lavas in the Faroe Islands region are divided into the Lower, Middle and Upper Basalt Formations (Rasmussen & Noe-Nygaard, 1970; Waagstein, 1988). Individual basalt beds in the Lower and Upper Formations have average thicknesses of about 20 and 10 m respectively. Sediment layers up to 10 m thick between basalt beds are found within the Lower and Upper Formations, but most interbasaltic sediment layers in these two formations are less than 1 m thick. In the Middle Formation individual basalt beds are thin and sediments are virtually absent (Rasmussen & Noe-Nygaard, 1970). The Glyvursnes-1 hole intersects both the Upper and Middle Formations and the Vestmanna-1 hole intersects the Middle and Lower Formations. In addition, the Lopra-1/1A hole on the island of Suduroy, drilled in 1981 and deepened in 1996, intersects the Lower Formation. The analysis of log and VSP data from this hole is described in Christie *et al.* (2006). These three holes provide an outstanding source of data for the determination of both the petrophysical and seismic properties of basalts in the Faroe Islands region and how these properties might vary laterally. The studies have been pursued in anticipation of continued interest in petroleum exploration in the Faroese area.

The structure of this paper is as follows: we describe the acquisition of the vertical VSP data acquired from the Glyvursnes-1 and Vestmanna-1 holes; we determine effective Q values from these data; we then attempt to estimate the scattering Q, using both a 1-dimensional model and a 3-dimensional numerical model; we investigate the possible range of values of intrinsic Q, based on the theory of Pointer *et al.* (2000) and Chapman (2003); finally we discuss some implications of our results.

VSP DATA ACQUISITION

The near zero-offset VSP profile at Glyvursnes, southern Streymoy, surveyed approximately 300 m of the Upper Basalt Formation and 300 m of the Middle Basalt Formation at 10 m intervals from 50 m to 600 m depth. A two-metre deep pit was excavated down to bedrock, 14 m from the borehole, and a single sleeve Sodera 2.46 litre air gun was suspended in the water at a depth of approximately 1.5 m. The borehole receiver was a custom-made I/O 3-component sensor containing SM-7M 10Hz geophones, and a hydraulic bow spring was used to clamp the receiver to the borehole wall at a pressure of ~ 2000 psi for each depth recording. A Geometrics ES-3000 seismometer was used to record the VSP survey at a sampling interval of 0.125 milliseconds and a record length of 1.95 seconds. No filters were applied to the raw data at the time of acquisition. A monitor hydrophone was positioned beneath the source pit within a slim hole at a depth of approximately 10 m.

A second near zero-offset VSP experiment was carried out at Vestmanna Sund, north-western Streymoy, through 500 m of the Middle Basalt Formation at 5 m intervals from 50 m to 500 m depth. Two Haliburton sleveguns, each with a capacity of 0.65 litres, were chained to flotation buoys and suspended at a depth of approximately 1.5 m in a two-metre diameter natural rock pool situated 18 m from the borehole. The same borehole receivers were used as at Glyvursnes, at a sampling interval of 0.5 milliseconds and a record length of 4.995 seconds. No filters were applied to the raw data at the time of acquisition. A monitor hydrophone was placed in the borehole at a constant depth of 20 m throughout the experiment

ESTIMATION OF EFFECTIVE Q

The spectral ratio method is widely used to estimate the attenuation of seismic data. It is applied in the frequency domain and compares the spectrum of a seismic wave entering an attenuative medium with its spectrum as it emerges. Q and the propagation velocity are assumed to be independent of frequency.

The amplitude of a seismic signal in relation to the source amplitude is given by:

$$A = A_0 \exp(-\pi fx / Qc) \qquad \textbf{(1)}$$

where A= amplitude at depth x, A_o = source amplitude, f = frequency, x = depth, Q = seismic quality factor and c = wave propagation velocity. Comparing traces from two depths,

$$\ln(\frac{A_2}{A_1}) - \ln(\frac{A_{02}}{A_{01}}) = \frac{-\pi f \delta t_{2-1}}{Q} \qquad \textbf{(2)}$$

where δt_{2-1} is the difference in travel times. If the source is constant throughout the experiment, $A_{02} = A_{01}$ and effective Q can be derived from a plot of ln (A_2 / A_1) against frequency f using:

$$Q = \frac{-\pi \delta t_{2-1}}{(slope\ of\ \ plot)} \qquad \textbf{(3)}$$

The VSP data was first time-aligned and median-filtered, to suppress the interference from upgoing waves. For two traces with a depth interval of (x_2 - x_1), time gates were applied to remove the short period multiples and preserve, as far as possible, only the first arrival. The time gates were tapered on both sides with half Hanning windows (Figures 1a, 2a). The amplitude spectra of the pair of traces were inspected (Figures 1b, 2b), to determine the bandwidth over which the spectral ratio was relatively stable. As small variations in the chosen frequency range could produce large fluctuations in the measured Q, several bandwidths were chosen and used in error estimation. A linear regression by least squares was performed on the scatter plots of the spectral ratios (Figures 1c, 2c). Then a Q value was derived using equation 3.

The analysis was repeated for all VSP trace pairs, using a constant depth separation of 250 metres. This relatively large interval was chosen to reduce the variance of the Q estimate, as recommended by White (1992).

Vestmanna

Good quality VSP data were acquired at the Vestmanna field site due to a constant source signature throughout the experiment and a generally low back-ground noise level. A broad frequency band from 10 – 700 Hz was achieved due to the excellent source coupling to the bed rock. The analysis over 250-metre intervals produced a modal value of Q of ~ 30 (Figure 3). While there are anomalously high outliers, these occurred at depth levels where short period multiples created numerous minima in the trace spectra, and where the spectral ratios were stable only over a narrow bandwidth. Under these circumstances, the high values are likely to reflect large uncertainty rather than actual physical properties. The Q value derived from comparing the uppermost trace and the lowermost trace is ~ 40±10. There was no evidence, within the uncertainties illustrated in Figure 3, of any significant variation of Q with depth.

Glyvursnes

The frequency bandwidth of the Glyvursnes VSP data was narrower than we had expected due, we believe, to relatively poor source to bed-rock coupling. Although the source pit was excavated to bed-rock, it was of necessity constructed in soft recent deposits. We encountered water leakage problems, so the water level in the pit was not constant throughout the experiment. This resulted in some variation in the source wavelet spectrum with time. In addition, the monitor hydrophone was poorly positioned, much too close to the pit. This resulted in hydrophone signal spectra that bore little relation to the spectra of the downhole signals. However, the hydrophone provided an estimate of the variability of the source spectra even though it could not be used to obtain a precise source amplitude spectrum correction. The spread of Q values in Figures 4 and 5 encompass any uncertainty in the estimates due to source variability. Results for Q ranged from ~ 5 - 70 (Figure 4). There was also evidence of an increase in Q with depth. In the upper half of the VSP survey (50 - 320 m) the mean and modal Q value is ~ 20 (Figure 5a), while in the lower half (320 - 600m) the mean and modal Q increase to ~ 30 (Figure 5b). The value derived from comparing the uppermost trace and the lowermost trace is ~ 25±5.

ESTIMATION OF 1-D SCATTERING Q

The rock masses in the field area display distinct horizontal layering, rendering 1-D scattering a candidate mechanism for the low effective Q values observed in real VSP data. Acoustic impedance values fluctuate strongly (Figure 6), which potentially could create much multiple interference. The frequency and magnitude of these fluctuations in acoustic impedance are noticeably different in the top 300 m of the Glyvursnes hole compared to the remainder of the logs (Figure 6b) which corresponds to the depth interval of the Upper Basalt Formation. A corresponding difference in 1-D scattering attenuation should arise. To test this hypothesis, 1-D acoustic modelling was carried out using a reflectivity algorithm by Kennett (1979), which produces theoretical P-wave seismograms for an explosive source in a multilayered elastic medium.

Synthetic seismograms were generated for the same intervals as the VSP surveys, 50 – 500 m for Vestmanna and 50 – 600 m for Glyvursnes, using the primary wavelets of the respective 50 m VSP traces as input. The resulting output wavelets were then isolated, tapered on either side with half Hanning windows, and analysed by the spectral ratio method. As with the analysis of the real VSP data, linear regression by least squares was performed only over the bandwidth where the spectral ratio was stable. Figures 7a & 8a show that there is far less broadening of the first arrival in the 1-D medium than in the real data (Figures 1a, 2a). The spectral shape of the wavelet exiting a 1-D medium (Figures 7b, 8b) is not as strongly modified (Figures 1b, 2b). The derived 1-D scattering Q for Glyvursnes was 50-80 and for Vestmanna 80-110.

The upper and lower halves of the Glyvursnes log were then analysed separately to determine whether the obvious change in log character resulted in a change of scattering attenuation. The primary wavelet of the VSP trace at 50 m depth was used as the input for the upper section model and the primary wavelet of the 320 m trace was the input for the lower section. In the upper section, the 1-D scattering Q value is estimated to be 20-40. The wavelet from the lower section shows very little broadening or spectral modification and the estimated 1-D scattering Q is greater than 100-200.

ESTIMATION OF 3-D SCATTERING Q

Having established that predicted 1-D scattering cannot fully account for the effective Q values seen in the VSP data, we investigate whether significant apparent attenuation might result from seismic wave scattering due to three-dimensional variations in basalt structure. The main short-coming of our study is that we have no way of determining the true three-dimensional structure within the immediate vicinity of the Glyvursnes and Vestmanna holes. So we construct a hypothetical model, based on field evidence of basalt structure, which we believe reflects the extent of the lateral variation that is likely to exist.

Two distinct basalt morphological types occur in the Faroe Plateau Lava Group (S. R. Passey, quoted in Bondre *et al,.* 2004), and limited exposure can be viewed in the field area of the VSP experiments. The first type is a low frequency, massive tabular lithology, akin to that described by Jerram (2002). This type is predominant in the Lower and Upper Formations in the Faroes. The second is composed of hummocky flows between 1 and 5 metres in thickness. These are akin to compound braided basalts described by Jerram (2002), and may be tube-fed (Bondre *et al.*, 2004). In cross-section, they may appear as lobes tens of metres in length, and are thought to be predominant in the Middle Formation and thus in the Vestmanna locality. At the resolution of seismic wavelengths, this second morphological type is more internally varied, possibly giving rise to more 3-D scattering than the tabular form.

A 3-D model based on the latter basalt type was constructed, using an algorithm which propagated basalt flows of a specified thickness and width over existing terrain. The model resolution was set to 1.5 m per cell. A multi-fractal topography with low relief (<5 m) and cell dimensions of 320 x 320 was used as the first surface. Successive flows were built up, each with a thickness of 2 cells and a width of 12 cells, starting from the lowest point on the southern edge of the model, towards the north. The flows were allowed to meander towards lower topography but were not allowed to pool laterally or terminate before reaching the northern side. This simulated viscous lava with substantial pressure from the source, and had the effect of creating flow tubes of regular size but varying position. The model was built up to 4600 flows, or approximately 300 cells height, and then truncated to 300 x

300 x 300 to remove edge effects. Seismic velocities were then assigned to the framework of basalt tubes by sampling the Vestmanna P-wave velocity log such that there was an approximate tie between the distribution of velocities in the model and the 1-D log with depth. An approximate linear relationship between P-wave velocity and density was established from the log data. This relationship, (density = 0.15 kg s m^{-4} V_p + 2000 kg m^{-3}) was used to define the density of the basalt tubes. Figure 9 shows the resulting 3-D velocity model (referred to below as model A). To provide a means of comparison with the results in the previous section, a three dimensional plane layered model with one dimensional velocity and density variation in the depth direction was also constructed. The velocity/depth profile taken from the centre of the model in Figure 9b was used and is shown in Figure 9d. This we refer to as model B.

A 3D discrete numerical elastic lattice method was used to simulate elastic wave propagation through the basalt models. The numerical model consists of particles, representing blocks of intact rock, arranged on a cubic lattice which interact with Hooke's Law forces. The algorithm is described in detail by O'Brien and Bean (2004), with supporting theoretical and practical detail to be found in Monette and Anderson (1994) and Toomey and Bean (2000). A 300 x 300 x 400 particle grid was used with a grid spacing of 1.5 metres. A source was input as a force in the z (depth) direction on the particle in the centre of the model at 75 metres depth. The peak and centre frequency of the source wavelet was 100 Hz with a bandwidth from 0 to 200 Hz. The time sample interval was 0.0002 s. The grid spacing and sample interval were chosen to avoid the problems of numerical stability and dispersion. Poisson's ratio was fixed at 0.25 by setting the bond-bending constant to zero as described in O'Brien and Bean (2004).

3-D synthetic seismic data were calculated for models A and B. Figure 10a shows part of the wavefield after it has travelled 425 m from the source in model A. Note the variation in the amplitude of the wavelet with horizontal position. This contrasts with negligible variations in wavelet shape and amplitude observed for model B. Figure 10b shows results from two orthogonal horizontal spreads of vertical receivers at 500 m depth. The source position is at the mid point of the spreads; spread length is 150 m and receiver interval is 15 m (see Figs. 9a and b). In Figure 10b the signals for model B, which are virtually identical for all receiver positions, is compared with two signals for model A representing the greatest observed departure from the result of model B. In Figure 10c, the amplitude spectrum for the model B signal is compared with spectra for the 20 receivers with model A. Note that 3-D scattering can result in both an increase and decrease in spectral amplitude compared to the 1-D case. However, the most important result from this study is that the variation of the apparent attenuation that can be estimated from all the spectra in Figure 10c is small compared to the errors in our estimates of 1-D scattering quoted in the last section. Hence, we conclude that departures from horizontal layering of the basalts is unlikely to be a significant factor in any explanation of the causes of low values of effective Q obtained from our VSP data.

ESTIMATION OF INTRINSIC Q

If the observed data cannot be explained entirely by some form of elastic wave scattering, then an anelastic mechanism is the only alternative explanation. Using the simple inverse relationship between effective, intrinsic and scattering Q mentioned above, we deduce that required values of intrinsic Q vary from infinity in the top half of the Glyvursnes sequence, where there is little difference between our estimates of effective and scattering Q, to as low as approximately 45 at Vestmanna. These numbers vary greatly within the uncertainty limits of our estimates. For example, it is possible to attribute the observed effective Q of 20 in the shallower sections at Glyvursnes to a combination of scattering Q and intrinsic Q, both with a value of 40. Our limited aim is to determine whether values of intrinsic Q as low as 40 are realistic on the basis of existing theory and our knowledge of the petrophysical properties of Faroes basalts.

Fluctuating stresses in a rock caused by the passage of a seismic wave induce pore pressure gradients at the scale of the seismic wavelength and also at the scale of individual grains, pores and micro-cracks. Mavko and Jizba (1991) and Dvorkin *et al.* (1995) described how seismic attenuation results from the squirt flow of fluid between pores and micro-cracks. However, doubts have been expressed about the magnitude of squirt flow induced attenuation at exploration seismic frequencies (Gist, 1994; Pride *et al.*, 2003). Hudson *et al.* (1996) proposed the equant porosity model of wave induced fluid flow as diffusion from aligned cracks into a porous matrix material, which is applicable over a wide frequency range. Pointer *et al*. (2000) subsequently extended this theory to the case of randomly oriented cracks. Chapman (2003) developed a model with coupled fluid motion on two scales: the grain scale and the fracture scale. Fractures are assumed to be large with respect to grain size but are small with respect to wavelength so that equivalent media theory is applicable. The model consists of randomly oriented micro-cracks and spherical pores at the grain scale and aligned fractures. This approach was originally developed by Chapman *et al.* (2002) for the case when there are no fractures.

Provisional results from the analysis of 28 core samples and neutron porosity logs from the Glyvursnes and Vestmanna holes by members of the Seifaba research group include estimates of porosity and permeability (Japsen and Waagstein, personal communication). The basalt sections can be simply classified as consisting of lava core and lava crust or breccia. Very approximately, there are equal proportions of these lithologies in the two holes. Average porosities from the core analysis and the neutron porosity logs calibrated by the core data are 4% for the lava core and 15% for the lava crust. Core sample estimates of permeability for lava core and lava crust are 10^{-17} m^2 and 5.0×10^{-16} m^2 respectively. For our modelling, we have assumed an average porosity of 10% and a permeability range from 10^{-17} to 10^{-16} m^2.

An important constraint is provided by the work of Bais *et al.* (2006). From an analysis of the offset VSP data acquired at Vestmanna they have concluded that P-wave seismic anisotropy within the basalts is negligible. Consequently, we have used only two theoretical models which include micro-cracks or fractures with random orientations. These are the theory of Chapman (2003) with fracture density set to zero and the randomly oriented cracks with equant porosity (equant-random) model described by Pointer *et al.* (2000). We assume that the rocks are 100% saturated and water filled. Other known parameters for our homogeneous model are listed in Table 1.

For the equant-random model, required unknown parameters are crack radius, crack density and crack aspect ratio. The frequencies corresponding to the peaks in the attenuation curves in Figure 11 are equal to the inverse of the relaxation time of the fluid flow, which is proportional to (permeability/crack radius^2). Hence crack radius is determined to be 0.001 m since we know permeability and require peak attenuation to be at 100 Hz. The amplitude of the peak is governed by crack density and crack aspect ratio. Figure 11 shows curves for a crack density of 0.05 and crack aspect ratios of 0.1, 0.03 and 0.01, models 1, 2 and 3. As might be expected, the rock becomes more compliant as the crack aspect ratio decreases and consequently the intrinsic attenuation increases. Also shown in Figure 11 is the effect of increasing the value of rock matrix permeability of model 2 with all other parameters unchanged (model 4). This has no influence on the amplitude of the peak attenuation, but moves the peak to a higher frequency. The curve could be moved back to a lower frequency by increasing the crack radius. Hence, in the examples in Figure 11, the same result can be achieved with a permeability of 10^{-16} m^2 and a crack radius of 0.003 m or a permeability of 10^{-17} m^2 and a crack radius of 0.001 m.

Required unknown parameters for the Chapman (2003) theory are the micro-crack density, crack aspect ratio and fluid relaxation time. Figure 11 shows results for a crack density of 0.05 and crack aspect ratios of 0.01 and 0.03, in models 5 and 6. Fluid relaxation time was chosen so that the peak in the attenuation curve is at approximately the same frequency as obtained with the equant-random model. Relaxation times for the two models differed by a factor of 10: 2.5×10^{-3} s for the Chapman model and 2.5×10^{-4} s for the equant-random model. All the examples shown in Figure 11 have predicted values of intrinsic Q of between 100 and 45 within the frequency band of our observed VSP data.

Velocity dispersion of between 100 and 150 m/s is also predicted over a frequency range from 100 Hz to 24 kHz. The later value is the dominant frequency of our sonic logging tool. In principle, this could be detected by comparing the VSP travel times with integrated log times. Unfortunately, we experienced considerable difficulties with the calibration of our sonic log data and it was not possible to estimate dispersion induced positive drift from the combination of observed negative and positive drift in the two holes.

DISCUSSION

Our attempt to separate and quantify the effects of scattering and intrinsic attenuation is based on a number of assumptions that should be questioned. Our use of the spectral ratio technique to obtain a single Q value from a particular pair of signals is certainly common practice but is not entirely satisfactory. Q is known to be a frequency dependent quantity (Sams *et al.*, 1997) and any estimate over a restricted frequency band should be clearly associated with the frequency band that was selected.

1-D scattering attenuation is critically dependent on the character of the acoustic impedance log. We have noted how observable differences in the Glyvursnes log above and below 300 m depth results in a dramatic difference in 1-D scattering attenuation. Although the weight of evidence from other studies referred to in the introduction suggests that 1-D scattering is the dominant cause of seismic attenuation in basalts of the North Atlantic region, this study provides evidence that this may not be a reliable general conclusion.

Our analysis of 3-D scattering attenuation is based on only one hypothetical model. However, we believe we have constructed an upper limit of likely lateral variability, and consequently our conclusion about the effect of 3-D scattering is conservative. Nevertheless, this is not proof and further experimentation could reveal plausible 3-D structures that result in significant scattering attenuation.

Likewise, our study of intrinsic attenuation demonstrates that this could be a significant mechanism in Faroes basalts but does not prove the point. We can only suggest that our estimated model parameters, crack density, crack aspect ratio and crack radius are realistic. A crack density of 0.05 is not unusual in comparison with field data reviewed by Crampin (1994) and the laboratory data of Peacock *et al.* (1994). Observed micro-crack aspect ratios of less than 0.01 have been reported in the review by Kranz (1983). Attenuation is inversely proportional to crack aspect ratio. So our choice of modelled aspect ratios is conservative. Micro-crack radius is a complete unknown. However, if we permit ourselves some flexibility in the choice of in-situ permeability, a range of values of micro-crack radius is acceptable since the same result is obtained for constant values of (permeability/crack radius^2).

We stated earlier that our choice of only random crack intrinsic attenuation models was prompted by the finding that seismic P-wave anisotropy at Vesmanna was negligible (Bais *et al.,* 2006). Currently there exist some unresolved issues concerning the confidence limits that should be associated with this result. This is a critical matter because intrinsic attenuation would increase significantly if randomly oriented cracks became aligned, with a resulting P-velocity anisotropy of 1-2%. In other regions where velocity anisotropy is detected, one might reasonably expect relatively low values of intrinsic Q.

CONCLUSIONS

Values of seismic Q determined from VSP data acquired at wells at Lopra, Glyvursnes and Vestmanna in the Faroe Islands are all sufficiently low to be a dominant cause of the poor quality of seismic reflection images. However, the possible causes of the low Q have been found to vary between the three borehole localities. Christie *et al*. (2006) conclude that 1-D scattering is the dominant attenuation mechanism at Lopra. It is possible to come to the same conclusion for the upper basalt formation in the top half of the Glyvursnes hole. However, within the middle basalt formation in the bottom half of the Glyvursnes hole and at Vestmanna, very little attenuation can be attributed to 1-D scattering. Results from 3-D elastic wave numerical modelling with a hypothetical basalt model constructed on the basis of field observations indicate that very little scattering attenuation is caused by lateral variations in basalt structure. However, the low values of effective Q observed at Glyvursnes and Vestmanna can be explained as resulting from a combination of 1-D scattering and intrinsic attenuation due to seismic wave induced fluid flow within pores and micro-cracks. This study adds to the now substantial number of observations of seismic attenuation within basalt sequences in the North Atlantic region and reinforces the general conclusion that low values of effective Q are to be expected. However, the causes of the high attenuation may vary greatly from one locality to another.

ACKNOWLEDGEMENTS

We thank the Sindri Group for financial support and permission to publish the results in this paper. The SeiFaBa project is funded collectively by oil companies operating in the Faroe sector. We are grateful for colleagues in the SeiFaBa project for allowing us to include petrophysical data in this paper that is not currently released to the public domain. Members of the SeiFaBa research group, in addition to named authors of this paper are Peter Japsen, Jens Moller, Dan Olsen, Niels Springer, Nina Turner, Rasmus Rasmussen and Regin Waagstein (Geological Survey of Denmark and Greenland), Claus Andersen (Faroes Geological Survey), Lars Boldreel (University of Copenhagen), Jacob Petersen (Odegaard A/S) and Gary Mavko (Stanford University). We also thank Mark Chapman and Tim Pointer for generously sending us copies of their software. Any possible misuse of this software is entirely our responsibility.

REFERENCES

Bias, G., White, R.S., Worthington, M.H., Andersen, M.S. and the SeiFaBa group, 2006 . The seismic response of Faroe basalts from integrated borehole and wide-angle seismic data, 68th Annual International Meeting, EAGE, Vienna, expanded abstracts.

Bondre, N.R., Duraiswami, R.A. & Dole, G. 2004. A brief comparison of lava flows from the Deccan Volcanic Province and the Columbia-Oregon Plateau Flood Basalts: Implications for models of flood basalt emplacement. Proc*. Indian Acad. Sci. (Earth Planet. Sci.)*, **113**, no. 4, 809 - 817.

Chapman, M. 2003. Frequency-dependent anisotropy due to meso-scale fractures in the presence of equant porosity, *Geophysical Prospecting*, **51**, 369-379.

Chapman, M., Zatsepin, S.V. and Crampin, S. 2002. Derivation of a microstructural poroelastic model, *Geophysical Journal International*, **151**, 427-451.

Christie, P., Gollifer, I. and Cowper, D. 2006. Borehole seismic studies of a volcanic succession from the Lopra-1/1A borehole in the Faroe Islands, N.E.Atlantic, Geology of Denmark Survey, in press.

Crampin, S. 1994. The fracture criticality of crustal rocks, *Geophysical Journal International*, **118**, 428-436.

Dvorkin, J., Mavko, G. and Nur, A., 1995. Squirt flow in fully saturated rocks, *Geophysics*, **60**, 97-107.

Fliedner, M.M. and White, R.S. 2001. Sub-basalt imaging in the Faroe-Shetland Basin with large offset data, *First Break*, **19**, 247-252.

Gist, G.A. 1994. Fluid effects on velocity and attenuation in sandstones, *Journal of the acoustical society of America*, **96**, 1158-1173.

Holliger, K. 1996. Upper-crustal seismic velocity heterogeneity as derived from a variety of P-wave sonic logs, *Geophysical Journal International*, **125**, 813-829.

Holliger, K. 1997. Seismic scattering in the upper crystalline crust based on the evidence from sonic logs, *Geophysical Journal International*, **128**, 65-72.

Hudson,J.A., Liu, E. and Crampin, S. 1996. The mechanical properties of materials with interconnected cracks and pores, *Geophysical Journal International*, **124**, 105-112.

Japsen, P. et al. 2005. Preliminary results from investigations of seismic and petrophysical properties of Faroes basalts in the SeiFaBa project. In: Dore, A.G. and Vining, B. (eds.) Petroleum Geology: North-West Europe and Global Perspectives, *Proceedings of the 6th Petroleum Geology Conference*, Geological Society of London, pp. 1461-1470.

Jerram, D.A. 2002. Volcanology and facies architecture of flood basalts. In: Menzies, M.A., Klemperer, S.L., Ebinger, C.J. & Baker, J. (eds) *Volcanic Rifted Margins.* Geological Society of America, Special Papers, **362**, 121 - 135.

Kennett, B.L.N. 1979. Theoretical reflection seismograms for elastic media. *Geophysical Prospecting*, **27**, 301-321.

Kranz, R.L. 1983. Microcracks in rocks: a review, *Tectonophysics*, **100**, 449-480.

Lerche, I. and Menke, W. 1986. An inversion method for separating apparent and intrinsic attenuation in layered media, *Geophysical Journal of the Royal Astronomical Society*, **87**, 333-347.

Maresh, J. & White, R. S., 2005. Seeing through a glass, darkly: strategies for imaging through basalt, *First* Break*,* 23, 27−32.

Maresh, J., White, R.S., Hobbs, R.W. and Smallwood, J.R., 2006. Seismic attenuation of Atlantic margin basalts: observations and modelling, *Geophysics*, in press.

Martini, F. and Bean, C.J. 2002. Interface scattering versus body scattering in sub basalt imaging and application of prestack wave equation datuming, *Geophysics*, **67**, 1593-1601.

Mavko, G and Jizba, D. 1991. Estimating grain scale fluid effects on velocity dispersion in rocks, *Geophysics*, **56**, 1940-1949.

Monette, L. and Anderson, M.P. 1994. Elastic and fracture properties of the two-dimensional triangular and square lattices, *Modelling and simulation in materials science and engineering*, **2**, 53-66.

O'Brien, G.S. and Bean, C.J. 2004. A 3D discrete numerical elastic lattice method for seismic wave propagation in heterogeneous media with topography, *Geophysical Research Letters*, **31**, L14608, doi:1029/2004GL020069.

Peacock, S., McCann, C., Sothcott, C. and Astin, T.R., 1994. Seismic velocity in fractured: an experimental verification of Hudson's theory, *Geophysical Prospecting*, **42**, 27-80.

Pointer, T., Liu, E. and Hudson, J.A. 2000. Seismic wave propagation in cracked porous media, *Geophysical Journal* International, **142**, 199-231.

Pride *et al*. 2003. Permeability dependence of seismic amplitudes, *The Leading Edge*, **24**, No 6, 518-525.

Pujol, J. and Smithson, S. 1991. Seismic attenuation in volcanic rocks from VSP experiments, *Geophysics*, **56**, 1441-1455.

Pujol, J., Fuller, B.N. and Smithson, S.B. 1989. Interpretation of a vertical seismic profile conducted in the Columbia Plateau basalts, *Geophysics*, **54**, 1258-1266.

Rasmussen, J. and Noe-Nygaard, A. 1970. Geology of the Faroe Islands. *Geological sur of Denmark I. Series*. **25**, 1-142.
Rutledge, J.T. and Winkler, H. 1987. Attenuation measurements in basalt using vertical seismic profile data from the Eastern Norwegian Sea, 57th Annual International Meeting, SEG, expanded abstracts, 711-713.
Sams, M.S., Neep, J.P., Worthington, M.H. and King, M.S. 1997. The measurement of velocity dispersion and frequency dependent intrinsic attenuation in sedimentary rocks, *Geophysics*, **62**, 1456-1464.
Toomey, A. and Bean, C.J. 2000. Numerical simulation of seismic waves using a discrete particle scheme, *Geophysical Journal International*, **141**, 595-604.
Waagstein, R. 1988. Structure, composition and age of the Faroe basalt plateau. In: Morton,A.C. and Parson, L.M. (eds) Early Tertiary volcanism and the opening of the North-East Atlantic, *Geological Society of London, Special Publications*, **39**, 225-238.
White, R.E. 1992. The accuracy of estimating Q from seismic data. Geophysics, **57**, 1508 - 1511.

FIGURE CAPTIONS

Figure 1 (a) Downgoing wavelets at 50 m and 500 m in the Vestmanna borehole. The dotted curves are the tapered time gates.
(b) Amplitude spectra for the traces in 1(a).
(c) Spectral ratio plot. Linear regressions are performed over varying frequency ranges, avoiding incoherent regions in the bandwidth where possible.

Figure 2 (a) Downgoing wavelets at 50 m and 600 m in the Glyvursnes borehole. The dotted curves are the tapered time gates.
(b) Amplitude spectra for the traces in 2(a).
(c) Spectral ratio plot. Linear regressions are performed over varying frequency ranges, avoiding incoherent regions in the bandwidth where possible.

Figure 3. Histogram of effective Q measurements in the Vestmanna data, derived using the spectral ratio method, for a depth separation of 250 metres between traces.

Figure 4. Histogram of effective Q measurements in the Glyvursnes data, derived by the spectral ratio method, for a depth separation of 250 metres between traces.

Figure 5 (a) Histogram of effective Q measurements in Glyvursnes, 50 - 320 m.
(b) Histogram of effective Q measurements in Glyvursnes, 320 - 600 m.

Figure 6(a) Acoustic impedance log, Vestmanna.
(b) Acoustic impedance log, Glyvursnes.

Figure 7 (a) Input and output primary wavelets of synthetic seismograms, for a 1-D model of the 50 – 500 m interval of the Vestmanna velocity and density logs. The dotted curve is the tapered time gate.

(b) Amplitude spectra for the traces in 7(a).
(c) Spectral ratio of the input and output traces.

Figure 8 (a) Input and output primary wavelets of synthetic seismograms, for a 1-D model of the 50 – 600 m interval of the Glyvursnes velocity and density logs. The dotted curve is the tapered time gate.
(b) Amplitude spectra for the traces in 8(a).
(c) Spectral ratio of the input and output traces.

Figure 9 (a) View of varied velocity model parallel to flow direction, towards 'North'. The receivers are represented by black squares at the 500 metres depth level. The borehole is represented by the solid black line, and the source by a red circle.
(b) View of varied velocity model perpendicular to flow direction, towards 'West'.
The receivers are represented by black squares at the 500 metres depth level. The borehole is represented by the solid black line, and the source by a red circle.
(c) Top down view of the varied velocity model. Colour bar units are in m/s. The location of the borehole is marked by a white circle.
(d) Velocity log through model borehole.

Figure 10 (a) Snap shot of a portion of a wave propagating through the laterally variable velocity model in Figure 9.
(b) The solid curve is the signal recorded at a receiver at 500 m depth in the 1-dimensional model described in the text. The dashed and dotted curves are signals recorded at two different receivers at 500 m depth in the laterally variable model shown in Figure 9.
(c) The dotted curve is the spectrum of signals at any of the receiver positions at 500 m depth in the 1-dimensional model (see text for details). The 20 solid curves are the spectra of signals at the 20 receiver locations in the 3-D laterally variable model shown in Figure 9.

Figure 11. Modelled values of intrinsic Q as a function of frequency. Model parameters are listed in Table 1. See text for details.

Model 1 (••••) Equant-random model with crack aspect ratio of 0.1
Model 2 (oooo) Equant-random model with crack aspect ratio of 0.03
Model 3 (------) Equant-random model with crack aspect ratio of 0.01
Model 4 (solid curve) Equant-random model with model 2 parameters but permeability increased to 10^{-16} m^2
Model 5 (××××) Chapman(2003) model with crack aspect ratio of 0.03
Model 6 (……) Chapman(2003) model with crack aspect ratio of 0.01

TABLES

Compressional velocity (m/s)	5000
Shear velocity (m/s)	2650
Density (kg/m^3)	2600
Fluid velocity (m/s)	1500
Fluid density (kg/m^3)	1000
Fluid viscosity (mks)	9.0×10^{-4}
Rock matrix porosity	0.1
Rock matrix permeability (m^2)	10^{-16} - 10^{-17}
Crack radius (m)	0.001 – 0.003
Crack density	0.05
Crack aspect ratio	[0.01 0.03 0.1]
Fluid relaxation time (Chapman model) (s)	2.5×10^{-3}

Table 1. Model parameters used in the intrinsic attenuation modelling.

FIGURES

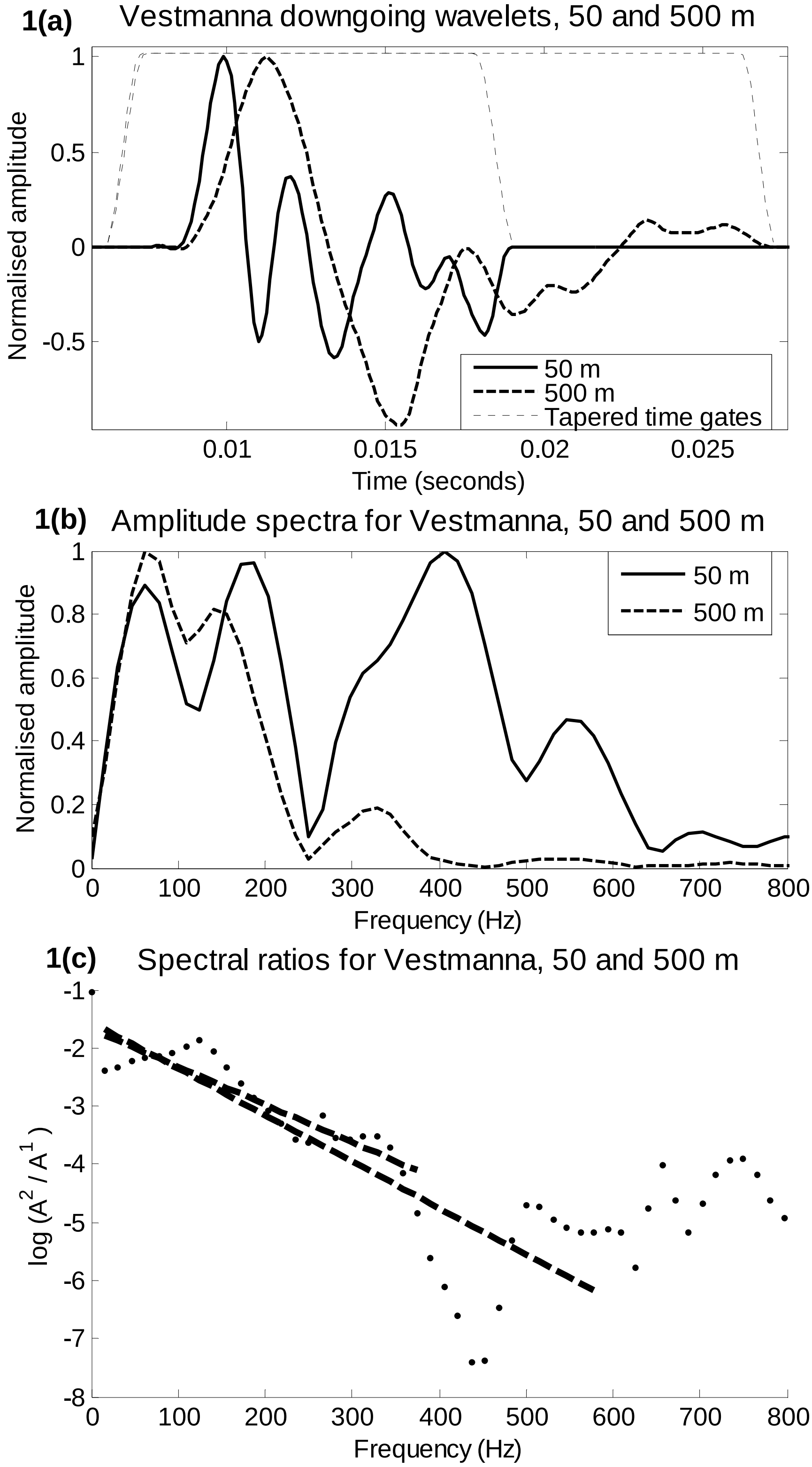

Figure 1

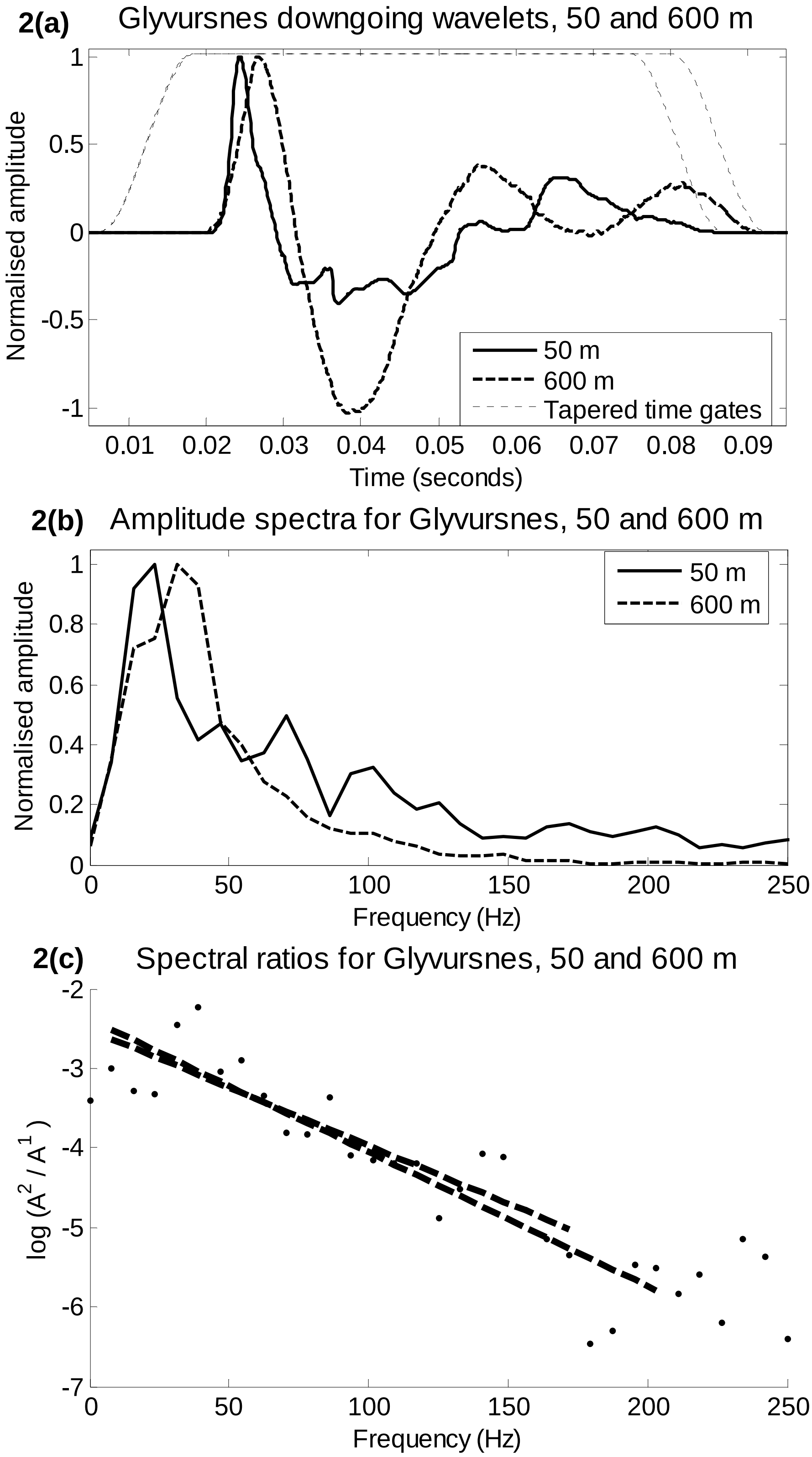
2(a)
Glyvursnes downgoing wavelets, 50 and 600 m
Normalised amplitude
Time (seconds)
50 m
600 m
Tapered time gates
2(b)
Amplitude spectra for Glyvursnes, 50 and 600 m
Normalised amplitude
Frequency (Hz)
50 m
600 m
2(c)
Spectral ratios for Glyvursnes, 50 and 600 m
log (A2 / A1)
Frequency (Hz)

Figure 2

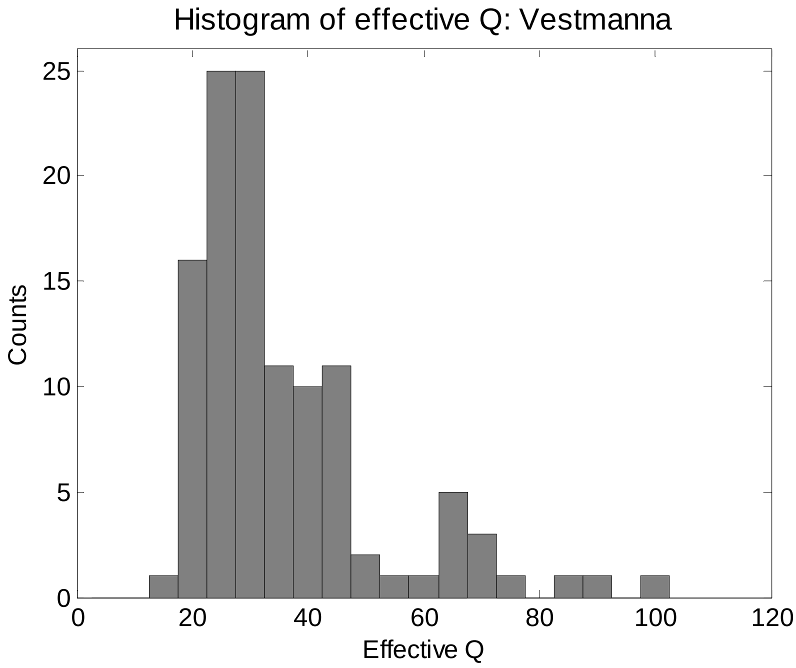

Figure 3

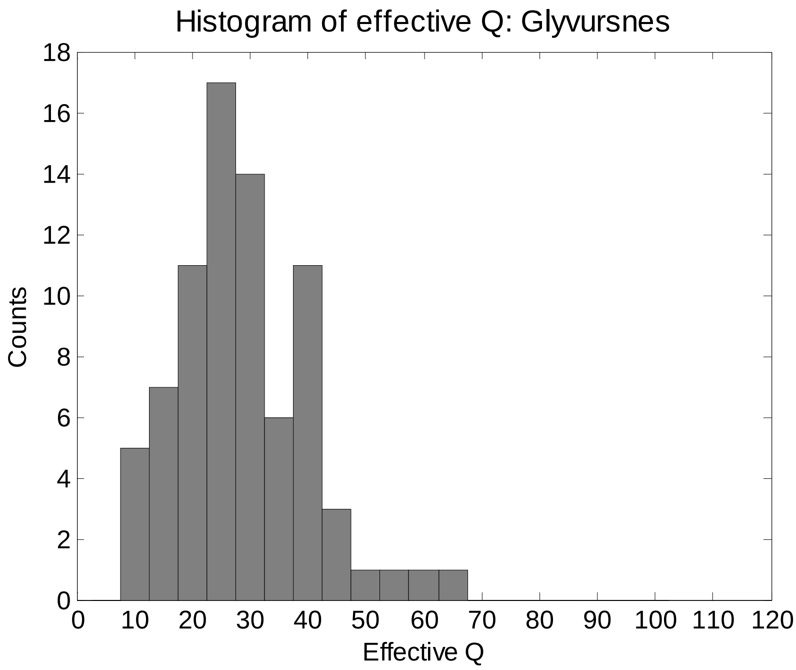

Figure 4

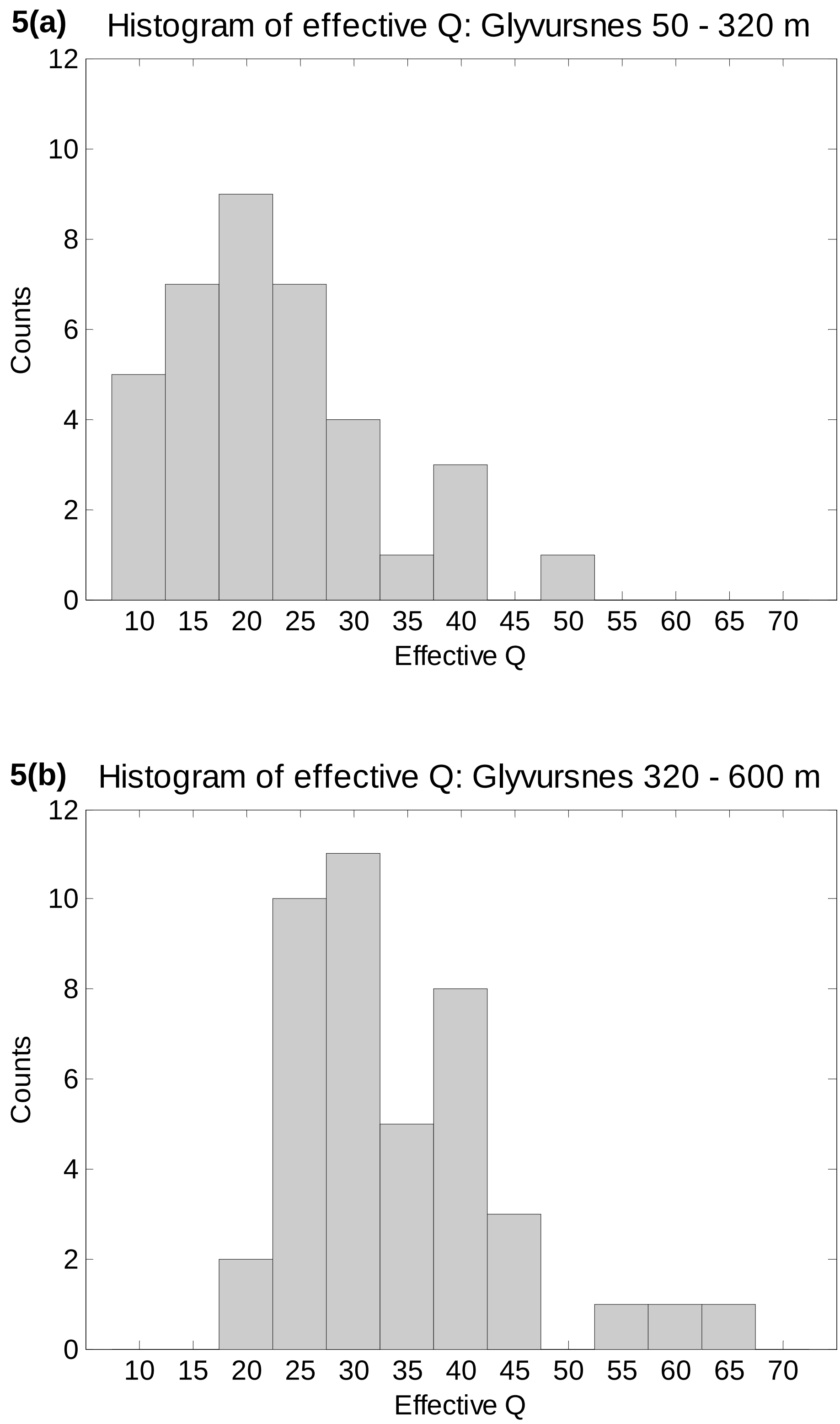
5(a)
Histogram of effective Q: Glyvursnes 50 - 320 m
Counts
Effective Q
5(b)
Histogram of effective Q: Glyvursnes 320 - 600 m
Counts
Effective Q

Figure 5

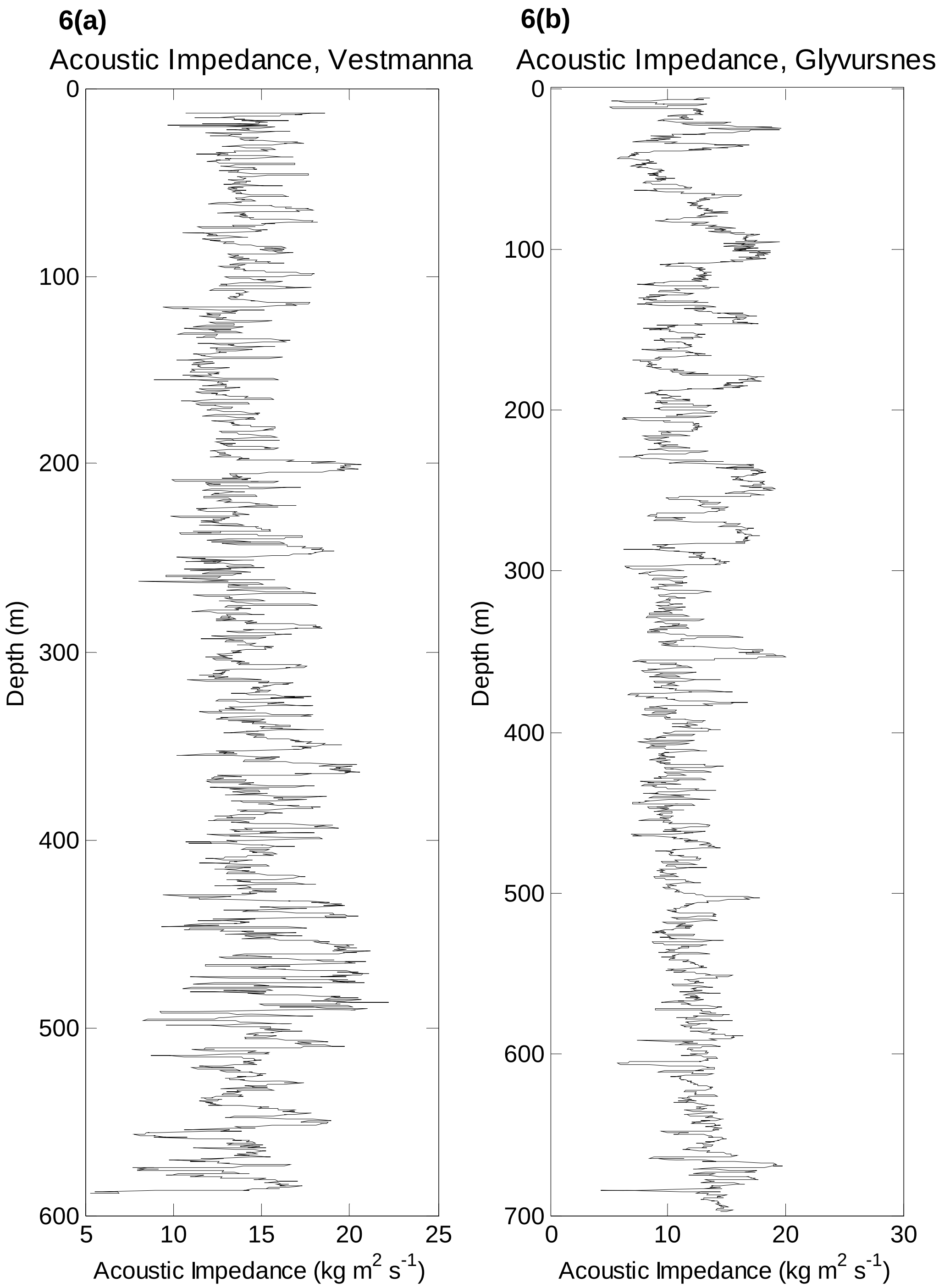
6(a)
Acoustic Impedance, Vestmanna
Depth (m)
0
100
200
300
400
500
600
5
10
15
20
25
Acoustic Impedance (kg m2 s-1)
6(b)
Acoustic Impedance, Glyvursnes
Depth (m)
0
100
200
300
400
500
600
700
0
10
20
30
Acoustic Impedance (kg m2 s-1)

Figure 6

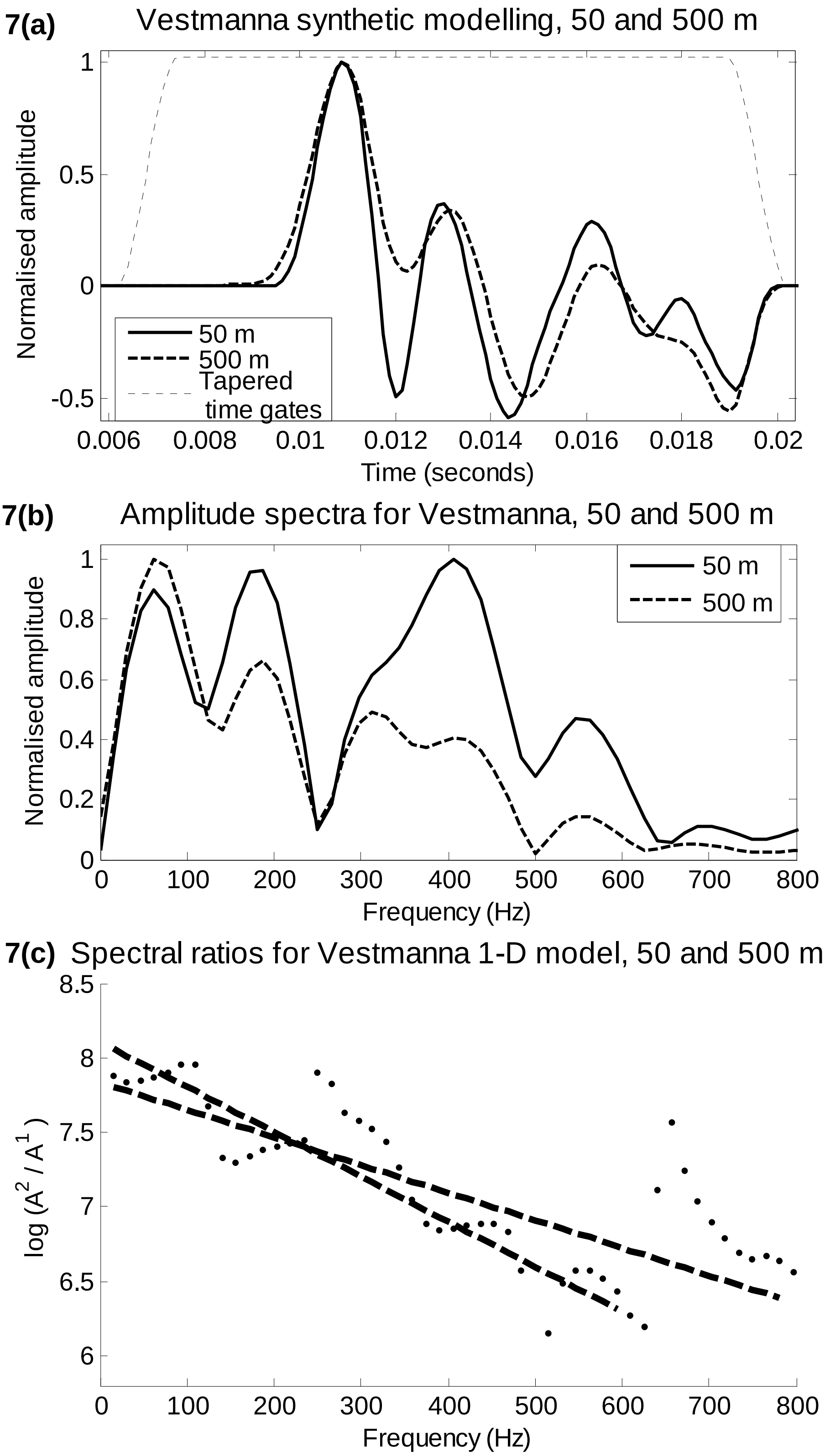

7(a)
Vestmanna synthetic modelling, 50 and 500 m
Normalised amplitude
Time (seconds)
50 m
500 m
Tapered time gates
7(b)
Amplitude spectra for Vestmanna, 50 and 500 m
Normalised amplitude
Frequency (Hz)
50 m
500 m
7(c)
Spectral ratios for Vestmanna 1-D model, 50 and 500 m
log (A2 / A1)
Frequency (Hz)

Figure 7

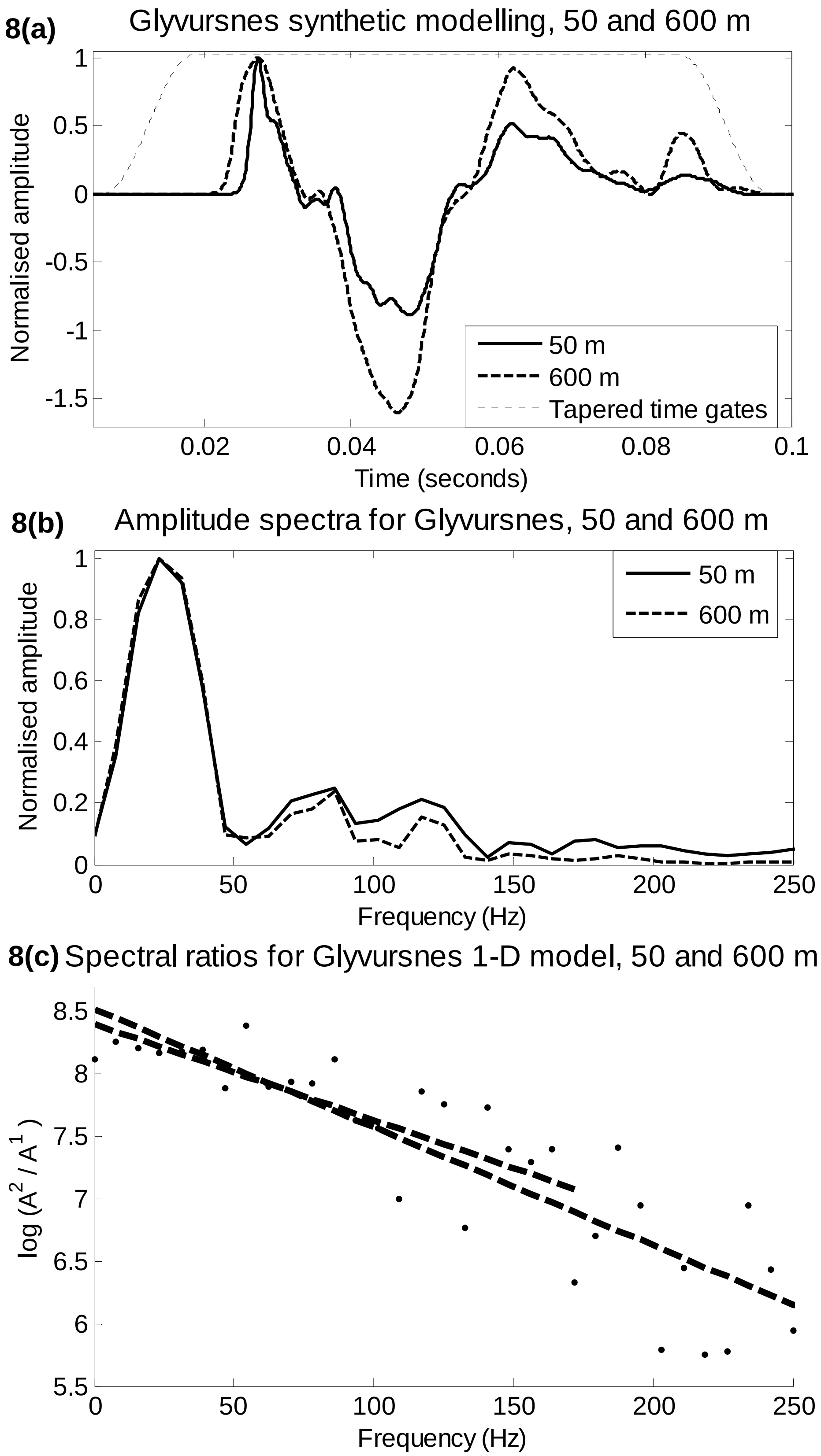
8(a)
Glyvursnes synthetic modelling, 50 and 600 m
Normalised amplitude
Time (seconds)
50 m
600 m
Tapered time gates
8(b)
Amplitude spectra for Glyvursnes, 50 and 600 m
Normalised amplitude
Frequency (Hz)
50 m
600 m
8(c) Spectral ratios for Glyvursnes 1-D model, 50 and 600 m
log (A2 / A1)
Frequency (Hz)

Figure 8

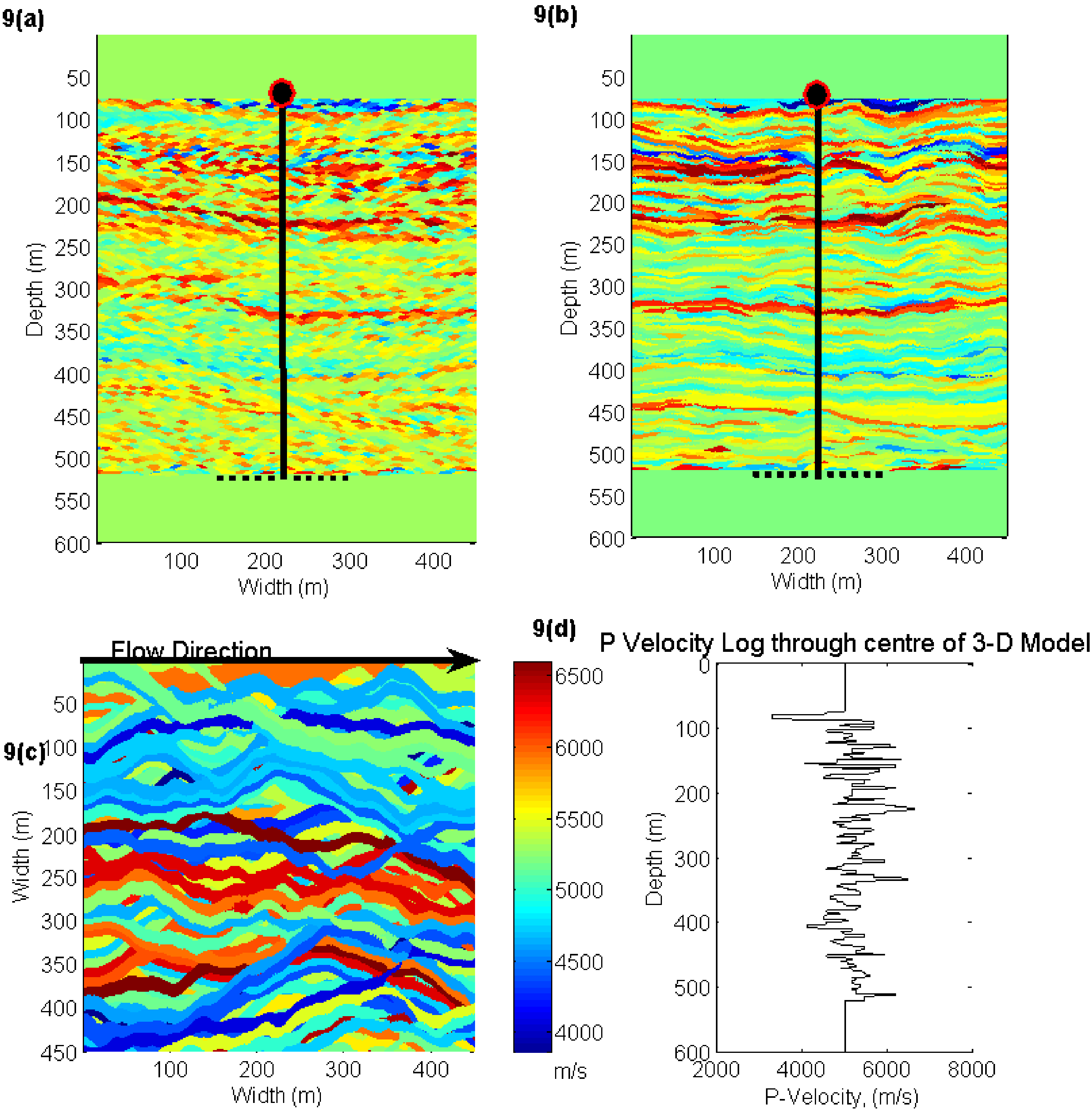
9(a)
Depth (m)
Width (m)
9(b)
Depth (m)
Width (m)
Flow Direction
9(c)
Width (m)
Width (m)
9(d)
m/s
P Velocity Log through centre of 3-D Model
Depth (m)
P-Velocity, (m/s)

Figure 9

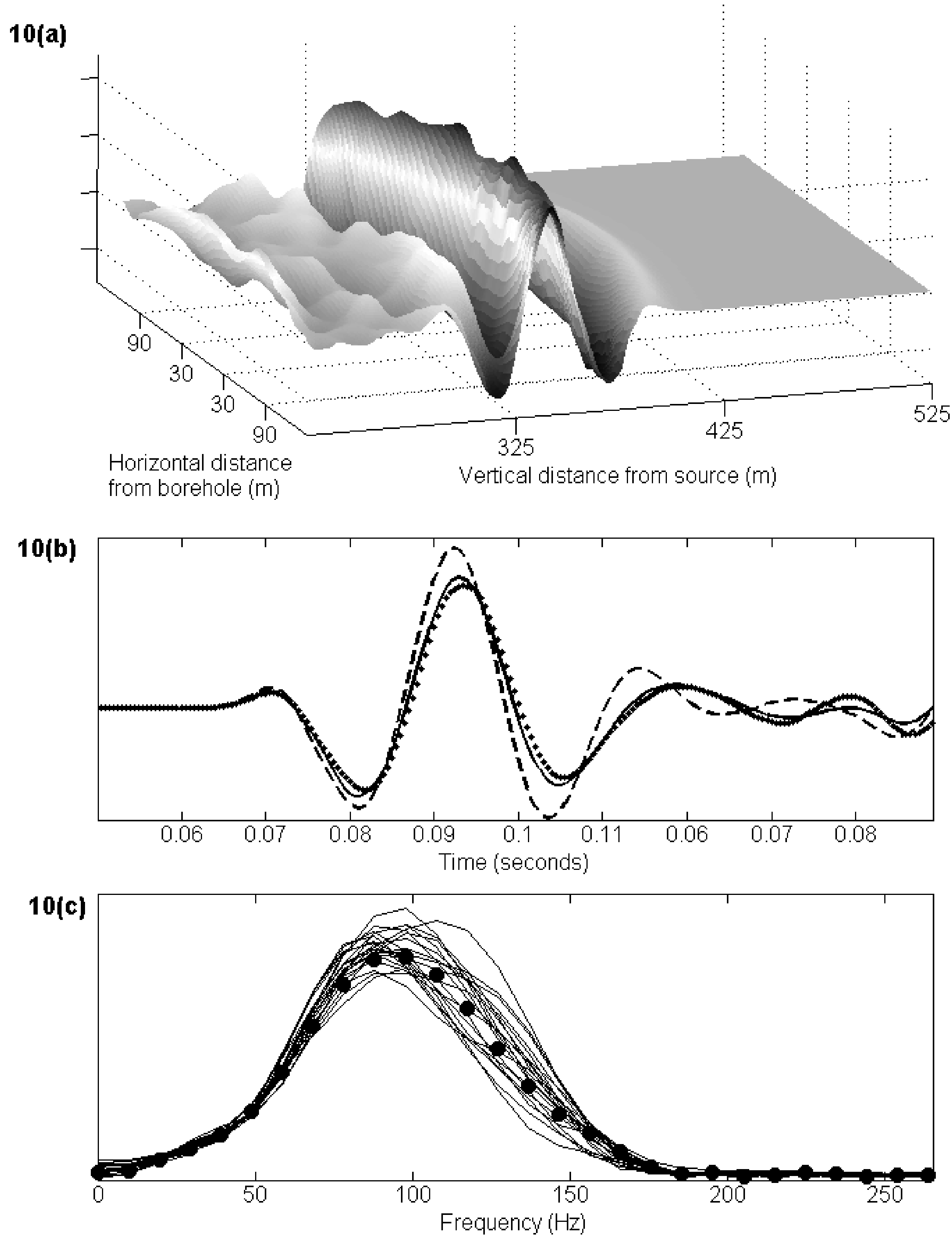
10(a)
90
30
30
90
Horizontal distance
from borehole (m)
325
425
525
Vertical distance from source (m)
10(b)
0.06
0.07
0.08
0.09
0.1
0.11
0.06
0.07
0.08
Time (seconds)
10(c)
0
50
100
150
200
250
Frequency (Hz)

Figure 10

11

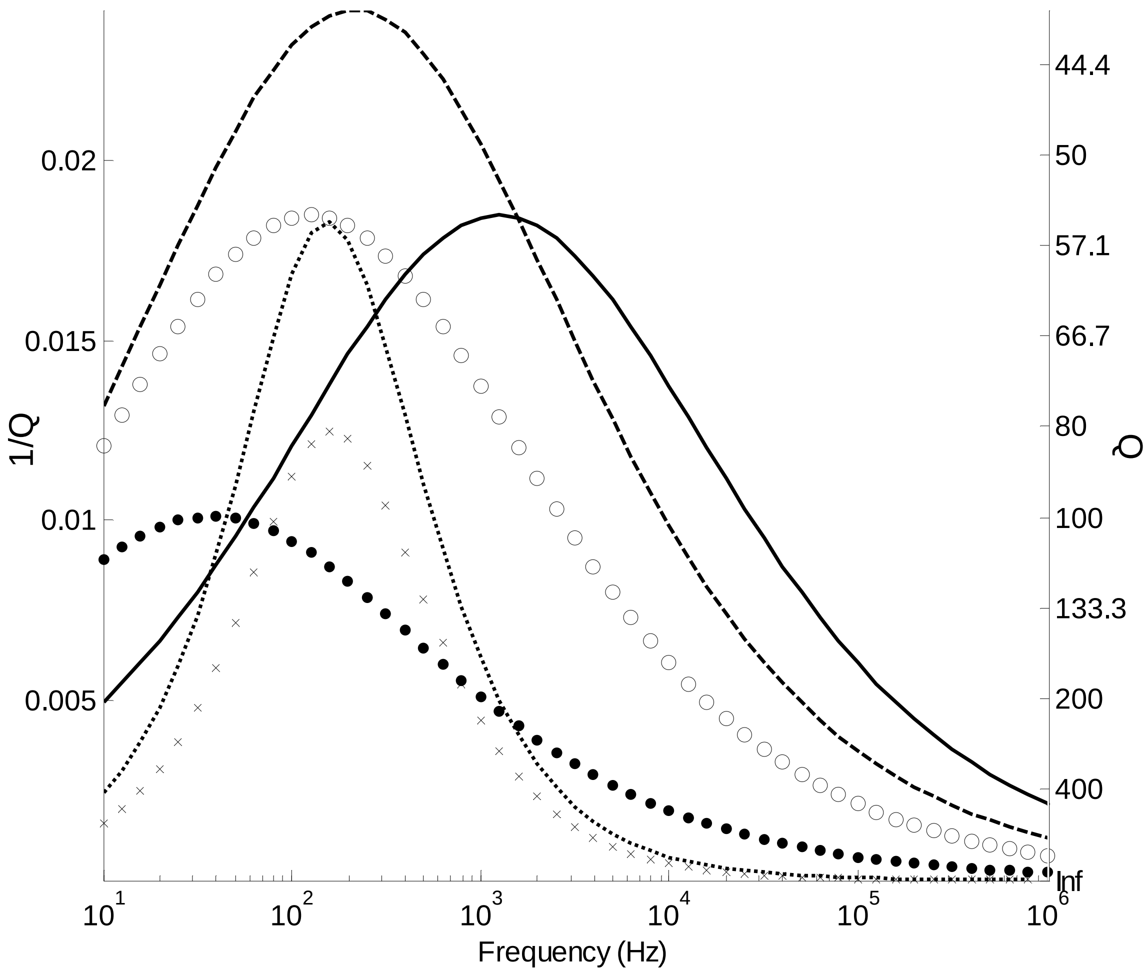

0.02
0.015
0.01
0.005
1/Q
44.4
50
57.1
66.7
80
100
133.3
200
400
Inf
Q
10^1
10^2
10^3
10^4
10^5
10^6
Frequency (Hz)

Figure 11